To the Graduate Council:

I am submitting herewith a dissertation written by Dee Hak-ki Wong (黃克基) entitled "Fire Modeling: Application of a Finite Element CFD Method to Three Dimensional Fire Simulation Based on Buoyant Viscous Flow with Thermal Radiation." I have examined the final copy of this dissertation for form and content and recommend that it be accepted in partial fulfillment of the requirements for the degree of Doctor of Philosophy, with a major in Engineering Science.

A. J. Baker, PhD
Major Professor

We have read this dissertation

and recommend its acceptance:

Accepted for the Council:

Associate Vice Chancellor and
Dean of The Graduate School

Fire Modeling:

Application of a Finite Element CFD Method to Three Dimensional Fire Simulation Based on Buoyant Viscous Flow with Thermal Radiation

A Dissertation

Presented for the

Doctor of Philosophy

Degree

The University of Tennessee, Knoxville

Dee Hak-ki Wong

(黃克基)

August 1995

DEDICATION

To my beloved wife,

Ms. Linda Susan Lefler

who patiently and persistently provided me

with the encouragement and words of wisdom

during a number of serious crises of this soul searching.

I did not earn this degree; **WE** have earned this degree.

And,

to my loving father,

Mr. Ting-fan Wong

(黃鼎勳先生)

who recently has resided in his spiritually peaceful domain

and is proud of our achievement.

Acknowledgments

I would like to gratefully thank my advisor, Professor A. J. Baker, for being a dedicated teacher and kind mentor. As a sagacious instructor, he enlightened me on the intricacy and versatility of finite-element CFD methodologies. As a mentor, he provided tremendous morale as well as emotional support during this profound soul searching.

I wish to express my sincere gratitude towards a number of good and bright friends at UT CFD Lab. Mr. Kwai-lam Wong, specializing in vorticity-velocity formulations and parallel processing, patiently helped me to better understand the formulations, matrix solvers and parallel computing. Mr. David Chaffin, an expert in Unix system, rescued me numerous times when I was frantically resolving "seemingly unresolvable" programming and computer problems. He and Dr. Subrata Roy enlightened me on advanced CFD theories and patiently showed me how to use some "user-friendly" software such as VI editor and Tecplot. Mr. Joseph Michael Barton was always available for turbulence and numerical consultation in addition to reviewing my convoluted technical notes. More importantly, without their sincere emotional support and encouragement during my life crises of the past year, this degree would be impossible.

I would like to gratefully thank Messr. Edward Schaub and Winston Holmes for their kind support of *AKCESS*.*, the selected finite element CFD code sponsored at the UT CFD Lab by Computational Mechanics Corporation in Knoxville, TN.

Last, but not the least, I would like to gratefully thank my doctoral committee members: Professors T. G. Carley, K. H. Kim and R. M. Kelso, for their enthusiastic participation and generous technical and financial support during this research program.

Abstract

Numerical fire simulations based on computational fluid dynamics (CFD), or field modeling, especially with compressible flows, three dimensions and turbulence have emerged and gained momentum since early 1980's. Nevertheless, none of the germane publications definitively determine the feasibility of buoyant incompressible laminar flows and applicability of thermal radiation. The primary objective of this research is to address these two issues. In addition, all these publications are based on either finite-difference or finite-volume algorithms, thereby rendering the application of finite-element method in this research area genuinely unique and original.

Assuming incompressible Navier-Stokes equations with constant fluid and thermophysical properties, *AKCESS.**, a general-purpose finite-element CFD code handling any convective/diffusive fluid simulation, has been adopted. Thus, the major challenge or the crux of this research is to develop and verify thermal radiation submodels therein, which robustly and efficiently handle both non-participating and participating media in conjunction with ad hoc verifications of non-zero Neumann temperature BC's.

To lessen the degrees of freedom of the Navier-Stokes conservation law (or PDE) system, and to circumvent the cumbersome derivation of the spatial discretization for the convection-diffusion-radiation term in the energy equation, the divergence of the radiative flux vector based on Naraghi's methods [60,61] is treated as a legitimate source term constituting the radiation field computed from the temperature field from the previous time station. Due to numerical stability issues and the assumption of laminar flow, certain inconsistencies among fluid, radiation and fire dimensionless groups exist in these

equations, resulting in use of a dual dimensionless systems: fluid, and radiation/ fire.

An elementary fire scenario in a 3x3x3 m enclosed adiabatic room with a central 10-node column 250 kW fire has been assumed. For an uniform 2-D grid of 16x16 elements, the computational results based on Rayleigh number of 1.E6 reasonably correlate with the overall hot-layer temperature predicted by an experimentally validated 2-zone fire model. A uniform 3-D grid produces similar results. With respect to the temporal-spatial temperature profiles based on 2-D simulations of the first 15 seconds, the radiative source (or sink) terms do not impact the scalar fields due to several orders of magnitude difference between nodal fire and radiative sources. However, further investigations on more complex fire scenarios are needed to generalize this conclusion.

Despite the problematic dual dimensionless systems, current findings of a fundamental fire scenario with easily reproducible results demonstrate that incompressible laminar flows are viable candidates for realistic fire simulations, thereby bridging the dichotomy of over-simplified 2-zone semi-empirical fire models and full-fledged CFD-fire models with complex features that are highly restricted to research community use only.

In order to realistically estimate the combined net (or incident) radiative and conductive (or convective) flux onto an analyst-defined target such as a fire sprinkler, heat detector, fusible link or even human skin located some distance away from the fire plume, or to perform conjugate heat transfer analysis at the fluid-solid interface for structural integrity, one must utilize a similar radiation submodel. This truly original, unique technique is readily transformed into a practical fire protection engineering tool for fire damageability studies, hence advancing the art and science of fire technology.

Nomenclature

English

A	area, m^2
$Ar=Gr/Re^2$	Archimedes number
Bo	Boltzmann Number, dimensionless
c	specific heat, kJ/(kg-K)
	coefficient
D	diameter, m
dss	discrete exchange factor, surface to surface
dsg	discrete exchange factor, surface to gas
dgs	discrete exchange factor, gas to surface
dgg	discrete exchange factor, gas to gas
dA	differential or discretized surface area, m^2
dV	differential or discretized volume, m^3
E	emissive power, kW/m^2
$Eu=p_o/\rho_o U_o^2$	Euler number, dimensionless
F_{ij}	view factor matrix, dimensionless
f_j	dimensionless kinematic flux vector
f_j^v	dimensionless viscous flux vector
G	irradiance or irradiation, kW/m^2
$Gr=[g(\Delta T_o/T_o)L_o]/\nu_o$	Grashof number, dimensionless
g	acceleration due to gravity, 9.81 m/s^2
h	height, m
	thickness, m
J	Jacobian matrix, dimensionless
K_a	absorption coefficient, 1/m
K_s	scattering coefficient, 1/m
$K_t=K_a+K_s$	extinct coefficient, 1/m
k	thermal conductivity, kW/(m-K)
L	Length, m
m	mass, kg
M	mass matrix, dimensionless
N	total number of summation index, dimensionless
N	finite element basis, dimensionless
n	unit normal vector, dimensionless
$Pe=U_oL_o/\alpha_o=RePr$	Peclet number, dimensionless
$Pr=\mu_o c_{p,o}/k_o=\nu_o/\alpha_o$	Prandtl number=0.7, dimensionless
p	pressure, Pa
Q	dimensionless state variable vector
Q	rate of heat release of fire, kW

q	heat rate, kW
	heat energy, kJ
R	radiosity, kW/m^2
Ra=GrPr	Rayleigh number, dimensionless
r	distance vector between nodes i and j
$Re=U_oL_o/\nu_o$	Reynolds number, dimensionless
s	dimensionless source term
T	temperature, K
t	time, s
U	reference velocity, m/s
u	velocity
x	coordinate, m

Greek

α	absorptivity, dimensionless
	thermal diffusivity, m^2/s
β	dimensionless compressibility coefficient
Δ, δ	differential, discrete, Kronecker delta
ε	emissivity, dimensionless
η	natural or local coordinate for finite element
$\Theta\equiv(T-T_o)/\Delta T_o$	dimensionless temperature
θ	Euler implicit value
ν	dynamic viscosity, m^2/s
π	3.1416
ρ	density, kg/m^3
	reflectivity, dimensionless
ϕ	included angle between distance vector and
	unit normal vector, degree
Ψ	weight function vector for Galerkin weak statement
Ω	discretized domain
$\omega\equiv K_s/K_t$	scattering albedo, dimensionless
σ	Stefan-Boltzmann Constant, 5.67E-11 $kW/(m^2\text{-}K^4)$
τ	transmittance, dimensionless
Σ	summation

Superscript

.	time rate, 1/s
//	flux, per unit area, $1/m^2$
///	per unit volume, $1/m^3$

T	transpose of a vector or matrix
p	iteration station
*	dimensionless quantity

Subscript

i, j, k	tensorial indices
e	elemental basis
o	reference or characteristic value
n	time station
b	blackbody
s	surface, sprinkler
f	fire
g	gas
H	hot wall
C	cold wall
r	radiation
c	conduction

Non-dimensionalization

$$x_j^* \equiv \frac{x}{L_o} \quad ; \quad u_j^* \equiv \frac{u_j}{U_o} \quad ; \quad t^* \equiv \frac{L_o}{U_o} \quad ; \quad p^* \equiv \frac{p}{\Delta p} \quad ; \quad \Delta p \equiv p_o = \rho_o U_o^2$$

$$\rho^* \equiv \frac{\rho}{\rho_o} \quad ; \quad \nu^* \equiv \frac{\nu}{\nu_o} \quad ; \quad \alpha^* \equiv \frac{\alpha}{\alpha_o} \quad ; \quad c_p^* \equiv \frac{c_p}{c_{p,o}}$$

$$Bo \equiv \frac{\rho_o c_{p,o} U_o \Delta T_o}{\sigma (\Delta T_o)^4} \quad ; \quad \Delta T_o \equiv T_{max} - T_{min} \quad ; \quad \dot{q}''_{r,o} \equiv \sigma (\Delta T_o)^4$$

$$\dot{q}''_{c,o} \equiv \frac{k_o \Delta T_o}{L_o} \quad ; \quad \dot{q}''_o \equiv \rho_o c_{p,o} U_o \Delta T_o = \dot{q}''_{c,o} \, Pe = \dot{q}''_{r,o} \, Bo \quad ; \quad \dot{q}'''_o \equiv \frac{\dot{q}''_{r,o}}{L_o}$$

Table of Content

Chapter		Page
1	**Introduction**	1
1.1	Historical Background	1
1.2	Objective	4
1.3	Originality and Significance	4
2	**Literature Overview**	5
2.1	Zone and Field Modeling	5
2.2	Zone Models	6
2.3	Field Models	7
2.3.1	Nineteen Seventies	8
2.3.2	Nineteen Eighties	9
2.3.3	Nineteen Nineties	12
2.4	CFD-Radiation Fire Simulations	18
2.5	CFD-Radiation	19
2.6	Summary of Literature Search	21
3	**Mathematical Models**	22
3.1	Governing Partial Differential Equations (PDE)	22
3.2	The Finite Element CFD Algorithm	24

3.2.1	Discretization of Divergence of Radiative Flux Vector	25
3.2.2	Finite Element Matrix Statement	26
3.3	Participating Thermal Submodel	27
3.4	Radiative Source (or Sink) Term Approach	31
4	**Results and Discussion**	33
4.1	Verifications of Pure Radiation Submodel	33
4.1.1	2-D Non-Participating Square Cavity	33
4.1.2	3-D Non-Participating Cube	36
4.1.3	1-D Participating Slab	38
4.2	Pure Radiation Benchmark Comparisons	39
4.2.1	2-D Participating Square Cavity	39
4.2.2	3-D Participating Cube	40
4.3	CFD-Radiation Implementation	41
4.3.1	Dimensionless Fluid and Heat Transfer Parameters	41
4.3.2	2-D CFD-Radiation Test Cases	44
4.3.3	3-D CFD-Radiation Test Cases	54
4.3.4	3-D Discrete Exchange Factors and Accuracy Study	61
4.4	Fire Simulations	64
4.4.1	Dual Dimensionless Systems	64
4.4.2	Fire Specifications	66

4.4.3	A 2-zone Model for Qualitative Check of Results	67
4.4.4	2-D Room Fire	68
4.4.5	3-D Room Fire	82
4.5	Fire Damageability Studies	91
4.6	Computational Considerations	95
5	**Conclusions**	97
References		98
Appendix A	2-D Benchmark Verification Solutions	105
A.1	Case 1: 2-D Thermal Cavity Steady State Solutions, Ra=1.E4	106
A.2	Case 2: 2-D Ad Hoc Benchmark Baseline Conductive Flux	107
A.3	Case 3: 2-D Verification of Combined Conductive and Radiative in a Non-Participating Medium, ε=1.0	108
A.4	Case 4: 2-D Verification of Combined Conductive and Radiative Flux in a Non-Participating Medium, ε=0.1	109
A.5	Case 5: Verification of Combined Conductive and Radiative Flux in a Participating Medium, ε=1.0	110
A.6	Case 6: Verification of Combined Conductive and Radiative Flux in a Participating Medium, ε=0.1	111
A.7	Case 7: 2-D Steady State Solutions of Participating Thermal Cavity, Fluid Ra=1.E4, Mesh=16x16	112
A.8	Case 8: Accuracy Study of 2-D Steady State Solutions of Participating Thermal Cavity, Fluid Ra=1.E4, M=32x32	114

Appendix B 3-D Benchmark Verification Solutions 120

B.1 Case 9: 2-D Thermal Cavity Steady State Solutions, Ra=1.E4 121

B.2 Case 10: 2-D Ad Hoc Benchmark Baseline Conductive Flux 124

B.3 Case 11: 2-D Verification of Combined Conductive and Radiative in a Non-Participating Medium, ε=1.0 125

B.4 Case 12: 2-D Verification of Combined Conductive and Radiative Flux in a Non-Participating Medium, ε=0.1 126

B.5 Case 13: Verification of Combined Conductive and Radiative Flux in a Participating Medium, ε=1.0 127

B.6 Case 14: Verification of Combined Conductive and Radiative Flux in a Participating Medium, ε=0.1 128

B.7 Case 15: 2-D Steady State Solutions of Participating Thermal Cavity, Fluid Ra=1.E4, Mesh=16x16x16 129

Appendix C 2-D Fire Simulation Solutions 132

C.1 Case 16: 2-D Fire Simulation, Pure Convection, Fluid Ra=1.E4 133

C.2 Case 17: 2-D Fire Simulation, Convection and Radiation, Fluid Ra=1.E4 134

C.3 Case 18: 2-D Fire Simulation, Pure Convection, Fluid Ra=1.E5 136

C.4 Case 19: 2-D Fire Simulation, Convection and Radiation, Fluid Ra=1.E5 137

C.5 Case 20: 2-D Fire Simulation, Pure Convection, Fluid Ra=1.E6 139

C.6 Case 21: 2-D Fire Simulation, Convection and Radiation, Fluid Ra=1.E6 140

C.7 Case 22: Accuracy Study of 2-D Fire Simulation, Fluid Ra=1.E6, Mesh=32x32 142

C.8 Case 23: 2-D Fire Simulation, Fluid Ra=1.E6, Small Opening, M=32x16 146

Appendix D 3-D Fire Simulation Solutions 148

D.1 Case 24: 3-D Fire Simulation, Fluid Ra=1.E4 149

D.2 Case 25: 3-D Fire Simulation, Fluid Ra=1.E5 152

D.3 Case 26: 3-D Fire Simulation, Fluid Ra=1.E6, t^*=5.33 155

D.4 Case 27: 3-D Fire Simulation, Fluid Ra=1.E5, Non-Uniform Grid 158

D.5 Case 28: 3-D Fire Simulation, Fluid Ra=1.E6, Non-Uniform Grid, t^*=16.4 161

Appendix E A Sample of Discrete Exchange Factor Subroutine 165

Appendix F *AKCESS**. Model File for Ra=1.E5, 3-D Fire Simulation 169

Appendix G *AKCESS**. Template File for Ra=1.E5, 3-D Fire Simulation 174

Appendix H *AKCESS**. Cdata File for RA=1.E4, 2-D CFD-Radiation and Fire Simulation 183

Vita 192

List of Figures

Title	Page
Fig. 1 2-D Verification Problem	34
Fig. 2 Designations of Boundary Normal Vectors	35
Fig. 3 2-D Benchmark Cube	40
Fig. 4 2-D Standard Thermal Cavity	44
Fig. 5 2-D Steady State Solutions of Standard Thermal Cavity	45
Fig. 6 3-Point Backward Finite Difference Algorithm	47
Fig. 7 2-D Hot Wall Temperatures	48
Fig. 8 2-D Cold Wall Temperatures	48
Fig. 9 2-D Steady State Solutions of Participating Thermal Cavity	52
Fig. 10 Accuracy Study of 2-D Steady State Solutions of Participating Thermal Cavity	53
Fig. 11 3-D Steady State Solutions of Standard Thermal Cavity	56
Fig. 12 3-D Mid x_1-x_2 Plane Hot Wall Temperatures	58
Fig. 13 3-D Mid x_1-x_2 Plane Cold Wall Temperatures	58
Fig. 14 3-D Steady State Solutions of Participating Thermal Cavity	60
Fig. 15 Nomenclature of Generic Geometrical Discrete Exchange Factors	62
Fig. 16 2-D Fire Simulation, Pure Convection, Fluid Ra=1.E4, Case 16	69
Fig. 17 2-D Fire Simulation, Convection and Radiation, Fluid Ra=1.E4, Case 17	70
Fig. 18 2-D Fire Simulation, Pure Convection, Fluid Ra=1.E5, Case 18	71

Fig. 19 2-D Fire Simulation, Convection and Radiation, Fluid Ra=1.E5, Case 19 72

Fig. 20 2-D Fire Simulation, Pure Convection, Fluid Ra=1.E6, Case 20 73

Fig. 21 2-D Fire Simulation, Convection and Radiation, Fluid Ra=1.E6, Case 21 74

Fig. 22 Accuracy Study of 2-D Fire Simulation, Fluid Ra=1.E6, M=32x32, Case 22 75

Fig. 23 2-D Fire Simulation, Small Opening, Fluid Ra=1.E6, M=32x16, Case 23 76

Fig. 24 2-D Fire Room Temoeratures 78

Fig. 25 3-D Fire Simulation, Fluid Ra=1.E4, Case 24 83

Fig. 26 3-D Fire Simulation, Fluid Ra=1.E5, Case 25 84

Fig. 27 3-D Fire Simulation, Fluid Ra=1.E6, Case 26 t=2.6 s 85

Fig. 28 3-D Fire Simulation, Fluid Ra=1.E5, Non-Uniform Grid 86

Fig. 29 3-D Fire Room Temperatures 89

List of Tables

	Title	Page
Table 1	Comparison of Analytical and Numerical Results for 1-D Participating Slab	38
Table 2	Comparison of 2-D Participating Cavity Dimensionless Emissive Power for Radflux and Benchmark Results	39
Table 3	Comparison of 3-D Participating Cube of Radflux and Benchmark Results	40
Table 4	Summary of 2-D Mid-Wall (x_2^*=0.5) Fluxes and Temperatures	49
Table 5	Summary of 2-D Mid-Wall (x_2^*=0.5) Non-Participating Fluxes and Temperatures	50
Table 6	Summary of 2-D Mid-Wall (x_2^*=0.5) Participating Fluxes and Temperatures	50
Table 7	Summary of 3-D Mid-Wall (x_2^*=0.5) Fluxes and Temperatures (Plane 9)	57
Table 8	Fluid and Fire (or Radiation) Systems for Fluid and Heat Transfer Groups	65
Table 9	Summary of Dimensionless Results of 2-D Fire Simulations	77
Table 10	Summary of Dimensionless Results of 2-D Fire Simulations	77
Table 11	Evan's Empirical Correlations for a Steady State **Ceiling** Jet Flow	87
Table 12	Summary of Dimensionless Results of 3-D Fire Simulations	88
Table 13	Summary of Dimensionless Results of 3-D Fire Simulations	88

Chapter One

Introduction

1.1 Historical Background

In performing fire hazard and risk assessment, fire professionals such as engineers, architects, building and fire officials, facility operators, insurers, and safety and risk managers need to determine the ultimate impact of fire on life safety, property loss and business interruption. Traditionally, the methodology of such assessment has been qualitative. Building construction is generically classified as *Combustible* or *Non-combustible*; and occupancy is classified as *Light*, *Ordinary* or *Extra* Hazard, in connection with the probabilistic notion of *Highly Unlikely*, *Likely* or *Highly Likely*. For many decades, this simplistic system has been the basis for formulating the current building and fire codes and regulations, and serving as the screening or "engineering" tool for the insurance industry as well as worldwide fire communities. Though elegantly simple, this qualitative approach has some significant drawbacks. First, as the technology advances rapidly, this simplistic classifying system is neither reasonable nor adequate to describe the extreme variations of the extent and magnitude of potential fire hazards and risks for most types of construction and occupancy. Second, the approach is highly subjective, often leading to confusion and controversy.

Since the early nineteen eighties, fire communities have realized these shortcomings. As a result, quantitative fire hazard analysis comprising both deterministic and probabilistic aspects has emerged and gained momentum. This new approach

attempts to specifically address some of those ever-agonizing issues such as: how hot are certain fuel packages (compositions of fires) in temperature (degrees) and in kilowatts per square meter of emissive power; what are concentrations of the fire products (or fire species including smoke) in parts per million or kilograms per second per cubic meter; what are net or incident heat fluxes onto the exposed environments in kilowatts per square meter; and are certain fire sprinklers, detectors and building construction designed adequately to suppress, control, detect or withstand the assumed fires under nontrivial fire scenarios? Moreover, what is the likelihood of the fire occurrence and the scope of fire damageability? Concerning the deterministic aspect only, this new approach employs outcomes of scientific or experimental fire research and incorporates advanced engineering modeling wherever appropriate. The hybrid of these two entities: empiricism and theoretical modeling, lays the foundation of the so-called "fire modeling", which had been coined in the early nineteen seventies, and is still in its very infancy.

To date, as we may know, "ordinary" fires are extremely complicated combustion processes, in which most of their physicochemical phenomena remain unknown. Limited to the present technology, basic descriptions of fire in terms of rate of heat energy release, average fire temperature, flame and plume geometries, fire species production rates, and horizontal and vertical flame spread rates must resort to empiricism and cannot be based on purely theoretical modeling. Fire research communities such as the Building and Fire Research Laboratory of US National Institute of Standards and Technology (NIST), Factory Mutual Research Corporation (FMRC), Southwest Research Institute (SwRI), Sandia National Laboratory, Lawrence Livermore National Laboratory (LLNL), Canadian

National Research Council (CNRC), UK Fire Research Station of British Research Establishment (BRE), Swedish Fire Research Center and Japan Fire Research Centre have jointly or independently developed these purely empirical correlations and the semi-empirical 2-zone PC-based (personal computer) fire models in the past few decades. Nevertheless, augmented by numerous standard and ad hoc fire tests, the scope of predictability of published empirical correlations and 2-zone models is rather limited to fairly simple fire scenarios. This is the reason that probabilistic models as well as field modeling or computational fluid dynamics (CFD) are necessary to supplement or even finally replace the empiricism of the deterministic methodologies in certain fire hazard and risk analyses.

While the empirical aspect focuses on the physicochemical phenomena of the fire plume and its flame, or the "near" field of an arbitrary, physically bounded fire enclosure, and the interactions of the plume and extinguishing media such as water and foam, the computational aspect usually is confined to the physical phenomena of the "far" field. Unlike most fire researchers, primarily interested in the near field to better understand phenomena of fire, practicing fire professionals usually are interested in the impact of fire and smoke in the far field only, since most components of the immediately exposed environment including fire protective devices under a direct flame impingement or fire engulfment would be instantaneously deformed or activated. It is the numerical aspect of the deterministic approach for fire hazard analysis that is of interest to this doctoral research program; namely, utilizing a feasible engineering transport model for numerical fire simulation.

1.2 Objective

As presented in the next chapter, Literature Overview, CFD fire simulations are neither original nor unique. Complex engineering models based on governing partial differential equations (PDE) embracing three dimensions, turbulence, compressibility, buoyancy, thermal radiation and mass transfer have been applied in fire simulations but are extremely cost-prohibitive. In addition, it is deemed that desperately needing well defined problems with easily reproducible results, the current development on CFD fire modeling lacks a sound foundation or protocol leading to a rigorous, versatile but feasible fire protection engineering tool for the future. Thus, in light of this lofty ambition, the objective of this research project is three-fold, *partially* addressing this long-term goal:

1. establish a benchmark fire scenario with readily reproducible numerical results;
2. determine if a purely laminar flow analysis is viable for fire simulations; and
3. under an elementary fire scenario, determine if thermal radiation is significant.

1.3 Originality and Significance

The original and significant contribution is a more realistic fire damageability study based on both conductive and radiative fluxes. Despite any significance of radiation on the scalar fields, CFD-radiation fire modeling indeed provides a necessary vehicle for the analysis. The adoption of the *Source-Function* approach for the radiative term in the energy equation is original, resulting in the elimination of the equation of (radiation) transfer (RTE) from the governing PDE system. Additionally, a finite element based CFD fire simulation system is unique.

Chapter Two

Literature Overview

2.1 Zone and Field Modeling

As mentioned in the previous chapter, the computational aspect is further subdivided into zone and field modeling, and both apply conservation laws. A typical two-zone model, dividing a conceived fire compartment into two dynamic control volumes, namely, the "hot" and "cold" layers, can be viewed as a special case of field modeling. Such simplifications seem highly idealized; however, they logically stem from physical observations of many fire experiments and real fire situations. The significant advantage of zone models is that their concomitant mathematical models, though substantially augmented by empiricism in terms of source terms, layer interface and boundary conditions, are merely a set of two or three coupled first-order non-linear ordinary differential equations, which can be solved quite easily and economically with the existing personal-computer (PC) technologies.

The above approach, which assumes that all scalar variables within the same layer or control volume are uniform and constant, sometimes is unrealistic. Naturally, a field model, essentially synonymous with CFD, utilizing dozens or even thousands of control volumes (finite volumes or elements), can be applied to situations where detailed solutions are needed or the applicability of zone modeling is no longer valid, such as in the case of highly irregular geometries of fire enclosures. However, the major drawback of field modeling is the enormous computational resources required that are sometimes

prohibitive, even for the fire research arena, let alone the fire communities in general.

It is predicted that as the computing technologies become more and more powerful and accessible, and CFD-fire theories mature, field modeling as a practical fire protection engineering tool would eventually surpass zone modeling.

2.2 Zone Models

In the mid-nineteen seventies, Emmons had formulated the very first documented zone model called Harvard Computer Fire Code [1], which has been upgraded and revised ever since. Originally, it could handle a single fire compartment only; now it can handle multiple-connected rooms. Unfortunately, fire communities had not been properly indoctrinated in the concept and utility of fire modeling, and the Harvard fire code has never been widely accepted. The most renowned single-room zone model is ASET [2], Available Safe Egress Time, written by Cooper at the Center for Fire Research of NBS (now NIST). With the advent of PC's in the early nineteen eighties, ASET-B, a revised version of ASET written in Basic in lieu of Fortran, can be run efficiently on a PC.

ASET was considered the state-of-the-art fire modeling tools in the fire protection consulting engineering industry in the era. The latest generation of zone modeling can simulate multiple-room fires. A state-of-the-art zone modeling code is HAZARD-I [3] predicated on FAST, a model for the transport of fire, smoke and toxic gases written by Jones [4] and Tanaka [5]. HAZARD-I, incorporating a non-participating thermal radiation enclosure model, can not only estimate field variables in fire compartments but can also predict toxicological effects on occupants by incorporating an evacuation model based on

the psychological aspect of group human behavior. Presently, there are dozens of zone models available to the public worldwide. Most zone models are experimentally validated by small-room fires and well accepted by the fire communities. Additional surveys of zone models can be found in [6-8]. In this research, FPETOOL [9] has been adopted for comparisons.

2.3 Field Models

Like solving most fluid, thermal and mass transfer engineering problems, such as combustion processes and furnace and rocket designs, fire modeling is based on the same set of basic conservation laws with some "slight" modifications. However, a comprehensive review of the past and current research work including the above general problems as a basis for this literature search would be neither practical nor fruitful due to the humongous volume of related literature. Moreover, there are hundreds of papers relating to these general problems being published every year. These published works are usually oriented towards combustion science and industrial applications instead of pure fire research, per se.

Hence, this literature review is limited only to those explicit studies of CFD fire modeling. The set of key words used in the computerized literature search includes:

1. fire or fire modeling;
2. CFD, numerical, computational or mathematical modeling; and
3. heat transfer, convection, radiation, or thermal radiation.

As expected, there are only a few dozen papers directly relating to this subject. Significant papers surveyed are discussed below.

2.3.1 Nineteen Seventies

Yang, et al [10] and Ku, et al [11] appear to be the first groups performing CFD Fire simulations in 1977. UNDSAFE-I (University of Notre Dame - Smoke and Fire Enclosures) [10] can handle two-dimensional unsteady compressible turbulent buoyant flows, utilizing a finite-difference algorithm restricted to single rectangular rooms with an opening such as window or door. The algebraic turbulence model is based on a Prandtl mixing-length theory. An "arbitrary" volumetric region is assigned to be a heat source for the fire. Only numerical examples have been presented without comparisons with fire experiments.

In the following year, Liu and Yang upgraded the code to UNDSAFE-II [12], which significantly added an one-dimensional radiation model for surface radiation, soot radiation, and non-gray gaseous radiation, in addition to refined algebraic turbulence models and numerical error and stability control mechanisms. However, the treatment of thermal radiation of the hot smoke layer within the fire enclosure was not clearly addressed. Additionally, no direct comparisons with experimental results had been made in [12], although this was the intent of upgrading the UNDSAFE code to include an adjacent room for experimental correlations at the doorway. These research work along with other similar research activities were virtually unknown to the fire communities; therefore, no practical applications had been documented.

2.3.2 Nineteen Eighties

The most active group in numerical fire modeling is the British research team comprising Markatos, Kumar, Cox, Galea and Hoffman, applying the now-commercial general-purpose CFD packages such as FLOW3D, FLUENT and PHOENICS. JASMINE, a specialized computer fire code written by BRE [13,14] and based on PHOENICS, has been compared with experimental data at LLNL and found "somewhat" correlated. JASMINE can handle nine degrees of freedom: three velocity components, pressure, enthalpy, mixture and mass fraction of the fuel (2-phase reaction flows), the turbulent kinetic energy and its dissipation rate. Moreover, it is the first three-dimensional unsteady compressible k-ε turbulent flow CFD code coupling species transfer equations and a radiation submodel, attempting to capture details of both the near and far fields. FLOW3D is based on a finite-volume algorithm with an optional QUICK or HUW scheme.

During the same period, NIST and Japanese fire research groups had jointly sponsored some sporadic internal research programs on numerical fire modeling. Criticizing the arbitrary empiricism of a k-ε turbulence model, Baum, et al [15] implemented large-scale buoyant convection and smoke aerosol coagulation into their CFD fire simulations. The authors contend that physical measurements obtained by McCaffrey [16] and other fire experimentalists indicate that laboratory scale fire plumes are dominated by eddies of low frequency (typically two to five hertz) and length scales comparable to the local plume width, significantly deviating from the turbulent plume profiles predicted by Ku, et al [11] and Markatos and Cox [17] with the k-ε model.

Further, Baum, et al have been convinced that large-scale macroscopically resolvable motion is responsible for most transport of mass, momentum, and energy except at boundaries. In addition, small-scale physical and chemical processes, which control heat and mass transfer to boundaries, as well as most combustion and smoke aerosol phenomena, are ultimately to be imbedded in a systematic way into the large-scale flow.

In the near field, the combustion and smoke formation zone is replaced by a prescribed source of heat and particulate matter. Heat transfer to the boundaries is ignored. The large-scale transport is then calculated directly from the equations of motion. The introduction of coagulation into the large scale flow pattern is to allow consideration of more complex small scale processes. The authors also introduced a "particle tracking" system based on a Lagrangian representation. Interestingly, expanding their original work [18,19] based on compressible flows in the near field, the authors employed an incompressible laminar flow with a Boussinesq approximation for the far field only. A velocity-vorticity formulation in conjunction with an interchangeable dimensionless perturbed energy and density equation has been adopted.

Unlike typical dimensionless systems, their dimensionless reference velocity and temperature (or density) were based on empiricism, thereby eliminating Reynolds, Grashof, Prandtl, Rayleigh, Euler and Peclet Numbers. It is deemed that the adoption of an incompressible flow with a Boussinesq approximation and an equation of state (the ideal gas law) for pressure in the far field is problematic, while the near field is based on a compressible flow exclusively utilizing an equation of state. In addition, the authors had not addressed the implementation and compatibilities of two distinct density fields

as well as enforcement of conservation of mass in the near and far fields. The former does not enforce the solenoidal velocity vector field, whereas the latter does.

A typical grid ranges from 20x20x20 to 54x54x24. Consequently, a Cray-1 has been utilized and the cpu time ranges to 1000 seconds. Despite the innovative approach of combining empiricism and theoretical modeling using discrete Fourier transforms, this research work, in addition to a more recently related work [20], has never been widely publicized by fire communities. Thus, there had been no practical fire simulation based on this hydrodynamic model inspired by the so-called "salt-water wedges" phenomenon arising from a characteristic gravity front starting from the near field spreading down to the far field. Nevertheless, Baum, et al continued this methodology into the nineteen nineties. Their current work will be further discussed in the next section.

Morita, et al [21] has explicitly described the numerical aspect of CFD-fire modeling among the above papers. Their research are based on two-dimensional unsteady compressible k-ε turbulent flows. The CFD formulation is based on a 3-point upwind finite differencing method. The fire source is a "line"-typed fire characterized by an array of constant Dirichlet temperature nodes on a wall. The fire temperature is 800° C. Their major observation is that the time interval and space mesh be chosen less than 10 msec and 5 cm, respectively, for a high Reynolds number such as 500 or above. Unfortunately, values of other important dimensionless groups and their reference parameters in addition to experimental correlations have not been reported.

In the late nineteen eighties, the British group applied the CFD packages mentioned earlier in this section to simulate actual enclosure fires for aircraft cabins,

shopping malls, and small office rooms [22-25]. A body-fitted coordinate (BFC) formulation was utilized for the aircraft cabin fires. The number of cells (or finite volumes) ranges from 2000 to 24,000. The predicted temperature profiles of a huge closed stadium fire were reported to correlate well with experimental data collected from the stadium.

Concurrently, a fire research group in Hong Kong headed by Chow applied SIMPLER and PISO algorithms to simulate corridor, tunnel and atrium fires [26,27] based on two-dimensional compressible viscous buoyant turbulent flows.

The first and unique experimental-numerical research work was conducted by Alpert and Delichatsios [28] of FMRC. The study involves the interaction of water spray from fire sprinklers and the fire plume with the consideration of two-phase flows. TEACH-T, an upwind finite-difference code (with an alternating direction implicit (ADI) scheme) developed by FMRC accommodating fairly small grids, required improvements on numerical accuracy, stability and convergence.

2.3.3 Nineteen Nineties

In general, fire simulations were based on three-dimensional compressible turbulent buoyant flows. Usually, dimensionless systems were not used. Chow and Fong [29], and Hoffmann and Galea [30] continued the unfinished mission launched by FMRC; namely, studies of the interaction of water spray and the fire plume. Both research were purely numerical experiments without experimental correlations or definitive conclusions.

The most significant achievement for a practical CFD fire simulation is the notorious King's Cross underground (subway) station fire in London in 1987 that killed thirty-one people and severely injured numerous others. There are several unique features of this retrospective fire simulation. First, this is the first CFD fire simulation utilized in an actual fire investigation. Second, a group of customized medium-scale experiments was conducted to augment the necessary physical data needed for numerical simulations. Third, with the aid of numerical solutions produced by Simcox, et al [31] from Harwell Laboratory (UK) using FLOW3D, an unusual fire phenomenon called *trench effect* was discovered by the UK government fire investigation team. The trench effect is that the fire flame, usually perpendicular to the ground, bends approximately 90° and spreads extremely rapidly through the train tunnels as well as the passenger escalators in the subway, induced by the strong mechanical ventilation and the longitudinal-shaped architectural branches of the subway system.

Impressed by this application, another group of NIST fire researchers comprising Davis, Forney and Klote [32] has recently adopted FLOW3D to simulate three-dimensional multiple-room fires, producing good experimental correlations except in the near field. Thereafter, despite on-going in-house developmental activities on CFD fire simulations performed by Baum, et al, NIST has applied FLOW3D to other field modeling research activities such as the ASHRAE (American Society of Heating, Refrigerating and Air-Conditioning Engineers, Inc.) project [33] and a Navy's 19F4 fire fighting trainer [34]. The ASHRAE project models the fire smoke beneath non-smooth or highly irregular ceilings, thereby shaping the future design basis for fire detection

systems.

Wong of SwRI [35] has attempted to upgrade an existing generic two-dimensional steady turbulent finite-element CFD code called TURBO2T to three-dimensional unsteady fire simulations. However, the work had not been completed and there are no meaningful numerical results. TURBO2T, developed by Schnipke [36] is a hybrid of the conventional finite-element method and the SIMPLER algorithm, utilizing a streamline upwind scheme.

Satoh of Fire Research Institute of Japan [37] enhanced UNDSAFE-II to investigate the smoke and heat transport at the early stage of a room fire strongly influenced by mechanical ventilation. A smoke equation was added to the governing PDE system. Qualitative analysis of smoke movement based on these numerical results had been concluded.

Hadjisophocleous and Cacambouras of NCRC [38] have experimentally validated their numerical results based on a three-dimensional compressible viscous k-ε turbulent flow and a SIMPLER finite volume algorithm. The room is 2.8x2.8x2.2 m. The fire source is 60.9 kW, adjacent to the back wall of the room. The fire reached steady state after 90 seconds.

Chow, et al [39,40] expanded their field modeling research into atrium fires and practical fire services designs, primarily studying effects of hot smoke on HVAC (heating, ventilation and air-conditioning) systems by adding a smoke species equation to the governing PDE system.

McGrattan, et al [41] of NIST and Baum, et al [42,43] continue their unique CFD

modeling methodology based on [15,16,18-20] as mentioned in the previous section. Unlike [15] and [43], their current work primarily focuses on two dimensions only. Since [41-43] are technically identical, they are discussed together. There are a few issues concerning these three papers.

First, the authors recognize the issue concerning the coupling of large-scale and small-scale fields. Their resolution is to enforce the solenoidal velocity field whenever large, low-frequency, pulsating toroidal vortices occur in the global domain, and embed the so-called small-scale thermal elements into the large-scale flow field. However, this approach is equivalent to the merging of a compressible flow (i.e., near or small-scale) field and an incompressible (i.e., far or large-scale) flow field contained within one global domain. The authors did not address how to conserve the mass of fluid at the "dynamic" interface of these two distinct density fields. In a compressible flow field, density is a state or independent variable and enforces mass continuity, whereas in an incompressible flow field, density variations normally vanish by definition. Hence, in an incompressible flow field, the solenoidal velocity vector field functioning as a constraint to the governing PDE is the *sole* mechanism to conserve the mass of fluid, although an additional PDE for *mildy* variable density or other similar species equation is permitted.

This brings up the previous, seemingly problematic issue of incorporating an equation of state into an "incompressible" flow field. It has already replaced moderate density variations with a Boussinesq approximation in terms of an empirical Froude scaling called β based on the rate of heat release of fire and a physically perturbed density.

The second issue is similar to the first one. The three papers did not address the conservation of momentum at the dynamic interface of the small-scale and large-scale flow fields, since the governing PDE for the compressible flow field does not include a momentum equation, owing to the assumption of low Mach number combustion. Although this assumption allows the authors to remarkably conglomerate the mass and energy equations and the equation of state into a single, mathematically tractable scalar or Poisson equation, the use of a vorticity stream function momentum equation (or equation of motion) in the large-scale flow field which does not conserve momentum is difficult to justify.

The third issue is the "absence" of a turbulence model advocated in the papers. According to Barton [44], it is deemed that the large-eddy simulation in the subgrids of the large-scale flow field (at the expense of utilizing highly dense grids), similar to a k-ε turbulence model, is indeed a subset of turbulence modeling, despite any semantic difference. Therefore, Baum and McGrattan, et al have *incorporated* a turbulence model throughout their numerical fire research.

The fourth issue is thermal radiation. Baum, et al [42] did not incorporate any formal or generalized thermal radiation submodel into the governing PDE system. Instead, [42] adopted a highly restrictive *point-source* thermal radiation model for each thermal element in the combustion zone, implicitly assuming a non-participating medium between the fire source and its exposed environment. Neglecting view factors and most radiative properties and phenomena, a *point-source* model is a function of radial distance between the source and an user-defined target, and the rate of heat release of the fire

only. This also implies that the fire plume accompanied by its hot smoke layer away from the combustion zone does not project any radiative flux onto the environment. Although this assumption is valid for certain fire scenarios for simplicity, a much simpler method would be preferred, e.g. [45] adopting an algebraic empirical correlation [46,47] for the fire plume in conjunction with a *cylindrical* radiation model, or simply applying the stand-alone point-source model, in lieu of any costly CFD-fire simulation. References [41-43] did not include the studies of combined conductive (or convective) and radiative fluxes onto a target.

The last issue is Reynolds number. Although Baum, Rehm and McGrattan, et al take a different approach to derive the dimensionless equations without the use of a Rayleigh or Grashof number, these parameters must be embedded into their adopted PDE system in some manner. Noting that $Gr=[g(\Delta T_o/T_o)L_o^3]/\nu_o^2=Re^2$ in a conventional natural buoyancy approach and assuming T_{max}=400 K, T_{min}=300 K, L_o=3 m and ν_o=15.89E-6 m^2/s, Gr=3.E11, Re=5.47E5 and U_o=2.9 m/s. This Reynolds number is an order of magnitude higher than the range of 20,000-40,000 used in their simulations. There is an inconsistency in selecting this range based on their own dimensionless groups. For example, if a "mild" fire source of q_f=250 kW is selected and all reference thermophysical properties are based on standard air, then $U_o=(q_f g/\rho c_p T_o)^{1/3}$=1.89 m/s, $\beta=U_o/(gL_o)$=0.122, and finally, $Re=U_oL_o/\nu_o$=3.57E5, which is comparable to the conventional approach and also another order of magnitude higher than the selected range. This demonstrates that the authors, Baum and McGrattan, et al [41-43] also encountered the same predicament of using dual dimensionless systems.

Restricted to two-dimensional analysis only, their simulations employed grid sizes of 768x192 and 3072x192 cells. The numerical results have been validated with a "salt-water" experiment conducted by Chan and Zukoski [48] and a backdraft experiment conducted by Fleischmann [49]. Using a Schwarz-Christoffel mapping package and an ADI scheme, a typical computation required between 20 and 100 Mbytes of memory and up to 50 hours of cpu time on an IBM RISC system/6000 workstation. To accommodate high Reynolds number, grids with up to half a million cells had been used.

2.4 CFD-Radiation Fire Simulations

In the previous sections, thermal radiation has never be formally discussed or incorporated. FLOW3D seems to have a legitimate three-dimensional thermal radiation enclosure sub-model called RAD3D, written by Guilbert [50]. It is based on a probabilistic approach, utilizing the Monte Carlo Method or a flux model to discretize the RTE, in lieu of the traditional Hottel's zonal method [51]. Unfortunately, no quantitative comparisons between CFD and CFD-radiation fire simulations [52] were made. Only a qualitative judgement that the radiative effect is very "important" in the near field was made.

There are at least two rigorous papers discussing CFD-radiation fire simulations. Fusegi and Farouk [53] of Drexel University have incorporated a k-ε turbulence and P_1-Approximation radiation module, adding an additional PDE for RTE into their 2-D finite-difference incompressible constant-properties viscous buoyant flow code. This paper reports a number of interesting observations regarding effects of turbulence and thermal

radiation, which is further subdivided into gas radiation and gas-soot radiation. However, the paper does not affirmatively conclude the important relevance of participating-radiative effects for fire simulations, except that the radiative effect is significant near the wall. Unfortunately, the detailed information of the construction of the fire source in terms of geometry and nodal kW/m^3 were not available, and their results cannot be practically reproduced. Furthermore, it is noted that laminar flow dominates the hot smoke layer and the cold region except in the immediate fire plume (near field), and the various radiative effects virtually have no impact on the velocity field in any case run.

Based on a 6-flux radiation model, the second paper is written by Kumar, Gupta and Cox [54]. Similar to the previous work, some regions of the simulated small room are not significantly affected by radiation; some regions are "qualitatively significant" affected. Both groups show that the incorporation of thermal radiation does not necessarily result in overall higher temperature profiles. On the contrary, some regions of their rooms have lower temperature profiles as a result of thermal radiation.

It is not clear from these two papers whether thermal radiation has a legitimate role in fire protection simulation as a practical engineering tool.

2.5 CFD-Radiation

In addition to [53, 54], only a few papers [55-58] on this subject (without fire applications) have been surveyed to gain some insight as to the general approach of CFD-radiation algorithms. All papers, considering non-gray (spectrally dependent) but not necessarily anisotropically scattering media, adopt an additional PDE for RTE, and

discretize the divergence of radiative flux vector along with the spatial convective and diffusive terms. The major drawback of this approach is not only an added degree of freedom to the governing PDE but also an inefficient algorithm resulting from an extra discretization for the radiative term in the energy equation. Among these papers, only Yucel's [55] approach explicitly treats the divergence of radiative flux vector as a "self-sustained" or independent source term (actually a sink term) in the energy equation, although the RTE is needed. This *source-term* approach serendipitously coincides with the intuitive strategy of this research, which is crucially based on the following papers. At high Rayleigh number, Fusegi, et al [56] had also adopted inconsistent dimensionless groups for convection and radiation.

A number of pure radiation papers have been surveyed from the ASME (American Society of Mechanical Engineers) heat transfer literature [59]. Among these papers, it is considered that the 2-D and 3-D *Source-Function* methods by Naraghi, et al [60,61] are the most versatile and numerically efficient algorithms. First, they can handle gray and anisotropically scattering, emitting and absorbing media inside gray-diffuse enclosures, although this research considers gray and non-scattering gases inside blackbody enclosures only. Second, their methods circumvent the expensive numerical integration of differential exchange factors, arising from either the 6-flux model or the zonal method. Third, the discretization method is highly adaptable to any existing CFD code and any matrix solver for nodal radiosities (or radiosity vector) with minimal modifications.

2.6 Summary of Literature Search

Although this overview does not include every published paper directly related to the CFD fire modeling, it is believed that the literature search is reasonably comprehensive and realistically reflects the chronology and the state-of-the-art of numerical fire modeling. Based on this search, the following observations can be made:

1. the significant role of laminar flow for fire simulations has never been formally studied;
2. a fundamental, *reproducible* benchmark fire scenario exclusively for CFD fire modeling does not exist;
3. the significant role of participating thermal radiation for fire simulations is not clear;
4. the use of finite element CFD methodologies for fire simulations does not exist;
5. the use of dimensionless systems for CFD fire simulations is rare; and for those related research works based on a dimensionless system, the predicament of dual dimensionless systems seemingly has been inherent in the analysis but never properly addressed; and
6. the application of combined conductive (or convective) and radiative flux to fire damageability studies does not exist.

Chapter Three

Mathematical Models

3.1 Governing Partial Differential Equations (PDE)

The general dimensionless incompressible laminar Navier-Stoke equations with a Boussinesq approximation can be cast into the parabolic conservation law form [62].

$$L(\{Q\}) = \frac{\partial\{Q\}}{\partial t^*} + \frac{\partial}{\partial x_j^*}\left(\{f_j\} - \{f_j^v\}\right) - \{s\} = \{O\} \tag{3-1}$$

where, the state variable is

$$\{Q\} = \{Q(x_i^*, t^*)\} = \left\{u_1^*,\ u_2^*,\ u_3^*,\ \Theta^*\right\}^T$$

and

$$\{f_j\} = \left\{u_1^* u_j^* + \frac{1}{Eu}\frac{p^*}{\rho^*}\delta_{1j},\ u_2^* u_j^* + \frac{1}{Eu}\frac{p^*}{\rho^*}\delta_{2j},\ u_3^* u_j^* + \frac{1}{Eu}\frac{p^*}{\rho^*}\delta_{3j},\ u_j^*\Theta^*\right\}^T$$

$$\{f_j^v\} = \left\{\frac{\nu^*}{Re}\frac{\partial u_1^*}{\partial x_j^*},\ \frac{\nu^*}{Re}\frac{\partial u_2^*}{\partial x_j^*},\ \frac{\nu^*}{Re}\frac{\partial u_3^*}{\partial x_j^*},\ \frac{\alpha^*}{Pe}\frac{\partial\Theta^*}{\partial x_j^*}\right\}^T$$

$$\{s\} = \left\{0,\ -\frac{Gr}{Re^2}\beta^*\Theta^* g_2,\ 0,\ -\frac{1}{Bo}\left(\frac{\partial \dot{q}_{rj}^{*'''}}{\partial x_j^*} - \frac{\dot{q}^{*'''}}{\rho^* c_p^*}\right)\right\}^T$$

The pertinent thermal-radiative definitions are

$$Bo \equiv \frac{\rho_o c_{p,o} u_o \Delta T_o}{\sigma (\Delta T_o)^4} \; ; \quad \Theta^* \equiv \frac{T - T_{\min}}{T_{\max} - T_{\min}} \; ; \quad \Delta T_o \equiv T_{\max} - T_{\min} \; ; \quad \dot{q}''_{r,o} \equiv \sigma (\Delta T_o)^4 \; ; \quad \dot{q}'''_o \equiv \frac{\dot{q}''_{r,o}}{L_o}$$

The other dimensionless parameters and groups are listed in the Nomenclature.

Solutions of Eqn (3-1) must be constrained by the incompressibility condition of a solenoidal velocity vector field as discussed in Chapter Two, namely,

$$\frac{\partial u_j^*}{\partial x_j^*} = 0 \tag{3-2}$$

This requirement is handled in the present study via the algorithm of Williams [62] as implemented in *AKCESS*.*. Included therein is an accompanying segregated Poisson equation for the genuine pressure field

$$L(p^*) = \frac{\partial}{\partial x_i^*}\left(\frac{\partial p^*}{\partial x_i^*} + u_j^* \frac{\partial u_i^*}{\partial x_j^*} - \frac{\partial}{\partial x_j}\left(\frac{\nu^*}{Re}\left(\frac{\partial u_i^*}{\partial x_j^*} + \frac{\partial u_j^*}{\partial x_i^*}\right)\right) + \frac{Gr}{Re^2}\beta^*\Theta^* g_i^*\right) = 0 \tag{3-3}$$

for evaluating the pressure term in $\{f_j\}$. $\{Q\}$, $\{f_j\}$ and $\{f_j^v\}$ are the state variable and the kinematic flux and viscous flux vectors, respectively, while $\{s\}$ denotes the source term.

For simplicity, the assumption of constant fluid and thermophysical properties has been made. Although allowing variable density is beyond the scope of this research, the impact of this feature could be scrutinized in a future work. For example, with or without a Boussinesq approximation, Bell, et al [64] admit finite-amplitude density variations, necessitating an additional degree of freedom accompanied by a fifth state variable, ρ^*.

3.2 The Finite Element CFD Algorithm

Stemming from variational calculus, tensor field theory and linear algebra, finite-element CFD methods are deemed to be among the most versatile and powerful algorithms. There are some advantages of finite-element methods over other CFD methods. First, "free" natural boundary conditions are readily provided to handle Neumann (or flux) boundary conditions. Second, although only rectangular domains are considered here, finite-element methods appear the best discretizing candidates for handling highly irregular geometries. Lastly, finite-element methods can naturally incorporate higher-order polynomial trial functions, or other innovative, improved interpolation functions, to handle more challenging problems concerning numerical accuracy, stability and convergence. However, other CFD methods have some advantages over finite-element methods, e.g., simpler discretizing formulations and computer coding. Treatments of finite-element CFD methods can be found in the text written by Baker [65].

The specific projection method used to enforce the continuity equation in the adopted finite-element CFD code, *AKCESS.** [66], is based on Williams' [63] Continuity Constraint Method. The essence of finite-element CFD discretization is briefly discussed. The solution to Eqn (3-1) can be approximated by the Galerkin Weak Statement (GWS^h).

$$(3\text{-}4) \qquad GWS^h = \bigcup_{e=1}^{e=M} \left(\int_{\Omega_e} \Psi_i \left(\frac{\partial N}{\partial t^*} \{Q\} - N\{s\} \right) d\Omega_e - \int_{\Omega_e} \frac{\partial \Psi_i}{\partial x_j^*} \left(N \{f_j\} - N \{f_j^v\} \right) d\Omega_e \right)$$

$$+ \bigcup_{e=1}^{e=M} \left(\oint_{\partial\Omega_e \cap \partial\Omega} \Psi_i \left(N \{f_j\} - N \{f_j^v\} \right) n_j d\sigma_{\partial\Omega} \right) = \{O\} \qquad , \qquad j \le i \le N$$

and,

$$\{Q\}=\{Q(x_i^*,t^*)\}\approx\{Q^h(x_i^*,t^*)\}=\bigcup_{e=1}^{e=M}\{Q_e(x_i^*,t^*)\} \quad ; \quad \{Q(x_i^*,t^*)\}_e\equiv\{N(\eta_i)\}^T\{Q(t^*)\}_e$$

Green's theorem has been applied to project the divergence operator from the flux vectors, $\{f_j\}$ and $\{f_j^v\}$, onto the approximation (global) trial space, Ψ_i, and to produce the closed surface integral in Eqn (3-4); namely, the *natural* boundary condition in the *GWS*^{h}.

3.2.1 Discretization of Divergence of Radiative Flux Vector

The divergence of radiative flux vector of the 4-th component of the source-term vector, s_4, in Eqn (3-4), can be decomposed into two partial derivatives:

$$-\Psi_i\,(Ns_4) = -\Psi_i\frac{\partial\left(N\dot{q}_{r,j}^{*''}\right)}{\partial x_j^*} = \left(N\dot{q}_{r,j}^{*''}\right)\frac{\partial\Psi_i}{\partial x_j^*} - \frac{\partial}{\partial x_j^*}\left[\Psi_i\left(N\dot{q}_{r,j}^{*''}\right)\right] \tag{3-5}$$

At the elemental level, the first term on the right-handed side of Eqn (3-5) becomes

$$\int_{\Omega_e}\frac{\partial\Psi_i}{\partial x_j^*}\left(N\dot{q}_{r,j}^{*''}\right)d\Omega_e\equiv\int_{\Omega_{e,gas}}\Psi_i\frac{\partial\left(N\dot{q}_{rg,j}^{*''}\right)}{\partial x_j^*}d\Omega_e \tag{3-6}$$

The left-hand side of Eqn (3-6) is equivalent to an elemental gas volume integral associated with components of the viscous flux vector of Eqn (3-4). By invoking the Gaussian theorem, the second partial derivative of the right-hand side of Eqn (3-5) becomes

$$(3\text{-}7) \qquad -\int_{\Omega_e}\frac{\partial}{\partial x_j^*}\left(\Psi_i\, N\, \dot{q}^{*''}_{rg,j}\right)d\Omega_e = -\oint_{\partial\Omega_e\cap\partial\Omega}\Psi_i\, N\, \dot{q}^{*''}_{rs,j}\, n_j d\sigma_{\partial\Omega_e}$$

which is the *radiative* natural boundary condition in Eqn (3-4).

3.2.2 Finite Element Matrix Statement

The finite-element method uses a spatial semi-discretization, Ω^h, of the continuum domain Ω, made up of the union of a set of non-overlapping subdomains Ω_e or finite elements. As shown in Eqn (3-4), $\{Q\}\equiv\{Q(t^*)\}$ is the array of the state variable approximation coefficients at the geometric nodes of Ω^h. In the Galerkin method, the global trial space becomes an expression on Ω_e in the form $\Psi_i=N_i\equiv N$, where N_i is a polynomial of degree k in the finite-element basis set. The assembled global matrix statement for Eqn (3-4) results in the following first-order nonlinear matrix equation:

$$(3\text{-}8) \qquad GWS^h = [M]\frac{d\{Q\}}{dt^*} + \{R(\{Q\})\} = \{O\}$$

$[M]$ and $\{R\}$ are a global rank square matrix and a "residual" column matrix. $\{R\}$ is a nonlinear function of $\{Q\}$, and contains contributions from all terms in Eqn (3-4) except the temporal term, i.e., convection, diffusion, source and boundary conditions. Using the θ-implicit, one-step Euler or Crank-Nicolson temporal discretization, the terminal algebraic statement using Eqn (3-8) is

$$(3\text{-}9) \qquad \{FQ\} = [M]\left(\{Q_{n+1}\}-\{Q_n\}\right) + \Delta t^*\left(\theta\{R\}_{n+1} + (1-\theta)\{R\}_n\right) = \{O\}$$

Finally, a quasi-Newton iterative algorithm is used to solve Eqn (3-9). The basic statement for this nonlinear matrix solutions process is

$$[J]^{p}_{n+1}\{\delta Q\}^{p+1}_{n+1} = -\{FQ\}^{p}_{n+1} \tag{3-10}$$

$$\{Q\}^{p+1}_{n+1} = \{Q\}^{p}_{n+1} + \{\delta Q\}^{p+1}_{n+1}$$

where,

$$[J] \equiv \left[M + \theta\Delta t \cdot \frac{\partial\{R\}}{\partial\{Q\}}\right]$$

$$\{Q\}^{0}_{n+1} = \{Q\}_{n} \quad ; \quad \{FQ\}^{0}_{n+1} = \{FQ\}_{n}$$

Subscript n denotes the time station, and superscript p denotes the iteration step. Quasi-Newton approximations depend on the simplification of the Jacobian matrix, $[J]$. This algorithm clearly demonstrates the legitimacy of calculating the radiation field at the next time station based on the temperature field of the current time station. Thus, the radiation and temperature fields as well as other scalar fields are coupled, despite the absence of the RTE.

Other aspects of the selected finite element algorithm regarding element formulations, continuity enforcement, control of dispersion error, numerical accuracy and convergence and stability, and linear algebra can be found in [62,63,65,66] or references cited therein.

3.3 Participating Thermal Radiation Submodel

Complete derivations of the RTE are fully discussed in many standard texts on thermal radiation, c.f. [51,67-69]. Hence, the theory is not repeated here. It is considered that Naraghi's, et al [60,61] *Source-Function* approach is the clever method for producing

an efficient numerical algorithm for handling most practical participating radiation engineering problems. Based on [60,61], the following set of dimensional "radiosity"-type discretization equations have been modified and generically coded for the two and three dimensional simulations in this research. In the interior gas domain, the discretized vector of the divergence of radiative flux is

$$(3\text{-}11) \qquad \frac{\partial \dot{q}''_{g,\,ik}}{\partial x_k} = 4(1-\omega_o)K_t\left(E_{bg,\,i} - \sum_{j=1}^{N_s} R_{s,\,j}\,\overline{dg_i s_j} - \sum_{j=1}^{N_g} R_{g,\,j}\,\overline{dg_i g_j}\right) = 4K_t(R_i - G_i)$$

and on boundaries, the discretized *net* surface radiative flux vector is

$$(3\text{-}12) \qquad \dot{q}''_{s,\,ik}\,n_k = \varepsilon\left(E_{bs,\,i} - \sum_{j=1}^{N_s} R_{s,\,j}\,\overline{ds_i s_j} - \sum_{j=1}^{N_g} R_{g,\,j}\,\overline{ds_i g_j}\right) = R_i - G_i$$

Similarly, in the gas domain, the discretized gas radiosity is

$$(3\text{-}13) \qquad R_{g,\,i} - \omega_o\sum_{j=1}^{N_s} R_{s,\,j}\,\overline{dg_i s_j} - \omega_o\sum_{j=1}^{N_g} R_{g,\,j}\,\overline{dg_i g_j} = (1-\omega_o)E_{bg,\,i}$$

and on boundaries, the discretized surface radiosity is

$$(3\text{-}14) \qquad R_{s,\,i} - (1-\epsilon)\sum_{j=1}^{N_s} R_{s,\,j}\,\overline{ds_i s_j} - (1-\epsilon)\sum_{j=1}^{N_g} R_{s,\,j}\,\overline{ds_i g_j} = \epsilon E_{bs,\,i}$$

where,

$$\overline{dg_i s_j} = \frac{\cos\phi_i\,\cos\phi_j\,\tau\,dA}{4\pi|r|^2} \qquad\qquad \overline{dg_i g_j} = \frac{\cos\phi_i\,\cos\phi_j\,\tau\,K_t\,dV}{4\pi|r|^2}$$

$$\overline{ds_i s_j} = \frac{\cos\phi_i \cos\phi_j \, \tau \, dA}{\pi |r|^2} \qquad \overline{ds_i g_j} = \frac{\cos\phi_i \cos\phi_j \, \tau \, K_t \, dV}{\pi |r|^2}$$

$$\tau = \tau(r) = \tau(r(x_i, x_j)) = e^{-K_t |r(x_i, x_j)|}$$

Upon discretization, all the nodal or elemental radiative flux vectors in Eqns (3-11) and (3-12) become components of a second-rank tensor denoted by q_{ik}'' in the global domain. Subscripts *b*, *s* and *g* denote blackbody, surface (or boundary) and gas, respectively. For clarity, subscript *r* for radiation (versus conduction) has been dropped. In Eqns (3-11)-(3-14), subscript *i* specifically signifies the sending (or "from") node or element, and subscript *j* signifies the receiving (or "to") node or element, while subscript *k* denotes a dummy summation index. ϖ_o, K_t, τ and ε are the *i*-th nodal (or elemental) radiative properties for scattering albedo, total absorption coefficient, transmittance and emissivity, respectively. *R*, *E*, and *G* are vectors of radiosity, emissive power and irradiation (or irradiance). **r** denotes the distance vector between Nodes (or Elements) *i* and *j*. *dss*, *dsg*, *dgs* and *dgg* are the differential direct exchange factor matrices. For gas nodes, cos ϕ=1. *dA* and *dV* specifically refer to the discretized (or differential) surface area and volume of *j*-th node or element, respectively. n_k is the unit normal vector on boundaries.

In this research, the basic assumption is a gray, absorbing, emitting and non-scattering gaseous medium within a blackbody enclosure. Furthermore, for simplicity, $K_a=K_t=1.0$ m^{-1} (heptane pool fire [47]); $\varpi_o=K_s=0.$ m^{-1}; and $\varepsilon=1.0$, thereby crucially circumventing mass transfer equations for fire species (e.g. H_2O, CO_2, soot and other significant hydrocarbon and nitrous products), which are necessary for the enormous

computations of variable radiative properties. If incorporated, these equations would alarmingly add several degrees of freedom to Eqn (3-1), overwhelming most existing computing resources.

The issue of the dynamic layers of participating (hot) gas and non-participating (cold) gas can be resolved by comparing nodal or elemental temperatures among themselves. At any time step, if any gas node is "cold", then the entries of the differential exchange factor matrices associated with this node, whether be an originating or receiving node, are set to zero. The analyst can arbitrarily define such a "cold" temperature, say, $T=T_{min}=294.4$ K (70° F). While the coding effort to implement this feature and the cpu time for this *bubble searching* are nominal, the computations for the exchange factor matrices are extremely costly especially for three dimensions. For simplicity, the fire enclosure assumes a homogeneous participating medium. Hence, in this research, the matrices are computed at the initial time step only. It is recommended that a future study be conducted to investigate the validity of the assumption, or explore other viable alternatives of handling the moving interface between the hot and cold layers.

For non-scattering media and blackbody surfaces, nodal radiosities equal their own blackbody emissive powers, remarkably eradicating the time-consuming radiosity matrix equations, namely, Eqns (3-13) and (3-14). This observation is extremely important for three-dimensional simulations, otherwise, enormous computing time would be involved.

For non-participating media, the divergence of radiative flux vector vanishes; but the surface integral for the dot product of the inward unit normal vector and radiative flux becomes a non-zero Neumann boundary condition as shown in Eqn (3-12). This set of

equations of radiation discretization fits perfectly into finite-element CFD methodology taking advantage of natural boundary conditions as shown in the classical Galerkin Weak Statement [62] for approximating the solution to Eqn (3-4) as shown in the previous section. On the contrary, the direction of unit normal vector in Eqn (3-1) points outward. This subtle but important distinction is illustrated by an numerical example in the next chapter.

Eqns (3-11)-(3-14) implicitly assume one-point Gaussian quadrature for the irradiance vector. For better accuracy of the irradiance vector, or in case of irregular geometrical domains, higher-order numerical integration schemes would be necessary.

In CFD-radiation or pure radiation modeling, the following important rules apply within a closed radiation field.

$$\text{(3-15)} \qquad \sum_{j=1}^{N_s} \overline{dg_i s_j} + \sum_{j=1}^{N_t} \overline{dg_i g_j} \simeq 1.0 \quad ; \quad \sum_{j=1}^{N_t} \overline{ds_i g_j} + \sum_{j=1}^{N_s} \overline{ds_i s_j} \simeq 1.0$$

$$\text{(3-16)} \qquad \sum_{i=1}^{N_t} \frac{\partial \dot{q}''_{g,ik}}{\partial x_k} dV_i + \sum_{i=1}^{N_s} \dot{q}''_{s,ik}\, n_k\, dA_i \simeq 0$$

Although these two equations are not required for the computation of the divergence of radiative flux vector for gases and net radiative fluxes for boundary surfaces, these two equations are a critical tool for checking the integrity of any adopted radiation algorithm as well as the accuracy of the resultant numerical solutions.

3.4 Radiative Source (or Sink) Term Approach

In contrast to the reviewed literature [53-58] on CFD-radiation and possibly the

majority of related published work, the divergence of radiative flux vector, which is often discretized along with the conductive flux (diffusive term) as well as the convective term, has been extracted from the spatial gradient and becomes a legitimate "source" term in Eqn (3-1). Physically, it is a sink term in the energy equation. This salient advantage is twofold. First, it is adaptable to existing CFD methodologies virtually without modifications Second, it allows CFD-analysts to focus on selections or developments of numerically efficient and robust submodels exclusively for handling this source term. Theoretically, this source-term approach seems to fully or partially decouple the radiation field from the temperature field, which is *a priori* unknown and is required for the computation of the radiative source term. As discussed in the previous section, this deviation from the conventional approach does not present any difficulty, since, in practice, the known temperature field from the current time station is used to evaluate the radiation field of the next time station via an implicit Euler temporal scheme.

The bonus of this approach is the elimination of another degree of freedom for Eqn (3-1); namely, the state variable member for the RTE, at the expense of evaluating the radiative source term. Interestingly and coincidentally, Yucel's, et al [55] finite-difference iterative procedure, though employing an explicit RTE, is methodologically congruent to this approach, i.e., computing the radiative field for the new time station first via solutions of the RTE (a Poisson-type equation) solely based on the temperature field from the current time station.

This completes the scope of theoretical considerations leading to the developed and implemented model.

Chapter Four

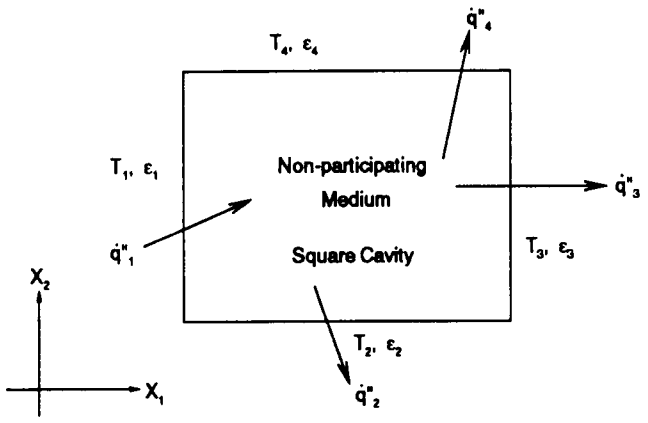
Results and Discussion

There are four main topics in this chapter. The first topic verifies the accuracy of a developed radiation submodel called Radflux, against closed form analytical solutions, which are basically limited to very simple non-participating cases, in addition to an one-dimensional participating slab. The second topic compares numerical results from Radflux with the test cases presented in the adopted radiation papers [60,61]. The third topic verifies the correct implementation of non-zero Neumann boundary conditions comprising conductive and radiative fluxes in a CFD domain. Finally, under a fundamental fire scenario, the third topic validates the CFD-Radiation fire simulations against a 2-zone PC fire model called FPETOOL [9] developed by NIST. It is the last topic that crucially determines the viability of incompressible laminar flows and the importance of thermal radiation for fire simulations. Finally, the relevance of fire damageability to this research and some numerical observations are discussed.

4.1 Verifications of Pure Radiation Submodel

There are three test cases. The first one is a two-dimensional non-participating medium. The second one is a three-dimensional non-participating medium. The third case is a one-dimensional participating slab.

4.1.1 2-D Non-Participating Square Cavity



T_1=1366.7 K (2000° F)

T_2=T_3=T_4=294.4 K (70° F)

ε_1=1.0

ε_2=ε_3=ε_4=0.5

L_1=L_2=L_3=L_4=1.0 m

Fig.1 2-D Verification Problem

Based on the Hottel's cross-string method [67], the symmetric view factor matrix for the problem defined in Fig. 1 is

$$F_{ij} = \begin{bmatrix} 0 & .29289 & .41421 & .29289 \\ .29289 & 0 & .29289 & .41421 \\ .41421 & .29289 & 0 & .29289 \\ .29289 & .41421 & .29289 & 0 \end{bmatrix} \tag{4-1}$$

By summing any row or column in Eqn (4-1), the summation rule in Eqn (3-15) is satisfied. Noting $R_i - \rho G_i = E_i$, $E_i = \varepsilon E_{b,i}$ and $G_i = R_j F_{ij}$, and invoking Kirchoff's Law, i.e., $\varepsilon = \alpha$ (implying $\rho = 1-\varepsilon$), the radiosity matrix equation is

$$\begin{bmatrix} 1 & -(1-\epsilon_1)F_{12} & -(1-\epsilon_1)F_{13} & -(1-\epsilon_1)F_{14} \\ -(1-\epsilon_2)F_{21} & 1 & -(1-\epsilon_2)F_{23} & -(1-\epsilon_2)F_{24} \\ -(1-\epsilon_3)F_{31} & -(1-\epsilon_3)F_{32} & 1 & -(1-\epsilon_3)F_{34} \\ -(1-\epsilon_4)F_{41} & -(1-\epsilon_4)F_{42} & -(1-\epsilon_4)F_{43} & 1 \end{bmatrix} \begin{Bmatrix} R_1 \\ R_2 \\ R_3 \\ R_4 \end{Bmatrix} = \begin{Bmatrix} \epsilon_1 E_{b,1} \\ \epsilon_2 E_{b,2} \\ \epsilon_3 E_{b,3} \\ \epsilon_4 E_{b,4} \end{Bmatrix} \tag{4-2}$$

Finally, defining $E_{b,i} \equiv \sigma(\Delta T_i)^4$ and $\Delta T_i \equiv T_i - T_{min}$ along with other parameters defined in Fig.1 and noting $q_i'' = R_i - G_i$, the solutions of radiosity, irradiation and *net* radiative flux are

$$(4\text{-}3)\qquad \begin{Bmatrix} R_1 \\ R_2 \\ R_3 \\ R_4 \end{Bmatrix} = \begin{Bmatrix} 74.96 \\ 17.63 \\ 20.61 \\ 17.63 \end{Bmatrix} \frac{kW}{m^2} \quad ; \quad \begin{Bmatrix} G_1 \\ G_2 \\ G_3 \\ G_4 \end{Bmatrix} = \begin{Bmatrix} 18.82 \\ 35.26 \\ 41.22 \\ 35.26 \end{Bmatrix} \frac{kW}{m^2} \quad ; \quad \begin{Bmatrix} \dot{q}_1'' \\ \dot{q}_2'' \\ \dot{q}_3'' \\ \dot{q}_4'' \end{Bmatrix} = \begin{Bmatrix} 56.14 \\ -17.63 \\ -20.61 \\ -17.63 \end{Bmatrix} \frac{kW}{m^2}$$

By thermodynamics convention, the direction of heat flow (hence the sign of heat rate) is positive when heat is transferred from the environment into the system. Conversely, for the opposite direction of heat flow, the sign of heat rate is negative. This convention stems from the First Law of Thermodynamics. Based on the signs of net radiative fluxes in Eqn (4-3), the directions of heat flow in Fig. 1 have been correctly assumed by physical reasoning. Observing that directions of unit normal vectors on boundaries for the pure radiation and CFD fields are directly opposite, as shown in Fig. 2, n_k in Eqn (3-12) for computing the boundary radiative in the CFD field can be problematic. The best way to resolve this issue is to negate <u>all</u> the signs of the calculated fluxes in Eqn (4-3) prior to sending them to the CFD computation. Mathematically, the resultant "scalar" n_k can be derived by taking the nodal dot products between the radiation and CFD fields. For example, for Side 1, $\{1,0\}^T_{rad} \bullet \{-1,0\}^T_{CFD} = -1$.

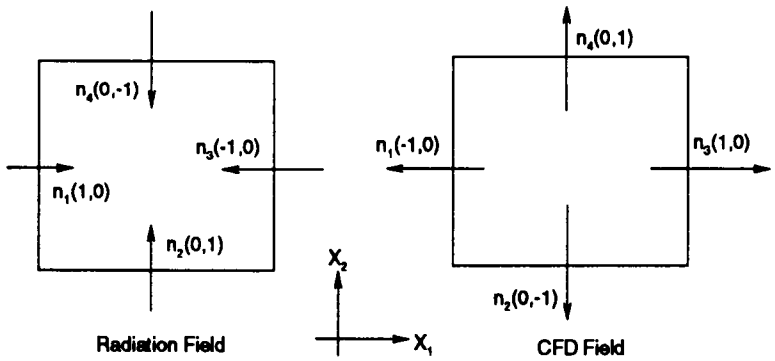


Fig. 2 Designations of Boundary Normal Vectors

In the CFD field, a negative heat of a node or an element implies that the heat is being transferred from this node to the remaining nodes in the domain. Conversely, the node receives heat from the rest of the domain or a source, resulting in a temperature increase.

In this test case, a one element mesh was used. The net radiative flux vector computed in Radflux is $\{56.07, -17.67, -20.70, -17.67\}^T$ kW/m^2. Compared with the analytical solution in Eqn (4-3), the numerical results generated by Radflux are slightly different due to decimal places used in the view factors. The analytical solution was truncated at five decimal places, whereas the latter carried sixteen significant figures via double precison on a 64-bit workstation.

The net *radiative* heat rate of the cavity is 1.E-10 kW, which satisfies Eqn (3-16).

4.1.2 3-D Non-Participating Cube

Similar to the two-dimensional test case, the three-dimensional test problem is defined as follows. T_1=1366.7 K, T_2=T_3=T_4=T_5=T_6=294.4 K. ε_1=1.0, ε_2=ε_3=ε_4=ε_5=ε_6=0.5. L=W=H=1.0 m. By symmetry, the resultant view factors [68] are: F_{ij}=0.2 if i≠j; F_{ij}=0. if i=j. Finally, the analytical solutions are

$$(4\text{-}4)\quad \begin{Bmatrix} R_1 \\ R_2 \\ R_3 \\ R_4 \\ R_5 \\ R_6 \end{Bmatrix} = \begin{Bmatrix} 74.96 \\ 12.49 \\ 12.49 \\ 12.49 \\ 12.49 \\ 12.49 \end{Bmatrix} \frac{kW}{m^2} \quad ; \quad \begin{Bmatrix} G_1 \\ G_2 \\ G_3 \\ G_4 \\ G_5 \\ G_6 \end{Bmatrix} = \begin{Bmatrix} 12.49 \\ 24.98 \\ 24.98 \\ 24.98 \\ 24.98 \\ 24.98 \end{Bmatrix} \frac{kW}{m^2} \quad ; \quad \begin{Bmatrix} \dot{q}_1'' \\ \dot{q}_2'' \\ \dot{q}_3'' \\ \dot{q}_4'' \\ \dot{q}_5'' \\ \dot{q}_6'' \end{Bmatrix} = \begin{Bmatrix} 62.47 \\ -12.49 \\ -12.49 \\ -12.49 \\ -12.49 \\ -12.49 \end{Bmatrix} \frac{kW}{m^2}$$

The three-dimensional mesh is 2x2x2 elements. The numerical solutions, computed at centroidal nodes of the six surfaces by Radflux are

$$(4\text{-}5)\qquad \begin{Bmatrix} R_1 \\ R_2 \\ R_3 \\ R_4 \\ R_5 \\ R_6 \end{Bmatrix} = \begin{Bmatrix} 74.96 \\ 14.73 \\ 14.73 \\ 14.73 \\ 14.73 \\ 18.35 \end{Bmatrix} \frac{kW}{m^2} \quad ; \quad \begin{Bmatrix} G_1 \\ G_2 \\ G_3 \\ G_4 \\ G_5 \\ G_6 \end{Bmatrix} = \begin{Bmatrix} 12.50 \\ 29.47 \\ 29.47 \\ 29.47 \\ 29.47 \\ 36.70 \end{Bmatrix} \frac{kW}{m^2} \quad ; \quad \begin{Bmatrix} \dot{q}_1'' \\ \dot{q}_2'' \\ \dot{q}_3'' \\ \dot{q}_4'' \\ \dot{q}_5'' \\ \dot{q}_6'' \end{Bmatrix} = \begin{Bmatrix} 62.46 \\ -14.74 \\ -14.74 \\ -14.74 \\ -14.74 \\ -18.35 \end{Bmatrix} \frac{kW}{m^2}$$

Quantitatively, these numerical results, though not as accurate as those in the two-dimensional case, are comparable to the analytical results. The primary reason for the discrepancy is the impact of the coarse mesh on view factor calculations. In the 2-D case, a closed-form view factor formula, i.e., cross-string method, is coded, reproducing the "exact" view factors regardless of the mesh density. In 3-D cases, a similar closed-form formula is not available. Thus, the *dss* formula in Eqn (3-14) must be used, setting τ=1.0. As discussed in Chapter 3, the accuracy of one-point Gaussian quadrature heavily depends on the quality (density) of mesh. However, in this particular case, it is inappropriate to increase the mesh, since the problem definition would change, resulting in a very different set of analytical solutions.

As a result, there is a significant imbalance of heat rate of -13.8 kW within the enclosure, compared with the total heat input of 62.4 kW. For dense grids, Eqns (3-15) and (3-16) are well satisfied. For example, for a mesh of 6x6x6 elements, the heat rate imbalance is substantially reduced to -0.08 kW.

4.1.3 1-D Participating Slab

It is impossible to have an analytical solution for a participating medium for two or three dimensions. Assuming a semi-infinite gray slab bounded by blackbody surfaces, and K_a=1.0 m^{-1} and K_s=0. m^{-1}, the analytical results, based on the solution of linear nonhomogeneous Fredholm integral equation derived by Brewster [71], are compared with the numerical results via Radflux in Table 1.

Table 1 Comparison of Analytical and Numerical Results for 1-D Participating Slab

Position, τ	Analytical	Radflux
0.17	0.68	0.65
0.33	0.58	0.58
0.50	0.50	0.51
0.67	0.40	0.44
0.83	0.35	0.40

Since the intent of this exercise is to verify the accuracy of *two* and *three* dimensions of Radflux for a participating medium, and there is no one dimensional version in Radflux, a mesh of 6x6x6 elements has been selected. The slab coordinate is a normalized optical thickness, τ, ranging from zero to unity. The results are dimensionless temperatures based on normalized blackbody emissive powers of gas nodes located at the centroidal points of the seven vertical planes. The dimensionless Dirichlet temperatures of the first (hot) plane and the last (cold) plane are unity and zero, respectively. These results show that Radflux produces good correlations with the analytical results for the participating case.

4.2 Pure Radiation Benchmark Comparisons

There are two test cases in this section. The first comparison is a two-dimensional problem based on [60], and the other is a three-dimensional problem based on [61].

4.2.1 2-D Participating Square Cavity

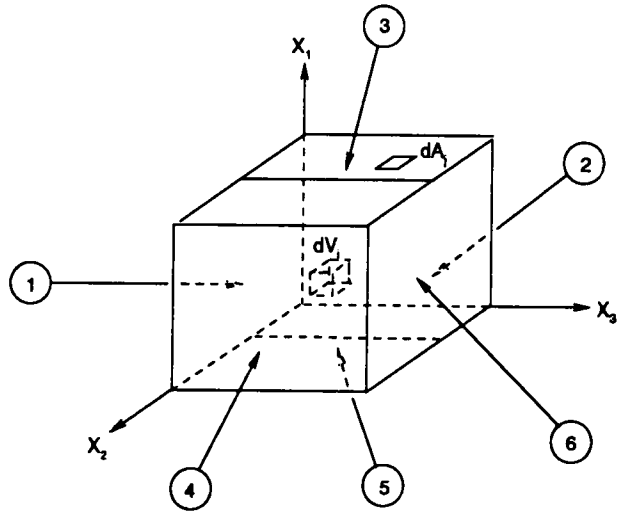
With reference to Fig. 1, the problem is redefined as follows. Optical thickness≡ $L_1=L_2=1$, $K_a=K_t=1.0$ m^{-1}, and $\varpi_o=0.$ implying $K_s=0.$ m^{-1}. $E_1^*=1.0$, $E_2^*=E_3^*=E_4^*=0.0625$, $E_i^*=E_i/E_o$, where $E_o\equiv\sigma(\Delta T_o)^4$ and $\Delta T_o\equiv T_{max} - T_{min}=(1366.7-294.4)$ K=1072.3 K, with $\varepsilon_i=1.0$. Thus, $E_o=79.4$ kW/m^2 and $E_2=4.7$ kW/m^2. The mesh is 6x6 elements. The comparison of dimensionless blackbody emissive power along the horizontal centerline between the pair of hot and cold walls is summarized in Table 2.

Table 2 Comparison of 2-D Participating Cavity Dimensionless Emissive Power for Radflux and Benchmark Results

Position	E_g, kW/m^2	Radflux	Benchmark
0.25	85.5	0.43	0.43
0.50	49.1	0.24	0.28
0.75	25.8	0.16	0.18

Radflux is in good agreement with the benchmark case [60]. It is estimated that the discrepancies are due to a better Gaussian quadrature algorithm adopted by Naraghi, et al [60] in computing the benchmark. The net heat rate of this enclosure is approximately 2.0 kW, compared with a total heat input of 74.96 kW, a nominal 3% error.

4.2.2 3-D Participating Cube



$L_1=L_2=L_3=1$ m

$E_1^*=E_2^*=E_3^*=1.0$

$E_4^*=E_5^*=E_6^*=0.$

$K_t=1.0\ m^{-1}$, $\varpi_o=0.75$

$\varepsilon_i=1.0$

$q_g''/E_o=4$, $E_o=74.96\ kW/m^2$

Fig.3 3-D Benchmark Cube

The problem is defined in Fig. 3. As shown in Table 3, results of dimensionless centerline gas temperatures from Radflux correlate well with the benchmark solutions [61]. The heat rate imbalance of the enclosure is less than 0.5 kW, compared with a total heat generation of 299.84 kW. The mesh again is 6x6x6 elements. Overall, these results of correlation with the available benchmarks are considered excellent.

Table 3 Comparison of 3-D Participating Cube of Radflux and Benchmark Results

Position, m	E_g, kW/m^2	Θ^*, Radflux	Θ^*, Benchmark
0.167	409.8	1.529	1.515
0.333	414.3	1.533	1.516
0.500	409.9	1.529	1.513
0.667	398.2	1.518	1.503
0.833	375.7	1.496	1.485

4.3 CFD-Radiation Implementation

There are two parts in this benchmarking process; namely, two- and three-dimensional cases. Each part consists of seven test cases to methodically verify the correct implementation of both conductive and radiative fluxes on boundaries for a CFD benchmark problem, the "thermal cavity". Choice of this problem did create non-dimensionalization problems as discussed herein. For clarity, all tabular scalar fields including radiation are contained in the appendices.

It is deemed this process was absolutely necessary in this research, due to the lack of an appropriate thermal cavity benchmark for CFD with radiation. This leads to a very important issue concerning dimensionless convective and radiative groups.

4.3.1 Dimensionless Fluid and Heat Transfer Parameters

Several research groups have performed CFD-radiation benchmark cases. Reproducing their results proved impossible, however, since none of these papers reported all necessary reference or characteristic parameters. It is also suspected that their dimensionless fluid and heat transfer groups are not entirely consistent.

Yucel, et al [55] did not report dimensional reference parameters such as T_{max}, T_{min}, L_o, and Reynolds number, which was implied to be unity. Their test case, though simple, is not reproducible. Draoui, et al [57] and Shih, et al [72] did not mention any dimensional reference values.

Fusegi, et al [56] had reported all dimensional characteristic parameters; however, the Reynolds number was not explicitly stated. Similar to this research, their work had

encountered the problematic issue of non-dimensionalization. First, though *freely* selected at users' discretion, a reference length of 0.11 m is unrealistic for any practical fire simulation. If a realistic reference length is selected (say, 3 m), then for Ra=4.5E6, $\Delta T_o/T_o$=5.16E-5 which has no meaningful application. It is evident that the authors traded a realistic length scale for a meaningful temperature difference. The paper was intended for fire simulations but was confined to CFD-radiation analysis only.

It is concluded that although the well publicized thermal cavity serves as an excellent tool for benchmarking from the CFD numerical standpoint, it is not suitable for any *actual* engineering application due to the impractical temperature difference resulting from the unit length scale for representative laminar flow Ra number. This is based on the observation that, for most purely convective engineering problems without the effects of fire and radiation, Rayleigh number would predominantly fall in the order of E10 or larger for common engineering fluids such as air, whereupon the flow would be turbulent. The real issue is that the non-dimensional Ra-scaling is vital to the CFD benchmarking, leading to *inadvertent* negligence of the consistency with realistic engineering data. Moreover, it is believed that all referenced results are based on the unit length scale except Fusegi's, et al benchmark [56]. Using a small reference length scale (hence a reasonable ΔT_o) has caused serious numerical problems with the standard CFD benchmark, hence also in this research. In summary, for a *practical* benchmark definition, the current CFD benchmark *usually* requires unit length scale precluding a high Ra number (i.e., E10 or higher) without employing a turbulence model.

The second inconsistency in Fusegi's et al [56] paper is that the thermophysical

properties are actually based on air as a "fire" gas at T_o=555 K in lieu of an assumed CO_2-H_2O-soot mixture. Based on the same temperature and the corresponding saturated vapor pressure, Ra=1.38E7 for pure CO_2 and Ra=5.5E10 for H_2O. In reality, the fire plume and gas layer contain a mixture of fire species and "hot" air, while the cold layer contains pure air only.

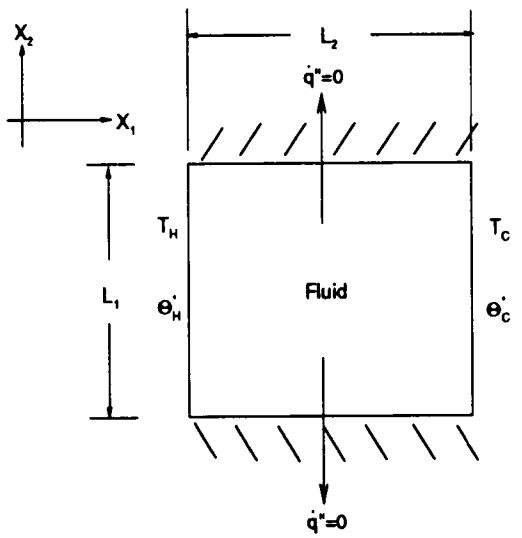
Therefore, it is exceedingly challenging to model a realistic fire scenario with Ra=3.1E10, Re=2.1E5, Gr=4.4E5, Pe=1.5E6, assuming Pr=0.7 and $Ar=Gr/Re^2=1$. Realistic fluid-thermal reference parameters are α_o=125E-6, m^2/s, ν_o=88E-6 m^2/s, k_o=58E-6 kW/m^2, ρ_o=0.42 kg/m^3, L_o=3 m, T_{max}=1366.7 K and T_{min}=294.4 K, based on pure air at normal pressure. As a result, ΔT_o=1072.3 K, T_o=830.6 K, U_o=6.16 m/s, t_o=0.48 s, and $p_o=\rho_o U_o^2$=16 Pa. Most importantly, Bo=40.65.

For CFD comparative purposes, the thermal cavity benchmark uses an unit length scale and a modest Rayleigh number, Ra≤1.E7. Hence, to accomplish the goal of this research, it was concluded that a dual dimensionless system would be necessary, one for the fluid and the other for the radiation (and fire). In a purely convective CFD analysis, this issue is not relevant as long as the unit reference length, hence the concomitant miniscule temperature difference, is not needed for interpreting with physical data. However, for CFD-radiation analysis, these reference parameters along with other fluid dimensionless groups must be determined or defined prior to selecting the Bo number. Otherwise, ΔT_o is essentially zero, thereby eradicating the entire radiative term in the energy equation since Bo becomes infinite. Hence, Bo=40.65 is used throughout the entire analysis, regardless of values of Ra and Re numbers selected for the benchmark

purpose, and of course, for the fire simulations in this research.

4.3.2 2-D CFD-Radiation Test Cases

Since the purpose is to verify the CFD-radiation implementation from the coding standpoint, the following set of dimensionless groups were selected: Ra=1.E4, Gr=1.4E4, Re=120, Ar=1, Pe=83.6, L_o=1 m, T_o=294.4 K, $\Delta T_o/T_o$=3.46E-6, Pr=0.7, ρ_o=1.16 kg/m^3, ν_o=15.89E-6 m^2/s, α_o=22.5E-6 m^2/s, k_o=26.3E-6 kW/(m-K), U_o=1.9E-3 m/s, t_o=524.4 s, p_o=2.21E-3 Pa, K_i=1.0 m^{-1}, K_s=0. m^{-1}, ε_i=1.0 and Bo=40.65. Except for the Bo number, all defined parameters are consistent with the dimensionless groups stated in Eqn (3-1). However, as far as the input is concerned, only Re, Ar, Pe and Bo are needed.



$L_o=L_1=L_2$=1 m

$T_H=T_o+\Delta T_o$

$T_C=T_o$

Θ_H^*=1.0 (hot wall)

Θ_C^*=0. (cold wall)

Fig. 4 Standard 2-D Thermal Cavity

Case 1 is the 2-D steady-state solution for the standard thermal cavity CFD benchmark as shown in Fig. 4, which serves as the baseline for the subsequent analyses. The mesh is 16x16 elements. The graphical solution is shown in Fig. 5 and the details

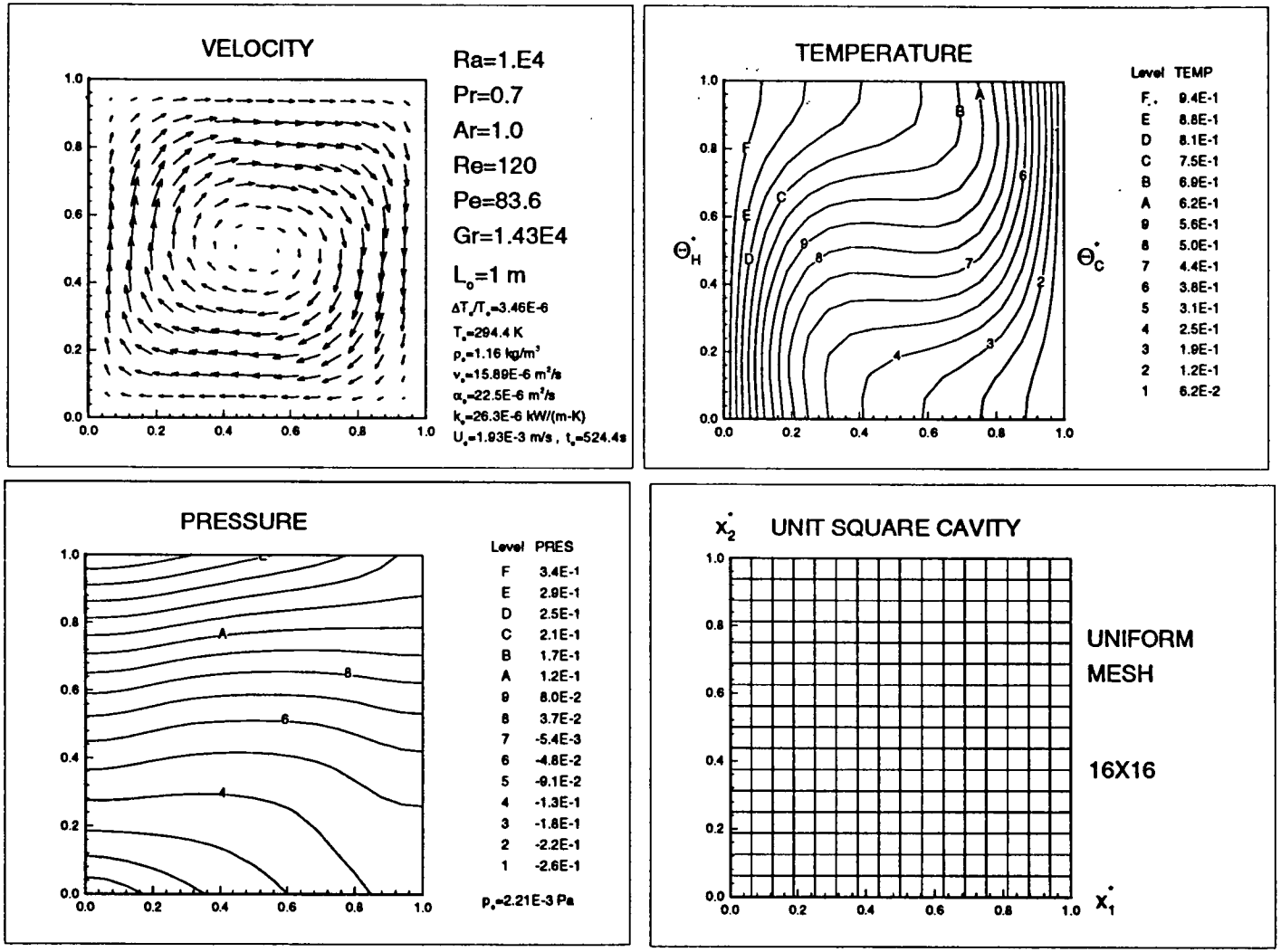


Fig. 5 2-D Steady State Solutions of Standard Thermal Cavity, Ra=1.E4, Case 1

of the computed dimensionless scalar fields are summarized in Appendix A.1. These results reproduced past experience, and were compared with [63] and found numerically accurate for the present purpose.

Due to the unavailability of *reproducible* CFD-radiation benchmark, Cases 2 - 6 are specifically designed to establish a referential CFD-radiation benchmark for this research, hence examining the radiative effects on the hot and cold wall temperature distribution of the cavity:

(1) Case 2: 2-D Ad Hoc Benchmark Baseline, Conductive Fluxes;

(2) Case 3: 2-D Conductive and Radiative Fluxes, Non-Participating Medium, ε=1.0;

(3) Case 4: 2-D Conductive and Radiative Fluxes, Non-Participating Medium, ε=0.1;

(4) Case 5: 2-D Conductive and Radiative Fluxes, Participating Medium, ε=1.0; and

(5) Case 6: 2-D Conductive and Radiative Fluxes, Participating Medium, ε=0.1

Both the conductive and radiative fluxes constitute a non-zero Neumann boundary condition. The following is the protocol for this verification process. First, the conductive fluxes at the hot and cold are computed, based on the converged temperature field of Case 1. The calculated conductive fluxes then replace the hot and cold Dirichlet temperature boundary conditions with non-zero Neumann boundary conditions, namely, the calculated conductive fluxes. Theoretically, since the conductive fluxes are estimated by the steady-state temperature field, the replacement *should* allow the original hot and cold wall temperatures to remain nominally held. If this step is verified, then the calculated conductive fluxes can be legitimately served as a baseline for comparisons of computed wall temperatures as a result of various types of radiative fluxes.

Using the resultant temperature profile from Case 1 and Eqn (4-6), all boundary conductive fluxes can be approximately computed, based on the Fourier Law and a 3-point backward second-order finite difference formula in Eqn (4-6) and Fig. 6, and Case 1 gas nodal temperatures normal to the boundaries.

$$(4\text{-}6) \qquad \frac{\partial \Theta_w^*}{\partial x_j^*} \simeq \frac{\Theta_{w+2}^* + \Theta_{w+1}^* - 2\Theta_w^*}{2\Delta n_1^* + \Delta n_2^*}$$

$$\dot{q}_{c,j}^{*''} n_j = -\frac{1}{Pe}\frac{\partial \Theta_w^*}{\partial x_j^*} n_j$$

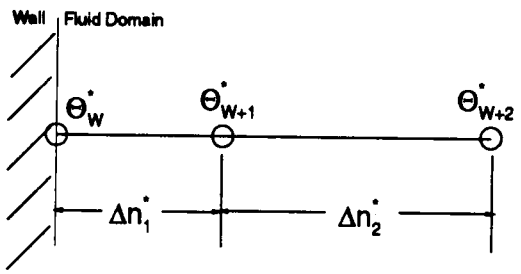


Fig.6 3-Point Backward Finite Difference Algorithm

Subscripts w, w+1 and w+2 denote wall, immediate off-wall and the second off-wall nodes. n denotes the discretized dimensionless length normal to the wall node.

Cases 2 - 6 compute the new wall temperature distribution at one time step after the replacement of Dirichlet wall temperatures with various types of dimensionless Neumann boundary conditions. The resultant computed temperature fields are summarized in A.2-A.6 of Appendix A, respectively. Additionally, the computed wall temperature distributions are summarized in Figures 7 and 8.

A number of observations have been made during this process. First, in Case 2, the hot wall temperature ranges from 0.955 to 0.991 and the cold wall temperature ranges from 0.008 to 0.044. Thus, the wall temperatures are reasonably close within 5% to the original Dirichlet values, qualifying the computed conductive fluxes as the baseline for the comparison of different kinds of radiative fluxes.

Second, the distribution of purely conductive fluxes is diagonally symmetrical in

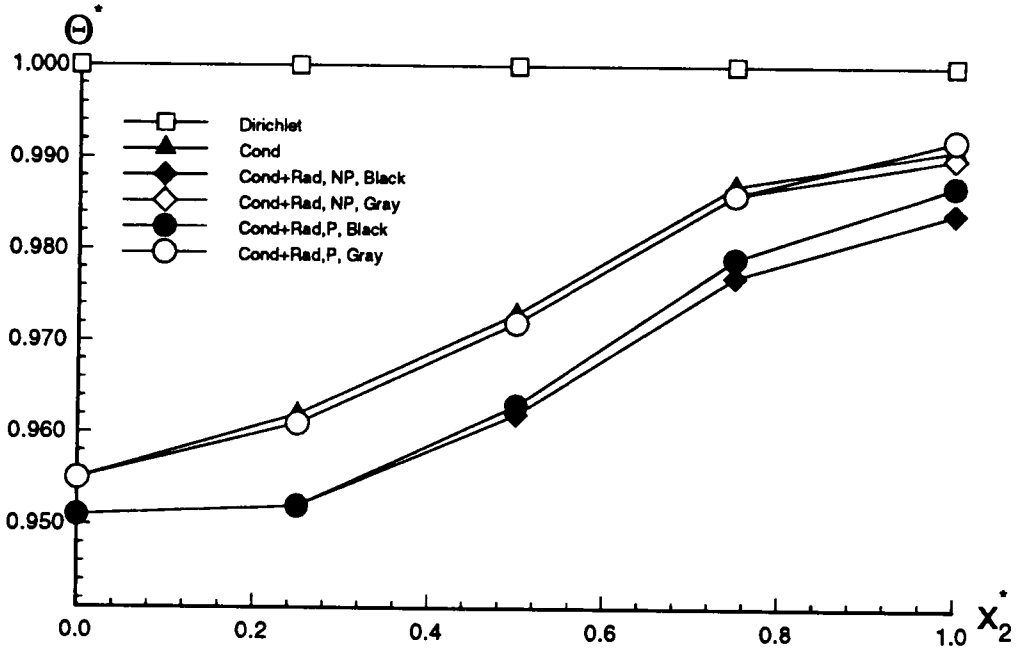


Fig. 7 2-D Hot Wall Temperatures

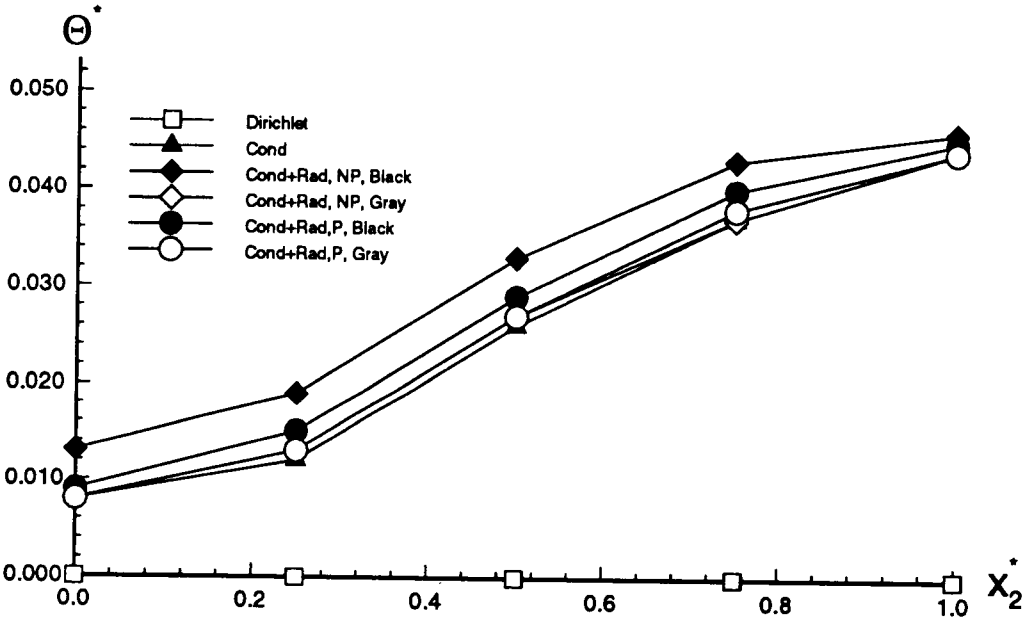


Fig. 8 2-D Cold Wall Temperatures

magnitude but opposite in sign, thus obeying the First Law of Thermodynamics. When either of the vertical walls increases its *positive* flux in the radiation field, which is equivalent to the decrease of the *positive* flux in the CFD field, the wall temperature decreases. Conversely, the wall temperature increases when either wall decreases its positive flux. This important observation is entirely consistent with comparisons among the above cases, as well as the theory discussed in Section 4.1.1. For example, on the hot wall at x_2^*=0.5, Θ^*=0.973 for the baseline conductive flux (Case 2). When the flux increases slightly in Case 3, the nodal temperature (Θ^*) at the same location decreases to 0.962. Conversely, on the cold wall at x_2^*=0.5, Θ^* increases from 0.026 to 0.033 as a result of a slight decrease of heat flux. This observation is summarized in Table 4, where cond and NP denote conductive and non-participating cases, respectively.

Table 4 Summary of 2-D Mid-Wall (x_2^*=0.5) Fluxes and Temperatures

Flux	q_H''	Θ_H^*	q_C''	Θ_C^*
cond	278.E-4	0.973	-278.E-4	0.026
NP	220.E-4	0.962	-138.E-4	0.033

Another observation is the effect of emissivity. For non-participating media, the *magnitude* of radiative flux is directly proportional to the emissivity. As a result, the radiative fluxes decrease at the hot wall and increase at the cold wall. This phenomenon is indeed reflected in Cases 3 and 4 (Tables 6 and 7). Based on the previous observation, the hot wall temperature increases and the cold wall temperature decreases. For example,

the mid-wall radiative fluxes and temperatures are summarized in Table 5.

Table 5 Summary of 2-D Mid-Wall (x_2^*=0.5) NP Radiative Fluxes and Temperatures

ε	$q_{r,H}''$	Θ_H^*	$q_{r,C}''$	Θ_C^*
1.0	220.E-4	0.962	-338.E-4	0.033
0.1	161.E-4	0.972	-93.E-4	0.027

Likewise, Table 6 summarizes the same type of data for the participating medium.

Table 6 Summary of 2-D Mid-Wall (x_2^*=0.5) Participating Fluxes and Temperatures

ε	$q_{r,H}''$	Θ_H^*	$q_{r,C}''$	Θ_C^*
1.0	195.E-4	0.963	-53.E-4	0.029
0.1	45.E-4	0.972	-108.E-4	0.027

Again, when the *positive* fluxes increase, the corresponding temperatures decrease. Furthermore, the participating effect is substantial at the cold wall only when all the walls are blackbody. When the emissivities are very low, the participating effect is significant at the hot wall only.

The fourth observation is that despite the problematic dimensionless issues discussed in Section 4.3.1, the dimensionless conductive and radiative fluxes are comparable. Lastly, in Appendix A.5, the radiative "source" field vividly depicts the buoyant plume (or the radiative *neutral* interface) along the vertical, hot wall and the

ceiling. The heat rate imbalance in this case is less than 1 kW out of the total heat rate input of 74 kW from the hot wall.

Two additional cases for the participating thermal cavity have been performed:

(1) Case 7 - 2-D Steady State Solutions of a Participating Thermal Cavity, Fluid Ra=1.E4, Mesh=16x16; and

(2) Case 8 - 2-D Steady State Solutions of a Participating Thermal Cavity, Fluid Ra=1.E4, Mesh=32x32.

Summary data for the solutions are graphed in Figures 9 and 10. Their companion scalar fields are summarized in A.7 and A.8 of Appendix A. The purpose of Case 8 is to conduct an accuracy study via mesh refinement by doubling the mesh of Case 7. The predicted numerical results are practically identical. For example, in both cases, the centroidal temperatures are identical, i.e., 0.72. Additionally, it is noted that u_1^* equals 0.090 and 0.088 for Cases 7 and 8 at the center of the ceiling, respectively.

Compared with Case 1, the overall temperature profile of Case 7 dramatically increases. For example, in the middle of the cavity, the purely convective temperature is 0.49, whereas the participating medium temperature is 0.72. This observation confirms the qualitative (or intuitive) theory that the gas temperature profile would increase for a participating medium, presuming that the absorbing effect overwhelms the emitting and scattering effects. However, under non-Dirichlet temperature boundary conditions (the hot Dirichlet boundary condition is a perpetual heat supply) and different heat sources (finite heat supplies such as combustion or fire), the CFD-radiation fire simulation does

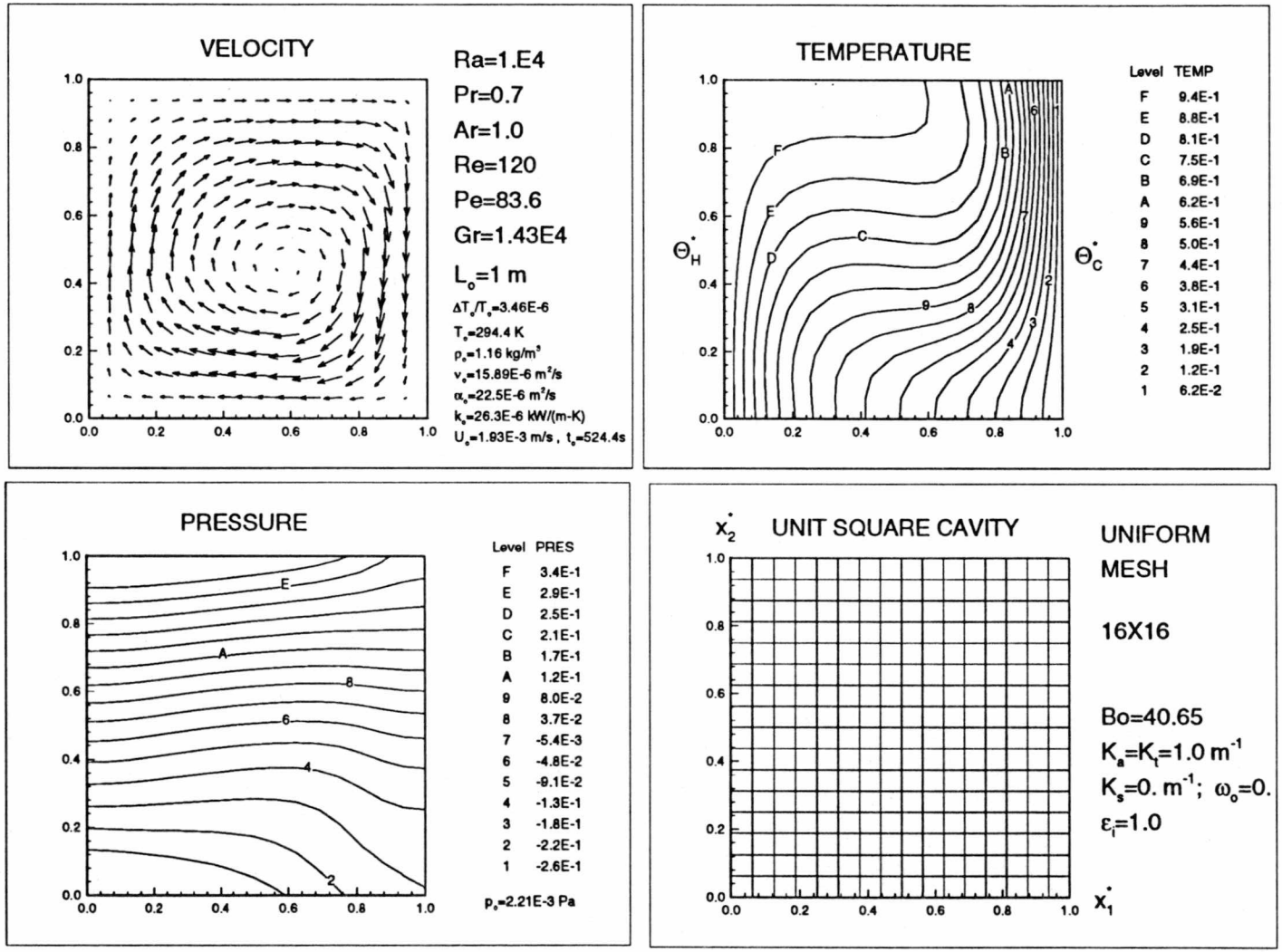


Fig. 9 2-D Steady State Solutions of Participating Thermal Cavity, Ra=1.E4, Case 7

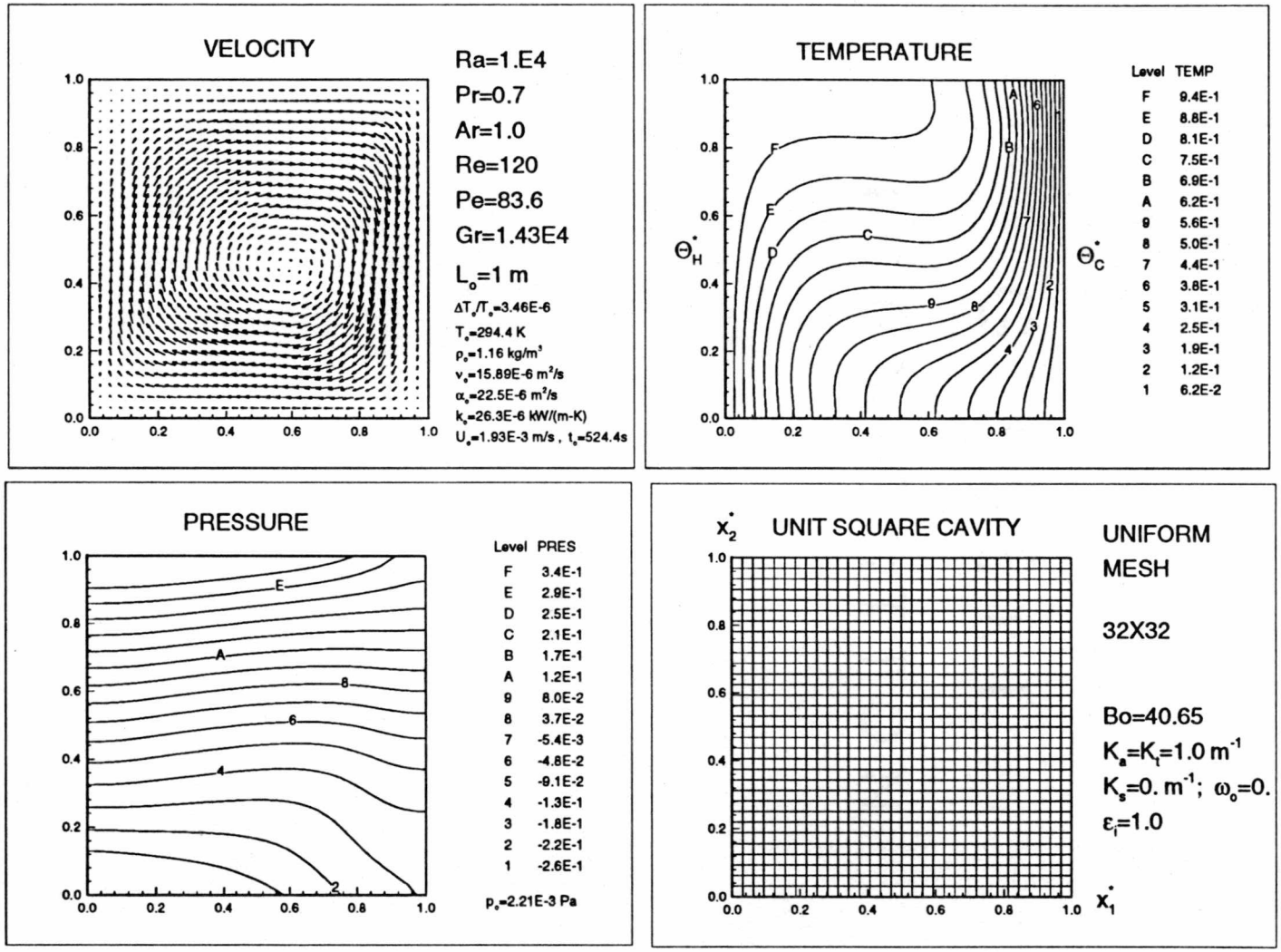


Fig. 10 Accuracy Study of 2-D Steady Participating Thermal Cavity, Ra=1.E4, Case 8

not necessarily manifest the similarly profound effect. This crucial effect will be further studied later in this chapter. The imbalance of the total radiative heat transfer rate inside the cavity is approximately -1.8 kW, compared with the total heat rate input of 74 kW.

In addition, it is noted that the velocities moderately decrease and increase along the hot and cold walls, respectively, as a result of participating medium definition. For example, at the middle of the hot wall, u_2^*=0.195 and 0.135 for Cases 1 and 7, respectively. At the middle of the cold wall, u_2^*=-0.195 and -0.242, respectively. Likewise, the ceiling velocity decreases and the floor velocity increases as a result of the participating medium. For example, in the middle of the ceiling, u_1^*=0.123 and 0.09 for Case 1 and 7, respectively. In the middle of the floor, u_1^*=-0.123 and -0.141, respectively. Due to the participating medium, the velocity profile no longer maintains its symmetry in the middle of the cavity as shown in Figures 9 and 10.

4.3.3 3-D CFD-Radiation Test Cases

In this subsection, the six test cases for two dimensions are repeated in three dimensions. The purpose of this exercise is to *verify* the three-dimensional CFD-radiation implementation, and compare with the two-dimensional results. For the same fluid and heat transfer parameters of the two dimensional cases, the three-dimensional test cases are:

(1) Case 9 - 3-D Steady State Solutions of Standard Thermal Cavity, Ra=1.E4;

(2) Case 10 - 3-D Ad Hoc Benchmark Baseline Conductive Fluxes;

(3) Case 11- 3-D Conductive and Radiative fluxes, Non-Participating Medium, ε=1.0;

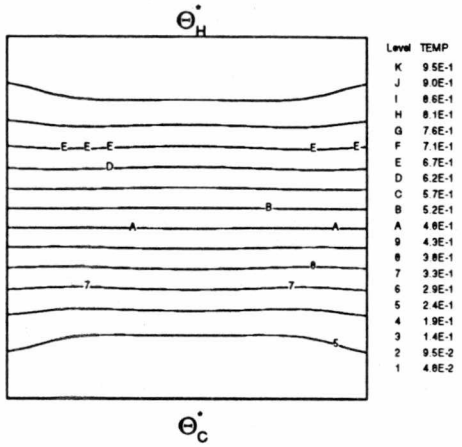
(4) Case 12- 3-D Conductive and Radiative fluxes, Non-Participating Medium, ε=0.1;

(5) Case 13- 3-D Conductive and Radiative fluxes, Participating Medium, ε=1.0; and

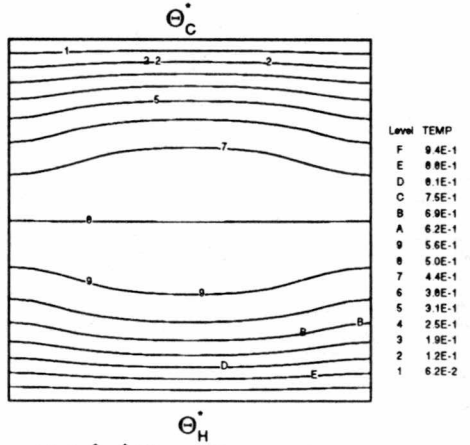
(6) Case 14- 3-D Conductive and Radiative fluxes, Participating Medium, ε=0.1;

With reference to Fig. 3 in Section 4.2.2, surfaces 1 and 6 are the hot and cold walls, respectively. Surfaces 2-5 are the adiabatic walls. The graphical steady state solutions of the standard convective thermal cavity of Case 9 are shown in Fig. 11. In order to meaningfully compare with two dimensional results, all three-dimensional results are based on the mid-plane of x_1^* and x_2^* coordinates. Since there are 17 *vertical* planes in the print fields, Plane 9 would be the mid-plane. Appendices B.1-B.6 summarize the numerical results for Cases 9-14, respectively. Overall, results of these seven three-dimensional cases are comparable with their corresponding two-dimensional counterparts. The uniform mesh is 16x16x16 elements.

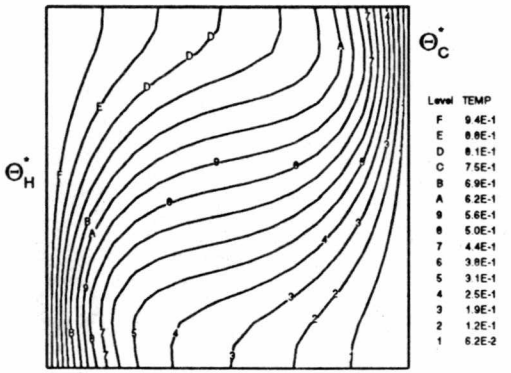
In Case 9, the velocity components are comparable as shown in Figures 5 and 11, and Appendices A.1 and B.1. For example, in the middle of ceiling, u_1^*=0.123 and 0.154 for the two and three dimensional convective (standard) cavities, respectively. In the middle of the hot wall, u_2^*=0.195 and 0.134, respectively. Finally, for the centroidal temperature, both cases equal 0.49. Therefore, the temperature field is acceptable for computing various types of flux in Cases 10-14. Moreover, it is interesting to note that u_3^* is highly symmetrical at the mid-plane of x_1^* and x_2^* coordinates (Plane 9). For example, Plane 8 is the "mirror" of Plane 10, except their signs are reversed, implying the opposite directions of the "paired" velocity components.



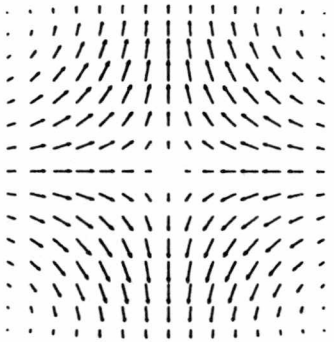
Mid x_3^*-x_2^* Plane Temperature



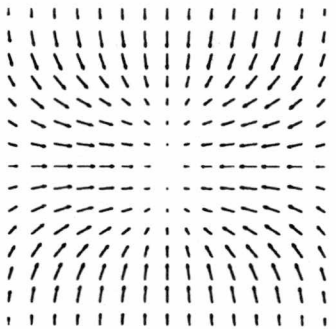
Mid x_1^*-x_3^* Plane Temperature



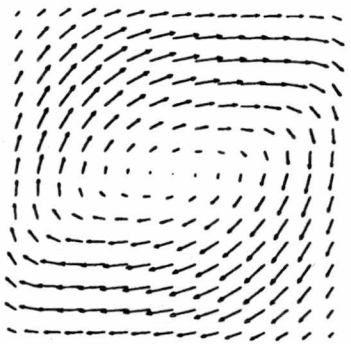
Mid x_1^*-x_2^* Plane Temperature



Mid x_3^*-x_2^* Plane Velocity



Mid x_1^*-x_3^* Plane Velocity



Mid x_1^*-x_2^* Plane Velocity

Fig.11 3-D steady State Solutions of Standard Thermal Cavity, Fluid Ra=1.E4, Case 9

In this particular three dimensional *rectangular* problem, Eqn (4-6) for calculating the boundary conductive fluxes still applies. For non-rectangular domains and non-Cartesian coordinates, Eqn (4-6) must be modified to account for nodal temperatures near the boundary element, which do not necessarily align with the unit normal vector.

Analogous to Figures 7 and 8, Figures 12 and 13 summarize the hot and cold wall temperatures of Plane 9. For the hot wall, the three dimensional temperature ranges from 0.945 to 0.995, whereas the two dimensional temperature ranges from 0.950 to 0.993. For the cold wall, the three dimensional temperature ranges from 0.004 to 0.056, whereas the two dimensional temperature ranges from 0.008 to 0.046. Unlike the monotonically increasing two dimensional temperature slopes, the three dimensional temperature profiles have significant concavities near the top of the wall. The encouraging observation is that in both dimensionalities, the pattern of curves are identical. For the hot wall, the descending order of temperature curves is: conductive, gray participating, gray non-participating, participating blackbody and non-participating blackbody. The descending order for the cold wall is exactly reverse.

To numerically compare with the two dimensional mid-wall temperatures in Tables 4-6, Tables 7 summarizes all the three dimensional mid-wall temperatures.

Table 7 Summary of 3-D Mid-Wall (x_2^*=0.5) Fluxes and Temperatures (Plane 9)

Flux Type	q_H''	Θ_H^*	q_C''	Θ_C^*
cond	237.E-4	0.977	-237.E-4	0.022
NP, ε=1.0	207.E-4	0.967	-96.E-4	0.027
NP, ε=0.1	182.E-4	0.976	-68.E-4	0.023
P, ε=1.0	190.E-4	0.968	-46.E-4	0.024
P, ε=0.1	190.E-4	0.976	-31.E-4	0.022

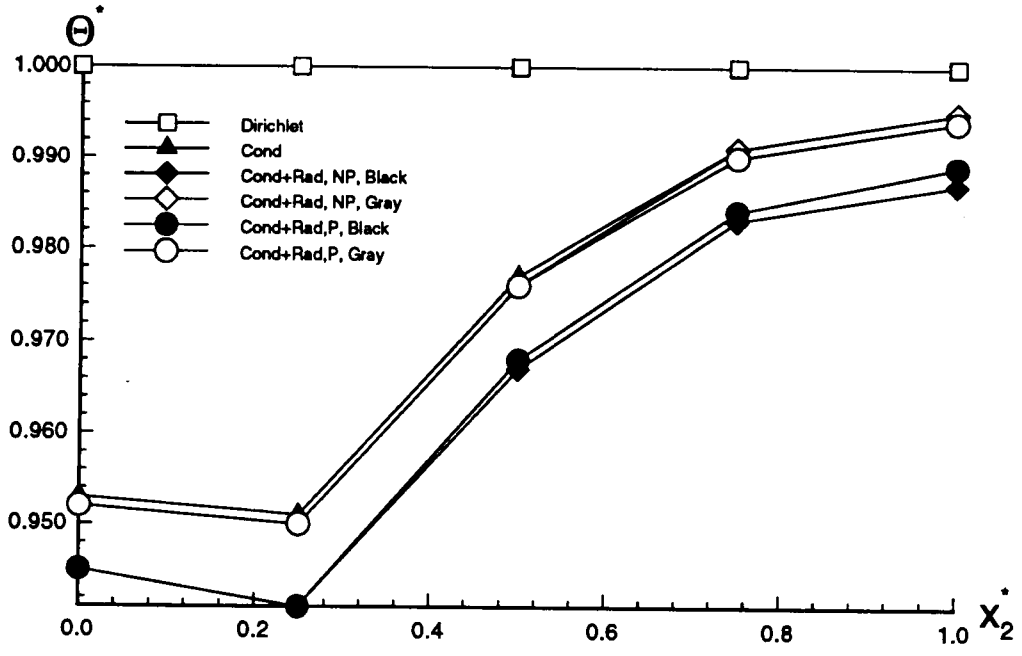


Fig. 12 3-D Hot Wall Temperatures

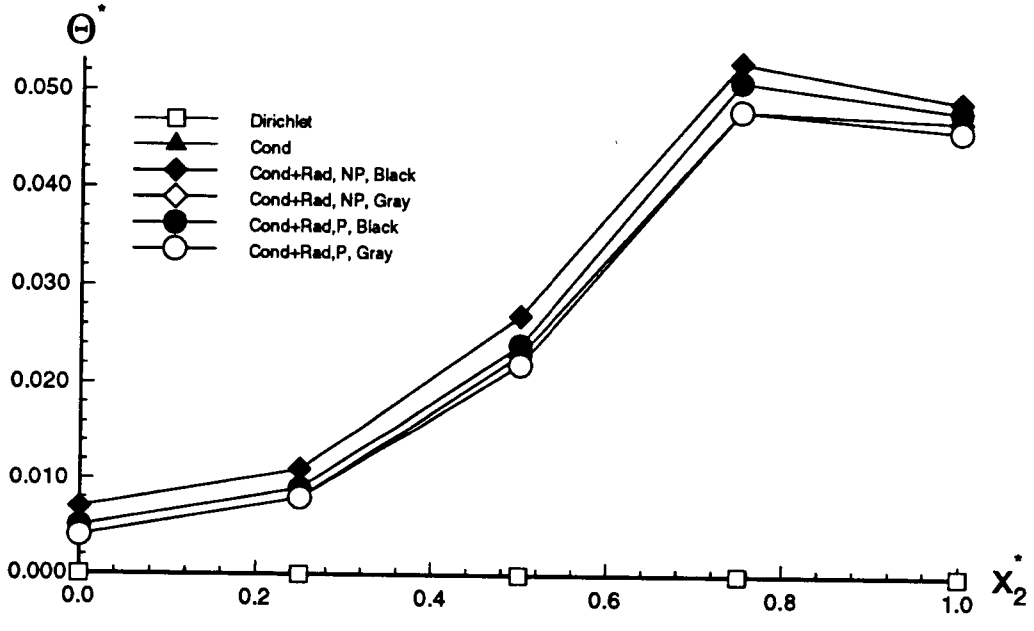


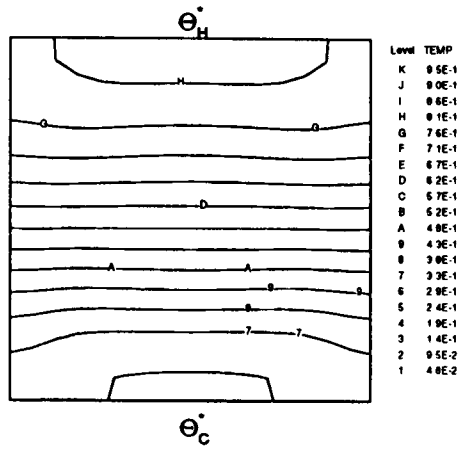
Fig. 13 3-D Cold Wall Temperatures

Again, cond, NP and P denote conductive, non-participating and participating cases. These results correlate well with Tables 4-6. Thus, the implementation of three dimensional CFD-radiation has been verified.

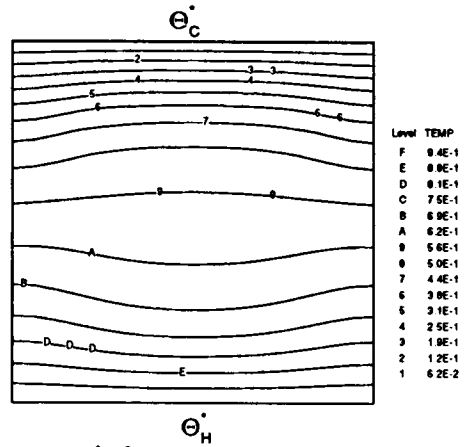
The last case in this subsection is Case 15, 3-D Steady State Solution of a Participating Thermal Cavity, Fluid Ra=1.E4, Mesh=16x16. The graphical solutions are summarized in Figure 14, and the numerical solutions are summarized in Appendix B.6. Compared with solutions of Case 9, Appendix B.1, the three dimensional participating thermal case only moderately impacts the scalar fields. Using the previous examples for the two dimensional caparisons, the ceiling velocity (u_1^*) equals 0.160 and 0.154 for the participating and non-participating cases. The mid-hot wall velocity (u_2^*) equals 0.138 and 0.134, respectively. The mid-cold wall velocity equals -0.143 and -0.133, respectively. The significant difference in terms of velocity profile is that the participating case is no longer symmetrical in the center of the cavity. In fact, similar to Figures 9 and 10, the "eye" of the vortex slightly shifts towards the bottom of the cold wall. For the u_3^* components, the "mirror" phenomenon still exists; however, the overall magnitude is slighter greater in the participating case. For example, near the center of the cavity, u_3^* equals 0.166 and 0.136, respectively.

The centroidal center temperature equals 0.58 in the participating case, compared with 0.49 of the two and three dimensional non-participating cases and 0.72 of the two dimensional participating case.

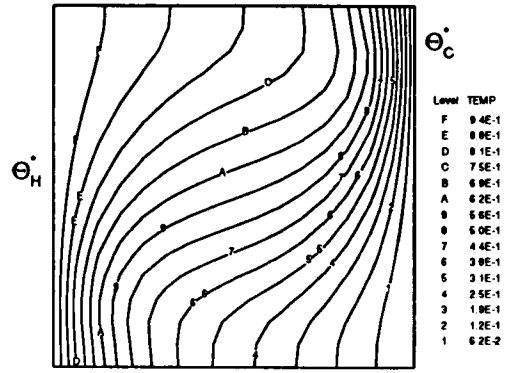
To compare with the radiation fields of the two and three dimensional participating cases, Tables 13 and 22 are used. The overall boundary radiative fluxes are comparable.



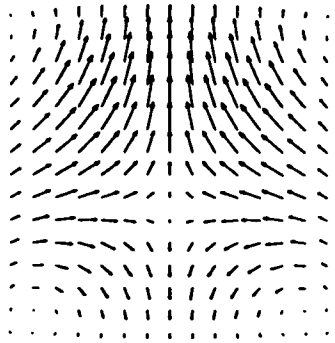
Mid x^*_3-x^*_2 Plane Temperature



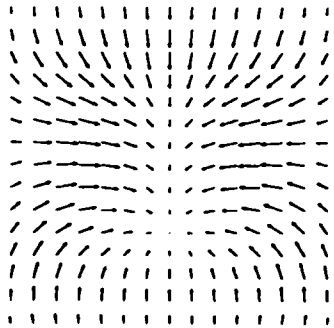
Mid x^*_1-x^*_3 Plane Temperature



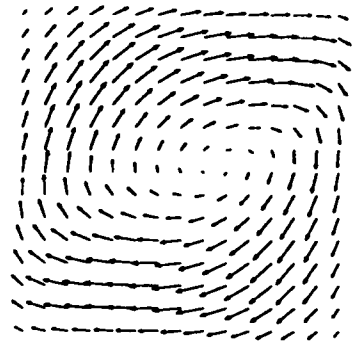
Mid x^*_1-x^*_2 Plane Temperature



Mid x^*_3-x^*_2 Plane Velocity



Mid x^*_1-x^*_3 Plane Velocity



Mid x^*_1-x^*_2 Plane Velocity

Fig.14 3-D steady State Solutions of Participating Thermal Cavity, Fluid Ra=1.E4

For example, the mid-hot wall fluxes (dimensionless) are 177.E-4 and 175.E-4 for two and three dimensional cases, respectively. The mid-cold wall fluxes are -53.E-4 and -49.E-4, respectively, However, the distributions of divergence of radiative fluxes are slightly different. First, in the two dimensional case, the positive radiative *sources* accumulate adjacent to the hot wall only, whereas the plume-like, positive sources distribute over the top of the hot wall as well as the large portion of the ceiling in the three dimensional case. The centroidal radiative *sink* equals -344.E-4 and -500.E-4 for the two and three dimensional cases, respectively.

4.3.4 3-D Discrete Exchange Factors and Accuracy Study

The crux of the developed thermal radiation submodel, Radflux, is the formulation and computations of the matrices for the four types of discrete exchange factor mentioned in Eqn (3-14).

In two dimensional cases, the effort is relatively minimal if the total number of nodes or elements is less than 1000. However, in any *practical* three dimensional problems, the mesh would normally equal or exceed 16x16x16 elements or 5000 nodes. Therefore, the *minimum* size of the global "view factor" matrix comprising the above four sub-matrices is [5000, 5000]. Such a humongous matrix presents two numerical challenges, namely, computational intensity and memory.

With respect to the computational intensity, the components of the four types of matrices are examined in Figure 15. The first determination is the three components of the distance vector, $\mathbf{r}(x_i^*, x_j^*)$, based on the nodal coordinates of i-th and j-th nodes. The

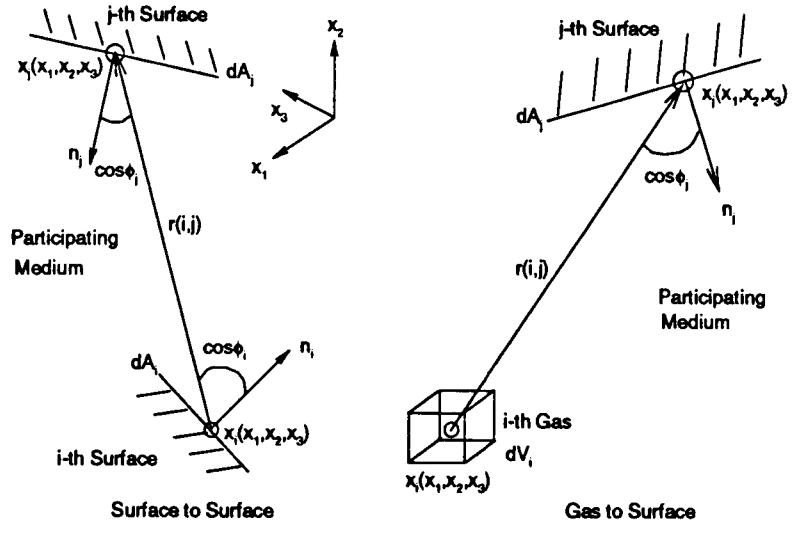


Fig. 15 Nomenclature of Generic Geometrical Discrete Exchange Factors

second determination is the three components of the boundary unit normal vector (note: the unit normal vector does not apply to a gas node or element). For rectangular domains, this determination is trivial, since there are only six predetermined unit normal vectors. If the domain can be reasonably described by a common curvilinear coordinate system such as cylindrical or spherical, the determination is still manageable since all the boundary unit normal vectors can be represented by a simple, closed-form analytical expression. However, for other irregular domains, three dimensional differential geometry analysis involving vectorial dot and cross products must be utilized. In that case, the computation can be very expensive.

The third determination is the differential or discretized boundary surface areas and interior gas volumes. Again, for *uniform, rectangular* domains, this task is trivial.

Otherwise, this can be complex and expensive even for a non-uniform Cartesian grid. The fourth determination is cos ϕ, which is equal to the dot product of the unit normal vector and the normalized distance vector. This task is computationally expensive. Finally, τ, an exponential function of the distance vector and the extinct coefficient, is also expensive.

The second challenge is computer memory. For the full-rank global matrix of [5000, 5000] alone, the required memories are 98 and 196 MBytes for single and double precision, respectively. However, due to the high degree of symmetry of the problem, both the computation and memory can be reduced by 50% or more. To take advantage of the symmetry, however, the submodel would be highly restrictive or require an enormous software development effort to accommodate the flexibility of symmetrical and non-symmetrical problems. Radflux does not incorporate this flexibility. To highlight some of the complexity of the global matrix, the primary subroutine for the view factor is excerpted in Appendix E.

It was intended to perform an accuracy study for the three dimensional steady state participating thermal cavity based on a doubling mesh, i.e., 32x32x32 elements. But this would require a view factor global matrix of [33^3, 33^3]=[35937, 35937] or 5.17 GBytes for single precision. Obviously, this computing requirement exceeds the available resources in this research. Therefore, it is recommended that a future study be performed to explore much more efficient algorithms based on simplified radiation models in conjunction with more effective and *compact* software developments to handle the three dimensional participating problems.

4.4 Fire Simulations

This section contains the results of a two- and a three-dimensional fire simulation based on an elementary fire scenario. The fire enclosure is a room measuring 3x3x3 m, similar to the standard ASTM (American Society of for Testing and Materials) fire test room. Since, in the inchoate stage of fire, heat transfer from the fire to the construction of a well insulated room is minimal, the wall temperature BCs are assumed adiabatic.

4.4.1 Dual Dimensionless Systems

As discussed in Sections 2.3.3 and 4.3.1, the dual dimensionless system is again used due to the constraint of moderate Rayleigh number and unit reference length. For the fluid system simulation state is fully specified via three parameters: Gr (or Ra), Re and Pe, assuming Pr=0.7, Ar=1.0 and Eu=1 (implying $p_o=\rho_o U_o^2$). If Ra is determined by selecting the implied parameters: T_{max}, T_{min}, L_o and ν_o, then Re and Pe are fixed accordingly. In the low and moderate ranges of Ra number, Bo would be approaching infinity as $\Delta T_o/T_o \approx 0$. While the *fluid* Ra number ranges from 1.E4 to 1.E6 for numerical reason, the Bo number is again set to 40.65. Table 8 summarizes the dual system.

For a genuine fire, there is of course only *one* reference system. In this CFD simulation, the physical interpretation of the dimensionless numerical results is based on the *fire* reference set. Hence, there is a subtle but very important implication. In calculating the dimensionless conductive flux based on Eqn (4-6), the Peclet number of the fluid system must be used. In contrast to the dimensionless radiative flux, which is calculated in a dimensional radiation field first, the dimensionless conductive flux is

Table 8 Fluid and Fire (or Radiation) Systems for Fluid and Heat Transfer Groups

Group	Fluid Ra=1.E4	Fluid Ra=1.E5	Fluid Ra=1.E6	Fire Ra=3.1E10
Explicit parameters:				
Pr	0.7	0.7	0.7	0.7
Gr	1.43E4	1.43E5	1.43E6	4.43E10
Ar	1.0	1.0	1.0	1.0
Re	120	378	1195	2.10E5
Pe	84	265	837	1.47E5
Bo	40.65(or $\approx\infty$)	40.65(or $\approx\infty$)	40.65(or $\approx\infty$)	40.65
Implied fluid or convective parameters:				
L_o, m	1.0	1.0	1.0	3.0
$\Delta T_o/T_o$	3.68E-7	3.68E-6	3.68E-5	1.291
T_{min}, K	294.4	294.4	294.4	294.4
T_{max}, K	294.4	294.4	294.4	1366.7
ΔT_o, K	$\approx$0.	$\approx$0.	$\approx$0.	1072.3
T_o, K	294.4	294.4	294.4	830.6
ν_o, m^2/s	15.89E-6	15.89E-6	15.89E-6	88.E-6
α_o, m^2/s	22.5E-6	22.5E-6	22.5E-6	125.E-6
k_o, kW/(m-K)	26.3E-6	26.3E-6	26.3E-6	58.E-6
$c_{p,o}$, kJ/(kg-K)	1.0	1.0	1.0	1.1
ρ_o, kg/m^3	1.16	1.16	1.16	0.42
U_o, m/s	1.9E-3	6.0E-3	1.9E-2	6.16
t_o, s	526.3	166.7	52.6	0.487
p_o, Pa	4.19E-6	4.19E-5	4.19E-4	15.94
Implied fire and radiation parameters:				
K_a, m^{-1}	1.0	1.0	1.0	1.0
K_s, m^{-1}	0.	0.	0.	0.
ϖ_o	0.	0.	0.	0.
ε	1.0	1.0	1.0	1.0
$q''_{c,o}$, kW/m^2	$\approx$0.	$\approx$0.	$\approx$0.	2.073E-2
$q''_{r,o}$, kW/m^2	$\approx$0.	$\approx$0.	$\approx$0.	74.96
q''_o, kW/m^2	$\approx$0.	$\approx$0.	$\approx$0.	3.05E3
$q'''_{f,o}$, kW/m^3	$\approx$0.	$\approx$0.	$\approx$0.	1.015E3

calculated from the dimensionless CFD field which senses the *fluid* Peclet number. However, to translate the dimensionless conductive fluxes into dimensional fluxes, the Peclet number of the fire system, or the common reference heat flux to both conduction and radiation, would be used. Noting $q''_{r,o} \equiv \sigma(\Delta T_o)^4 = 74.96$ kW/m^2, and $q''_{c,o} \equiv k_o \Delta T_o / L_o$ $= 2.1E\text{-}2$ kW/m^2, the common reference heat flux, $q''_o = \rho_o c_{p,o} U_o \Delta T_o = Pe(q''_{c,o}) = Bo(q''_{r,o})$ $= 3.05E3$ kW/m^2. Thus, $q''_c = q''_o(q''^*_c)$ and $q''_r = q''_o(q''^*_r)$.

The rationality of the dual dimensionless system is based on physical observations that the majority of the flow regime in the hot smoke layer outside the immediate vicinity of the fire plume is deemed quasi-laminar flow. Since the intent of this research is not to study the physicochemical phenomena of fire plume, this engineering improvisation is justified.

4.4.2 Fire Specifications

A small pool fire of 250 kW is located in the center of the room floor. The fire diameter and flame height are 0.2658 and 1.868 m, respectively. The flame height is estimated by the Heskestad (FMRC) correlation [73]: $h_f = -1.02D_f + 0.235Q_f^{0.4}$, where h_f, D_f and Q_f denote flame height, fire diameter and rate of heat release in meters and kW. To derive these geometrical parameters, heptane is assumed as the fuel package. Based on Babrauskas' experimental data [47], the "infinite" pyrolysis mass rate (mass flux) is 0.101 kg/(m^2-s) and the net heat of combustion is 44.6 MJ/kg. Finally, the base area of fire equals the rate of heat release divided by the product of the mass flux and heat of combustion. Coincidentally, the experimental $K_t \approx 1.1$ m^{-1}.

Assuming a right circular cylinder, the fire volume equals 0.1037 m^3. Consequently, the heat generation per unit volume, q_f''', equals 2411.4 kW/m^3 and subsequently, $q'''^*=(L_o/q''_{r,o})q_f'''=96.5$. This dimensionless fire source term would be normalized by the Boltzmann number for insertion into the CFD simulation (see Eqn (3-1)). Finally, $q'''^*=2.37$.

4.4.3 A 2-zone Model for Qualitative Check of Results

To establish a baseline for comparisons of results, the given fire scenario was simulated by FPETOOL [9], an experimentally validated 2-zone PC based model. At 15 seconds, the model predicts the hot smoke layer would be 2 m thick and the "average" temperature of the hot layer is approximately 400 K. This translates into $\Theta^*\approx 0.1$ at $t^*\approx 30$. Of course, in reality, the flame and the ceiling temperatures would be much higher than this layer temperature due to the shortcoming of a zone model.

The use of the zone model result in this research is not to estimate the accuracy of the CFD-generated solutions *vis-a-vis*, but instead to "qualitatively" serve as a reasonably physical check for the credibility of generated solutions of this innovative approach, which involves some unresolved, complex issues. For example, if the overall interpreted dimensional temperature resulting from a fire simulation is over 1000 K or less than 300 K for the same duration, then there exists some major fallacy in the formulation of the mathematical model, or the dual dimensionless system, or the fire specification, or any combination thereof, presuming the verified CFD-radiation code is correctly implemented.

4.4.4 2-D Room Fire

Based on the standard 16x16 mesh, the fire is characterized as a vertical single line consisting of 10 nodes starting at the floor. To compensate for the absence of three dimensionality, the dimensionless nodal fire sources is multiplied by a 3-D "coefficient", $C_{3D} \equiv W_f/L_3 \approx 0.0983$, where W_f ($\equiv V_f/A_f = 0.295$ m) is the equivalent depth of the fire in the z- or x_3-direction. Thus, the net dimensionless fire heat source is 0.233 per node. Based on $t^*=30$ ($t \approx 15$ s) and a closed unit square domain (i.e., $x_1^*=x_2^*=1$ and $L_1=L_2=3$ m) discretized in a 16x16 mesh (unless otherwise specified), the following two dimensional fire simulations have been executed:

(1) Case 16 - 2-D Fire Simulation, Pure Convection, Fluid Ra=1.E4;

(2) Case 17 - 2-D Fire Simulation, Convection and Radiation, Fluid Ra=1.E4;

(3) Case 18 - 2-D Fire Simulation, Pure Convection, Fluid Ra=1.E5;

(4) Case 19 - 2-D Fire Simulation, Convection and Radiation, Fluid Ra=1.E5;

(5) Case 20 - 2-D Fire Simulation, Pure Convection, Fluid Ra=1.E6;

(6) Case 21 - 2-D Fire Simulation, Convection and Radiation, Fluid Ra=1.E6;

(7) Case 22 - Accuracy Study of 2-D Fire Simulation, Fluid Ra=1.E6, Mesh=32x32; and

(8) Case 23 - 2-D Fire Simulation, Fluid Ra=1.E6, Small Opening, Mesh=32x16.

The word "fluid" used here for Rayleigh number is to emphasize the distinction between the fluid and fire Rayleigh numbers. In this fire scenario, the latter is always 3.1E10.

Figures 16-23 present the graphical solutions of Cases 16-23, respectively. Appendix C.1-C.7 summarize the respective numerical data of scalar and radiative fields.

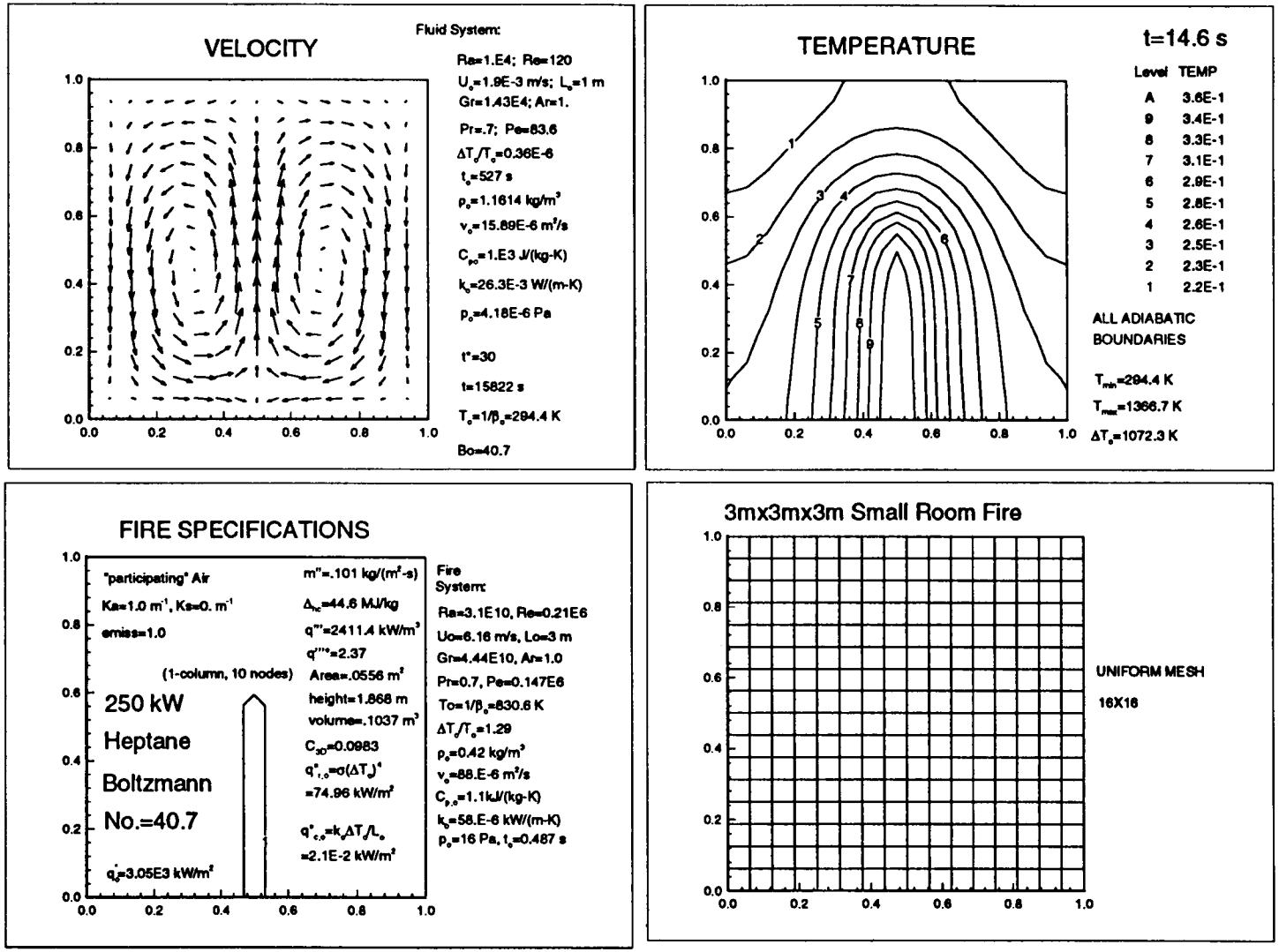


Fig. 16 2-D Fire Simulation, Pure Convection, Fluid Ra=1.E4, Case 16

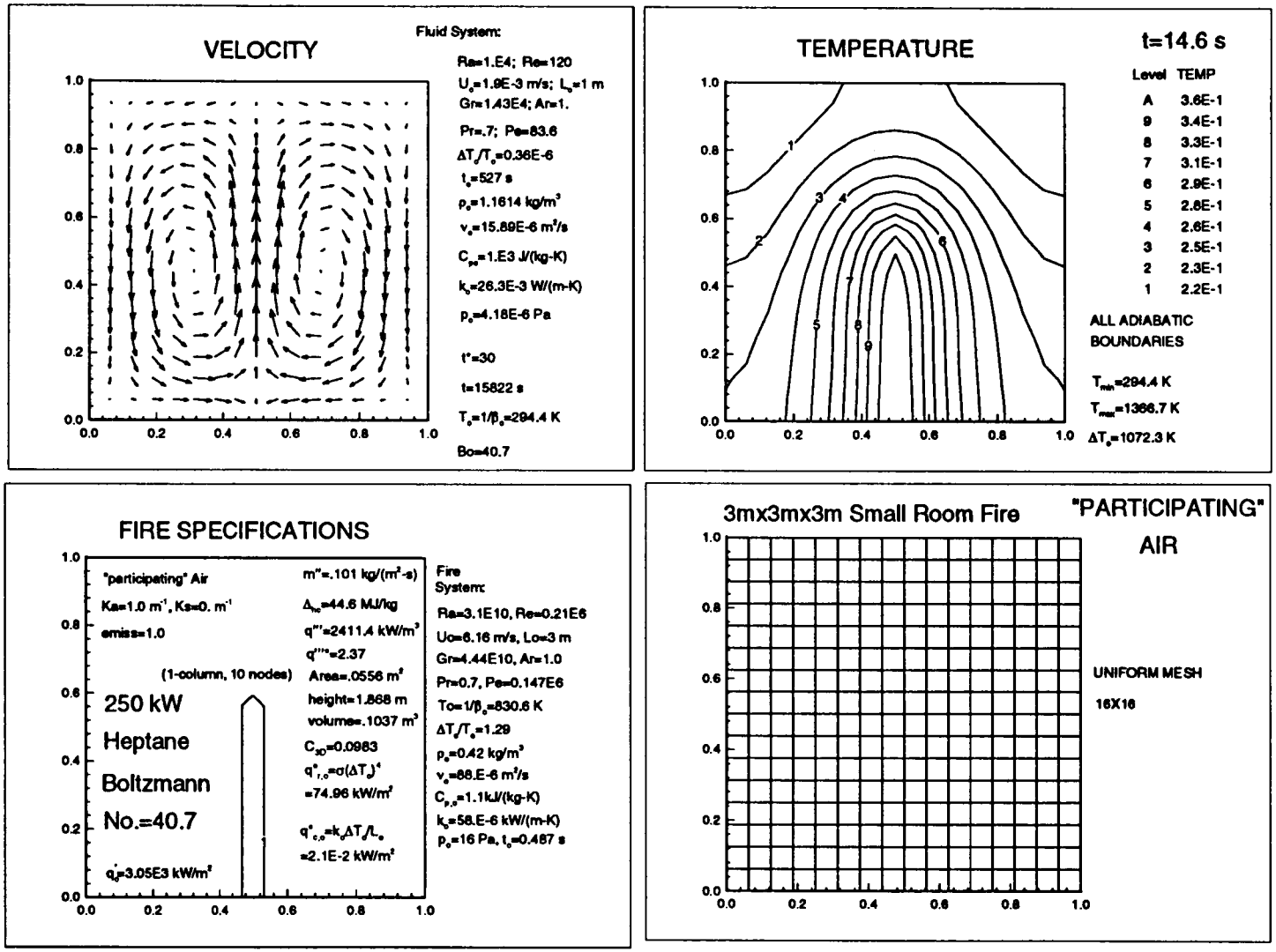


Fig. 17 2-D Fire Simulation, Convection and Radiation, Fluid Ra=1.E4, Case 17

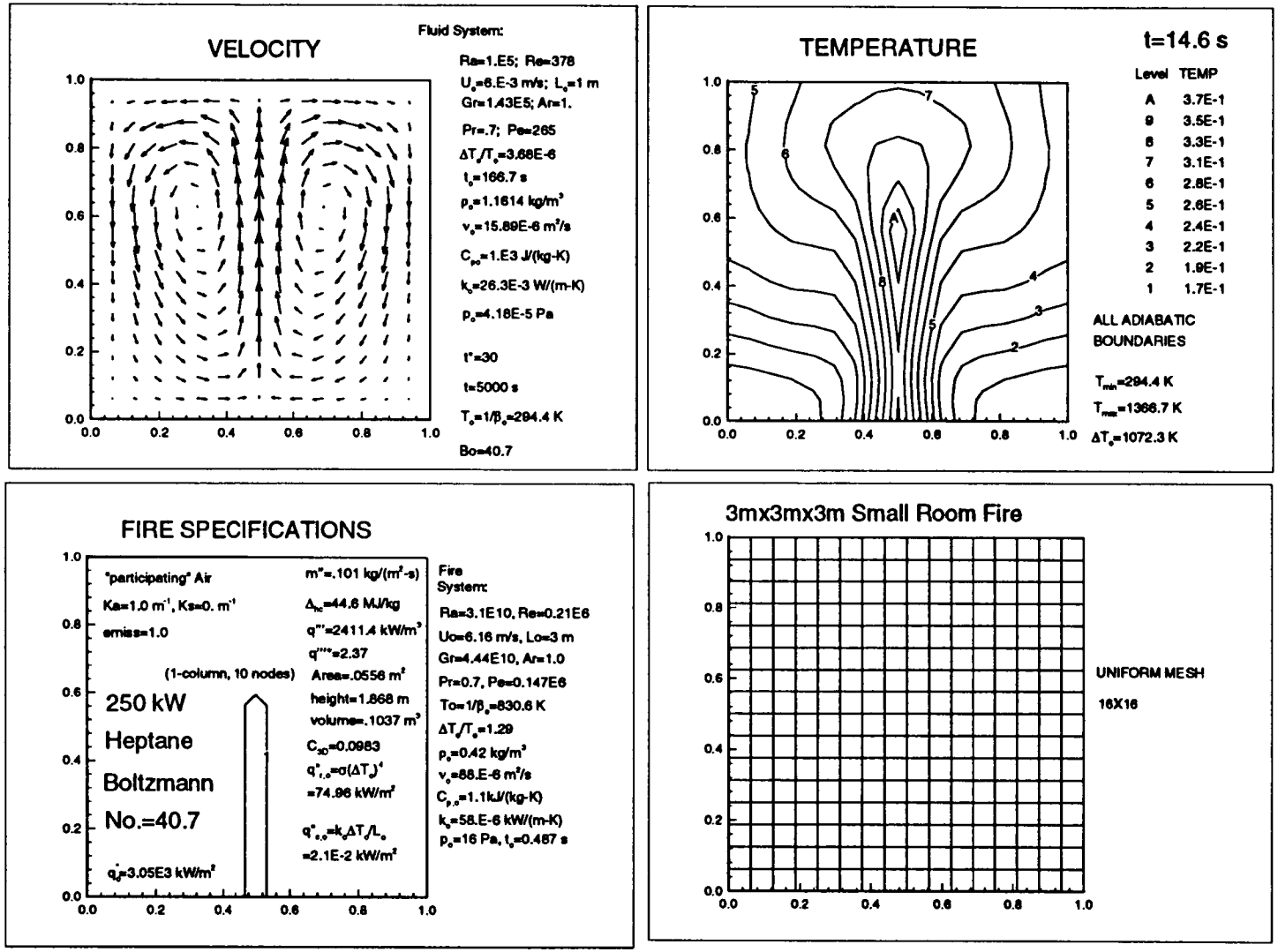


Fig. 18 2-D Fire Simulation, Pure Convection, Fluid Ra=1.E5, Case 18

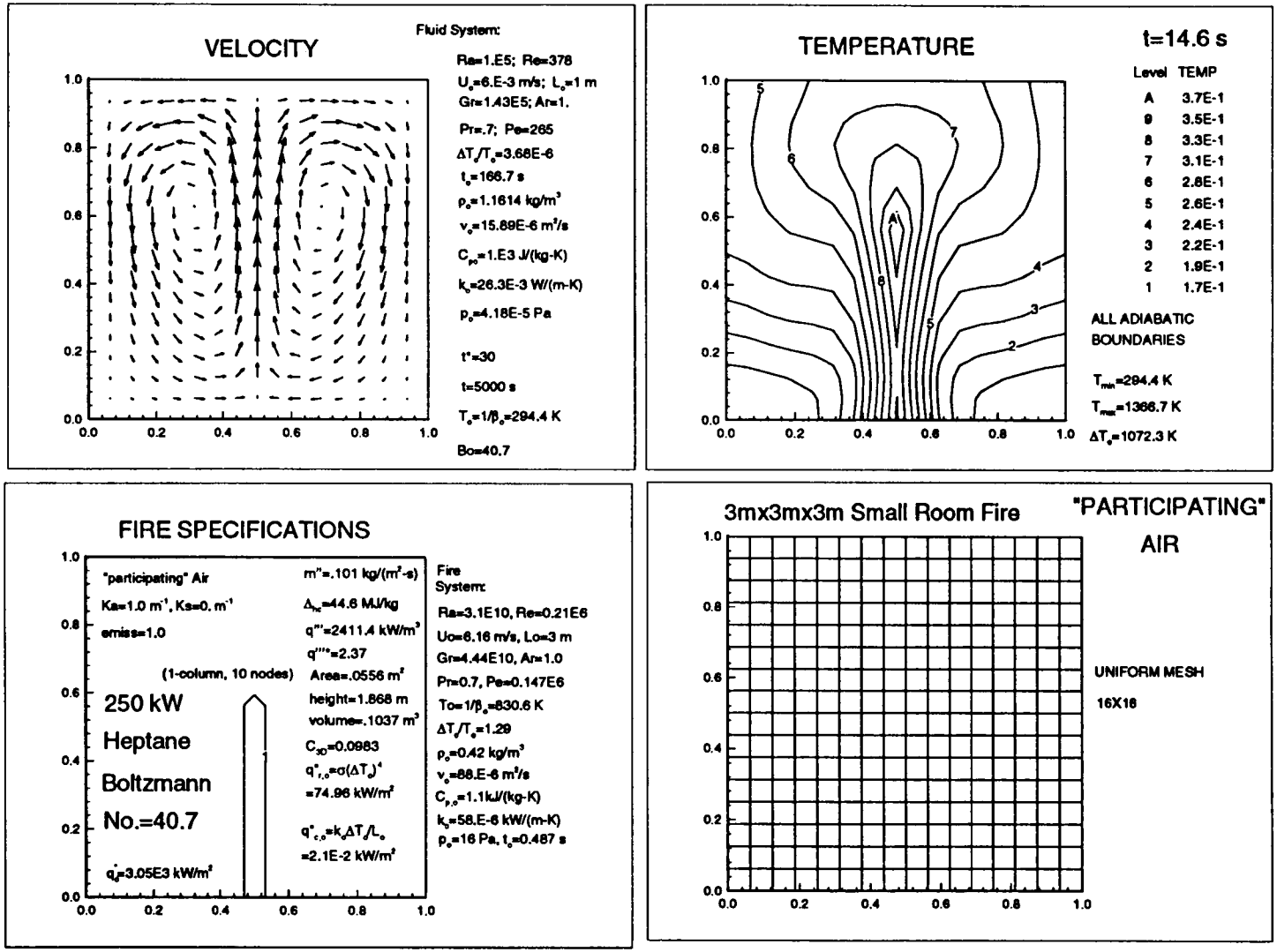


Fig. 19 2-D Fire Simulation, Convection and Radiation, Fluid Ra=1.E5, Case 19

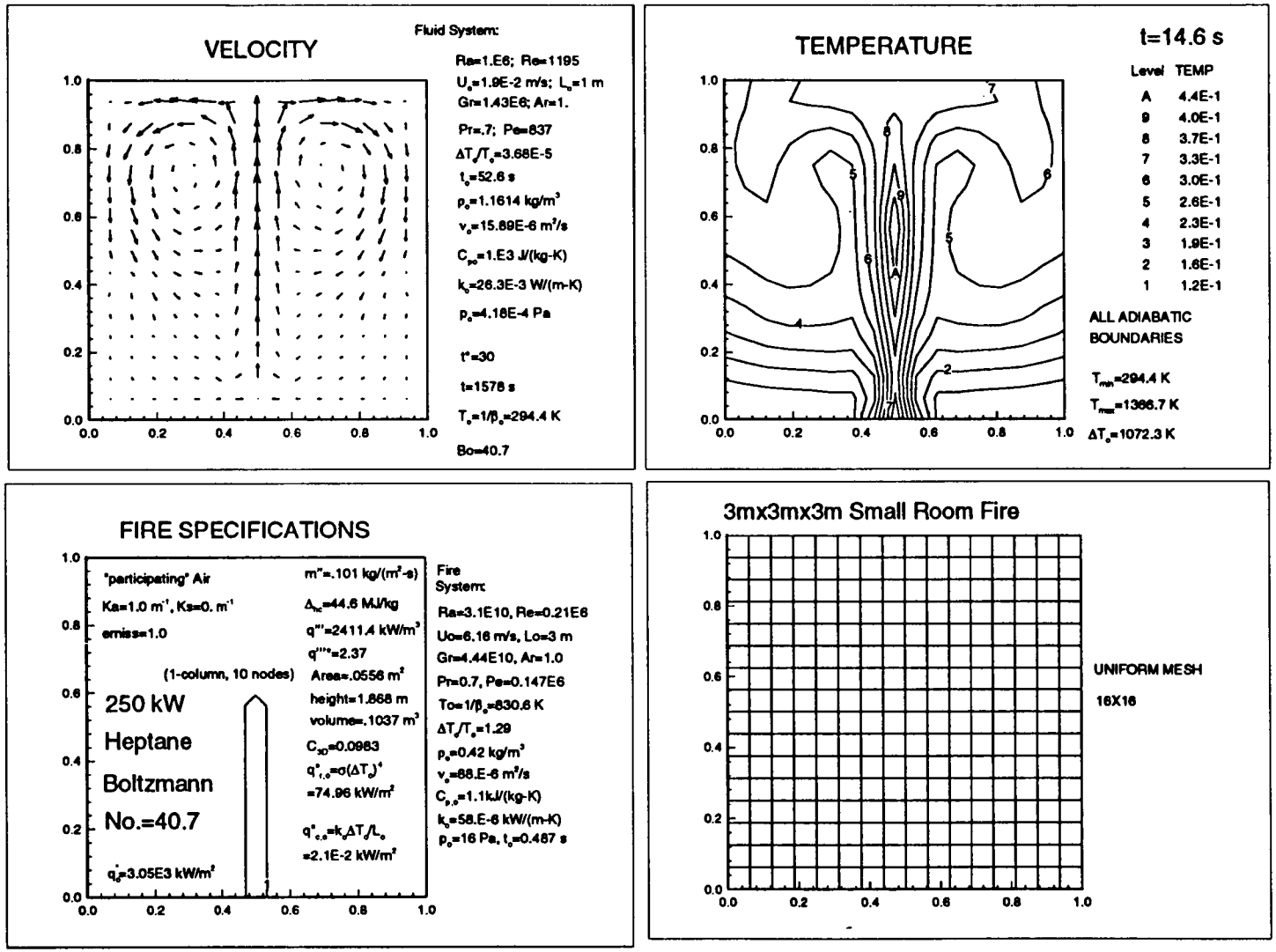


Fig. 20 2-D Fire Simulation, Pure Convection, Fluid Ra=1.E6, Case 20

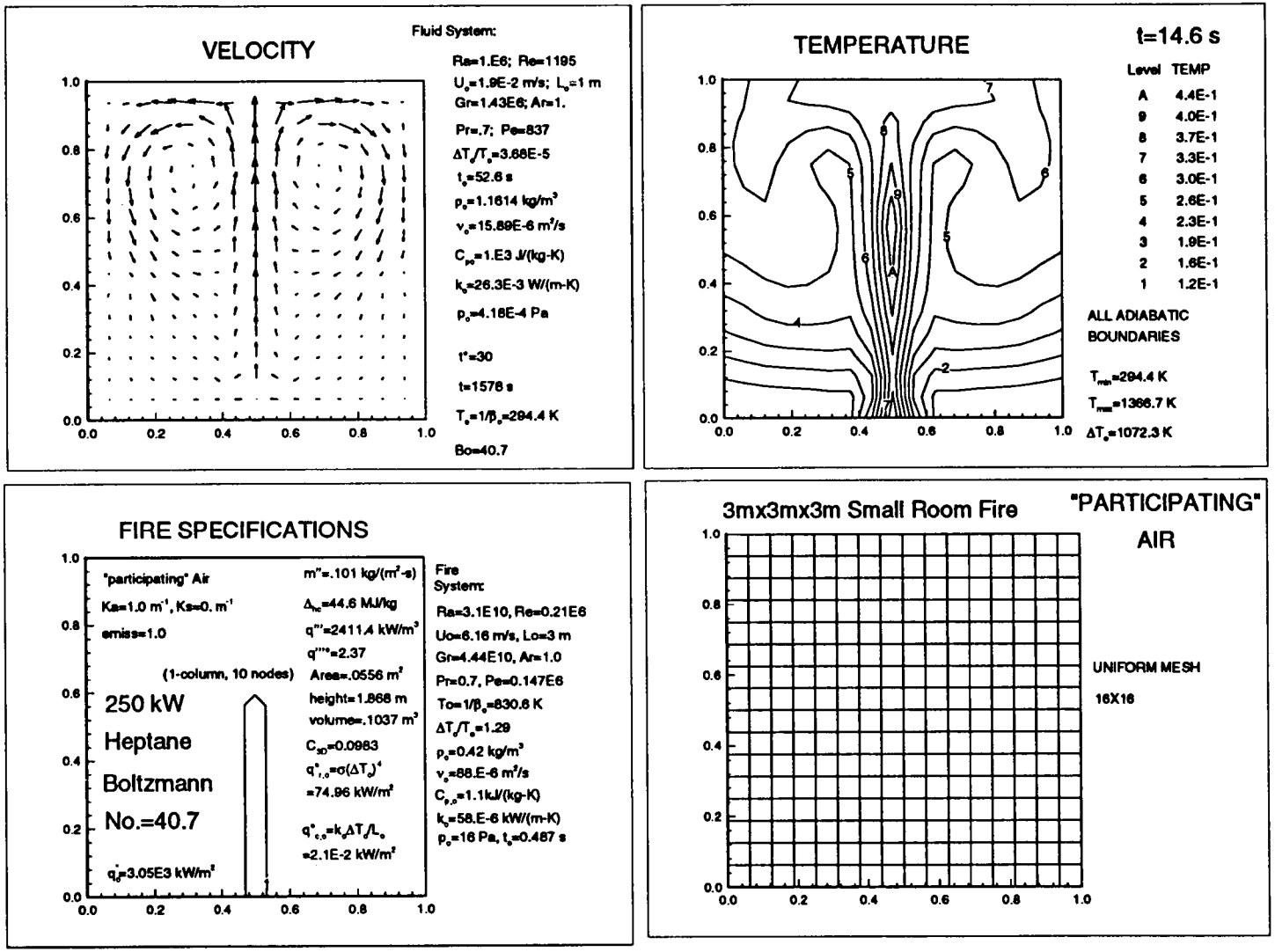


Fig. 21 2-D Fire Simulation, Convection and Radiation, Fluid Ra=1.E6, Case 21

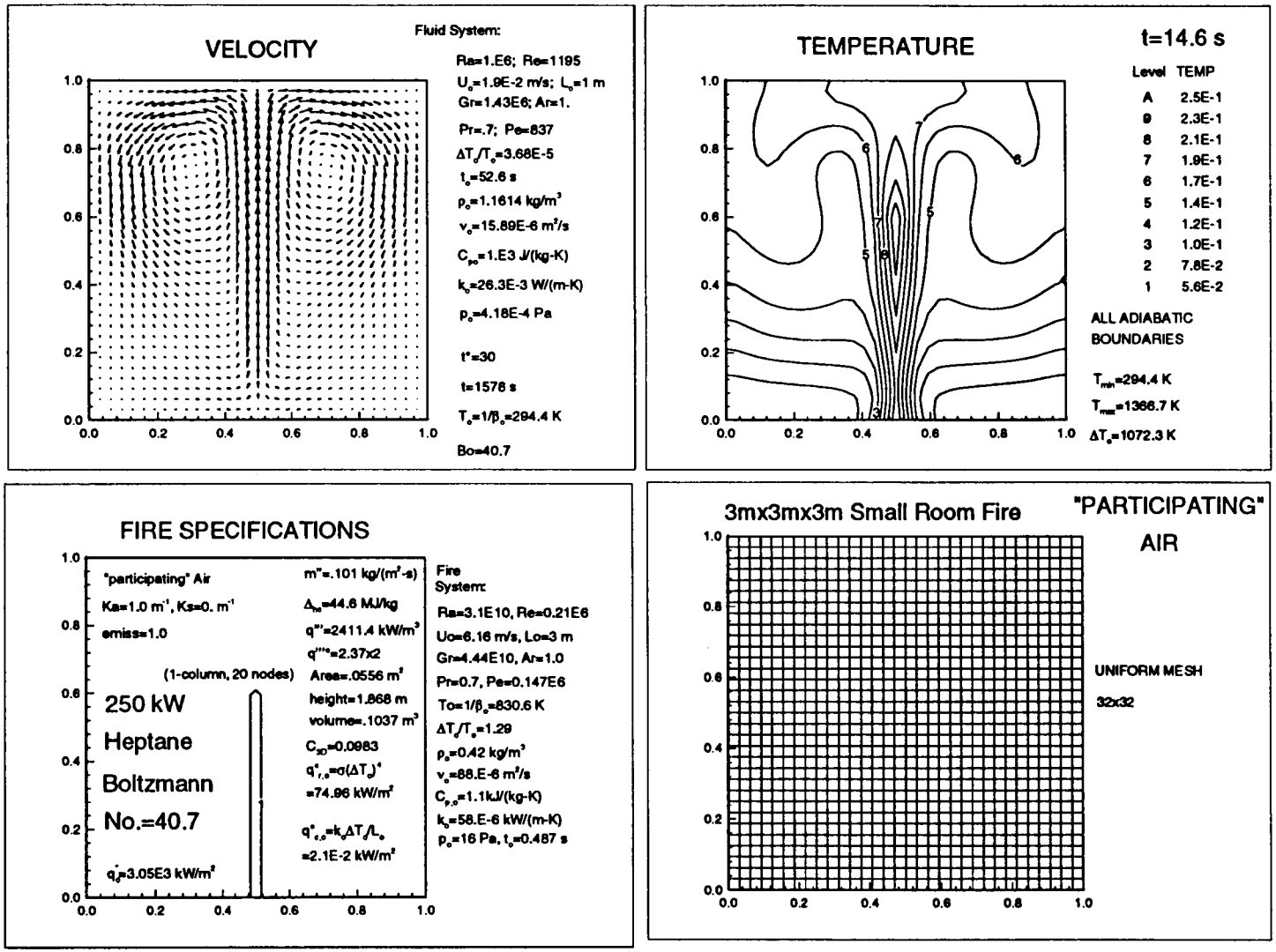


Fig. 22 Accuracy Study of 2-D Fire Simulation, Fluid Ra=1.E6, M=32x32, Case 22

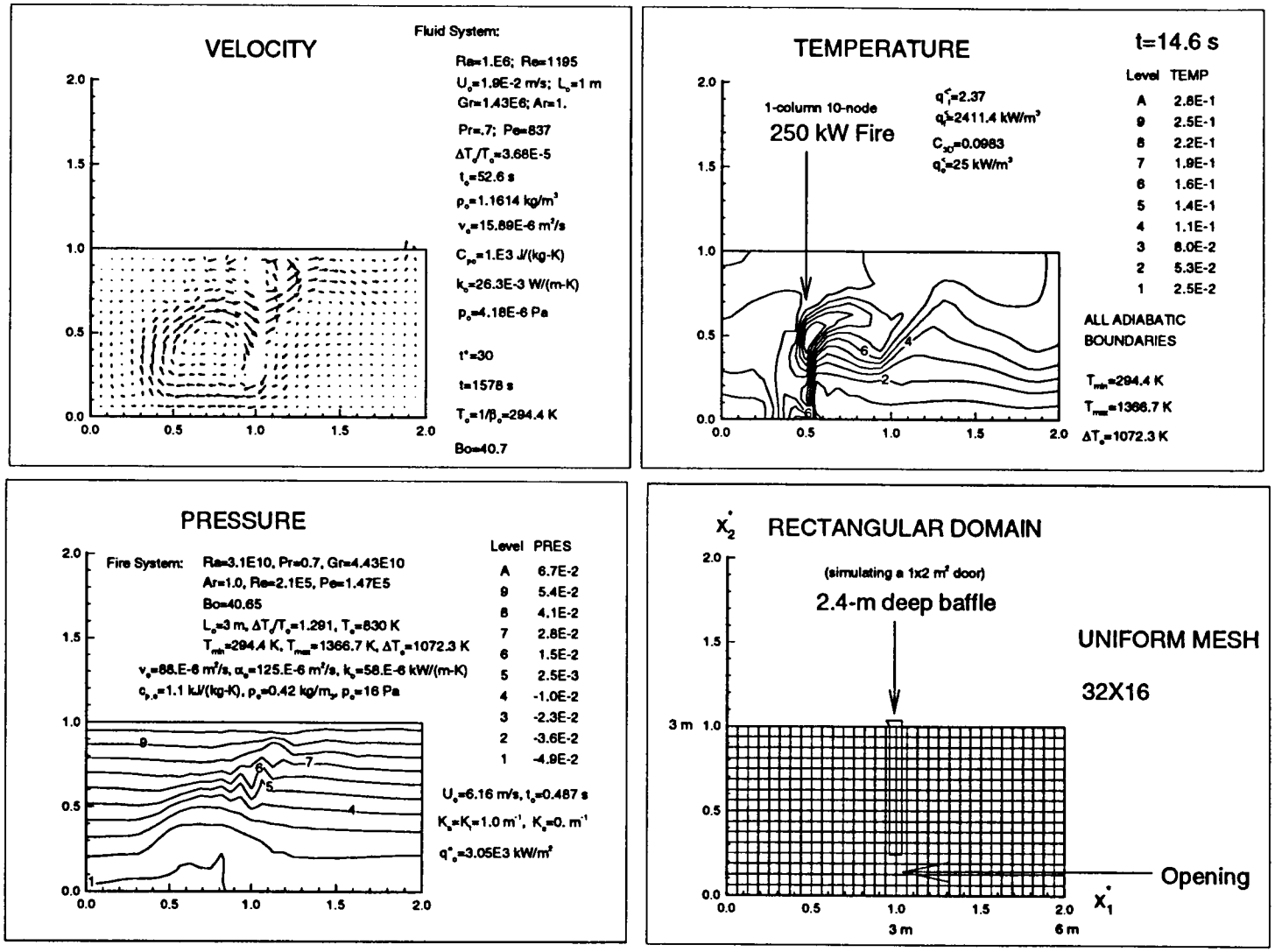


Fig.23 2-D Fire Simulation, Small Opening, Fluid Ra=1.E6, Mesh=32x16, Case 23

For comparisons, the maximum dimensionless velocity (i.e., u_2^* along the vertical centerline of fire), temperature, conductive and radiative fluxes and divergence of radiative flux are summarized in Table 9. C and R denote convection and radiation.

Table 9 Summary of Dimensionless Results of 2-D Fire Simulations

Case	u_2^*	Θ^*	$q_c^{*'''}$	$q_r^{*'''}$	$\nabla \bullet q_r^{*'''}$
Ra=E4, C	0.0751	0.376	n/a	n/a	n/a
Ra=E4, CR	0.0732	0.373	-691.E-6	-50.E-6	265.E-5
Ra=E5, C	0.2270	0.397	n/a	n/a	n/a
Ra=E5, CR	0.2270	0.393	-442.E-6	-48.E-6	293.E-5
Ra=E6, C	0.3750	0.473	n/a	n/a	n/a
Ra=E6, CR	0.3750	0.470	-254E-6	152E-6	439.E-5
Ra=E6, C,32[2]	0.3550	0.509	n/a	n/a	n/a
Ra=E6, Open	0.1490	0.295	n/a	n/a	n/a

Table 10 translates data in Table 32 into engineering units.

Table 10 Summary of Dimensional Results of 2-D Fire Simulations

Case	u_2, m/s	T, K	q_c'', kW/m^2	q_r'', kW/m^2	$\nabla \bullet q_r''$, kW/m^3
Ra=E4, C	0.4626	697.6	n/a	n/a	n/a
Ra=E4, CR	0.4509	694.4	-2.1076	-0.1525	2.69
Ra=E5, C	1.3983	720.1	n/a	n/a	n/a
Ra=E5, CR	1.3983	715.8	-1.3481	-0.1464	2.98
Ra=E6, C	2.3100	801.6	n/a	n/a	n/a
Ra=E6, CR	2.3100	798.4	-0.7747	-0.4636	4.46
Ra=E6, C,32[2]	2.1868	840.2	n/a	n/a	n/a
Ra=E6, Open	0.9178	610.7	n/a	n/a	n/a

The gas temperature distribution along the vertical line at x_1^*=0.25 (x_1=1.5 m) for all cases are summarized in Figure 24, in comparison to the FPETOOL prediction.

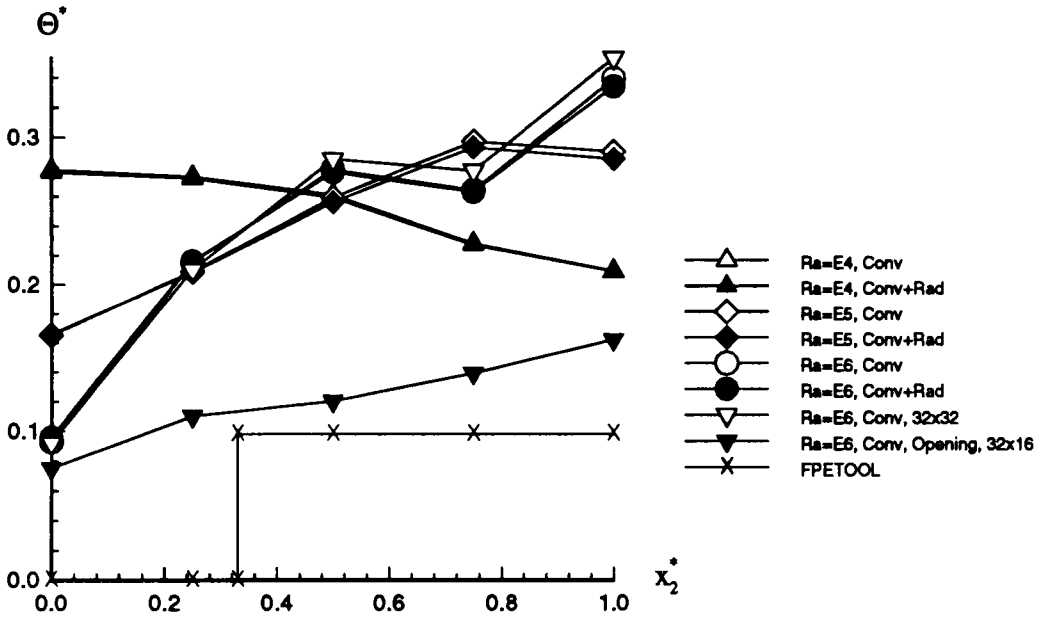


Fig. 24 2-D Fire Room Temperatures at x_1^*=0.25 (x_1=1.5 m), t^*=30. (t=15 s)

A number of significant observations have been made for these two dimensional fire simulation results. Foremost and most important is that addition of thermal radiation does not materially affect the scalar fields, since the velocity and temperature fields are virtually identical in the pure convection and convection-participating radiation cases. The logical explanation is that this is due to the extremely low order of magnitude of the divergence of radiative flux compared with its fire heat source counterpart. In Table 9, the former is order of 3.E-3, whereas the fire heat source is order 2.E-1. Physically, this means that the fire itself transfers approximately 3.0 kW/m^3 out of 237 kW/m^3 (2411 kW/m^3 for 3-D) to its environment, including the hot and cold layers and all walls, in the form of thermal radiation. Though quite minimal, the fire plume consistently lowers its temperature in the cases allowing thermal radiation.

In Figure 24, the fire room temperature at x_1^*=0.25 for Ra=1.E5 and 1.E6 are

quite comparable and consistent with physical observations, displaying the characteristic of "hot" and "cold" layers. The temperature curve for Ra=1.E4 along with Figures 16 and 17, is non-physical, since the floor temperature is higher than the ceiling temperature. However, all predicted room fire temperatures are significantly higher than the 400 K estimated by FPETOOL. The average temperature of the "hot" layer for both Ra=1.E5 and 1.E6 is $\Theta^* \approx 0.2$ or 500 K. As discussed earlier, the temperature from FPETOOL is only a *physical* guide and not usable for estimating the accuracy of the CFD solutions. Therefore, it is deemed that results from Ra=1.E5 and 1.E6 are reasonably predictive.

The other important aspect of fire modeling is the prediction of the velocity field. Unfortunately, none of the existing zone models has this capability. However, based on the fire experiments in general, the fire plume can generate a gas speed ranging from 1 to 10 m/s [72,73]. In Table 10, both Ra=1.E5 and 1.E6 are qualified for this range. Again, Ra=1.E4 is approximately an order of magnitude less than the physical results.

Appendices C.2, C.3 and C.9 show that the conductive and radiative fluxes are highly comparable. They all attain their maximum values in the center of the ceiling, which divides the symmetries of both types of flux in the fire room.

The solution accuracy study for Ra=1.E6 shows that the adopted standard mesh may be marginally acceptable for the fire problem at hand. For example, the centroidal temperature for is 0.278 and 0.285 for the standard and dense meshes. This slight difference is possible due to the nodal statement of data for the fire for the dense mesh. In the dense mesh, a single, vertical 20-node column was used. The nodal fire sources were double. The proper way is to redetermine the distribution of the nodal fire sources

based on the fire geometry.

Case 22 was intended to study the air entrainment effect and the impact on temperature field of the small room fire in case the door was open. The predicted velocity and temperature fields seem physically plausible, depicting the effect of "fresh" air entrainment and the phenomena of flicking flame and overall decreasing temperature in the fire room. However, the baffle has caused a serious numerical instability, resulting in a negative nodal temperature computed in the middle of the door opening. The numerical difficulty may be due to the inadequate mesh, the large time step (although $\Delta t^*=0.25$ was used), or the high Ra number, or even the robustness of the CFD algorithm, or any combination thereof.

There is one major underlying flaw in this case. The problem is ill-defined from the physical standpoint. The baffle must have a physical "thickness" occupying the computational domain. It is noted that the gas immediately outside the baffle is being heated up instantaneously by the gas in the front of the baffle (inside the fire room) while the air temperature in the door remains very low. For example, the dimensionless temperature air in the entire opening is 0.025 whereas the average gas temperature near the back of the baffle (outside the fire room) is 0.18. It is nonphysical. Moreover, the gas temperature adjacent to the back of the baffle is generally higher than the front-gas and baffle temperatures, manifesting serious dispersion (oscillation) errors.

The explanation for this flaw is that the baffle acts like an infinitely conductive material in the gas domain, rendering the gas temperatures near both sides of the baffle similar. To rectify this problem, a solid domain entailing a two dimensional conduction

model is required. A less desirable but more pragmatic alternative is to incorporate the gas boundary along the physical periphery of the baffle, totally neglecting the conductive heat transfer from the fire room into the contiguous non-fire room. In this fire scenario, the latter seems acceptable because the simulation time is very short. However, a rigorous study on this problem is considered beyond the scope of this research, and therefore, is recommended as a future examination. This is an important issue in fire simulation, since many actual fire scenarios anticipate openings through non-adiabatic or thermally thin barriers, e.g., doors, windows, glass panels, HVAC supplies and outlets.

In summary, it is deemed that laminar flow is a feasible approach for practical fire simulation despite the problematic dimensionless issue and some resolvable numerical difficulties such as dispersion error control and stability. Among the three Ra numbers tested, Ra-1.E6 seems to best model reality and is also the most challenging in terms of numerical stability. For example, Δt^* cannot be greater than 0.25 for Ra=1.E6, whereas in other cases 0.5 or greater is acceptable. In this fire scenario, thermal radiation does not impact the scalar fields. Owing to the limited scope of these fire model data sets, further studies are required to generalize this finding, involving more complex fire scenarios such as longer simulated periods, more intense fires and different sets of radiative properties including the moving interface of the hot and cold layers discussed previously. Interestingly, this observation is very different from the previous analysis on the participating thermal cavity, where the participating medium strongly influences the scalar fields. Thus, it is logically concluded that different boundary conditions and types of heat sources dictate the significance of thermal radiation in *similar* problems.

4.4.5 3-D Room Fire

Based on the observation from the two dimensional fire simulations that thermal radiation does not materially impact the CFD predicted scalar fields, pure convection cases have not been executed in the three dimensional analyses. The following CFD-radiation-fire simulations have been executed:

(1) Case 24 - 3-D Fire Simulation, Fluid Ra=1.E4;

(2) Case 25 - 3-D Fire Simulation, Fluid Ra=1.E5;

(3) Case 26 - 3-D Fire Simulation, Fluid Ra=1.E6, t^*=5.33 (t=2.6 s);

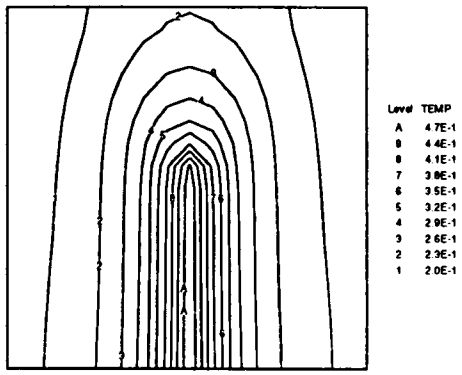
(4) Case 27 - 3-D Fire Simulation, Fluid Ra=1.E5, Non-Uniform Mesh; and

(5) Case 28 - 3-D Fire Simulation, Fluid Ra=1.E6, Non-Uniform Mesh, t^*=16.4, (t=8 s).

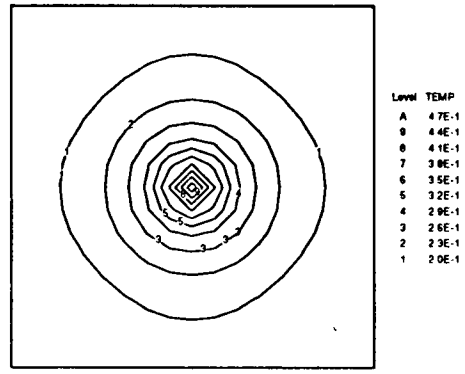
All solutions (except Case 28) and numerical scalar fields are graphically summarized in Figures 25-28 and in Appendices D.1-D.5. The Tecplot data for Case 28 was wiped out when Case 28 diverged. The only converged results are for Cases 24, 25 and 27.

Comparing Figure 25 with Figure 16, the temperature profiles of the two and three dimensional cases are very similar, although the overall maximum temperature in the fire flame vicinity is approximately 100 K higher in the three dimensional case (Figure 25). Coordinates x_1^* and x_3^* span the horizontal planes while x_2^* is the vertical axis. The centroidal base of fire is located at the dimensionless coordinates $x_1^*=0.5=x_2^*$ and $x_3^*=0$. By symmetry, the three dimensional mid x_1^*-x_2^* and x_2^*-x_3^* plane velocity profiles in Figure 25 are identical and similar to the two dimensional profile in Figure 16.

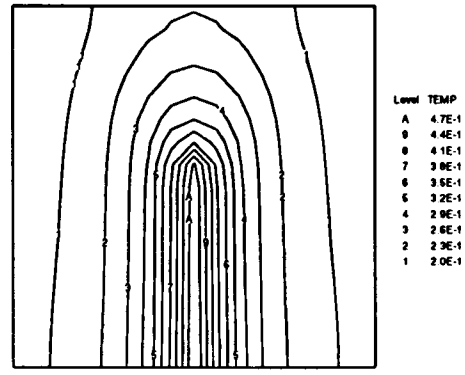
However, for Ra=1.E5, the two dimensional temperature profile in Figure 18 with a "T"-pattern is more realistic than the three dimensional "column"-pattern temperature



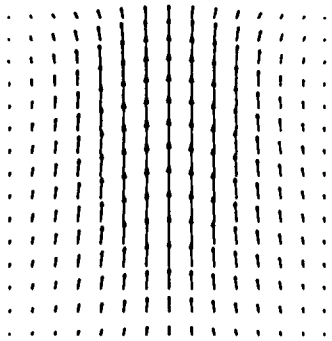
Mid x_3^*-x_2^* Plane Temperature



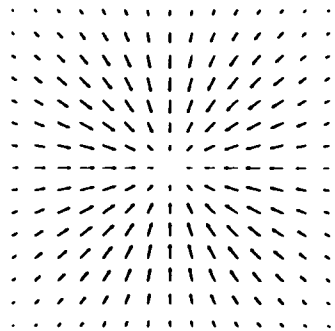
Mid x_1^*-x_3^* Plane Temperature



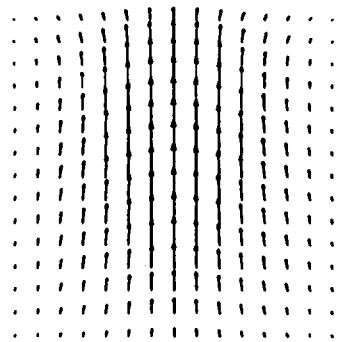
Mid x_1^*-x_2^* Plane Temperature



Mid x_3^*-x_2^* Plane Velocity

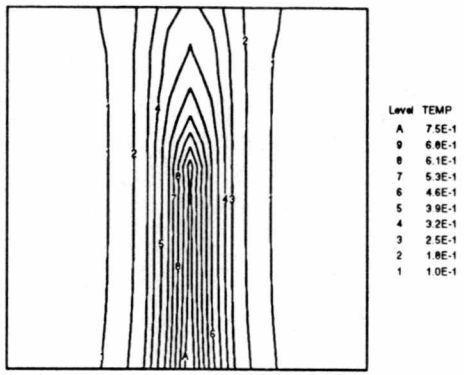


Mid x_1^*-x_3^* Plane Velocity



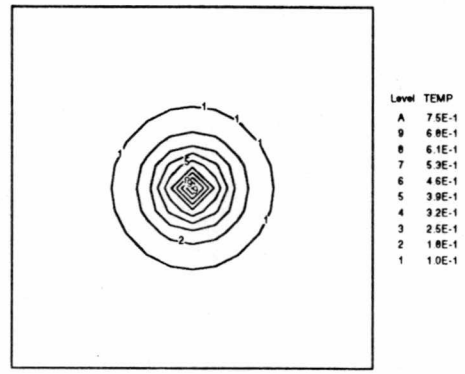
Mid x_1^*-x_2^* Plane Velocity

Fig. 25 3-D Fire Simulation, Fluid Ra=1.E4, Case 24



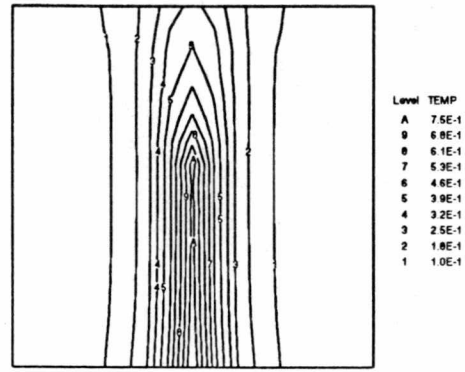
Level TEMP
A 7.5E-1
9 6.8E-1
8 6.1E-1
7 5.3E-1
6 4.6E-1
5 3.9E-1
4 3.2E-1
3 2.5E-1
2 1.8E-1
1 1.0E-1

Mid x_3^*-x_2^* Plane Temperature



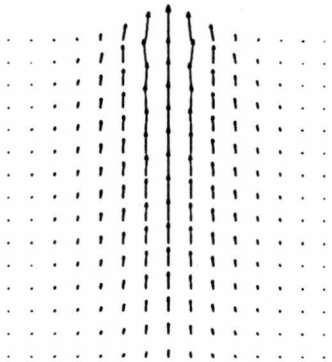
Level TEMP
A 7.5E-1
9 6.8E-1
8 6.1E-1
7 5.3E-1
6 4.6E-1
5 3.9E-1
4 3.2E-1
3 2.5E-1
2 1.8E-1
1 1.0E-1

Mid x_1^*-x_3^* Plane Temperature

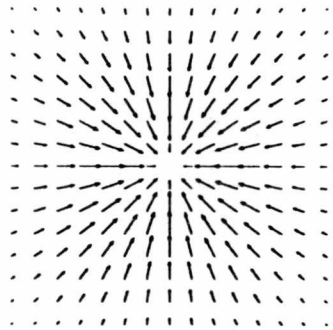


Level TEMP
A 7.5E-1
9 6.8E-1
8 6.1E-1
7 5.3E-1
6 4.6E-1
5 3.9E-1
4 3.2E-1
3 2.5E-1
2 1.8E-1
1 1.0E-1

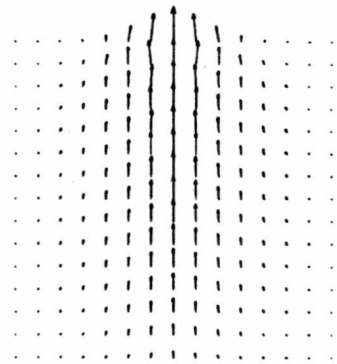
Mid x_1^*-x_2^* Plane Temperature



Mid x_3^*-x_2^* Plane Velocity

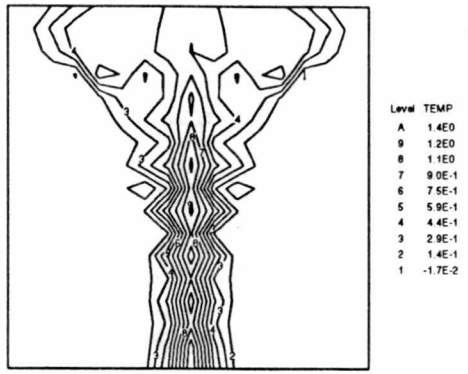


Mid x_1^*-x_3^* Plane Velocity

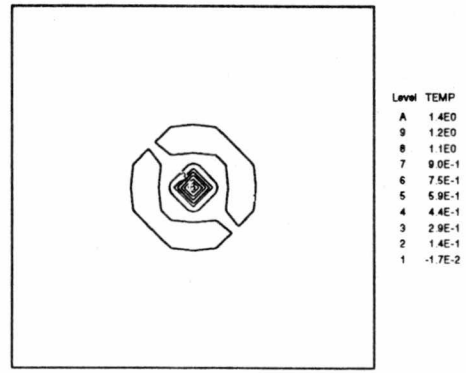


Mid x_1^*-x_2^* Plane Velocity

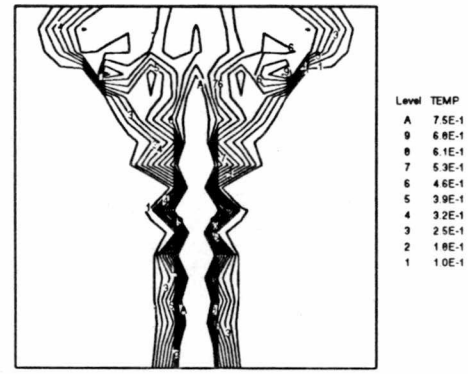
Fig. 26 3-D Fire Simulation, Fluid Ra=1.E5, Case 25



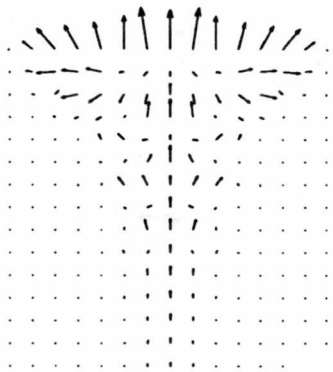
Mid x_3^*-x_2^* Plane Temperature



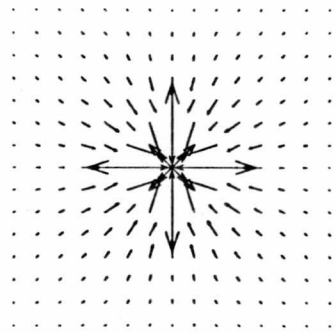
Mid x_1^*-x_3^* Plane Temperature



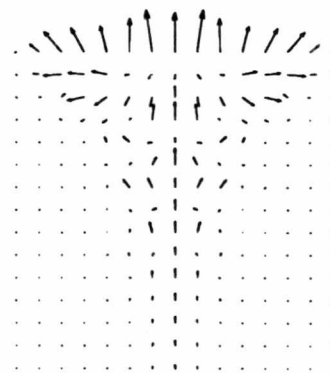
Mid x_1^*-x_2^* Plane Temperature



Mid x_3^*-x_2^* Plane Velocity

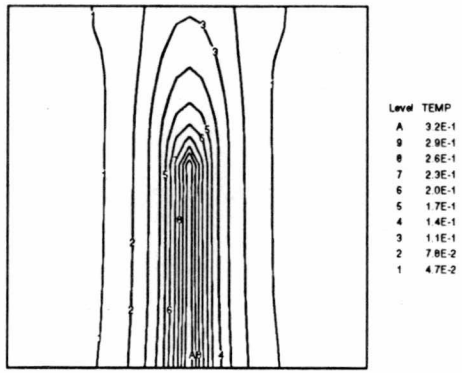


Mid x_1^*-x_3^* Plane Velocity

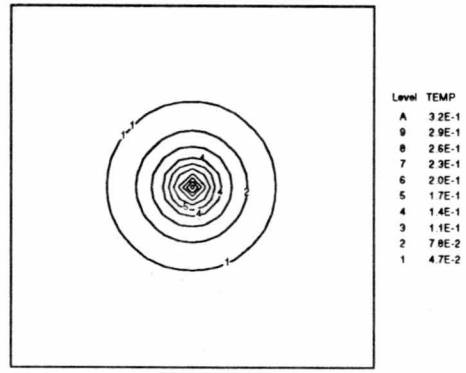


Mid x_1^*-x_2^* Plane Velocity

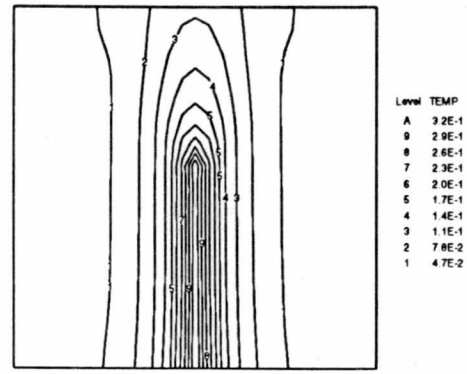
Fig. 27 3-D Fire Simulation, Fluid Ra=1.E6, t^*=5.33 (t=2.6 s), Case 26



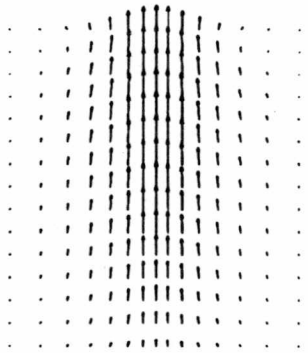
Mid x_3^*-x_2^* Plane Temperature



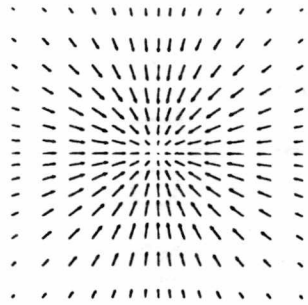
Mid x_1^*-x_3^* Plane Temperature



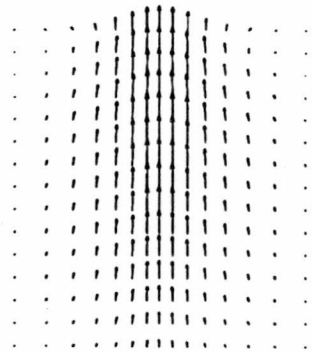
Mid x_1^*-x_2^* Plane Temperature



Mid x_3^*-x_2^* Plane Velocity



Mid x_1^*-x_3^* Plane Velocity



Mid x_1^*-x_2^* Plane Velocity

Fig. 28 3-D Fire Simulation, Fluid Ra=1.E5, Non-Uniform Grid, Case 27

profile in Figure 26. Based on Evan's ceiling jet flow empirical correlations [73], the ceiling($x_2^* \approx 1.0$) temperature and velocity as a function of x_1^* are summarized in Table 11.

Table 11 Evan's Empirical Correlations for a Steady State **Ceiling** Jet Flow

x_1^*	x_1, m	u, m/s	T, K
0.5	1.5 (plume centerline)	4.20	400.7
0.25, 0.75	0.75, 2.25	1.50	348.4
0., 1.0	0., 3.0	0.85	328.4

The temperature contour lines away from the plume centerline in the ceiling for the three dimensional case remain "cold", whereas the temperature contour lines in the two dimensional case have developed the uniformly "hot" layer across the entire ceiling, manifesting the T-pattern profile. However, it is possible that for longer simulated periods, the three dimensional cases may yield better correlations, as the fire simulation periods approach to steady state. It is noted in both Figures 25 and 26, the air entrainment phenomenon is vividly demonstrated in the mid x_1^*-x_3^* plane velocity profiles, where all transverse velocities are directed towards the plume centerline.

Prior to the occurrence of the diverged solutions of Ra=1.E6 at t^*=5.33, the Tecplot (graphical post processor) data was saved and translated into Figure 27. Despite a very short fire duration and the oscillations of temperature contour lines in the hot layer (due to computed negative temperatures), the fire plume, air entrainment, and hot and cold layers are vividly displayed.

Figure 28 for the non-uniform grid of Ra=1.E5 essentially captures the same temperature and velocity profiles of Figure 25, except the magnitudes of both the overall

temperature and velocity are reduced due to the erroneously lower fire intensity.

The maximum dimensionless velocity, temperature, conductive and radiative fluxes and divergence of radiative flux vector, as established in the two dimensional fire simulations, are summarized in Table 12, where NU denotes a non-uniform grid with attraction towards the fire plume or the vertical centerline of the fire room. The maximum dimensionless velocity, temperature and divergence of radiative flux vector should be located on the vertical centerline of the fire plume, but this may not necessarily coincide with the room centroid. For the dimensionless conductive and radiative fluxes, physically, they must be located in the center of the ceiling, although computationally they may be located in the middle of the four walls.

Table 12 Summary of Dimensionless Results of 3-D Fire Simulations

Case	u_2^*	Θ^*	$q_c^{*''}$	$q_r^{*''}$	$\nabla \cdot \mathbf{q}_r^{*''}$
Ra=E4	0.3030	0.495	-149.E-5	-2.0E-5	145.E-4
Ra=E5	0.9190	0.819	-195.E-5	+2.0E-4	110.E-3
Ra=E5, NU	0.3690	0.352	-783.E-6	-2.0E-6	421.E-5
Ra=E6†	3.4200	1.500	-183.E-5	+3.0E-3	100.E-2
Ra=E6, NU†	2.9500	1.330	-398.E-5	+1.3E-3	891.E-3

† solution eventually diverges.

Table 13 converts the data in Table 12 into engineering units.

Table 13 Summary of Dimensional Results of 3-D Fire Simulations

Case	u_2, m/s	T, K	q_c'', kW/m^2	q_r'', kW/m^2	$\nabla \cdot \mathbf{q}_r''$, kW/m^3
Ra=E4	1.8666	825	-4.5445	-0.0610	14.727
Ra=E5	5.6610	1172	-5.9475	+0.6100	111.728
Ra=E5, NU	2.2176	672	-2.3882	-0.0061	4.276
Ra=E6†	21.067	1903	-5.5815	+9.1500	1015.67
Ra=E6, NU†	18.172	1721	-12.1390	+3.9650	905.000

The maximum velocities and temperatures of the three dimensional cases for Ra=1.E4 and 1.E5 are higher than their two dimensional counterparts. Comparing Table 13 with Table 10, average flame temperatures are 700 K and 1000 K in two and three dimensions.

The "average" room fire temperature would be determined by the imaginary, single column of thermocouples located at a quadrant centroidal point (0.25, 0, 0.25) on the bottom horizontal plane, namely, the floor. Figure 29 summarizes the "average" room fire temperature at $x_1^*=x_3^*=0.25$ ($x_1=x_3=1.5$ m) as a function of the vertical axis ($x_2^*=0.$, 0.25, 0.50 and 1.00). Comparing the two dimensional average room fire temperature as shown in Figure 24 with the three dimensional average room fire temperature in Figure 29, the average room temperature of three dimensions is significantly lower in three dimensions (0.1) than in two dimensions (0.2) at all Ra numbers. Hence, the three dimensional average temperatures (<u>not</u> necessarily the temperature distribution, especially near the ceiling) correlate better with FPETOOL.

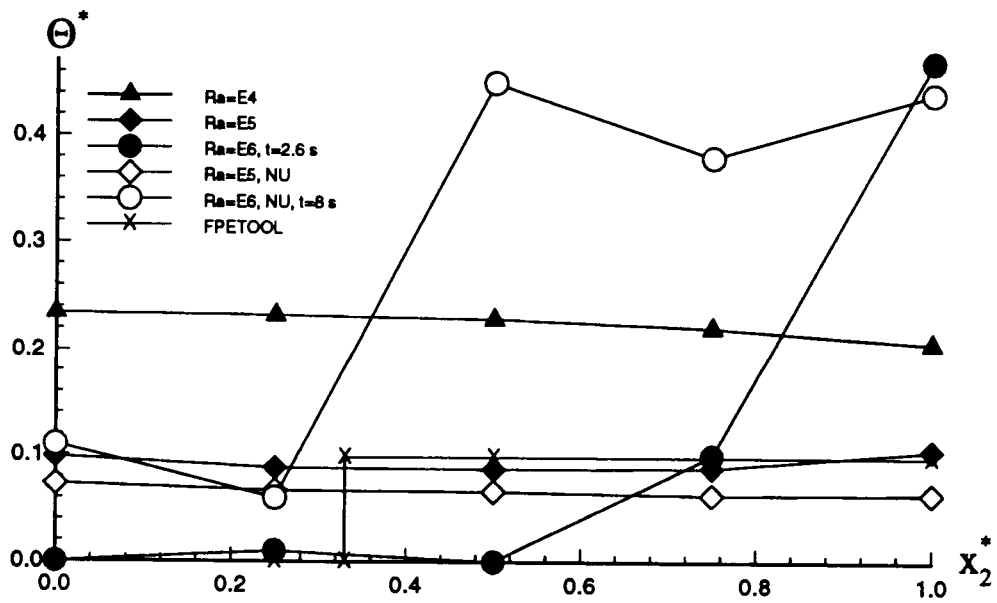


Fig. 29 3-D Fire Room Temperatures at $x_1^*=x_3^*=0.25$

Based on Ra=1.E4 and 1.E5, the average maximum conductive fluxes at the center of the ceiling are 1.7 and 5.19 kW/m^2 for two and three dimensions. Correspondingly, the maximum radiative fluxes are 0.15 and 0.31 kW/m^2. The reason for the diverse spectrum of conductive fluxes and slight difference in radiative fluxes is that the flame temperatures are higher in three dimensions than in two dimensions possibly due to an inaccuracy in three dimensional adjustment coefficient, C_{3D}, in the construction of the two dimensional fire. Based on the resulting plume temperatures (versus the entire hot layer temperatures), the three dimensional data are more realistic. For the two dimensional fluxes at Ra=1.E6, the conductive and radiative fluxes are 0.77 and 0.46 kW/m^2, respectively. This reverses the trend that the conductive flux predominates the radiative flux in the low range of Ra number, when more realistic flame and hot layer temperatures are predicted in a high Ra number.

Case 26 for Ra=1.E6 diverged even at a very small time increment, i.e., $\Delta t^*=0.01$. Consequently, Case 25 for Ra=1.E5 was repeated as Case 27, with a non-uniform mesh refinement in the fire plume vicinity based on the same nodal fire sources. However, since the numerical data are consistently lower in the non-uniform mesh, the discrepancy is due strictly to the assigned nodal fire sources, which truly depend on the nature of discretization of domain. A non-uniform grid does change the elemental (or nodal) volumes, necessitating the corresponding change of q''' to retain the same total rate of energy release in the computational domain. Since the mesh was refined near the fire, the total heat release energy was lower in Case 27, thereby yielding the overall lower temperature numerical results. The corollary of this numerical experiment is that under

mesh refinement, the fire must be reconstructed to accurately reflect the equivalent total volumetric energy release rate into the computational domain.

The last numerical experiment, Case 28, was to attempt to encourage convergence for the unsuccessful trial at Ra=1.E6, Case 26. However, the solution process diverged at t^*=16.34 using Δt^*=0.25. Therefore, it is concluded that the standard mesh M=16x16x16 is inadequate for a 3-D room fire simulation for Ra≥1.E6. Despite the numerical difficulties, it is considered that Ra=1.E6 is the best candidate for fire simulation, based on the qualitative aspect of the numerical temperature and velocity solutions from Case 26. The justification for this contention is that the "T"-pattern demarcating the hot and cold layer provides the most realistic temperature profile among all cases. In addition, the flame temperature is within the range of 1500 K, correlating well with the general experimental and analytical data. Nevertheless, Ra=1.E5 is deemed viable.

In summary, the three dimensional simulation results seem more realistic regarding the fire plume and the hot and cold layers in terms of velocity and temperature. However, the numerical computational requirements for three dimensional simulations are definitely challenging.

4.5 Fire Damageability Studies

One of the most important aspects of quantitative fire hazard analysis is the study of fire damageability. Primarily, this concept utilizes the theory of heat transfer to estimate the "incident" heat flux (technically, net flux) onto an analyst-defined target.

Typically, a target is a fire protective device such as fire sprinkler, heat detector, thermally fusible elements of fire damper and fire door, protective equipment, flammable commodities, structural assemblies and human skin. There are two approaches in this study. First, the estimated heat flux is used to compare with an experimentally determined critical (threshold) flux. If the calculated flux exceeds the published data, fire damage would be physically possible. The second approach is to couple the estimated flux with a conduction or comparable heat transfer model, such as semi-infinite slab and lumped capacity method, to determine the surface or internal temperature of the target. If the calculated temperature exceeds the ignition temperature, then a fire damage would also be possible.

Although it may be true that the radiation field does not significantly affect the scalar fields in most practical fire simulations (versus pure fire research), the powerful utility of CFD-radiation should not be underestimated in light of fire damageability studies. Prior to this research, fire communities worldwide usually have to over-simplify their heat transfer model by assuming a purely radiative or convective flux [74]. Predominantly, a purely radiative flux is utilized due to the simplicity of *point-source* model. The consideration of combined radiative and convective or radiative and conductive fluxes was highly formidable. As a result of this research, a more realistic fire damageability study is feasible by considering the combined flux.

For example, from Appendix C.5, the dimensionless conductive and radiative fluxes at the center of the ceiling are 2.54E-4 and 1.53E-4, respectively. From Section 4.4.1, the respective heat fluxes for two dimensions are 0.77 and 0.46 kW/m^2, resulting

in a total *net* thermal flux of 1.23 kW/m^2 at t=15s. This magnitude can physically cause a third degree skin burn but far below the ignition of wooden materials with an average critical heat of 12 kW/m^2 [75].

Another practical example is to determine whether this flux level would actuate a fire sprinkler at the same location. The current practice is to utilize the lumped capacity method for the thermally fusible link of the sprinkler. Applying the heat balance at the the control volume of the link, $A_s q''_s(t)=(\rho_s V_s c_{p,s})dT(t)/dt$. For simplicity, q''_s is linearized from zero to 1.23 kW/m^2 during the simulated period. Then, the average, "constant" flux is approximately 0.615 kW/m^2 from t=0 to t=15 s. Unfortunately, the thermophysical properties as well as details of the fusible links usually are not published as they usually are proprietary. To proceed with the illustration, ρ_s=7000 kg/m^3, $c_{p,s}$=0.2 kJ/(kg-K), A_s=0.645E-3 m^2 (1 in^2, one side only), and $V_s=A_s h_s$=(0.645E-3 m^2)(3.175E-3 m)=2.048E-6 m^3, assuming a thickness of 1/8" (h_s) for the link. Then the mass of the link is 14.3E-3 kg (or 14.3 grams). The analytical solution of the above simplified ordinary differential equation is:

$$T(t) = \frac{\dot{q}''_s A_s}{m_s c_{p,s}} (t-t_i) + T_i \qquad (4-1)$$

For t_i=0 s, t=15 s and T_i=294.4 K (70° F), the increased temperature is only 2.0 K (7.5° F). The *ordinary* operating temperature of a fire sprinkler based on NFPA 13 (National Fire Protection Association Codes and Standards) is 165° F (347 K). Therefore, it is predicted that the sprinkler would not be activated. However, if "both" sides of the fusible link are considered (or the mass is over-estimated), then the increased temperature

would double accordingly, or the instantaneous temperature of the link would be 298.4 K (77° F). Moreover, *if* the net total heat flux is based on the "pre-diverged" three dimensional results of 14.73 kW/m^2 for Ra=1.E6, then the sprinkler would actuate and the wooden ceiling in the center of the fire room would burn.

It is interesting to note that at lower room temperatures, the conductive flux dominates, whereas the radiative flux is higher than the conductive flux after the plume temperature has "picked up" to speed. This is one of the drawbacks to adopt a rate-of-heat-energy-release basis versus Dirichlet-temperature basis to describe the temporal development of fire. The former, though taking advantage of the experimental results, cannot immediately bring the fire temperature up to its maximum value, i.e., 1000~1500 K at zero time step. Physically, any fire almost instantaneously attains this temperature range and its corresponding maximum emissive power. It is deemed that once this issue has been resolved, the two dimensional simulations would better predict flame and plume temperatures, hence the resultant fluxes. In the incipient stage, the exposing heat flux including conductive and radiative to its environment is very low due to the relatively small flame geometry. For simplicity and erring on the conservation side, a fully developed fire has been assumed at zero time step.

Another practical utility of the combined radiative and conductive flux is a more realistic conjugate heat transfer analysis at the interface of fluid and solid media for the modeling of fire endurance of building construction. Although a multi-dimensional consideration is a highly challenging task, a one-dimensional constant properties conduction model is feasible. This utility advances the existing technology of modeling

structural fire endurance and possibly facilitates cost-effective and efficient testing designs for fire barriers.

4.6 Computational Considerations

The primary computing resource has been a Sun Sparc 20 workstation. Heavily depending on the mesh size (1x1 to 16x16x16 elements) and type of radiation medium, the cpu time ranges from seconds to several days. The most time-consuming aspect is the view factor (discrete exchange factor) calculations as discussed in Section 4.3.4. This explains why the one-point Gaussian quadrature was adopted at the expense of scarifying some accuracy provided by higher-order integration schemes. Furthermore, a homogenous radiative medium was assumed, otherwise, view factors would have to be evaluated at each time step. This is far beyond the available computing capabilities.

Including the participating radiation submodel, it took approximately 30 seconds and 8 minutes of cpu time to compute one iteration for two- and three-dimensional cases, respectively. Usually, one time step takes two to four iterations to converge the solution to a predetermined level, say, ±1.E-4 for all state variables. The linear algebra solvers in *AKCESS.** employ a combination of factored tensor product and GMRES with incomplete LU preconditioner. Gaussian elimination and Gauss-Seidel are used for the radiation submodel. If Radflux is run independently, it only takes approximately one cpu hour to compute the view factors for the same problem, since Radflux does not compete with *AKCESS.** for memory and cpu time. In light of the major finding in this research, namely, the insignificant impact of thermal radiation on the scalar fields, it is appropriate

(economical) to compute the radiation field only in the last time step, hence the boundary radiative flux for the fire damageability studies.

Numerical stability plays a critical role in the demand for computing time. At a high Rayleigh number≥1.E6, the number of iterations increases and the Ra number dictates a much smaller time step. As discussed in Section 4.4.5, for a three-dimensional fire simulation, the solutions diverged at Ra=1.E6, regardless of time step. The only recourse is to increase the mesh, or to decrease the time step, or both. Overall, the dimensionless time step was between 0.01 and 0.5. In general, two dimensional cases took an hour to reach a steady state solution for a mesh of 16x16 elements, whereas three-dimensional cases (16x16x16 elements) took one to several days, depending on the nature of the problem.

From the life safety standpoint, fire communities are interested in the fire simulation period of five to thirty minutes. However, for the fire endurance of building construction, fire communities are interested in the simulation period of one to four hours. For the first type of application, 1200~7200 time stations are required, based on $\Delta t^*=0.25$. This can be very expensive even for two dimensions. To circumvent the costly cpu time, this research has selected a short duration to fully explore the engineering issues of laminar flow and thermal radiation.

Chapter Five

CONCLUSIONS

Imbued with the advancement of art and science of fire protection engineering, the objective of this research has been to explore the feasibility of CFD fire simulation for practical fire hazard analysis and fire protection designs. It is deemed that the current capability in this arena is not adequate for developing a sound and viable tool for practicing fire professionals. Nowadays, field modeling (CFD) is still viewed as a *prime dona* research "toy" that is not easily accessible to the majority of the professionals. One of the major obstacles has been computing resources, but this is rapidly becoming moderated. The second significant factor is the lack of a sensible protocol funneling the fire communities' efforts to develop such tool.

This research has touched some fundamental issues concerning CFD fire modeling:

(1) laminar flow is a viable candidate despite the dual dimensionless issue;

(2) unlike the participating thermal cavity, thermal radiation does not significantly impact the computed velocity and temperature fields (~0.1%) in this preliminary study on CFD-radiation fire modeling;

(3) easy, practical, and more importantly, totally *reproducible* fire benchmark cases are established;

(4) the utility of combined radiative and conductive (or convective) flux for a more realistic fire damageability study is demonstrated; and

(5) a standard finite element CFD methodology has been applied to fire modeling.

REFERENCES

References

[1] Mitler, H.E., and Emmons H.W., Documentation for CFC V, the Fifth Harvard Computer Fire Code, Harvard Home Fire Project T.R.#45 and NBS-GCR 81-344, NIST, Gaithersburg, MD, USA, 1981

[2] Cooper, L.Y., "A Mathematical Model for Estimating Available Safe Egress Time in Fires," Fire and Materials, V.6, N3 and 4, pp.135-144, 1982

[3] Bukowski, R.W., Peacock, R.D., Jones, W.W., and Forney, C.L., "HAZARD-I Fire Hazard Assessment Method," NIST Handbook 146, Volume II, NIST, Gaithersburg, MD, USA, 1988

[4] Jones, W.W., "A model for othe Transport of Fire, Smoke and Toxic Gases (FAST)," NBSIR 84-2934, NIST, Gaithersburg, MD, USA, 1984

[5] Tanaka, T., "A model of Multiroom Fire Spread," NBSIR 83-2718, NIST, Gaithersburg, MD, USA, 1983

[6] Budnick, E.K. and Walton, W.D., "Computer Fire Models," Fire Protection Hankdbook, 16th Ed., pp.21-(25-30), National Fire Protection Association, Boston, MA, USA, 1986

[7] Mitler, H.E., "Mathematical Modeling of Enclosure Fires," NISTIR 90-4294, NIST, Gaithersburg, MD, USA, May 1991

[8] Freidman, R., "An International Survey of Computer Models for Fire and Smoke," J. of Fire Protection Engr., 4(3), pp. 81-92, 1992

[9] Nelson, H.E., *FPETOOL: Fire Protection Engineering Tools for Hazard Estimation*, NISTIR Report 4380, NIST, Gaithersburg, MD, USA, 1991

[10] Yang, K.T., and Chang L.C., "UNDSAFE-I: A Computer Code for Buoyant Flow in an Enclosure," NBS-GCR 77-84, NIST, Gaithersburg, MD, USA, 1977

[11] Ku, A.C., Doria, M.L., and Lloyd J.R., "Numerical Modeling of Unsteady Buoyant Flows Generated by Fire in a Corridor," The 16-th International Symposium on Combustion, August 15-20, Pittsburg, PA, USA, 1976

[12] Liu, V.K., and Yang, K.T., "UNDSAFE-II: A Computer Code for Buoyant Turbulent Flow in an Enclosure with Thermal Radiation," NBS-GCR-78-150, 1978

[13] Markatos, N.C., Pericleous, K.A., and Cox, G., "A Novel Approach to the Field Modeling of Fire," PCH PhysicoChemical Hydrodynamics, Vol 7, No.2/3, pp 125-143, 1986

[14] Cox, G., Kumar, S., and Markatos, N.C., "Some Field Model Validation Studies," Fire Safety Science-Proceedings of the First International Symposium, pp.159-171, 1986

[15] Baum, H.R., and Rehm, R.G., "Calculations of Three Dimensional Buoyant Plumes in Enclsoure," Combustion Science and Technology, Vol.40, pp.55-77, 1984

[16] McCaffrey, B., "Purely Buoyant Diffusion Flames: Some Experimental Results," NBSIR 79-1910, NIST, 1979

[17] Markatos, N.C. and Cox, G., "Turbulent Buoyant Heat Transfer in Enclosures Containing a Fire Source," Proceedings of The Seventh International Heat Transfer Conference, V.6, Hemisphere, London, p.373, 1982

[18] Rehm, R.G. and Baum, H.R., "The Equations of Motion for Thermally Driven Buoyant Flows," NBSJ Res. 83, 297, NIST, Gaithersburg, MD, 1978

[19] Baum, H.R. and Rehm, R.G., "Numerical Computation of Large-scale Fire Induced Flows," The Eighth International Conference on Numerical Methods in Fluid Dynamics, Springer-Verlag, Berlin, Germany, V.170, p.124, 1982

[20] Baum, H.R. and McCaffrey, B.J., "Fire Induced Flow Field - Theory and Experiment," Fire Safety Science - Proceedings of the Second International Symposium, pp. 129-148, 1988

[21] Morita, M., Hirota, M., and Oka, Y., "Numerical Analaysis and Computational Methods of Heat Flow in Fire Compartment," Fire Safety Science-Proceedings of the Second International Symposium, pp.189-1988

[22] Galea, E.R., and Markatos, N.C., "Prediction of Fire Development in Aircraft," 2nd International Phoenics Users Conference, London, Nov 1987

[23] Galea, E.R., and Markatos, N.C., "Modelling of Aircraft Cabin Fires," Fire Safety Science-Proceedings of the Second International Symposium, pp.801-810, 1988

[24] Galea, E., "On the Field Modelling Approach to the Simulation of Enclosure Fires," J. of Fire Protection Engineering, Vol.1, No.1, pp.11-22, 1989

[25] Waters, R.A., "Stansted Terminal Building and Early Atrium Studies," J. of Fire Protection Engineering, Vol.1, No.2, pp.63-76, 1989

[26] Chow, W.K., and Leung, W.M., "Application of Field Models for Simulating Building Fires at the Preflashover Stage," J. of Hong Kong Engineer, pp.25-27, July, 1988

[27] Chow, W.K. and Leung, W.M., "Application of Field Model to Tunnel Fire Service Design," Proceedings of 6th International Symposium of Aerodynamics and Ventilation of Vehicle Tunnels Paper H1, 495, 1988

[28] Alpert, R.L., and Delichatsios, M.M., "Calculated Interaction of Water Droplet Sprays with Fire Plumes in Compartments," NBS-GCR-86-520, 1986

[29] Chow, W.K., and Fong, N.K., "Numerical Simulation on Cooling of the Fire-Induced Air Flow by Sprinkler Water Spray," Fire Safety Journal, Vol.17, No.4, pp.263-290, 1991

[30] Hoffmann, N.A., and Galea, E.R., "On the Eulerian-Eulerian Approach to Fire-Sprinkler Modelling," J. of Fire Protection Engineering, Vol.3, No.4, pp.123-136, 1991

[31] Simcox, S., Wilkes, N.S., and Jones, I.P., "Computer Simulation of the Flows of Hot Gases from the Fire at King's Cross Underground Station," Fire Safety Journal, Vol.18, No.1, pp.49-73, 1991

[32] Davis, W.D., Forney, G.P., and Klote, J.H., "Field Modeling of Room Fire," NISTIR 4673, Nov., 1991

[33] Forney, G.P., Davis, W.D., and Klote, J.H., "Simulating the Effect of Beamed Ceilings on Smoke Flow, Part I. Comparison of Numerical and Experimental Results," NISTIR 4994, Dec., 1992

[34] Forney, G.P. and Davis, W.D., "Analyzing Strategies for Eliminating Flame Blown-down Occurring in the Navy's 19F4 Fire Fighting Trainer," NISTIR 4825, Gaithersburg, MD, USA, 1992

[35] Wong, D.H., "Three-dimensional, Field Modeling of Enclosure Fires," Sothwest Research Institute IR Project 01-9604, Feb., 1991

[36] Schnipke, R.J., and Rice, J.G., "A Streamline Upwid Finite-Element Method for Laminar and Turbulent Flow," PhD Dissertation, University of Virgina, UVA/643092/MAE86/342, Jun., 1986

[37] Satoh, K., "Numerical Study of Smoke and Heat Spread at Early Stage of Room Fires," Report of the 4th CIB W14 Workshop on Fire Modeling, NISTIR 4338, NIST, Gaithersburg, MD, USA, 1990

[38] Hadjisophocleous, G.V. and Cacambouras, M., "Computer Modeling of Compartment Fires," J. of Fire Protection Engineering, 5(2), pp. 39-52, 1993

[39] Chow, W.K., "Application of Field Modeling Technique on Fire Services Design," Far East Conference on Environmental Quality, ASHRAE, Hong Kong, 1991

[40] Chow, W.K. and Wong, W.K., "A Study of the Fire Aspect of Atria in Hong Kong," Fire Safety Science-Proceedings of The Third International Symposium, pp. 335-344, 1991

[41] McGrattan, K.B., Rehm, R.G. and Baum, H.R., "Fire-Driven Flows in Enclosures," J. of Computational Physics, 110, pp. 285-291, 1994

[42] Baum, H.R., Ezekoye, K.B., McGrattan, K.B. and Rehm, R.G., "Mathematical Modeling and Computer Simulation of Fire Phenomena," Theoretical Computational Fluid Dynamics, 6, pp. 125-139, 1994

[43] Rehm, R.G., Haum, H.R., Lozier, D.W., Tang, H. and Sims, J., "Buoyant Convection in an Inclined Enclosure," Fire Safety Science-Proceedings of The Third International Symposium, pp.313-323, 1991

[44] Barton, J.M., private communication, Analytical Methods, Inc., Redmond, WA, USA, 1995

[45] Evans, D.D., "Ceiling Jet Flow," Fire Protection Engineering Handbook, SFPE/NFPA, 1st Ed., Boston, MA, USA, 1988

[46] Babrauskas, V., "Pool Fires: Burning Rates and Heat Fluxes," Fire Protection Handbook, 16th Ed., NFPA, Boston, MA, USA, p.21-36, 1986

[47] Chan, W.R., Zukoski, E.E. and Kubota, T., "Experimental and Numerical Studies on Two-Dimensional Gravity Currents in a Horizontal Channel," Guggenheim Jet Propulsion Center, CIT, Pasadena, CA, USA, 1992

[48] Fleischmann, C.M., Pagni, P.J. and Williamson, R.B., "Backdraft Experiments," PhD Thesis, Civil Engineering Department, University of California, Berkeley, CA, 1993

[49] Guilbert, P.W., "Comparison of Monte Carlo and Discrete Transfer Methods for Modelling Thermal Radiation," AERE-R 13423 HCCP/R22/1989, Harwell Laborartory, Mar., 1989

[50] Hottel, H.C., and Sarofim, A.F., *Radiative Transfer*, McGraw Hill, pp.256-296, 1967

[51] Burns, A.D., Clarke, D.S., Guilbert, P., Jones, I.P., Simcox, S. and Wilkes, N.S., "The Application of CFD to the Modelling of Fires in Complex Geometries," Computational Fluid Dynamics, V1, pp.517-534, 1992

[52] Fusegi, T and Farouk, B., "Numerical Study on Interactions of Turbulent Convection and Radiation in Compartment Fires," Fire Science Technology, Vol. 8, No.1, pp.15-28, 1988

[53] Kumar, S., Gupta, A. K. and Cox, G., "Effects of Thermal Radiation on the Fluid Dynamics of Compartment Fires," Fire Safety Science-Proceedings of the Third International Symposium, pp.345-354, 1991

[54] Yucel, A., Acharya, S. and Williams, M. L., "Natural Convection and Radiation in a Square Enclosure," Numerical Heat Transfer, Part A, Vol.15, pp.261-278, 1989

[55] Fusegi, T., Farouk, B. and Kuwahara, K., "3-D Natural Convection-Radiation Interactions in a Cube Filled with Gas-Soot Mixtures," Fire Safety Science-Proceedings of the Third International Symposium, pp.366-374, 1991

[56] Draoui, A., Allard, F. and Beghein, C, "Numerical Analysis of Heat Transfer by Natural Convection and Radiation in Participating Fluids Enclosed in Square Cavities," Numerical Heat Transfer, Part A, Vol.20, pp.253-261, 1991

[57] Fusegi, T. and Farouk, B., "Laminar and Turbulent Natural Convection-Radiation Interactions in a Square Enclosure Filled with a Nongray Gas," Numerical Heat Transfer, Part A, Vol.15, pp.303-322, 1989

[58] *Radiation Heat Transfer*, Heat Transfet Divion V.154, ASME, 1990

[59] Naraghi, M. H. N. and Kassemi, M., "Analysis of Radiative Transfer in Rectangular Enclosures Using a Discrete Exchange Factor Method," Journal of Heat Transfer, Vol.111, pp.1117-1119, November 1989

[60] Huan, J. and Naraghi, M.H.N., "Analysis of Radiative Heat Transfer in Three-Dimensional Absorbing, Emitting, and Scattering Media - A Source Function Approach," ASME, HTD-Vol.154, pp.59-66, Nov., 1990

[61] Baker, A. J., and Kim, J. W., "A Taylor Weak-Statement Algorithm for Hyperbolic Conservation Laws," International Journal for Numerical Methods in Fluids, Vol.7, 1987

[62] Williams, P. T., "CCM Continuity Constraint Method: A Finite-Element Computational Fluid Dynamics Algorithm for Incompressible Navier-Stokes Fluid Flows," Oak Ridge National Laboratory ORNL/TM-12389, September 1993[62] Ozisik, M. N.,

[63] Bell, J. B. and Marcus, D. L., "A Second-Order Projection Method for Variable-Density Flows," Journal of Computational Physics, Vol. 101, pp.334-348, 1992

[64] Baker, A. J., *Finite Element Computational Fluid Mechanics*, McGraw Hill, 1983

[65] *AKCESS*.4CFD for Finite Element CFD Modeling in *AKCESS*.* User Guide, Computational Mechanics Corporation, Knoxville, TN 37919, USA, 1994

[66] Ozisik, M.N., *Radiation Transfer and Interactions with Conduction and Convection*, Wiley.

[67] Sparrow, E. M. and Cess, R. D., *Radiation Heat Transfer*, Revised Edition, Brooks/Cole Publishing Company

[68] Siegel, R. and Howell, J., *Thermal Radiation Heat Transfer*, Second Edition, Hemisphere/McGraw-Hill, 1981

[69] Incropera, F.P. and DeWitt, D.P., *Fundamentals of Heat Transfer*, Wiley, p.634, 1981

[70] Brewster, M.Q., *Thermal Radiative Transfer and Properties*, Wiley, p.372, 1992

[71] Shih, T.M. and Ten, A.L., "Combined Convective and Radiative Recirculating Flows in Enclosures," J. of Numerical Heat Transfer, V.8, pp.149-167, 1985

[72] Heskestad, G., "Fire Plume," *Fire Protection Engineering Handbook*, 1st Ed., SFPE/NFPA, Boston, MA, 1988

[73] Evans, D., "Ceiling Jet Flow," *Fire Protection Engineering Handbook*, 1st Ed., SFPE/NFPA, Boston, MA, 1988

[74] Wong, D. H.,"Fire Damageability Due to Thermal (Heat) Flux," SFPE/NFPA Engineering Seminars, New Orleans, LA, USA, May 1992

[75] Drysdale, D., *Introduction to Fire Dynamics*, Wiley, 1985

Appendix A

2-D Benchmark Verification Solutions

A.1 Case 1: 2-D Thermal Cavity Steady State Solutions, Ra=1.E4

PURE CONVECTION
BC's: No slip; Vertical Dirichlet Temp. and Horizontal Adiabatic Walls
Explict Parameters: Ra=1.E4, Pr=0.7, Ar=1.0, Gr=1.43E4, Re=120, Pe=83.6
Implict Parameters: Lo=1 m, Nu=15.89E-6 m2/s, To=294.4 K, dTo=3.68E-7
ko=26.3E-6 m2/s, po=2.21E-3 Pa, rho,o=1.16 kg/m3
alpha,o=22.5E-6 m2/s, Uo=1.9E-3 m/s, to=527.4 s

U1 EXP -3 PLANE 1

1:	2:	3:	4:	5:	6:	7:	8:	9:	10:	11:	12:	13:	14:	15:	16:	17:
0	0	0	0	0	0	0	0	0	0	0	0	0	0	0	0	0
0	8	37	67	95	113	123	126	123	117	112	106	100	87	66	18	0
0	10	51	92	131	160	177	184	183	177	168	155	141	113	78	18	0
0	11	54	96	137	166	185	194	196	191	182	166	146	111	70	16	0
0	11	53	91	126	150	166	174	177	175	167	153	130	96	56	12	0
0	10	49	80	106	122	132	138	141	141	136	124	103	72	39	7	0
0	9	41	62	77	84	89	93	96	98	95	86	69	45	20	3	0
0	7	30	39	43	42	43	45	48	51	51	45	32	16	1	0	0
0	4	15	12	6	-1	-4	-3	0	3	4	1	-6	-12	-15	-4	0
0	0	-1	-16	-32	-45	-51	-51	-48	-45	-43	-42	-43	-39	-30	-7	0
0	-3	-20	-45	-69	-86	-95	-98	-96	-93	-89	-84	-77	-62	-41	-9	0
0	-7	-39	-72	-103	-124	-136	-141	-141	-138	-132	-122	-106	-80	-49	-10	0
0	-12	-56	-96	-130	-153	-167	-175	-177	-174	-166	-150	-126	-91	-53	-11	0
0	-16	-70	-111	-146	-166	-182	-191	-196	-194	-185	-166	-137	-96	-54	-11	0
0	-18	-78	-113	-141	-155	-168	-177	-183	-184	-177	-160	-131	-92	-51	-10	0
0	-18	-66	-87	-100	-106	-112	-117	-123	-126	-123	-113	-95	-67	-37	-8	0
0	0	0	0	0	0	0	0	0	0	0	0	0	0	0	0	0

U2 EXP -3 PLANE 1

1:	2:	3:	4:	5:	6:	7:	8:	9:	10:	11:	12:	13:	14:	15:	16:	17:
0	0	0	0	0	0	0	0	0	0	0	0	0	0	0	0	0
0	8	11	11	8	5	1	0	-1	-2	-1	-1	-2	-6	-11	-18	0
0	37	52	52	41	26	11	0	-6	-10	-10	-11	-16	-32	-58	-72	0
0	66	93	92	74	49	24	4	-9	-17	-22	-27	-40	-67	-106	-116	0
0	99	138	135	107	71	37	9	-10	-23	-33	-45	-67	-107	-154	-155	0
0	129	176	168	132	88	47	15	-9	-27	-43	-63	-94	-143	-193	-182	0
0	157	208	193	147	97	53	19	-7	-28	-50	-77	-118	-173	-222	-198	0
0	180	230	205	152	99	56	22	-3	-27	-54	-88	-136	-195	-238	-202	0
0	195	241	206	148	96	56	25	0	-25	-56	-96	-148	-206	-241	-195	0
0	202	238	195	136	88	54	27	3	-22	-56	-99	-152	-205	-230	-180	0
0	198	222	173	118	77	50	28	7	-19	-53	-97	-147	-193	-208	-157	0
0	182	193	143	94	63	43	27	9	-15	-47	-88	-132	-168	-176	-129	0
0	155	154	107	67	45	33	23	10	-9	-37	-71	-107	-135	-138	-99	0
0	116	106	67	40	27	22	17	9	-4	-24	-49	-74	-92	-93	-66	0
0	72	58	32	16	11	10	10	6	0	-11	-26	-41	-52	-52	-37	0
0	18	11	6	2	1	1	2	1	0	-1	-5	-8	-11	-11	-8	0
0	0	0	0	0	0	0	0	0	0	0	0	0	0	0	0	0

TEMPERATURE EXP -2 PLANE 1

1:	2:	3:	4:	5:	6:	7:	8:	9:	10:	11:	12:	13:	14:	15:	16:	17:
100	96	92	89	87	84	82	80	78	75	72	68	61	52	37	19	0
100	96	92	89	86	84	82	80	78	75	73	69	62	53	39	20	0
100	95	91	87	84	82	80	78	76	75	72	69	63	54	40	21	0
100	94	89	84	81	78	76	75	74	72	71	68	63	54	40	21	0
100	92	86	80	76	73	72	70	70	69	68	66	61	53	39	20	0
100	90	82	75	70	67	66	65	65	65	64	63	58	50	37	19	0
100	88	78	70	65	61	60	60	60	60	60	59	55	47	34	18	0
100	86	75	65	59	55	54	54	55	55	55	54	50	43	31	16	0
100	85	71	60	54	50	49	49	49	50	50	49	45	39	28	14	0
100	83	68	56	49	45	44	44	44	45	45	44	40	34	24	13	0
100	81	65	52	44	40	39	39	39	39	39	38	34	29	21	11	0
100	80	62	49	41	36	35	34	34	34	33	32	29	24	17	9	0
100	79	60	46	38	33	31	30	29	29	27	26	23	19	13	7	0
100	78	59	45	36	31	28	27	25	24	23	21	18	15	10	5	0
100	78	59	45	36	30	27	24	23	21	19	17	15	12	8	4	0
100	79	60	46	37	30	26	24	21	19	17	15	13	10	7	3	0
100	80	62	47	38	31	27	24	21	19	17	15	12	10	7	3	0

A.2 Case 2: 2-D Ad Hoc Benchmark Baseline Conductive Flux

PURE CONVECTION
BC's: No slip; Vertical Non-zero Neumann. and Horizontal Adiabatic Walls
Explict Parameters: Ra=1.E4, Pr=0.7, Ar=1.0, Gr=1.43E4, Re=120, Pe=83.6
Implict Parameters: Lo=1 m, Nu=15.89E-6 m2/s, To=294.4 K, dTo=3.68E-7
ko=26.3E-6 m2/s, po=2.21E-3 Pa, rho,o=1.16 kg/m3
alpha,o=22.5E-6 m2/s, Uo=1.9E-3 m/s, to=527.4 s

TEMPERATURE EXP -3 PLANE 1

1:	2:	3:	4:	5:	6:	7:	8:	9:	10:	11:	12:	13:	14:	15:	16:	17:
991	965	929	899	871	846	824	803	782	759	729	686	621	522	383	193	44
993	963	926	895	867	843	821	800	781	759	731	692	632	536	395	201	38
992	957	914	879	849	824	804	786	769	751	729	695	641	549	408	207	38
989	946	892	848	813	788	769	755	742	730	713	686	637	549	409	207	38
987	930	861	806	764	737	720	710	703	696	685	663	619	534	398	201	37
983	913	825	757	708	678	663	657	655	653	647	630	590	509	378	191	35
980	894	787	706	650	618	604	601	603	606	604	590	552	476	352	177	33
976	874	749	656	593	560	547	546	551	557	557	544	508	436	321	161	30
973	856	713	608	540	505	493	494	499	505	506	494	459	391	286	143	26
969	838	678	563	491	455	442	442	448	452	452	439	406	343	250	125	23
966	822	647	523	447	409	395	393	395	398	395	381	349	293	212	105	19
964	808	621	490	409	369	352	346	344	342	336	321	291	242	174	86	16
962	798	601	464	380	336	314	303	296	289	279	262	235	193	138	69	12
961	792	590	450	362	313	286	269	257	244	230	211	185	151	107	53	10
961	792	591	450	358	304	270	248	230	213	195	175	150	120	85	42	7
961	798	604	463	367	307	268	240	218	198	178	156	132	104	73	36	6
955	806	616	477	378	313	270	240	217	196	175	153	128	100	70	34	8

CONDUCTIVE FLUX EXP -4 PLANE 1

1:	2:	3:	4:	5:	6:	7:	8:	9:	10:	11:	12:	13:	14:	15:	16:	17:
110	6	11	14	16	16	14	12	9	4	-1	-9	-19	-26	-24	-13	-556
70	0	0	0	0	0	0	0	0	0	0	0	0	0	0	0	-385
82	0	0	0	0	0	0	0	0	0	0	0	0	0	0	0	-397
104	0	0	0	0	0	0	0	0	0	0	0	0	0	0	0	-398
134	0	0	0	0	0	0	0	0	0	0	0	0	0	0	0	-387
168	0	0	0	0	0	0	0	0	0	0	0	0	0	0	0	-367
205	0	0	0	0	0	0	0	0	0	0	0	0	0	0	0	-342
242	0	0	0	0	0	0	0	0	0	0	0	0	0	0	0	-311
278	0	0	0	0	0	0	0	0	0	0	0	0	0	0	0	-278
311	0	0	0	0	0	0	0	0	0	0	0	0	0	0	0	-242
342	0	0	0	0	0	0	0	0	0	0	0	0	0	0	0	-205
367	0	0	0	0	0	0	0	0	0	0	0	0	0	0	0	-168
387	0	0	0	0	0	0	0	0	0	0	0	0	0	0	0	-134
398	0	0	0	0	0	0	0	0	0	0	0	0	0	0	0	-104
397	0	0	0	0	0	0	0	0	0	0	0	0	0	0	0	-82
385	0	0	0	0	0	0	0	0	0	0	0	0	0	0	0	-70
556	13	24	26	19	9	1	-4	-9	-12	-14	-16	-16	-14	-11	-6	-110

A.3 Case 3: 2-D Verification of Combined Conductive and Radiative Flux in a Non-Participating Medium, e=1.

CONVECTION + RADIATION
BC's: No slip; Vertical Non-zero Neumann and Horizontal Adiabatic Walls
Explict Parameters: Ra=1.E4, Pr=0.7, Ar=1.0, Gr=1.43E4, Re=120, Pe=83.6
Bo=40.65
Implict Parameters: Lo=1 m, Nu=15.89E-6 m2/s, To=294.4 K, dTo=3.68E-7
ko=26.3E-6 m2/s, po=2.21E-3 Pa, rho,o=1.16 kg/m3
alpha,o=22.5E-6 m2/s, Uo=1.9E-3 m/s, to=527.4 s
black surfaces

TEMPERATURE EXP -3 PLANE 1

1:	2:	3:	4:	5:	6:	7:	8:	9:	10:	11:	12:	13:	14:	15:	16:	17:
984	966	929	899	871	846	824	803	782	759	729	686	621	522	383	192	46
984	965	926	895	867	843	821	800	781	759	731	692	632	536	396	200	42
983	959	914	879	849	824	804	786	769	751	729	695	641	549	408	206	43
980	949	893	848	813	788	769	755	742	730	713	686	637	549	409	206	44
977	934	862	806	764	737	720	710	703	696	685	663	619	534	398	200	43
974	916	826	757	708	678	663	657	655	653	647	630	590	509	378	190	41
970	897	788	706	650	618	604	601	603	606	604	590	552	476	352	176	39
966	878	751	656	593	560	547	546	551	557	557	544	508	436	321	160	36
962	859	714	608	540	505	493	494	499	505	506	494	459	391	287	142	33
959	842	680	563	491	455	442	442	448	452	452	439	406	343	250	123	29
956	826	649	524	447	409	395	393	395	398	395	381	349	293	212	104	26
954	812	622	490	409	369	352	346	344	342	336	321	291	242	174	85	22
952	801	603	465	380	336	314	303	296	289	279	262	235	193	138	67	19
951	795	592	450	362	313	286	269	257	244	230	211	185	151	107	52	15
952	795	592	450	358	304	270	248	230	213	195	175	150	120	85	41	13
954	801	605	464	367	307	268	240	218	198	178	156	132	104	73	35	12
951	809	618	477	378	313	270	240	217	196	175	153	128	100	70	33	13

RADIATIVE FLUX EXP -4 PLANE 1

1:	2:	3:	4:	5:	6:	7:	8:	9:	10:	11:	12:	13:	14:	15:	16:	17:
153	80	59	44	32	24	19	15	11	6	0	-8	-21	-35	-44	-45	-42
174	0	0	0	0	0	0	0	0	0	0	0	0	0	0	0	-98
188	0	0	0	0	0	0	0	0	0	0	0	0	0	0	0	-110
197	0	0	0	0	0	0	0	0	0	0	0	0	0	0	0	-120
204	0	0	0	0	0	0	0	0	0	0	0	0	0	0	0	-127
209	0	0	0	0	0	0	0	0	0	0	0	0	0	0	0	-132
214	0	0	0	0	0	0	0	0	0	0	0	0	0	0	0	-136
217	0	0	0	0	0	0	0	0	0	0	0	0	0	0	0	-138
220	0	0	0	0	0	0	0	0	0	0	0	0	0	0	0	-138
221	0	0	0	0	0	0	0	0	0	0	0	0	0	0	0	-138
222	0	0	0	0	0	0	0	0	0	0	0	0	0	0	0	-136
222	0	0	0	0	0	0	0	0	0	0	0	0	0	0	0	-133
219	0	0	0	0	0	0	0	0	0	0	0	0	0	0	0	-129
213	0	0	0	0	0	0	0	0	0	0	0	0	0	0	0	-124
197	0	0	0	0	0	0	0	0	0	0	0	0	0	0	0	-118
153	0	0	0	0	0	0	0	0	0	0	0	0	0	0	0	-112
88	-51	-108	-124	-125	-121	-115	-109	-102	-96	-90	-84	-78	-72	-67	-62	-106

A.4 Case 4: 2-D Verification of Combined Conductive and Radiative Flux in a Non-Participating Medium, e=0.1

CONVECTION + RADIATION
BC's: No slip; Vertical Dirichlet Temp. and Horizontal Adiabatic Walls
Explict Parameters: Ra=1.E4, Pr=0.7, Ar=1.0, Gr=1.43E4, Re=120, Pe=83.6, Bo=40.65
Implict Parameters: Lo=1 m, Nu=15.89E-6 m2/s, To=294.4 K, dTo=3.68E-7
ko=26.3E-6 m2/s, po=2.21E-3 Pa, rho,o=1.16 kg/m3
alpha,o=22.5E-6 m2/s, Uo=1.9E-3 m/s, to=527.4 s, gray walls

TEMPERATURE EXP -3 PLANE 1

1:	2:	3:	4:	5:	6:	7:	8:	9:	10:	11:	12:	13:	14:	15:	16:	17:
990	965	929	899	871	846	824	803	782	759	729	686	621	522	383	193	44
992	963	926	895	867	843	821	800	781	759	731	692	632	536	395	201	38
991	957	914	879	849	824	804	786	769	751	729	695	641	549	408	207	38
989	948	893	848	813	788	769	755	742	730	713	686	637	549	409	207	39
986	932	863	806	764	737	720	710	703	696	685	663	619	534	398	201	37
983	914	827	757	708	678	663	657	655	653	647	630	590	509	378	191	36
979	896	789	706	650	618	604	601	603	606	604	590	552	476	352	177	33
976	876	751	656	593	560	547	546	551	557	557	544	508	436	321	161	30
972	858	714	608	540	505	493	494	499	505	506	494	459	391	286	143	27
969	840	680	563	491	455	442	442	448	452	452	439	406	343	250	125	23
966	824	649	523	447	409	395	393	395	398	395	381	349	293	212	105	20
963	810	623	490	409	369	352	346	344	342	336	321	291	242	174	86	16
961	800	603	465	380	336	314	303	296	289	279	262	235	193	138	68	13
960	794	592	450	362	313	286	269	257	244	230	211	185	151	107	53	10
960	794	593	450	358	304	270	248	230	213	195	175	150	120	85	42	8
961	800	605	463	367	307	268	240	218	198	178	156	132	104	73	36	7
955	808	618	477	378	313	270	240	217	196	175	153	128	100	70	34	8

RADIATIVE FLUX EXP -4 PLANE 1

1:	2:	3:	4:	5:	6:	7:	8:	9:	10:	11:	12:	13:	14:	15:	16:	17:
153	116	90	68	50	35	23	12	3	-6	-18	-32	-50	-68	-80	-85	-84
156	0	0	0	0	0	0	0	0	0	0	0	0	0	0	0	-88
157	0	0	0	0	0	0	0	0	0	0	0	0	0	0	0	-89
159	0	0	0	0	0	0	0	0	0	0	0	0	0	0	0	-91
159	0	0	0	0	0	0	0	0	0	0	0	0	0	0	0	-92
160	0	0	0	0	0	0	0	0	0	0	0	0	0	0	0	-92
161	0	0	0	0	0	0	0	0	0	0	0	0	0	0	0	-93
161	0	0	0	0	0	0	0	0	0	0	0	0	0	0	0	-93
161	0	0	0	0	0	0	0	0	0	0	0	0	0	0	0	-93
161	0	0	0	0	0	0	0	0	0	0	0	0	0	0	0	-93
161	0	0	0	0	0	0	0	0	0	0	0	0	0	0	0	-93
161	0	0	0	0	0	0	0	0	0	0	0	0	0	0	0	-92
161	0	0	0	0	0	0	0	0	0	0	0	0	0	0	0	-92
160	0	0	0	0	0	0	0	0	0	0	0	0	0	0	0	-91
158	0	0	0	0	0	0	0	0	0	0	0	0	0	0	0	-91
152	0	0	0	0	0	0	0	0	0	0	0	0	0	0	0	-90
148	4	-58	-80	-87	-90	-90	-90	-90	-89	-89	-88	-88	-87	-87	-86	-89

A.5 Case 5: 2-D Verification of Combined Conductive and Radiative Flux in a Participating Medium, e=1.0

CONVECTION + RADIATION

BC's: No slip; Vertical Non-zero Neumann and Horizontal Adiabatic Walls

Explict Parameters: Ra=1.E4, Pr=0.7, Ar=1.0, Gr=1.43E4, Re=120, Pe=83.6, Bo=40.65

Implict Parameters: Lo=1 m, Nu=15.89E-6 m2/s, To=294.4 K, dTo=3.68E-7, ko=26.3E-6 m2/s
po=2.21E-3 Pa, rho,o=1.16 kg/m3, alpha,o=22.5E-6 m2/s, Uo=1.9E-3 m/s
to=527.4 s, Ka=Kt=1.0 1/m, Ks=0. 1/m, Omega,o=0, black surfaces

TEMPERATURE EXP -3 PLANE 1

1:	2:	3:	4:	5:	6:	7:	8:	9:	10:	11:	12:	13:	14:	15:	16:	17:
987	966	929	899	871	846	824	803	782	759	729	686	621	522	383	193	45
987	964	926	895	867	843	821	800	781	759	731	692	632	536	396	201	40
985	958	914	879	849	824	804	786	769	751	729	695	641	550	408	207	40
982	947	891	848	814	788	769	755	742	730	713	686	637	549	409	207	41
979	932	860	806	764	737	720	710	703	696	685	663	619	535	398	201	40
975	914	825	757	708	678	663	657	655	653	647	630	590	509	378	191	38
971	895	787	707	650	618	604	602	604	606	604	590	552	476	352	177	35
967	876	749	656	594	560	548	547	552	557	557	544	509	436	321	161	32
963	858	713	609	541	506	494	494	500	506	506	494	460	392	287	143	29
960	840	678	564	492	456	443	443	448	453	452	440	406	344	250	124	25
957	824	648	524	448	410	396	393	396	398	395	382	350	293	212	105	22
954	810	621	491	410	370	352	346	345	343	337	321	292	242	174	86	18
952	800	602	465	381	337	315	304	297	290	280	263	235	194	139	68	15
951	794	591	451	363	314	287	270	257	245	230	212	186	151	108	53	12
951	794	591	451	359	304	271	248	230	213	196	175	150	120	85	42	9
952	800	604	464	368	307	268	241	219	199	179	157	132	104	73	36	8
951	807	616	477	378	313	270	241	217	196	175	153	128	100	70	34	9

RADIATIVE FLUX EXP -4 PLANE 1

1:	2:	3:	4:	5:	6:	7:	8:	9:	10:	11:	12:	13:	14:	15:	16:	17:
77	50	47	39	34	30	28	26	24	21	17	9	0	-10	-16	-16	-26
117	0	0	0	0	0	0	0	0	0	0	0	0	0	0	0	-43
135	0	0	0	0	0	0	0	0	0	0	0	0	0	0	0	-50
148	0	0	0	0	0	0	0	0	0	0	0	0	0	0	0	-54
159	0	0	0	0	0	0	0	0	0	0	0	0	0	0	0	-56
170	0	0	0	0	0	0	0	0	0	0	0	0	0	0	0	-57
179	0	0	0	0	0	0	0	0	0	0	0	0	0	0	0	-56
187	0	0	0	0	0	0	0	0	0	0	0	0	0	0	0	-55
195	0	0	0	0	0	0	0	0	0	0	0	0	0	0	0	-53
201	0	0	0	0	0	0	0	0	0	0	0	0	0	0	0	-51
206	0	0	0	0	0	0	0	0	0	0	0	0	0	0	0	-48
209	0	0	0	0	0	0	0	0	0	0	0	0	0	0	0	-46
212	0	0	0	0	0	0	0	0	0	0	0	0	0	0	0	-43
212	0	0	0	0	0	0	0	0	0	0	0	0	0	0	0	-40
209	0	0	0	0	0	0	0	0	0	0	0	0	0	0	0	-37
198	0	0	0	0	0	0	0	0	0	0	0	0	0	0	0	-33
71	-53	-69	-79	-76	-69	-62	-56	-50	-45	-40	-36	-32	-28	-25	-21	-25

DIVERGENCE OF RADIATIVE FLUX EXP -4 PLANE 1

1:	2:	3:	4:	5:	6:	7:	8:	9:	10:	11:	12:	13:	14:	15:	16:	17:
0	0	0	0	0	0	0	0	0	0	0	0	0	0	0	0	0
0	304	258	159	105	80	71	72	76	77	63	23	-51	-144	-208	-204	0
0	303	219	85	19	-2	1	19	42	60	61	28	-50	-159	-239	-238	0
0	232	100	-73	-151	-165	-140	-97	-48	-5	18	5	-62	-169	-253	-254	0
0	120	-61	-273	-356	-357	-312	-245	-172	-105	-58	-51	-100	-192	-266	-264	0
0	-9	-232	-468	-545	-531	-468	-383	-294	-211	-149	-124	-153	-222	-277	-268	0
0	-139	-389	-630	-692	-660	-584	-490	-393	-304	-234	-198	-208	-252	-285	-267	0
0	-261	-523	-754	-792	-743	-657	-560	-463	-375	-303	-261	-255	-276	-288	-264	0
0	-370	-630	-840	-853	-787	-696	-599	-506	-422	-354	-309	-291	-292	-287	-257	0
0	-462	-712	-895	-882	-803	-708	-615	-527	-450	-386	-340	-314	-299	-282	-248	0
0	-538	-770	-924	-888	-799	-702	-612	-531	-460	-401	-355	-322	-298	-272	-237	0
0	-594	-805	-930	-875	-778	-682	-595	-520	-455	-400	-355	-319	-289	-260	-225	0
0	-628	-815	-914	-845	-744	-648	-566	-496	-437	-386	-343	-307	-275	-245	-213	0
0	-634	-795	-874	-796	-694	-603	-527	-463	-409	-363	-323	-289	-258	-229	-200	0
0	-602	-732	-799	-723	-629	-547	-479	-423	-375	-334	-299	-267	-239	-213	-186	0
0	-517	-606	-668	-608	-535	-470	-416	-370	-331	-296	-266	-239	-214	-192	-168	0
0	0	0	0	0	0	0	0	0	0	0	0	0	0	0	0	0

A.6 Case 6: 2-D Verification of Combined Radiative and Conductive Flux in a Participating Medium, e=0.1

CONVECTION + RADIATION

BC's: No slip; Vertical Non-zero Neumann and Horizontal Adiabatic Walls

Explict Parameters: Ra=1.E4, Pr=0.7, Ar=1.0, Gr=1.43E4, Re=120, Pe=83.6, Bo=40.65

Implict Parameters: Lo=1 m, Nu=15.89E-6 m2/s, To=294.4 K, dTo=3.68E-7, ko=26.3E-6 m2/s po=2.21E-3 Pa, rho,o=1.16 kg/m3, alpha,o=22.5E-6 m2/s, Uo=1.9E-3 m/s to=527.4 s, Ka=Kt=1.0 1/m, Ks=0. 1/m, Omega,o=0, gray surfaces

TEMPERATURE EXP -3 PLANE 1

1:	2:	3:	4:	5:	6:	7:	8:	9:	10:	11:	12:	13:	14:	15:	16:	17:
992	964	928	898	871	846	824	803	782	758	729	686	621	522	383	193	44
992	958	922	892	864	840	819	799	779	757	730	692	631	536	396	202	38
991	952	910	876	846	822	802	784	767	750	727	695	641	550	409	208	39
989	941	888	846	812	786	768	753	741	729	712	685	637	549	410	208	39
986	926	858	804	763	736	719	709	702	695	684	662	619	535	399	202	38
983	909	822	756	707	678	663	657	655	653	647	630	590	510	379	192	36
979	890	785	706	650	618	604	602	604	606	604	590	553	476	353	178	33
976	872	748	656	594	561	548	547	552	557	557	545	509	437	322	162	30
972	853	712	608	541	506	494	495	500	506	507	494	460	392	288	144	27
969	836	678	564	492	456	444	443	449	453	453	440	407	344	251	126	23
966	820	647	524	448	410	396	394	397	399	396	382	350	294	213	106	20
963	806	621	491	411	370	353	347	345	343	337	322	292	243	175	87	16
961	796	601	466	382	337	316	304	297	290	280	263	236	194	139	69	13
960	790	590	451	363	315	287	270	258	245	231	212	186	152	108	54	10
960	790	591	451	359	305	272	249	231	214	196	176	151	121	86	43	8
961	797	604	464	369	308	269	241	219	199	179	157	133	105	74	37	7
955	806	616	477	378	313	270	241	217	196	175	153	128	101	70	34	8

RADIATIVE FLUX EXP -4 PLANE 1

1:	2:	3:	4:	5:	6:	7:	8:	9:	10:	11:	12:	13:	14:	15:	16:	17:
-132	-155	-158	-155	-146	-136	-126	-117	-109	-102	-96	-92	-90	-89	-88	-87	-103
-109	0	0	0	0	0	0	0	0	0	0	0	0	0	0	0	-122
-98	0	0	0	0	0	0	0	0	0	0	0	0	0	0	0	-127
-78	0	0	0	0	0	0	0	0	0	0	0	0	0	0	0	-129
-54	0	0	0	0	0	0	0	0	0	0	0	0	0	0	0	-128
-27	0	0	0	0	0	0	0	0	0	0	0	0	0	0	0	-125
-1	0	0	0	0	0	0	0	0	0	0	0	0	0	0	0	-120
23	0	0	0	0	0	0	0	0	0	0	0	0	0	0	0	-114
45	0	0	0	0	0	0	0	0	0	0	0	0	0	0	0	-108
64	0	0	0	0	0	0	0	0	0	0	0	0	0	0	0	-102
79	0	0	0	0	0	0	0	0	0	0	0	0	0	0	0	-96
91	0	0	0	0	0	0	0	0	0	0	0	0	0	0	0	-90
99	0	0	0	0	0	0	0	0	0	0	0	0	0	0	0	-85
102	0	0	0	0	0	0	0	0	0	0	0	0	0	0	0	-81
100	0	0	0	0	0	0	0	0	0	0	0	0	0	0	0	-78
93	0	0	0	0	0	0	0	0	0	0	0	0	0	0	0	-76
-5	-110	-128	-134	-128	-121	-114	-107	-101	-96	-91	-86	-82	-78	-76	-74	-74

DIVERGENCE OF RADIATIVE FLUX EXP -3 PLANE 1

1:	2:	3:	4:	5:	6:	7:	8:	9:	10:	11:	12:	13:	14:	15:	16:	17:
0	0	0	0	0	0	0	0	0	0	0	0	0	0	0	0	0
0	559	470	377	312	266	232	205	181	156	125	80	19	-48	-99	-120	0
0	537	436	334	266	222	193	173	157	139	115	77	21	-46	-101	-124	0
0	501	380	263	191	151	130	120	114	108	94	66	17	-47	-101	-125	0
0	454	312	179	105	70	57	56	60	64	60	42	2	-54	-103	-125	0
0	403	242	98	26	-2	-8	-2	8	18	22	12	-18	-64	-105	-123	0
0	354	179	32	-34	-57	-58	-48	-34	-21	-13	-18	-40	-75	-106	-119	0
0	310	126	-18	-76	-93	-91	-80	-65	-52	-43	-44	-60	-84	-106	-115	0
0	270	84	-54	-103	-115	-110	-99	-87	-74	-66	-66	-75	-91	-104	-111	0
0	237	51	-78	-119	-126	-121	-111	-100	-90	-83	-81	-86	-95	-102	-106	0
0	208	26	-93	-127	-131	-125	-116	-107	-99	-93	-91	-92	-96	-99	-101	0
0	186	9	-103	-131	-132	-126	-118	-111	-104	-99	-96	-95	-95	-95	-96	0
0	171	-2	-107	-131	-131	-125	-118	-111	-105	-100	-97	-94	-93	-92	-92	0
0	163	-6	-108	-129	-129	-123	-116	-110	-105	-100	-96	-93	-90	-89	-89	0
0	165	-3	-105	-127	-126	-121	-114	-109	-103	-99	-95	-91	-89	-87	-86	0
0	170	2	-100	-124	-125	-120	-114	-108	-103	-99	-95	-91	-88	-86	-85	0
0	0	0	0	0	0	0	0	0	0	0	0	0	0	0	0	0

A.7 Case 7: 2-D Steady State Solutions of Participating Thermal Cavity Fluid Ra=1.E4, Mesh=16x16

CONVECTION + RADIATION

BC's: No slip; Vertical Non-zero Neumann and Horizontal Adiabatic Walls
Explict Parameters: Ra=1.E4, Pr=0.7, Ar=1.0, Gr=1.43E4, Re=120, Pe=83.6, Bo=40.65
Implict Parameters: Lo=1 m, Nu=15.89E-6 m2/s, To=294.4 K, dTo=3.68E-7, ko=26.3E-6 m2/s po=2.21E-3 Pa, rho,o=1.16 kg/m3, alpha,o=22.5E-6 m2/s, Uo=1.9E-3 m/s, to=527.4 s, Ka=Kt=1.0 1/m, Ks=0. 1/m, Omega,o=0, black surfaces

U1 EXP -3 PLANE 1

1:	2:	3:	4:	5:	6:	7:	8:	9:	10:	11:	12:	13:	14:	15:	16:	17:
0	0	0	0	0	0	0	0	0	0	0	0	0	0	0	0	0
0	3	18	32	50	63	76	82	90	93	100	100	108	93	80	20	0
0	5	28	51	79	100	119	130	141	144	151	147	148	123	94	19	0
0	6	35	62	93	116	138	150	162	165	169	160	151	117	80	17	0
0	7	37	66	97	119	140	151	162	164	165	154	140	104	66	12	0
0	7	38	64	93	111	128	138	146	148	147	135	117	83	47	9	0
0	7	36	58	81	93	106	112	119	120	118	108	89	59	29	4	0
0	6	30	45	59	66	73	78	83	84	82	73	55	32	9	0	0
0	4	20	26	31	30	32	35	38	40	38	31	16	2	-9	-3	0
0	1	7	2	-3	-11	-13	-13	-12	-10	-13	-16	-26	-29	-28	-6	0
0	-1	-9	-25	-42	-55	-64	-67	-69	-67	-69	-68	-71	-59	-45	-9	0
0	-5	-27	-52	-79	-98	-114	-121	-126	-126	-126	-119	-111	-86	-58	-12	0
0	-8	-44	-77	-111	-134	-156	-168	-178	-179	-179	-165	-146	-107	-67	-13	0
0	-12	-57	-92	-130	-154	-179	-195	-210	-214	-213	-194	-168	-119	-72	-15	0
0	-12	-63	-94	-128	-147	-170	-187	-205	-213	-216	-199	-172	-121	-71	-13	0
0	-12	-51	-69	-90	-100	-115	-126	-141	-149	-154	-145	-129	-92	-56	-12	0
0	0	0	0	0	0	0	0	0	0	0	0	0	0	0	0	0

U2 EXP -3 PLANE 1

1:	2:	3:	4:	5:	6:	7:	8:	9:	10:	11:	12:	13:	14:	15:	16:	17:
0	0	0	0	0	0	0	0	0	0	0	0	0	0	0	0	0
0	3	4	6	5	4	3	2	1	1	2	0	0	-6	-10	-20	0
0	18	27	30	28	23	17	12	9	7	6	4	-4	-26	-65	-89	0
0	34	51	57	52	43	32	23	15	10	5	-1	-20	-56	-114	-135	0
0	56	83	89	81	67	50	35	22	13	2	-11	-42	-95	-169	-185	0
0	77	112	118	105	85	64	44	28	13	-2	-25	-67	-132	-210	-212	0
0	99	142	145	127	101	76	53	33	14	-8	-39	-93	-167	-246	-236	0
0	118	164	163	140	110	82	58	36	14	-14	-54	-115	-195	-268	-242	0
0	135	182	174	146	114	87	63	40	14	-19	-66	-135	-215	-280	-242	0
0	144	187	172	142	111	87	65	42	14	-23	-75	-146	-222	-273	-226	0
0	146	182	161	131	104	84	65	44	15	-25	-80	-149	-218	-257	-204	0
0	135	161	137	111	89	75	60	42	14	-24	-76	-139	-196	-221	-170	0
0	118	133	107	85	70	62	53	39	15	-19	-66	-119	-164	-180	-136	0
0	85	90	69	54	45	42	38	29	13	-11	-45	-83	-114	-123	-91	0
0	54	51	36	27	23	23	23	19	11	-3	-24	-47	-67	-73	-55	0
0	12	8	7	4	4	4	4	4	2	0	-4	-8	-14	-13	-12	0
0	0	0	0	0	0	0	0	0	0	0	0	0	0	0	0	0

(Cont'd)

A.7 Case 7: 2-D Steady State Solutions of Participating Thermal Cavity Fluid Ra=1.E4, Mesh=16x16

TEMPERATURE EXP -2 PLANE 1

1:	2:	3:	4:	5:	6:	7:	8:	9:	10:	11:	12:	13:	14:	15:	16:	17:
100	98	97	96	96	96	96	96	95	94	92	88	81	70	52	27	0
100	98	97	96	96	96	96	96	95	94	93	89	83	72	54	28	0
100	97	96	95	95	95	95	95	94	94	93	90	85	74	56	29	0
100	97	95	93	93	93	93	93	93	92	92	89	85	74	56	30	0
100	96	93	91	90	89	89	90	90	90	89	88	83	73	55	29	0
100	95	91	88	86	86	85	86	86	87	86	85	80	71	53	28	0
100	93	88	85	82	81	81	81	82	83	83	81	77	67	50	26	0
100	92	86	81	78	77	76	77	77	78	78	77	73	63	47	25	0
100	91	83	78	74	72	72	72	72	73	73	72	67	58	43	23	0
100	89	81	74	70	67	67	66	67	67	67	66	61	53	39	20	0
100	88	78	71	66	63	61	61	61	61	60	59	54	46	34	18	0
100	87	76	68	62	59	57	55	55	54	53	51	47	39	29	15	0
100	86	74	65	59	55	52	50	48	47	45	43	39	32	23	12	0
100	86	73	64	57	52	48	46	43	41	38	35	31	26	18	10	0
100	86	73	63	56	51	46	43	40	37	33	30	26	21	15	8	0
100	86	74	64	56	50	46	42	38	34	31	27	23	18	13	6	0
100	86	74	64	57	51	46	42	38	34	30	26	22	17	12	6	0

RADIATIVE FLUX EXP -4 PLANE 1

1:	2:	3:	4:	5:	6:	7:	8:	9:	10:	11:	12:	13:	14:	15:	16:	17:
74	19	6	-12	-25	-33	-37	-38	-38	-36	-33	-30	-26	-23	-20	-17	-24
139	0	0	0	0	0	0	0	0	0	0	0	0	0	0	0	-35
155	0	0	0	0	0	0	0	0	0	0	0	0	0	0	0	-39
164	0	0	0	0	0	0	0	0	0	0	0	0	0	0	0	-42
169	0	0	0	0	0	0	0	0	0	0	0	0	0	0	0	-45
172	0	0	0	0	0	0	0	0	0	0	0	0	0	0	0	-47
174	0	0	0	0	0	0	0	0	0	0	0	0	0	0	0	-48
175	0	0	0	0	0	0	0	0	0	0	0	0	0	0	0	-49
175	0	0	0	0	0	0	0	0	0	0	0	0	0	0	0	-49
175	0	0	0	0	0	0	0	0	0	0	0	0	0	0	0	-49
174	0	0	0	0	0	0	0	0	0	0	0	0	0	0	0	-48
172	0	0	0	0	0	0	0	0	0	0	0	0	0	0	0	-47
169	0	0	0	0	0	0	0	0	0	0	0	0	0	0	0	-45
164	0	0	0	0	0	0	0	0	0	0	0	0	0	0	0	-42
155	0	0	0	0	0	0	0	0	0	0	0	0	0	0	0	-39
139	0	0	0	0	0	0	0	0	0	0	0	0	0	0	0	-35
74	19	6	-12	-25	-33	-37	-38	-38	-36	-33	-30	-26	-23	-20	-17	-24

DIVERGENCE OF RADIATIVE FLUX EXP -4 PLANE 1

1:	2:	3:	4:	5:	6:	7:	8:	9:	10:	11:	12:	13:	14:	15:	16:	17:
0	0	0	0	0	0	0	0	0	0	0	0	0	0	0	0	0
0	167	61	-117	-230	-298	-333	-346	-341	-325	-302	-275	-246	-218	-192	-165	0
0	206	70	-140	-273	-352	-392	-404	-396	-376	-347	-313	-279	-245	-215	-183	0
0	230	77	-150	-297	-384	-428	-441	-432	-409	-376	-339	-301	-264	-230	-196	0
0	247	83	-156	-312	-405	-453	-468	-459	-434	-399	-360	-319	-279	-243	-206	0
0	259	87	-159	-321	-419	-470	-486	-478	-452	-416	-375	-332	-291	-253	-214	0
0	266	90	-160	-326	-428	-481	-498	-490	-464	-428	-385	-342	-299	-260	-220	0
0	270	92	-161	-329	-433	-487	-505	-497	-471	-434	-392	-347	-304	-264	-224	0
0	271	92	-161	-330	-434	-489	-508	-500	-474	-437	-394	-349	-305	-265	-225	0
0	270	92	-161	-329	-433	-487	-505	-497	-471	-434	-392	-347	-304	-264	-224	0
0	266	90	-160	-326	-428	-481	-498	-490	-464	-428	-385	-342	-299	-260	-220	0
0	259	87	-159	-321	-419	-470	-486	-478	-452	-416	-375	-332	-291	-253	-214	0
0	247	83	-156	-312	-405	-453	-468	-459	-434	-399	-360	-319	-279	-243	-206	0
0	230	77	-150	-297	-384	-428	-441	-432	-409	-376	-339	-301	-264	-230	-196	0
0	206	70	-140	-273	-352	-392	-404	-396	-376	-347	-313	-279	-245	-215	-183	0
0	167	61	-117	-230	-298	-333	-346	-341	-325	-302	-275	-246	-218	-192	-165	0
0	0	0	0	0	0	0	0	0	0	0	0	0	0	0	0	0

A.8 Case 8: Accuracy Study of 2-D Steady State Solutions of Participating Thermal Cavity Fluid Ra=1.E4, Mesh=32x32

CONVECTION + RADIATION

BC's: No slip; Vertical Non-zero Neumann and Horizontal Adiabatic Walls
Explict Parameters: Ra=1.E4, Pr=0.7, Ar=1.0, Gr=1.43E4, Re=120, Pe=83.6, Bo=40.65
Implict Parameters: Lo=1 m, Nu=15.89E-6 m2/s, To=294.4 K, dTo=3.68E-7, ko=26.3E-6 m2/s po=2.21E-3 Pa, rho,o=1.16 kg/m3, alpha,o=22.5E-6 m2/s, Uo=1.9E-3 m/s, to=527.4 s, Ka=Kt=1.0 1/m, Ks=0. 1/m, Omega,o=0, black surfaces

U1 EXP -3 PLANE 1

1:	2:	3:	4:	5:	6:	7:	8:	9:	10:	11:	12:	13:	14:	15:	16:	17:	18:	19:	20:
0	0	0	0	0	0	0	0	0	0	0	0	0	0	0	0	0	0	0	0
0	0	2	5	9	13	18	22	27	31	35	39	42	44	46	48	49	51	52	54
0	0	4	10	16	24	32	41	49	56	63	69	74	79	82	86	88	91	93	95
0	1	6	14	23	33	44	55	65	75	84	92	99	105	110	114	118	121	123	125
0	1	8	17	28	40	52	65	77	89	99	109	117	124	130	135	139	142	144	146
0	1	9	19	31	45	59	73	86	98	110	120	129	136	143	148	152	155	158	159
0	2	10	21	34	48	63	78	92	105	116	127	136	144	150	155	159	162	164	165
0	2	10	22	36	51	66	81	95	108	120	130	139	146	153	158	162	164	166	166
0	2	11	23	37	52	68	83	96	109	120	130	138	145	151	156	159	162	163	163
0	2	11	24	38	53	68	82	95	107	117	126	134	141	146	150	153	156	157	156
0	2	11	24	38	53	67	80	92	103	112	120	127	133	138	141	144	146	147	147
0	2	11	24	37	51	64	76	87	96	104	111	117	122	126	130	132	134	135	134
0	2	11	23	36	48	60	71	80	88	94	100	105	109	112	115	118	119	120	119
0	2	11	22	33	45	55	63	70	76	81	86	90	93	96	99	101	102	103	102
0	2	10	20	30	39	47	54	59	63	67	70	73	75	78	80	82	83	84	83
0	2	9	17	26	33	38	42	45	48	50	51	53	55	57	59	61	63	63	63
0	1	7	14	20	25	28	29	30	31	31	31	32	34	35	37	38	40	40	40
0	1	6	10	14	16	16	15	13	12	11	10	10	10	11	13	14	15	16	15
0	1	4	6	6	5	3	0	-3	-7	-10	-12	-13	-13	-13	-12	-11	-10	-10	-10
0	0	1	1	0	-5	-10	-16	-22	-27	-32	-35	-37	-39	-39	-39	-38	-38	-38	-38
0	0	-1	-4	-9	-16	-24	-33	-41	-48	-54	-59	-63	-65	-66	-67	-67	-67	-67	-66
0	0	-3	-9	-18	-28	-39	-50	-60	-69	-77	-83	-87	-91	-93	-95	-96	-96	-96	-96
0	-1	-6	-15	-27	-40	-53	-66	-78	-89	-98	-106	-112	-116	-120	-122	-124	-125	-125	-124
0	-2	-9	-21	-35	-51	-66	-81	-95	-107	-118	-127	-134	-140	-145	-148	-151	-152	-152	-152
0	-2	-12	-27	-43	-61	-78	-95	-109	-123	-134	-145	-153	-161	-167	-171	-175	-177	-177	-177
0	-3	-15	-32	-50	-69	-88	-105	-121	-135	-147	-158	-168	-176	-184	-190	-194	-197	-198	-197
0	-4	-18	-36	-56	-76	-95	-112	-128	-142	-155	-166	-177	-186	-194	-201	-207	-210	-212	-212
0	-4	-19	-39	-59	-79	-98	-114	-129	-143	-155	-167	-177	-187	-196	-204	-210	-215	-218	-218
0	-4	-20	-40	-60	-79	-96	-111	-124	-136	-148	-158	-168	-178	-187	-195	-202	-208	-211	-212
0	-4	-20	-39	-57	-74	-88	-100	-111	-121	-130	-139	-148	-156	-164	-172	-179	-185	-190	-192
0	-4	-18	-34	-48	-61	-72	-80	-88	-94	-101	-107	-114	-120	-127	-133	-139	-145	-149	-152
0	-3	-12	-22	-31	-38	-44	-48	-52	-55	-58	-61	-65	-68	-72	-76	-80	-84	-87	-89
0	0	0	0	0	0	0	0	0	0	0	0	0	0	0	0	0	0	0	0

```
  0   0   0   0   0   0   0   0   0   0   0   2   0   U1 FIELD CONT'D
 55  57  59  61  63  63  62  59  51  40  23   4   0
 97  99 101 103 104 102  98  90  76  56  31   8   0
127 129 130 130 128 124 116 104  85  61  33   8   0
147 148 147 146 142 135 124 108  87  61  32   7   0
160 159 157 153 147 138 125 106  84  57  30   7   0   (Cont'd) A.8  Case 8
165 164 160 155 147 136 121 101  78  52  26   6   0   Accuracy Study of
166 163 159 152 143 130 114  94  71  46  23   5   0   2-D Steady State
162 159 154 146 136 123 106  86  63  40  19   4   0   Solution Participating
155 151 145 137 127 113  96  76  55  34  16   3   0   Medium
144 141 135 126 115 101  85  66  47  28  13   2   0
132 128 122 113 102  89  73  56  38  22   9   1   0
117 113 107  99  88  75  60  44  29  16   6   1   0
100  96  91  83  72  60  47  33  20   9   3   0   0
 81  78  72  65  55  44  32  21  10   3   0   0   0
 61  57  52  45  37  27  17   8   1  -2  -3  -1   0
 38  35  31  25  17   9   2  -4  -8  -8  -6  -1   0
 14  11   7   3  -2  -8 -13 -17 -17 -14  -8  -2   0
-11 -13 -16 -20 -24 -27 -29 -29 -26 -20 -11  -2   0
-38 -40 -42 -44 -45 -46 -45 -42 -35 -25 -14  -3   0
-67 -67 -68 -68 -67 -65 -61 -54 -43 -30 -16  -3   0
-95 -95 -94 -92 -89 -83 -75 -64 -50 -34 -17  -4   0
-123-122-119-115-109-100 -89 -74 -57 -37 -19  -4   0
-150-147-142-136-127-115-100 -82 -62 -40 -20  -4   0
-174-170-164-155-143-128-110 -89 -66 -42 -21  -4   0
-194-189-181-170-156-139-118 -94 -69 -44 -21  -4   0
-209-203-194-182-166-146-123 -97 -71 -44 -21  -4   0
-215-210-200-187-170-149-125 -99 -71 -45 -21  -4   0
-211-206-197-184-167-147-123 -97 -70 -44 -21  -4   0
-191-188-181-170-155-136-114 -90 -65 -41 -20  -4   0
-153-151-146-138-127-112 -94 -74 -54 -34 -16  -3   0
 -91 -90 -88 -84 -78 -69 -58 -46 -33 -20  -9  -2   0
  0   0   0   0   0   0   0   0   0   0   0   0   0     U2  EXP -3
 1:  2:  3:  4:  5:  6:  7:  8:  9: 10: 11: 12: 13: 14: 15: 16: 17: 18: 19: 20:
  0   0   0   0   0   0   0   0   0   0   0   0   0   0   0   0   0   0   0   0
  0   0   0   1   1   1   1   1   1   1   1   1   1   0   0   0   0   0   0   0
  0   2   4   6   7   8   8   8   8   7   6   5   4   4   3   3   2   2   2   2
  0   5  10  13  16  17  18  18  17  15  14  12  10   9   7   6   5   5   4   4
  0   9  17  22  26  29  30  29  28  26  23  20  17  15  12  10   9   7   7   6
  0  14  25  33  39  42  43  42  40  37  33  29  25  21  18  15  12  10   9   7
  0  19  34  45  52  56  58  57  54  49  44  39  33  28  24  19  16  13  10   8
  0  25  44  58  67  72  73  71  67  62  55  49  42  35  29  24  19  15  12   8
  0  31  55  71  82  87  88  85  80  74  66  58  50  42  35  28  23  17  12   8
  0  37  65  85  97 102 103 100  93  85  76  67  57  48  40  32  25  19  13   7
  0  44  76  98 111 117 117 113 105  96  85  74  64  54  45  36  28  21  13   6
  0  51  87 112 126 131 131 125 116 105  93  81  70  59  49  39  30  22  13   4
  0  57  98 125 139 145 143 135 125 113 100  87  75  63  52  42  32  23  13   3
  0  64 108 137 152 156 153 144 132 119 105  92  79  67  55  45  34  24  13   2
  0  70 118 148 162 166 161 151 138 124 109  95  82  70  58  47  36  25  13   0
  0  76 127 157 171 173 167 156 142 127 112  98  84  72  60  49  38  26  13   0
  0  81 134 165 178 178 171 158 143 128 113  99  86  74  62  51  39  27  13  -1
  0  85 140 170 182 181 172 158 143 127 113  99  87  75  64  52  40  28  14  -2
  0  88 144 173 183 180 170 156 140 125 111  98  86  75  64  53  42  29  14  -2
  0  90 145 173 181 177 165 151 135 121 108  96  85  75  65  54  42  29  14  -3
  0  91 144 170 176 170 158 143 129 115 103  93  83  74  64  54  43  29  14  -3
  0  90 141 164 168 161 148 134 120 108  97  88  79  71  63  53  42  29  14  -3
  0  87 135 156 158 149 136 122 109  99  89  82  75  68  60  52  42  29  14  -2
  0  83 127 144 144 135 122 109  97  88  80  74  69  63  57  49  40  29  14  -2
  0  76 116 129 128 118 106  94  84  76  70  65  61  57  52  46  38  27  15   0
  0  68 102 112 109 100  88  78  69  63  59  55  53  50  46  41  34  26  14   1
  0  59  87  94  89  80  70  61  54  50  47  45  43  41  39  35  30  23  14   2
  0  48  69  74  69  61  52  45  40  36  35  34  33  32  31  29  25  20  13   4
  0  36  51  53  49  42  35  30  26  24  23  23  23  23  22  21  19  16  11   4
  0  24  33  34  30  25  20  17  15  14  13  13  14  14  14  14  13  11   8   4
  0  12  17  16  14  11   9   7   6   6   6   6   6   6   7   7   6   5   4   2
  0   3   4   3   3   2   1   1   1   1   1   1   1   1   1   1   1   1   1   0
  0   0   0   0   0   0   0   0   0   0   0   0   0   0   0   0   0   0   0   0
```

```
  0   0   0   0   0   0   0   0   0   0   0   0   0   U2 FIELD CONT'D
  0   0   0   0   0   0   0  -2  -3  -5  -6  -7   0
  2   2   2   2   1   0  -4 -10 -17 -24 -29 -24   0
  4   4   4   2   0  -5 -12 -23 -37 -49 -56 -44   0
  6   5   3   1  -3 -12 -24 -40 -59 -77 -83 -64   0
  6   4   2  -2 -10 -22 -39 -60 -84-105-110 -83   0
  6   3  -1  -8 -18 -34 -55 -81-109-132-135 -99   0
  4   0  -6 -15 -29 -48 -73-103-134-157-158-113   0   (Cont'd) A.8  Case 8
  2  -3 -12 -23 -40 -62 -91-125-158-181-178-126   0
  0  -7 -18 -32 -52 -78-110-146-180-202-195-136   0
 -2 -12 -25 -42 -64 -93-128-166-201-221-209-143   0
 -5 -17 -32 -52 -77-108-145-184-219-237-221-149   0
 -8 -22 -39 -61 -89-123-161-201-235-250-230-154   0
-11 -27 -46 -71-101-136-176-216-248-261-236-156   0
-14 -31 -53 -79-111-148-189-228-259-268-239-156   0
-16 -36 -59 -88-121-159-200-238-266-271-240-155   0
-19 -40 -65 -95-130-168-208-245-270-272-237-152   0
-21 -43 -70-101-136-175-214-249-271-269-232-147   0
-22 -46 -74-106-141-180-217-249-267-263-224-141   0
-24 -48 -76-109-144-181-217-246-261-254-214-133   0
-24 -49 -78-110-144-180-213-238-250-241-202-124   0
-24 -49 -77-109-142-175-205-228-237-225-187-114   0
-23 -48 -75-105-136-167-194-213-220-207-170-103   0
-22 -45 -71 -99-127-155-179-195-200-187-153 -92   0
-19 -40 -64 -90-116-140-161-174-177-165-134 -80   0
-15 -34 -56 -78-101-122-140-151-152-141-114 -68   0
-11 -27 -45 -65 -84-102-116-125-126-116 -94 -56   0
 -7 -20 -34 -50 -66 -80 -91 -98 -99 -91 -73 -44   0
 -3 -12 -23 -35 -47 -57 -66 -71 -72 -66 -53 -31   0
  0  -6 -13 -21 -29 -36 -42 -45 -46 -42 -34 -20   0
  0  -2  -6  -9 -13 -17 -20 -22 -22 -21 -17  -9   0
  0   0  -1  -2  -2  -3  -4  -5  -5  -4  -3  -2   0
  0   0   0   0   0   0   0   0   0   0   0   0   0   TEMPERATURE   EXP -2
 1:  2:  3:  4:  5:  6:  7:  8:  9: 10: 11: 12: 13: 14: 15: 16: 17: 18: 19: 20:
100  99  98  97  97  96  96  96  96  96  96  96  96  96  96  96  96  95  95  94
100  98  98  97  97  96  96  96  96  96  96  96  96  96  96  96  96  95  95  94
100  98  97  97  96  96  96  96  96  96  96  96  96  96  96  96  95  95  95  94
100  98  97  97  96  96  96  95  95  95  95  95  95  95  95  95  95  95  95  94
100  98  97  96  96  95  95  95  95  95  95  95  95  95  95  95  95  94  94  94
100  98  97  96  95  95  94  94  94  94  94  94  94  94  94  94  94  94  93  93
100  98  96  95  94  94  93  93  93  93  92  92  92  93  93  93  93  93  92  92
100  98  96  95  94  93  92  92  91  91  91  91  91  91  91  91  91  91  91  91
100  97  95  94  93  92  91  90  90  90  89  89  89  89  89  90  90  90  90  90
100  97  95  93  92  90  89  89  88  88  87  87  87  87  88  88  88  88  88  88
100  97  94  92  90  89  88  87  86  86  86  85  85  85  86  86  86  86  86  86
100  96  94  91  89  88  86  85  84  84  83  83  83  83  83  84  84  84  84  84
100  96  93  90  88  86  85  83  82  82  81  81  81  81  81  81  82  82  82  82
100  96  92  89  87  85  83  81  80  80  79  79  79  79  79  79  79  80  80  80
100  95  92  88  86  83  81  79  78  77  77  76  76  76  77  77  77  77  78  78
100  95  91  87  84  82  79  77  76  75  74  74  74  74  74  74  75  75  75  75
100  95  90  86  83  80  77  75  74  73  72  72  71  71  72  72  72  72  73  73
100  94  90  85  82  78  76  73  72  71  70  69  69  69  69  69  69  70  70  70
100  94  89  84  80  77  74  72  70  68  67  67  66  66  66  66  66  67  67  67
100  94  88  83  79  75  72  70  68  66  65  64  64  64  63  63  64  64  64  64
100  93  88  82  78  74  70  68  66  64  63  62  61  61  61  61  61  61  61  60
100  93  87  82  77  72  69  66  64  62  61  60  59  58  58  58  57  57  57  57
100  93  87  81  76  71  67  64  62  60  58  57  56  56  55  55  54  54  54  53
100  93  86  80  75  70  66  63  60  58  56  55  54  53  52  52  51  51  50  50
100  92  86  79  74  69  65  62  59  57  55  53  52  51  50  49  48  48  47  46
100  92  85  79  73  68  64  61  58  55  53  51  50  49  48  46  46  45  44  43
100  92  85  79  73  68  63  60  57  54  52  50  48  47  46  44  43  42  41  40
100  92  85  79  73  67  63  59  56  53  51  49  47  45  44  42  41  40  38  37
100  92  85  79  73  67  63  59  56  53  50  48  46  44  43  41  40  38  36  35
100  92  85  79  73  68  63  59  56  53  50  48  46  44  42  40  39  37  35  33
100  92  85  79  73  68  63  59  56  53  50  48  46  44  42  40  38  36  34  33
100  92  86  79  74  68  64  60  56  53  50  48  46  44  42  40  38  36  34  32
100  93  86  80  74  69  64  60  56  53  51  48  46  44  42  40  38  36  34  32
```

93	91	89	86	83	78	71	63	53	42	29	14	0
93	91	89	87	83	78	72	64	54	42	29	14	0
93	92	90	87	84	79	73	65	55	43	30	15	0
93	92	90	88	84	80	74	66	56	44	30	15	0
93	92	90	88	85	81	75	67	57	44	30	15	0
92	91	90	88	85	81	75	67	57	45	30	15	0
92	91	89	87	85	80	75	67	57	44	30	15	0
91	90	89	87	84	80	74	66	56	44	30	15	0
89	89	87	86	83	79	73	65	56	43	30	15	0
88	87	86	84	82	78	72	64	55	43	29	14	0
86	86	85	83	80	76	71	63	53	42	28	14	0
84	84	83	81	79	75	69	62	52	41	28	14	0
82	82	81	79	77	73	67	60	50	39	27	13	0
80	80	79	77	74	71	65	58	49	38	26	13	0
78	77	76	75	72	68	63	56	47	36	25	12	0
75	75	74	72	70	66	61	54	45	35	24	12	0
73	72	71	69	67	63	58	51	43	33	23	11	0
70	69	68	67	64	60	55	49	41	32	21	11	0
67	66	65	63	61	57	52	46	38	30	20	10	0
63	63	62	60	57	54	49	43	36	28	19	9	0
60	59	58	56	54	50	46	40	34	26	18	9	0
56	56	54	53	50	47	43	37	31	24	16	8	0
53	52	51	49	46	43	39	34	28	22	15	7	0
49	48	47	45	42	39	36	31	26	20	13	7	0
45	44	43	41	39	36	32	28	23	18	12	6	0
42	40	39	37	35	32	29	25	21	16	11	5	0
38	37	35	33	31	29	26	22	18	14	10	5	0
35	34	32	30	28	26	23	20	16	13	8	4	0
33	32	30	28	26	23	21	18	15	11	8	4	0
32	30	28	26	24	22	19	16	13	10	7	3	0
31	29	27	25	23	20	18	15	13	10	6	3	0
30	29	27	24	22	20	18	15	12	9	6	3	0
30	28	26	24	22	20	17	15	12	9	6	3	0

RADIATIVE FLUX EXP -4

1:	2:	3:	4:	5:	6:	7:	8:	9:	10:	11:	12:	13:	14:	15:	16:	17:	18:	19:	20:
75	40	31	17	4	-5	-13	-20	-26	-30	-34	-36	-38	-39	-39	-39	-39	-38	-37	-35
120	0	0	0	0	0	0	0	0	0	0	0	0	0	0	0	0	0	0	0
137	0	0	0	0	0	0	0	0	0	0	0	0	0	0	0	0	0	0	0
147	0	0	0	0	0	0	0	0	0	0	0	0	0	0	0	0	0	0	0
154	0	0	0	0	0	0	0	0	0	0	0	0	0	0	0	0	0	0	0
159	0	0	0	0	0	0	0	0	0	0	0	0	0	0	0	0	0	0	0
162	0	0	0	0	0	0	0	0	0	0	0	0	0	0	0	0	0	0	0
165	0	0	0	0	0	0	0	0	0	0	0	0	0	0	0	0	0	0	0
167	0	0	0	0	0	0	0	0	0	0	0	0	0	0	0	0	0	0	0
169	0	0	0	0	0	0	0	0	0	0	0	0	0	0	0	0	0	0	0
170	0	0	0	0	0	0	0	0	0	0	0	0	0	0	0	0	0	0	0
171	0	0	0	0	0	0	0	0	0	0	0	0	0	0	0	0	0	0	0
172	0	0	0	0	0	0	0	0	0	0	0	0	0	0	0	0	0	0	0
173	0	0	0	0	0	0	0	0	0	0	0	0	0	0	0	0	0	0	0
173	0	0	0	0	0	0	0	0	0	0	0	0	0	0	0	0	0	0	0
173	0	0	0	0	0	0	0	0	0	0	0	0	0	0	0	0	0	0	0
173	0	0	0	0	0	0	0	0	0	0	0	0	0	0	0	0	0	0	0
173	0	0	0	0	0	0	0	0	0	0	0	0	0	0	0	0	0	0	0
173	0	0	0	0	0	0	0	0	0	0	0	0	0	0	0	0	0	0	0
173	0	0	0	0	0	0	0	0	0	0	0	0	0	0	0	0	0	0	0
172	0	0	0	0	0	0	0	0	0	0	0	0	0	0	0	0	0	0	0
171	0	0	0	0	0	0	0	0	0	0	0	0	0	0	0	0	0	0	0
170	0	0	0	0	0	0	0	0	0	0	0	0	0	0	0	0	0	0	0
169	0	0	0	0	0	0	0	0	0	0	0	0	0	0	0	0	0	0	0
167	0	0	0	0	0	0	0	0	0	0	0	0	0	0	0	0	0	0	0
165	0	0	0	0	0	0	0	0	0	0	0	0	0	0	0	0	0	0	0
162	0	0	0	0	0	0	0	0	0	0	0	0	0	0	0	0	0	0	0
159	0	0	0	0	0	0	0	0	0	0	0	0	0	0	0	0	0	0	0
154	0	0	0	0	0	0	0	0	0	0	0	0	0	0	0	0	0	0	0
147	0	0	0	0	0	0	0	0	0	0	0	0	0	0	0	0	0	0	0
137	0	0	0	0	0	0	0	0	0	0	0	0	0	0	0	0	0	0	0
120	0	0	0	0	0	0	0	0	0	0	0	0	0	0	0	0	0	0	0
75	40	31	17	4	-5	-13	-20	-26	-30	-34	-36	-38	-39	-39	-39	-39	-38	-37	-35

(Cont'd) A.8 Case 8: Accuracy Study of 2-D Steady State Solution Participating Thermal Cavity, Fluid Ra=1.E4, Mesh=32x32

RADIATIVE FLUX SOLUTION FIELD CONTINUED

21:	22:	23:	24:	25:	26:	27:	28:	29:	30:	31:	32:	33:
-34	-32	-30	-28	-27	-25	-23	-22	-20	-19	-17	-15	-23
0	0	0	0	0	0	0	0	0	0	0	0	-33
0	0	0	0	0	0	0	0	0	0	0	0	-36
0	0	0	0	0	0	0	0	0	0	0	0	-38
0	0	0	0	0	0	0	0	0	0	0	0	-40
0	0	0	0	0	0	0	0	0	0	0	0	-41
0	0	0	0	0	0	0	0	0	0	0	0	-43
0	0	0	0	0	0	0	0	0	0	0	0	-44
0	0	0	0	0	0	0	0	0	0	0	0	-45
0	0	0	0	0	0	0	0	0	0	0	0	-46
0	0	0	0	0	0	0	0	0	0	0	0	-47
0	0	0	0	0	0	0	0	0	0	0	0	-48
0	0	0	0	0	0	0	0	0	0	0	0	-49
0	0	0	0	0	0	0	0	0	0	0	0	-49
0	0	0	0	0	0	0	0	0	0	0	0	-50
0	0	0	0	0	0	0	0	0	0	0	0	-50
0	0	0	0	0	0	0	0	0	0	0	0	-50
0	0	0	0	0	0	0	0	0	0	0	0	-50
0	0	0	0	0	0	0	0	0	0	0	0	-50
0	0	0	0	0	0	0	0	0	0	0	0	-49
0	0	0	0	0	0	0	0	0	0	0	0	-49
0	0	0	0	0	0	0	0	0	0	0	0	-48
0	0	0	0	0	0	0	0	0	0	0	0	-47
0	0	0	0	0	0	0	0	0	0	0	0	-46
0	0	0	0	0	0	0	0	0	0	0	0	-45
0	0	0	0	0	0	0	0	0	0	0	0	-44
0	0	0	0	0	0	0	0	0	0	0	0	-43
0	0	0	0	0	0	0	0	0	0	0	0	-41
0	0	0	0	0	0	0	0	0	0	0	0	-40
0	0	0	0	0	0	0	0	0	0	0	0	-38
0	0	0	0	0	0	0	0	0	0	0	0	-36
0	0	0	0	0	0	0	0	0	0	0	0	-33
-34	-32	-30	-28	-27	-25	-23	-22	-20	-19	-17	-15	-23

1:	2:	3:	4:	5:	6:	7:	8:	9:	10:	11:	12:	13:	14:	15:	16:	17:	18:	19:	20:
0	0	0	0	0	0	0	0	0	0	0	0	0	0	0	0	0	0	0	0
0	318	255	131	32	-48	-113	-166	-209	-243	-268	-287	-300	-309	-312	-312	-309	-304	-296	-287
0	371	291	146	31	-61	-135	-195	-242	-279	-306	-326	-340	-347	-350	-349	-344	-337	-328	-316
0	406	315	159	33	-67	-148	-213	-264	-303	-333	-353	-367	-375	-377	-375	-369	-361	-350	-337
0	433	335	170	36	-71	-158	-227	-281	-323	-354	-376	-390	-398	-400	-397	-391	-382	-370	-356
0	453	351	180	40	-72	-164	-237	-295	-339	-372	-395	-410	-418	-420	-417	-410	-400	-387	-372
0	470	364	189	44	-73	-168	-245	-305	-351	-386	-410	-426	-434	-436	-433	-426	-416	-402	-387
0	483	374	196	48	-73	-171	-251	-313	-362	-398	-423	-439	-448	-451	-448	-440	-429	-415	-399
0	493	383	201	51	-72	-173	-255	-320	-370	-407	-433	-451	-460	-463	-460	-452	-441	-427	-410
0	502	390	206	54	-72	-175	-258	-325	-376	-415	-442	-460	-470	-473	-470	-462	-451	-436	-419
0	508	395	210	56	-71	-176	-261	-329	-381	-421	-449	-467	-478	-481	-478	-471	-459	-444	-427
0	514	399	213	58	-70	-177	-263	-332	-385	-426	-455	-474	-484	-488	-485	-477	-466	-451	-434
0	518	403	216	59	-70	-177	-265	-334	-388	-429	-459	-478	-489	-493	-490	-483	-471	-457	-439
0	521	405	218	60	-70	-178	-266	-336	-391	-432	-462	-482	-493	-497	-495	-487	-476	-461	-443
0	523	407	219	61	-69	-178	-266	-337	-392	-434	-464	-484	-496	-500	-497	-490	-478	-463	-446
0	524	408	220	62	-69	-178	-267	-338	-393	-435	-466	-486	-497	-501	-499	-492	-480	-465	-448
0	525	409	220	62	-69	-178	-267	-338	-394	-436	-466	-486	-498	-502	-500	-492	-481	-466	-448
0	524	408	220	62	-69	-178	-267	-338	-393	-435	-466	-486	-497	-501	-499	-492	-480	-465	-448
0	523	407	219	61	-69	-178	-266	-337	-392	-434	-464	-484	-496	-500	-497	-490	-478	-463	-446
0	521	405	218	60	-70	-178	-266	-336	-391	-432	-462	-482	-493	-497	-495	-487	-476	-461	-443
0	518	403	216	59	-70	-177	-265	-334	-388	-429	-459	-478	-489	-493	-490	-483	-471	-457	-439
0	514	399	213	58	-70	-177	-263	-332	-385	-426	-455	-474	-484	-488	-485	-477	-466	-451	-434
0	508	395	210	56	-71	-176	-261	-329	-381	-421	-449	-467	-478	-481	-478	-471	-459	-444	-427
0	502	390	206	54	-72	-175	-258	-325	-376	-415	-442	-460	-470	-473	-470	-462	-451	-436	-419
0	493	383	201	51	-72	-173	-255	-320	-370	-407	-433	-451	-460	-463	-460	-452	-441	-427	-410
0	483	374	196	48	-73	-171	-251	-313	-362	-398	-423	-439	-448	-451	-448	-440	-429	-415	-399
0	470	364	189	44	-73	-168	-245	-305	-351	-386	-410	-426	-434	-436	-433	-426	-416	-402	-387
0	453	351	180	40	-72	-164	-237	-295	-339	-372	-395	-410	-418	-420	-417	-410	-400	-387	-372
0	433	335	170	36	-71	-158	-227	-281	-323	-354	-376	-390	-398	-400	-397	-391	-382	-370	-356
0	406	315	159	33	-67	-148	-213	-264	-303	-333	-353	-367	-375	-377	-375	-369	-361	-350	-337
0	371	291	146	31	-61	-135	-195	-242	-279	-306	-326	-340	-347	-350	-349	-344	-337	-328	-316
0	318	255	131	32	-48	-113	-166	-209	-243	-268	-287	-300	-309	-312	-312	-309	-304	-296	-287
0	0	0	0	0	0	0	0	0	0	0	0	0	0	0	0	0	0	0	0

21:	22:	23:	24:	25:	26:	27:	28:	29:	30:	31:	32:	33:	DIVERGENCE OF
-276	-264	-252	-240	-227	-215	-202	-190	-179	-168	-158	-144	0	RADIATIVE FLUX
-304	-290	-276	-261	-247	-233	-219	-205	-192	-180	-169	-155	0	
-323	-308	-292	-277	-261	-245	-230	-215	-202	-189	-176	-162	0	
-340	-324	-307	-290	-273	-257	-240	-225	-210	-196	-183	-168	0	
-356	-339	-321	-303	-285	-267	-250	-233	-218	-203	-190	-173	0	(Cont'd) A.8 Case 8
-370	-351	-333	-314	-295	-276	-258	-241	-225	-210	-196	-179	0	
-382	-363	-343	-324	-304	-285	-266	-248	-232	-216	-201	-183	0	
-392	-373	-353	-332	-312	-292	-273	-255	-237	-221	-206	-188	0	
-401	-381	-361	-340	-319	-299	-279	-260	-243	-226	-210	-192	0	
-408	-388	-367	-346	-325	-305	-284	-265	-247	-230	-214	-195	0	
-415	-394	-373	-352	-330	-309	-289	-269	-251	-233	-217	-198	0	
-420	-399	-378	-356	-334	-313	-292	-273	-254	-236	-220	-200	0	
-424	-403	-381	-359	-338	-316	-295	-275	-256	-238	-222	-202	0	
-426	-406	-384	-362	-340	-318	-297	-277	-258	-240	-223	-203	0	
-428	-407	-385	-363	-341	-319	-298	-278	-259	-241	-224	-204	0	
-429	-408	-386	-364	-342	-320	-299	-279	-259	-241	-224	-204	0	
-428	-407	-385	-363	-341	-319	-298	-278	-259	-241	-224	-204	0	
-426	-406	-384	-362	-340	-318	-297	-277	-258	-240	-223	-203	0	
-424	-403	-381	-359	-338	-316	-295	-275	-256	-238	-222	-202	0	
-420	-399	-378	-356	-334	-313	-292	-273	-254	-236	-220	-200	0	
-415	-394	-373	-352	-330	-309	-289	-269	-251	-233	-217	-198	0	
-408	-388	-367	-346	-325	-305	-284	-265	-247	-230	-214	-195	0	
-401	-381	-361	-340	-319	-299	-279	-260	-243	-226	-210	-192	0	
-392	-373	-353	-332	-312	-292	-273	-255	-237	-221	-206	-188	0	
-382	-363	-343	-324	-304	-285	-266	-248	-232	-216	-201	-183	0	
-370	-351	-333	-314	-295	-276	-258	-241	-225	-210	-196	-179	0	
-356	-339	-321	-303	-285	-267	-250	-233	-218	-203	-190	-173	0	
-340	-324	-307	-290	-273	-257	-240	-225	-210	-196	-183	-168	0	
-323	-308	-292	-277	-261	-245	-230	-215	-202	-189	-176	-162	0	
-304	-290	-276	-261	-247	-233	-219	-205	-192	-180	-169	-155	0	
-276	-264	-252	-240	-227	-215	-202	-190	-179	-168	-158	-144	0	
0	0	0	0	0	0	0	0	0	0	0	0	0	

Appendix B

3-D Benchmark Verification Solutions

B.1 Case 9: 3-D Thermal Cavity Steady State Solutions, Ra=1.E4

CONVECTION + RADIATION

BC's: No slip; Sides 1 and 6 Dirichlet temps, Sides 2-5 Adiabatic Walls
Explict Parameters: Ra=1.E4, Pr=0.7, Ar=1.0, Gr=1.43E4, Re=120, Pe=83.6,
Implict Parameters: Lo=1 m, Nu=15.89E-6 m2/s, To=294.4 K, dTo=3.68E-7,
ko=26.3E-6 m2/s, po=2.21E-3 Pa, rho,o=1.16 kg/m3,
alpha,o=22.5E-6 m2/s, Uo=1.9E-3 m/s, to=527.4 s

U1 EXP -3 PLANE 9

1:	2:	3:	4:	5:	6:	7:	8:	9:	10:	11:	12:	13:	14:	15:	16:	17:
0	0	0	0	0	0	0	0	0	0	0	0	0	0	0	0	0
0	33	64	91	114	132	144	151	154	155	154	151	145	136	115	70	0
0	49	93	131	162	185	202	213	221	224	224	220	211	193	157	92	0
0	55	104	143	172	192	207	217	225	230	231	229	219	197	154	87	0
0	56	105	140	164	177	186	192	197	201	202	200	189	165	123	65	0
0	54	99	128	144	150	151	152	154	156	156	152	140	116	80	38	0
0	49	86	107	114	112	108	106	105	104	103	96	83	60	34	11	0
0	40	67	77	75	67	59	55	52	51	47	39	25	7	-7	-10	0
0	27	41	38	27	15	6	2	0	-2	-7	-16	-28	-39	-41	-27	0
0	10	7	-8	-26	-40	-48	-51	-53	-55	-60	-67	-75	-77	-67	-40	0
0	-12	-34	-61	-83	-97	-103	-105	-105	-106	-109	-113	-114	-107	-86	-49	0
0	-38	-80	-116	-140	-152	-156	-156	-154	-153	-152	-150	-144	-128	-99	-54	0
0	-66	-124	-165	-189	-200	-203	-201	-197	-192	-186	-177	-164	-140	-105	-56	0
0	-87	-154	-197	-219	-229	-232	-230	-225	-217	-207	-192	-172	-143	-104	-55	0
0	-92	-157	-193	-211	-220	-224	-224	-220	-213	-202	-185	-162	-131	-93	-48	0
0	-70	-115	-136	-145	-151	-154	-155	-154	-151	-143	-131	-114	-91	-64	-33	0
0	0	0	0	0	0	0	0	0	0	0	0	0	0	0	0	0

U2 EXP -3 PLANE 9

1:	2:	3:	4:	5:	6:	7:	8:	9:	10:	11:	12:	13:	14:	15:	16:	17:
0	0	0	0	0	0	0	0	0	0	0	0	0	0	0	0	0
0	35	53	60	58	50	39	28	19	13	9	8	6	1	-11	-27	0
0	64	99	112	108	93	73	53	37	25	17	13	9	0	-25	-53	0
0	87	132	147	141	121	96	70	48	32	21	14	6	-10	-45	-77	0
0	104	154	168	158	133	104	75	52	34	21	10	-2	-26	-69	-98	0
0	116	167	176	159	129	98	70	47	29	14	0	-17	-49	-95	-115	0
0	125	172	172	147	114	83	56	35	18	2	-15	-40	-78	-122	-126	0
0	131	170	158	126	91	61	38	18	1	-15	-37	-68	-108	-144	-132	0
0	134	161	136	98	64	38	17	0	-17	-37	-64	-98	-136	-161	-133	0
0	132	144	108	68	37	15	-1	-18	-37	-61	-91	-125	-158	-170	-131	0
0	126	122	78	40	15	-2	-18	-35	-56	-83	-114	-147	-172	-172	-125	0
0	115	96	49	17	0	-14	-29	-47	-70	-98	-129	-158	-176	-167	-116	0
0	98	69	26	2	-10	-21	-34	-52	-75	-103	-133	-157	-168	-154	-103	0
0	77	45	10	-6	-14	-21	-32	-49	-70	-96	-121	-141	-147	-132	-87	0
0	53	25	0	-9	-13	-17	-25	-37	-54	-73	-93	-108	-111	-99	-64	0
0	27	11	-1	-6	-8	-10	-13	-19	-28	-39	-50	-58	-60	-53	-35	0
0	0	0	0	0	0	0	0	0	0	0	0	0	0	0	0	0

(Cont'd)
B.1 Case 9: 3-D Thermal Cavity Steady State Solutions, Ra=1.E4

U3 EXP -4 PLANE 8

1:	2:	3:	4:	5:	6:	7:	8:	9:	10:	11:	12:	13:	14:	15:	16:	17:
0	0	0	0	0	0	0	0	0	0	0	0	0	0	0	0	0
0	3	6	9	12	13	12	10	7	3	-1	-8	-17	-28	-38	-36	0
0	6	13	21	29	34	36	35	32	27	19	9	-3	-20	-39	-41	0
0	8	19	32	44	55	62	65	63	58	49	37	21	0	-24	-32	0
0	10	23	39	56	72	84	90	91	87	78	64	46	21	-6	-19	0
0	11	26	45	65	85	100	109	112	109	99	85	64	37	9	-7	0
0	12	28	49	72	94	111	122	126	123	113	97	74	47	19	2	0
0	12	29	51	77	100	118	130	134	130	120	103	79	51	25	7	0
0	10	28	52	79	103	121	133	136	132	121	103	79	52	28	10	0
0	7	25	51	79	103	120	130	134	130	118	100	76	51	29	12	0
0	2	19	47	74	97	113	123	126	122	111	94	72	48	28	12	0
0	-7	8	37	64	84	99	108	112	109	100	84	65	44	26	11	0
0	-19	-6	21	46	64	77	86	91	90	83	72	56	39	23	10	0
0	-33	-24	0	21	37	49	58	63	65	62	55	44	31	19	8	0
0	-41	-39	-20	-3	9	19	26	32	35	36	34	28	21	13	6	0
0	-37	-38	-28	-17	-8	-2	3	7	10	12	13	12	9	6	3	0
0	0	0	0	0	0	0	0	0	0	0	0	0	0	0	0	0

U3 EXP -4 PLANE 9

1:	2:	3:	4:	5:	6:	7:	8:	9:	10:	11:	12:	13:	14:	15:	16:	17:
0	0	0	0	0	0	0	0	0	0	0	0	0	0	0	0	0
0	0	0	0	0	0	0	0	0	0	0	0	0	0	0	0	0
0	0	0	0	0	0	0	0	0	0	0	0	0	0	0	0	0
0	0	0	0	0	0	0	0	0	0	0	0	0	0	0	0	0
0	0	0	0	0	0	0	0	0	0	0	0	0	0	0	0	0
0	0	0	0	0	0	0	0	0	0	0	0	0	0	0	0	0
0	0	0	0	0	0	0	0	0	0	0	0	0	0	0	0	0
0	0	0	0	0	0	0	0	0	0	0	0	0	0	0	0	0
0	0	0	0	0	0	0	0	0	0	0	0	0	0	0	0	0
0	0	0	0	0	0	0	0	0	0	0	0	0	0	0	0	0
0	0	0	0	0	0	0	0	0	0	0	0	0	0	0	0	0
0	0	0	0	0	0	0	0	0	0	0	0	0	0	0	0	0
0	0	0	0	0	0	0	0	0	0	0	0	0	0	0	0	0
0	0	0	0	0	0	0	0	0	0	0	0	0	0	0	0	0
0	0	0	0	0	0	0	0	0	0	0	0	0	0	0	0	0
0	0	0	0	0	0	0	0	0	0	0	0	0	0	0	0	0
0	0	0	0	0	0	0	0	0	0	0	0	0	0	0	0	0
0	0	0	0	0	0	0	0	0	0	0	0	0	0	0	0	0

U3 EXP -4 PLANE 10

1:	2:	3:	4:	5:	6:	7:	8:	9:	10:	11:	12:	13:	14:	15:	16:	17:
0	0	0	0	0	0	0	0	0	0	0	0	0	0	0	0	0
0	-3	-6	-9	-12	-13	-12	-10	-7	-3	1	8	17	28	38	36	0
0	-6	-13	-21	-29	-34	-36	-35	-32	-27	-19	-9	3	20	39	41	0
0	-8	-19	-32	-44	-55	-62	-65	-63	-58	-49	-37	-21	0	24	32	0
0	-10	-23	-39	-56	-72	-84	-90	-91	-87	-78	-64	-46	-21	6	19	0
0	-11	-26	-45	-65	-85	-100	-109	-112	-109	-99	-85	-64	-37	-9	7	0
0	-12	-28	-49	-72	-94	-111	-122	-126	-123	-113	-97	-74	-47	-19	-2	0
0	-12	-29	-51	-77	-100	-118	-130	-134	-130	-120	-103	-79	-51	-25	-7	0
0	-10	-28	-52	-79	-103	-121	-133	-136	-132	-121	-103	-79	-52	-28	-10	0
0	-7	-25	-51	-79	-103	-120	-130	-134	-130	-118	-100	-76	-51	-29	-12	0
0	-2	-19	-47	-74	-97	-113	-123	-126	-122	-111	-94	-72	-48	-28	-12	0
0	7	-8	-37	-64	-84	-99	-108	-112	-109	-100	-84	-65	-45	-26	-11	0
0	19	6	-21	-46	-64	-77	-86	-91	-90	-83	-72	-56	-39	-23	-10	0
0	33	24	0	-21	-37	-49	-58	-63	-65	-62	-55	-44	-31	-19	-8	0
0	41	39	20	3	-9	-19	-26	-32	-35	-36	-34	-28	-21	-13	-6	0
0	37	38	28	17	8	2	-3	-7	-10	-12	-13	-12	-9	-6	-3	0
0	0	0	0	0	0	0	0	0	0	0	0	0	0	0	0	0

(Cont'd)
B.1 Case 9: 3-D Thermal Cavity Steady State Solutions, Ra=1.E4

TEMPERATURE EXP -2 PLANE 1

1:	2:	3:	4:	5:	6:	7:	8:	9:	10:	11:	12:	13:	14:	15:	16:	17:
100	97	94	91	88	86	83	80	77	74	70	65	58	49	35	19	0
100	97	94	91	88	85	83	80	77	74	70	65	59	49	36	19	0
100	96	93	90	87	84	81	79	76	73	69	65	58	49	36	19	0
100	96	92	88	85	82	79	76	73	70	67	63	56	47	35	18	0
100	95	90	86	82	79	75	73	70	67	64	59	53	45	32	17	0
100	94	88	83	79	75	71	68	65	63	59	55	49	41	29	15	0
100	93	86	80	74	70	66	63	60	58	54	50	44	36	26	13	0
100	91	83	76	70	65	61	58	55	52	49	45	39	32	23	11	0
100	89	80	72	65	60	56	52	49	47	43	39	34	27	19	10	0
100	88	76	67	60	54	50	47	44	41	38	34	29	23	16	8	0
100	86	73	62	55	49	45	41	39	36	33	29	25	19	13	6	0
100	84	69	58	50	44	40	36	34	31	28	24	20	16	11	5	0
100	82	66	54	46	40	35	32	29	26	24	20	17	13	9	4	0
100	81	64	52	43	36	32	28	26	23	20	17	14	11	7	3	0
100	80	63	50	41	34	30	26	23	20	18	15	12	9	6	3	0
100	80	63	50	40	34	29	25	22	19	16	14	11	8	5	2	0
100	80	63	50	40	34	28	25	22	19	16	13	11	8	5	2	0

TEMPERATURE EXP -2 PLANE 9

1:	2:	3:	4:	5:	6:	7:	8:	9:	10:	11:	12:	13:	14:	15:	16:	17:
100	97	95	92	90	87	85	82	80	78	76	72	68	60	46	25	0
100	97	95	92	89	87	84	82	80	78	76	73	69	61	48	27	0
100	97	94	91	88	85	83	80	78	76	75	72	69	63	51	29	0
100	96	92	89	85	82	79	77	75	73	72	70	67	61	50	29	0
100	95	90	85	81	77	74	72	70	69	68	66	63	58	47	27	0
100	94	88	81	76	72	69	67	65	64	63	61	58	53	42	23	0
100	92	84	77	71	66	63	61	60	59	58	56	53	46	36	19	0
100	90	80	71	65	61	58	56	55	54	52	50	46	40	30	15	0
100	87	75	65	59	55	52	51	49	48	47	44	40	34	24	12	0
100	83	69	59	53	49	47	45	44	43	41	38	34	28	19	9	0
100	80	63	52	46	43	41	40	39	38	36	33	28	22	15	7	0
100	76	57	46	41	38	36	35	34	32	30	27	23	17	11	5	0
100	72	52	41	36	33	31	30	29	27	25	22	18	14	9	4	0
100	70	49	37	32	29	27	26	24	22	20	17	14	10	7	3	0
100	70	48	36	30	27	24	22	21	19	16	14	11	8	5	2	0
100	72	51	38	30	26	23	21	19	17	15	12	10	7	4	2	0
100	74	53	39	31	26	23	21	19	17	14	12	9	7	4	2	0

TEMPERATURE EXP -2 PLANE 17

1:	2:	3:	4:	5:	6:	7:	8:	9:	10:	11:	12:	13:	14:	15:	16:	17:
100	97	94	91	88	86	83	80	77	74	70	65	58	49	35	19	0
100	97	94	91	88	85	83	80	77	74	70	65	59	49	36	19	0
100	96	93	90	87	84	81	79	76	73	69	65	58	49	36	19	0
100	96	92	88	85	82	79	76	73	70	67	63	56	47	35	18	0
100	95	90	86	82	79	75	73	70	67	64	59	53	45	32	17	0
100	94	88	83	79	75	71	68	65	63	59	55	49	41	29	15	0
100	93	86	80	74	70	66	63	60	58	54	50	44	36	26	13	0
100	91	83	76	70	65	61	58	55	52	49	45	39	32	23	11	0
100	89	80	72	65	60	56	52	49	47	43	39	34	27	19	10	0
100	88	76	67	60	54	50	47	44	41	38	34	29	23	16	8	0
100	86	73	62	55	49	45	41	39	36	33	29	25	19	13	6	0
100	84	69	58	50	44	40	36	34	31	28	24	20	16	11	5	0
100	82	66	54	46	40	35	32	29	26	24	20	17	13	9	4	0
100	81	64	52	43	36	32	28	26	23	20	17	14	11	7	3	0
100	80	63	50	41	34	30	26	23	20	18	15	12	9	6	3	0
100	80	63	50	40	34	29	25	22	19	16	14	11	8	5	2	0
100	80	63	50	40	34	28	25	22	19	16	13	11	8	5	2	0

B.2 Case 10: 3-D Ad Hoc Benchmark Baseline Conductive Flux

PURE CONVECTION
BC's: No slip; Sides 1 and 6 Non-zero Neumann, Sides 2-5 Adiabatic Walls
Explict Parameters: Ra=1.E4, Pr=0.7, Ar=1.0, Gr=1.43E4, Re=120, Pe=83.6
Implict Parameters: Lo=1 m, Nu=15.89E-6 m2/s, To=294.4 K, dTo=3.68E-7
ko=26.3E-6 m2/s, po=2.21E-3 Pa, rho,o=1.16 kg/m3
alpha,o=22.5E-6 m2/s, Uo=1.9E-3 m/s, to=527.4 s

TEMPERATURE EXP -3 PLANE 9

1:	2:	3:	4:	5:	6:	7:	8:	9:	10:	11:	12:	13:	14:	15:	16:	17:
995	976	951	926	900	875	852	829	807	785	761	729	681	599	465	249	46
995	976	950	924	898	872	848	826	805	784	761	732	690	616	490	268	49
994	973	943	913	883	855	830	807	788	769	750	727	692	630	513	288	52
993	967	928	891	854	821	794	772	754	738	722	703	674	618	508	286	52
991	957	907	859	814	776	747	725	708	695	681	664	637	583	475	264	48
989	943	879	819	766	724	694	673	657	645	633	616	587	531	423	229	42
986	926	844	772	712	668	638	618	604	593	580	562	530	469	363	191	35
982	904	802	718	654	610	582	564	552	540	527	505	468	404	302	154	28
977	877	752	658	592	551	526	511	499	487	471	447	406	340	246	122	22
971	845	696	594	530	493	471	458	446	434	416	388	344	280	196	95	17
964	808	635	529	468	436	417	405	393	380	360	330	286	226	154	73	13
957	769	575	467	411	382	365	353	341	326	304	274	232	179	119	56	10
951	735	523	415	361	334	317	303	290	273	251	222	185	140	92	42	8
947	713	490	380	324	295	276	260	244	226	204	177	145	108	70	32	6
947	711	485	368	306	272	248	229	211	191	169	144	116	86	56	26	5
950	731	509	382	308	266	237	215	194	173	150	126	101	75	49	23	4
953	749	533	399	317	269	238	213	191	170	147	123	98	73	48	23	4

CONDUCTIVE FLUX EXP -4 PLANE 9

1:	2:	3:	4:	5:	6:	7:	8:	9:	10:	11:	12:	13:	14:	15:	16:	17:
46	0	0	0	0	0	0	0	0	0	0	0	0	0	0	0-460	
47	0	0	0	0	0	0	0	0	0	0	0	0	0	0	0-488	
53	0	0	0	0	0	0	0	0	0	0	0	0	0	0	0-516	
66	0	0	0	0	0	0	0	0	0	0	0	0	0	0	0-512	
87	0	0	0	0	0	0	0	0	0	0	0	0	0	0	0-476	
113	0	0	0	0	0	0	0	0	0	0	0	0	0	0	0-420	
147	0	0	0	0	0	0	0	0	0	0	0	0	0	0	0-357	
188	0	0	0	0	0	0	0	0	0	0	0	0	0	0	0-294	
237	0	0	0	0	0	0	0	0	0	0	0	0	0	0	0-237	
295	0	0	0	0	0	0	0	0	0	0	0	0	0	0	0-187	
357	0	0	0	0	0	0	0	0	0	0	0	0	0	0	0-146	
421	0	0	0	0	0	0	0	0	0	0	0	0	0	0	0-113	
477	0	0	0	0	0	0	0	0	0	0	0	0	0	0	0 -86	
513	0	0	0	0	0	0	0	0	0	0	0	0	0	0	0 -66	
517	0	0	0	0	0	0	0	0	0	0	0	0	0	0	0 -53	
489	0	0	0	0	0	0	0	0	0	0	0	0	0	0	0 -47	
461	0	0	0	0	0	0	0	0	0	0	0	0	0	0	0 -46	

B.3 Case 11: 3-D Verification of Combined Conductive and Radiative Flux in a Non-Participating Medium, e=1.0

CONVECTION + RADIATION

BC's: No slip; Sides 1 and 6 Non-zero Neumann, Sides 2-5 Adiabatic Walls

Explict Parameters: Ra=1.E4, Pr=0.7, Ar=1.0, Gr=1.43E4, Re=120, Pe=83.6, Bo=40.65

Implict Parameters: Lo=1 m, Nu=15.89E-6 m2/s, To=294.4 K, dTo=3.68E-7, ko=26.3E-6 m2/s po=2.21E-3 Pa, rho,o=1.16 kg/m3, alpha,o=22.5E-6 m2/s, Uo=1.9E-3 m/s to=527.4 s, black surfaces

TEMPERATURE EXP -3 PLANE 9

1:	2:	3:	4:	5:	6:	7:	8:	9:	10:	11:	12:	13:	14:	15:	16:	17:
987	978	950	926	900	875	852	829	807	785	761	729	681	599	466	249	49
988	977	949	924	898	872	848	826	805	784	761	732	690	616	490	267	53
987	974	943	913	883	855	829	807	788	769	750	727	692	630	514	287	56
985	968	928	891	854	821	794	772	754	738	722	703	674	618	508	285	56
983	958	907	859	814	776	747	725	708	695	681	664	637	583	475	263	53
980	945	879	819	766	724	694	672	657	645	633	616	587	530	423	228	46
976	928	844	772	712	668	638	618	604	593	580	562	530	469	363	190	39
972	906	802	718	654	610	582	564	552	540	526	505	468	404	302	153	33
967	879	752	658	592	551	526	511	499	487	471	447	406	340	246	121	27
961	847	695	594	530	493	471	458	446	434	416	388	344	280	196	94	22
954	810	635	529	468	436	417	405	393	380	360	329	286	226	154	72	18
947	771	575	468	411	382	365	353	341	326	304	274	232	179	120	55	14
941	737	523	415	361	334	317	303	290	273	251	222	184	140	92	41	11
936	715	490	380	324	295	276	260	244	226	204	177	145	108	70	32	9
936	713	484	368	306	272	248	229	211	191	169	144	116	86	56	25	8
940	733	508	382	308	266	237	215	194	173	150	126	101	75	49	22	7
945	751	533	399	317	269	238	213	191	170	147	123	98	73	48	22	7

RADIATIVE FLUX EXP -4 PLANE 9

1:	2:	3:	4:	5:	6:	7:	8:	9:	10:	11:	12:	13:	14:	15:	16:	17:
165	95	75	64	55	48	42	38	35	32	28	22	11	-4	-20	-27	-61
150	0	0	0	0	0	0	0	0	0	0	0	0	0	0	0	-77
159	0	0	0	0	0	0	0	0	0	0	0	0	0	0	0	-86
170	0	0	0	0	0	0	0	0	0	0	0	0	0	0	0	-93
180	0	0	0	0	0	0	0	0	0	0	0	0	0	0	0	-96
189	0	0	0	0	0	0	0	0	0	0	0	0	0	0	0	-98
196	0	0	0	0	0	0	0	0	0	0	0	0	0	0	0	-98
202	0	0	0	0	0	0	0	0	0	0	0	0	0	0	0	-98
207	0	0	0	0	0	0	0	0	0	0	0	0	0	0	0	-96
212	0	0	0	0	0	0	0	0	0	0	0	0	0	0	0	-93
216	0	0	0	0	0	0	0	0	0	0	0	0	0	0	0	-90
219	0	0	0	0	0	0	0	0	0	0	0	0	0	0	0	-86
221	0	0	0	0	0	0	0	0	0	0	0	0	0	0	0	-82
222	0	0	0	0	0	0	0	0	0	0	0	0	0	0	0	-77
221	0	0	0	0	0	0	0	0	0	0	0	0	0	0	0	-73
217	0	0	0	0	0	0	0	0	0	0	0	0	0	0	0	-67
157	-71	-124	-129	-122	-114	-105	-96	-87	-79	-72	-65	-59	-53	-47	-43	-71

RADIATIVE FLUX EXP -4 PLANE 1 OR 17 (x3=0. or 1.)

1:	2:	3:	4:	5:	6:	7:	8:	9:	10:	11:	12:	13:	14:	15:	16:	17:
131	79	63	52	42	34	27	21	15	9	2	-6	-15	-24	-29	-29	-55
119	60	40	29	21	15	10	6	2	-1	-6	-11	-19	-25	-29	-28	-51
127	57	32	19	10	3	-1	-4	-7	-9	-13	-17	-24	-30	-33	-31	-58
135	56	27	10	-1	-8	-13	-15	-17	-18	-20	-24	-29	-34	-36	-34	-62
142	54	18	-2	-15	-23	-27	-29	-29	-29	-30	-31	-35	-38	-39	-36	-66
148	48	7	-16	-31	-39	-42	-42	-41	-40	-39	-39	-40	-41	-40	-37	-68
152	41	-5	-32	-47	-54	-56	-54	-52	-49	-47	-45	-45	-43	-41	-37	-69
156	32	-20	-47	-61	-66	-66	-64	-60	-56	-53	-50	-47	-45	-41	-37	-69
159	22	-34	-61	-73	-76	-74	-70	-66	-61	-56	-52	-49	-45	-41	-36	-68
161	12	-48	-73	-82	-83	-79	-74	-68	-63	-58	-53	-49	-44	-40	-35	-67
163	1	-60	-83	-88	-86	-81	-75	-69	-63	-57	-52	-48	-43	-39	-34	-66
164	-8	-69	-89	-91	-87	-81	-74	-68	-62	-56	-51	-46	-41	-37	-33	-63
164	-16	-76	-91	-91	-85	-78	-72	-65	-59	-53	-48	-44	-39	-35	-32	-61
163	-22	-78	-90	-88	-81	-74	-67	-61	-55	-50	-45	-41	-37	-33	-30	-58
159	-24	-76	-85	-81	-75	-68	-62	-56	-51	-47	-42	-38	-35	-31	-28	-55
149	-20	-66	-73	-71	-66	-61	-56	-51	-47	-43	-39	-35	-32	-29	-26	-52
116	-25	-74	-87	-89	-86	-81	-76	-71	-66	-61	-56	-51	-47	-43	-39	-68

B.4 Case 12: 3-D Verification of Combined Conductive and Radiative Flux in a Non-Participating Medium, e=0.1

CONVECTION + RADIATION

BC's: No slip; Sides 1 and 6 Non-zero Neumann, Sides 2-5 Adiabatic Walls

Explict Parameters: Ra=1.E4, Pr=0.7, Ar=1.0, Gr=1.43E4, Re=120, Pe=83.6, Bo=40.65

Implict Parameters: Lo=1 m, Nu=15.89E-6 m2/s, To=294.4 K, dTo=3.68E-7, ko=26.3E-6 m2/s
po=2.21E-3 Pa, rho,o=1.16 kg/m3, alpha,o=22.5E-6 m2/s,
Uo=1.9E-3 m/s to=527.4 s, gray surfaces

TEMPERATURE EXP -3 PLANE 9

1:	2:	3:	4:	5:	6:	7:	8:	9:	10:	11:	12:	13:	14:	15:	16:	17:
995	976	951	926	900	875	852	829	807	785	761	729	681	599	466	249	47
994	976	950	924	898	872	848	826	805	784	761	732	690	616	490	268	49
994	973	943	913	883	855	829	807	788	769	750	727	692	630	513	288	53
992	967	928	891	854	821	794	772	754	738	722	703	674	618	508	286	52
991	957	907	859	814	776	747	725	708	695	681	664	637	583	475	264	48
988	943	879	819	766	724	694	672	657	645	633	616	587	530	423	229	42
985	926	844	772	712	668	638	618	604	593	580	562	530	469	363	191	35
981	904	802	718	654	610	582	564	552	540	526	505	468	404	302	154	28
976	877	752	658	592	551	526	511	499	487	471	447	406	340	246	122	23
970	845	696	594	530	493	471	458	446	434	416	388	344	280	196	95	18
963	808	635	529	468	436	417	405	393	380	360	329	286	226	154	73	14
956	769	575	467	411	382	365	353	341	326	304	274	232	179	119	56	10
950	735	523	415	361	334	317	303	290	273	251	222	184	140	92	42	8
946	713	490	380	324	295	276	260	244	226	204	177	145	108	70	32	6
946	711	485	368	306	272	248	229	211	191	169	144	116	86	56	26	5
949	731	509	382	308	266	237	215	194	173	150	126	101	75	49	23	4
952	749	533	399	317	269	238	213	191	170	147	123	98	73	48	23	4

RADIATIVE FLUX EXP -4 PLANE 9

1:	2:	3:	4:	5:	6:	7:	8:	9:	10:	11:	12:	13:	14:	15:	16:	17:
70	152	128	109	91	75	61	49	38	28	18	6	-9	-30	-49	-56	-131
177	0	0	0	0	0	0	0	0	0	0	0	0	0	0	0	-62
176	0	0	0	0	0	0	0	0	0	0	0	0	0	0	0	-66
177	0	0	0	0	0	0	0	0	0	0	0	0	0	0	0	-67
179	0	0	0	0	0	0	0	0	0	0	0	0	0	0	0	-68
180	0	0	0	0	0	0	0	0	0	0	0	0	0	0	0	-68
181	0	0	0	0	0	0	0	0	0	0	0	0	0	0	0	-68
181	0	0	0	0	0	0	0	0	0	0	0	0	0	0	0	-68
182	0	0	0	0	0	0	0	0	0	0	0	0	0	0	0	-68
182	0	0	0	0	0	0	0	0	0	0	0	0	0	0	0	-68
183	0	0	0	0	0	0	0	0	0	0	0	0	0	0	0	-67
183	0	0	0	0	0	0	0	0	0	0	0	0	0	0	0	-67
183	0	0	0	0	0	0	0	0	0	0	0	0	0	0	0	-66
183	0	0	0	0	0	0	0	0	0	0	0	0	0	0	0	-65
183	0	0	0	0	0	0	0	0	0	0	0	0	0	0	0	-64
185	0	0	0	0	0	0	0	0	0	0	0	0	0	0	0	-61
69	3	-52	-66	-69	-69	-69	-68	-67	-66	-65	-65	-64	-63	-62	-59	-133

RADIATIVE FLUX EXP -5 PLANE (1 or 17)

1:	2:	3:	4:	5:	6:	7:	8:	9:	10:	11:	12:	13:	14:	15:	16:	17:
-3	35	12	-3	-17	-29	-40	-50	-59	-69	-79	-90	-101	-112	-117	-114	-167
60	146	119	97	78	62	47	35	23	11	-1	-15	-30	-43	-52	-52	-119
58	140	111	88	68	52	37	25	14	3	-7	-20	-34	-47	-55	-56	-127
60	136	103	77	56	39	25	13	3	-5	-15	-26	-38	-50	-57	-58	-130
62	129	91	62	39	22	9	0	-9	-17	-25	-34	-44	-53	-59	-58	-132
64	121	77	45	21	4	-7	-15	-22	-29	-35	-42	-50	-56	-60	-59	-133
66	111	61	27	3	-12	-22	-29	-35	-40	-44	-50	-55	-59	-61	-59	-133
67	100	45	9	-13	-27	-35	-41	-45	-48	-52	-55	-58	-61	-62	-59	-134
68	88	28	-7	-27	-39	-46	-50	-53	-55	-57	-59	-61	-62	-62	-59	-134
69	76	12	-21	-39	-49	-54	-56	-58	-59	-61	-62	-62	-63	-62	-59	-133
69	64	-1	-33	-48	-56	-59	-61	-62	-62	-63	-63	-63	-63	-62	-59	-132
70	52	-13	-43	-55	-60	-62	-63	-64	-64	-63	-63	-63	-62	-61	-58	-131
70	43	-22	-49	-59	-63	-64	-64	-64	-64	-64	-63	-63	-62	-61	-58	-130
69	36	-28	-52	-61	-64	-65	-65	-64	-64	-63	-63	-62	-61	-60	-57	-128
69	34	-30	-53	-61	-64	-64	-64	-64	-63	-62	-62	-61	-60	-59	-56	-126
71	37	-27	-50	-58	-60	-61	-61	-61	-60	-59	-59	-58	-57	-56	-52	-119
-10	-55	-110	-129	-136	-137	-137	-136	-134	-133	-131	-130	-128	-126	-123	-116	-172

B.5 Case 13: 3-D Verification of Combined Conductive and Radiative Flux in a Non-Participating Medium, e=1.0

CONVECTION + RADIATION

BC's: No slip; Sides 1 and 6 Non-zero Neumann, Sides 2-5 Adiabatic Walls

Explict Parameters: Ra=1.E4, Pr=0.7, Ar=1.0, Gr=1.43E4, Re=120, Pe=83.6, Bo=40.65

Implict Parameters: Lo=1 m, Nu=15.89E-6 m2/s, To=294.4 K, dTo=3.68E-7, ko=26.3E-6 m2/s
po=2.21E-3 Pa, rho,o=1.16 kg/m3, alpha,o=22.5E-6 m2/s,
Uo=1.9E-3 m/s to=527.4 s, black surfaces, Ka=Kt=1 1/m, Ks=0 1/m

TEMPERATURE EXP -3 PLANE 9

1:	2:	3:	4:	5:	6:	7:	8:	9:	10:	11:	12:	13:	14:	15:	16:	17:
989	977	950	926	900	875	852	829	807	785	761	729	681	599	466	249	48
990	977	949	924	897	872	848	826	804	784	761	732	690	616	490	268	51
988	974	942	913	883	855	829	807	788	769	750	727	692	630	514	287	55
987	967	928	890	854	821	794	772	754	738	722	703	674	618	508	286	55
984	958	907	859	814	776	747	725	709	695	681	664	637	583	475	264	51
981	944	879	819	767	725	694	673	658	645	633	616	587	531	423	229	44
977	927	844	773	713	669	639	619	605	593	581	562	530	469	363	190	37
973	906	802	719	655	611	583	565	552	541	527	505	468	404	303	154	30
968	879	753	659	593	552	527	511	499	488	472	447	406	340	246	121	24
961	847	696	595	530	493	472	458	447	434	416	388	344	280	196	94	19
954	810	636	530	469	437	418	405	394	380	360	330	286	226	154	73	15
947	772	576	468	412	383	366	353	341	326	305	274	232	179	120	55	12
941	737	524	416	362	335	318	304	290	274	252	222	185	140	92	42	9
937	715	491	381	325	296	277	261	245	227	205	178	145	108	71	32	7
936	714	485	369	307	272	249	230	211	191	169	144	116	86	56	26	6
940	733	509	383	309	266	238	215	194	173	151	127	101	75	49	23	5
945	751	533	399	317	269	238	213	191	170	147	123	98	73	48	22	5

RADIATIVE FLUX EXP -4 PLANE 9

1:	2:	3:	4:	5:	6:	7:	8:	9:	10:	11:	12:	13:	14:	15:	16:	17:
119	67	56	50	45	41	39	37	35	33	30	25	16	2	-11	-17	-38
114	0	0	0	0	0	0	0	0	0	0	0	0	0	0	0	-47
126	0	0	0	0	0	0	0	0	0	0	0	0	0	0	0	-51
138	0	0	0	0	0	0	0	0	0	0	0	0	0	0	0	-54
150	0	0	0	0	0	0	0	0	0	0	0	0	0	0	0	-54
160	0	0	0	0	0	0	0	0	0	0	0	0	0	0	0	-53
171	0	0	0	0	0	0	0	0	0	0	0	0	0	0	0	-51
181	0	0	0	0	0	0	0	0	0	0	0	0	0	0	0	-49
190	0	0	0	0	0	0	0	0	0	0	0	0	0	0	0	-46
199	0	0	0	0	0	0	0	0	0	0	0	0	0	0	0	-43
206	0	0	0	0	0	0	0	0	0	0	0	0	0	0	0	-41
212	0	0	0	0	0	0	0	0	0	0	0	0	0	0	0	-38
217	0	0	0	0	0	0	0	0	0	0	0	0	0	0	0	-35
219	0	0	0	0	0	0	0	0	0	0	0	0	0	0	0	-32
219	0	0	0	0	0	0	0	0	0	0	0	0	0	0	0	-30
214	0	0	0	0	0	0	0	0	0	0	0	0	0	0	0	-28
151	-55	-92	-90	-80	-70	-61	-54	-47	-41	-36	-31	-27	-24	-21	-19	-32

DIVERGENCE OF RADIATIVE FLUX EXP -3 PLANE 9

1:	2:	3:	4:	5:	6:	7:	8:	9:	10:	11:	12:	13:	14:	15:	16:	17:
0	0	0	0	0	0	0	0	0	0	0	0	0	0	0	0	0
0	39	31	25	20	17	15	14	14	15	15	14	9	0	-13	-19	0
0	44	31	21	13	9	7	7	9	11	14	15	12	3	-12	-21	0
0	44	25	9	-1	-7	-8	-6	-2	1	5	8	8	1	-13	-22	0
0	40	13	-7	-20	-26	-26	-22	-17	-11	-6	-2	-1	-6	-17	-23	0
0	33	-1	-26	-39	-43	-41	-36	-29	-23	-16	-12	-11	-14	-21	-23	0
0	23	-19	-45	-56	-57	-52	-46	-38	-31	-25	-20	-19	-21	-23	-23	0
0	10	-39	-63	-69	-67	-60	-52	-44	-37	-31	-26	-24	-24	-24	-22	0
0	-6	-59	-78	-79	-73	-64	-55	-47	-40	-34	-30	-27	-26	-24	-21	0
0	-25	-77	-89	-85	-76	-66	-56	-48	-41	-35	-31	-28	-25	-22	-19	0
0	-44	-92	-96	-87	-76	-65	-56	-48	-41	-35	-31	-27	-24	-21	-18	0
0	-62	-102	-99	-87	-74	-63	-54	-46	-39	-34	-30	-26	-22	-19	-17	0
0	-76	-107	-98	-84	-71	-60	-51	-43	-37	-32	-28	-24	-21	-18	-15	0
0	-83	-107	-94	-79	-66	-55	-47	-40	-34	-29	-25	-22	-19	-16	-14	0
0	-82	-101	-87	-72	-60	-50	-42	-36	-31	-27	-23	-20	-17	-15	-13	0
0	-69	-86	-74	-62	-51	-44	-37	-32	-27	-24	-21	-18	-15	-13	-11	0
0	0	0	0	0	0	0	0	0	0	0	0	0	0	0	0	0

B.6 Case 14: 3-D Verification of Combined Conductive and Radiative Flux in a Participating Medium, e=0.1

CONVECTION + RADIATION

BC's: No slip; Sides 1 and 6 Non-zero Neumann, Sides 2-5 Adiabatic Walls

Explict Parameters: Ra=1.E4, Pr=0.7, Ar=1.0, Gr=1.43E4, Re=120, Pe=83.6, Bo=40.65

Implict Parameters: Lo=1 m, Nu=15.89E-6 m2/s, To=294.4 K, dTo=3.68E-7, ko=26.3E-6 m2/s po=2.21E-3 Pa, rho,o=1.16 kg/m3, alpha,o=22.5E-6 m2/s, Uo=1.9E-3 m/s to=527.4 s, gray surfaces, Ka=Kt=1 1/m, Ks=0 1/m

TEMPERATURE EXP -3 PLANE 9

1:	2:	3:	4:	5:	6:	7:	8:	9:	10:	11:	12:	13:	14:	15:	16:	17:
994	976	951	926	900	875	852	829	807	785	761	729	681	599	466	249	46
994	975	949	923	897	871	848	825	804	783	761	732	690	616	490	268	49
994	972	942	912	882	854	829	807	787	769	750	726	692	630	514	288	53
992	965	927	890	853	821	794	772	754	738	722	703	674	618	508	286	52
990	956	906	858	813	776	747	725	708	695	681	664	637	583	475	264	48
988	942	878	819	766	724	694	673	657	645	633	616	587	531	423	230	42
985	925	844	772	712	669	638	618	605	593	581	562	530	469	363	191	35
981	903	802	718	654	610	582	564	552	540	527	505	468	404	303	154	28
976	876	752	658	593	552	527	511	499	487	472	447	406	340	246	122	22
970	844	696	594	530	493	472	458	447	434	416	388	344	280	197	95	17
963	807	635	529	469	436	418	405	394	380	360	330	286	226	154	73	13
956	769	575	468	411	383	366	353	341	326	304	274	232	179	120	56	10
950	735	524	416	362	334	317	304	290	274	252	222	185	140	92	42	8
946	713	490	380	325	296	276	260	245	227	205	178	145	108	71	33	6
946	711	485	369	306	272	249	229	211	191	169	144	116	86	56	26	5
949	731	509	382	309	266	238	215	194	173	151	127	101	75	49	23	4
952	749	533	399	317	269	238	213	191	170	147	123	98	73	48	23	4

RADIATIVE FLUX EXP -5 PLANE 9

1:	2:	3:	4:	5:	6:	7:	8:	9:	10:	11:	12:	13:	14:	15:	16:	17:
183	123	104	90	78	68	60	53	47	41	35	26	14	-2	-20	-28	-28
149	0	0	0	0	0	0	0	0	0	0	0	0	0	0	0	-39
151	0	0	0	0	0	0	0	0	0	0	0	0	0	0	0	-40
156	0	0	0	0	0	0	0	0	0	0	0	0	0	0	0	-40
161	0	0	0	0	0	0	0	0	0	0	0	0	0	0	0	-39
168	0	0	0	0	0	0	0	0	0	0	0	0	0	0	0	-37
175	0	0	0	0	0	0	0	0	0	0	0	0	0	0	0	-35
183	0	0	0	0	0	0	0	0	0	0	0	0	0	0	0	-33
190	0	0	0	0	0	0	0	0	0	0	0	0	0	0	0	-31
196	0	0	0	0	0	0	0	0	0	0	0	0	0	0	0	-29
202	0	0	0	0	0	0	0	0	0	0	0	0	0	0	0	-28
206	0	0	0	0	0	0	0	0	0	0	0	0	0	0	0	-26
210	0	0	0	0	0	0	0	0	0	0	0	0	0	0	0	-25
211	0	0	0	0	0	0	0	0	0	0	0	0	0	0	0	-24
211	0	0	0	0	0	0	0	0	0	0	0	0	0	0	0	-23
209	0	0	0	0	0	0	0	0	0	0	0	0	0	0	0	-23
216	22	-27	-37	-37	-36	-34	-32	-30	-28	-27	-25	-24	-23	-22	-22	-20

DIVERGENCE OF RADIATIVE FLUX EXP -3 PLANE 9

1:	2:	3:	4:	5:	6:	7:	8:	9:	10:	11:	12:	13:	14:	15:	16:	17:
0	0	0	0	0	0	0	0	0	0	0	0	0	0	0	0	0
0	144	119	100	84	71	61	53	47	41	35	27	15	-2	-24	-37	0
0	141	114	91	73	60	50	43	38	34	30	25	16	0	-21	-37	0
0	137	104	76	55	40	31	26	23	21	20	17	11	-1	-22	-37	0
0	132	90	57	34	19	11	8	6	6	6	5	1	-9	-25	-37	0
0	125	74	37	13	0	-5	-7	-7	-6	-5	-5	-9	-17	-29	-36	0
0	115	55	17	-4	-14	-18	-18	-17	-16	-14	-15	-18	-24	-31	-35	0
0	103	35	-1	-19	-25	-27	-26	-24	-22	-21	-21	-24	-28	-32	-34	0
0	87	15	-17	-29	-33	-33	-31	-29	-27	-26	-26	-27	-29	-31	-32	0
0	69	-2	-29	-36	-37	-36	-34	-31	-29	-28	-28	-28	-29	-30	-30	0
0	51	-17	-37	-40	-39	-37	-35	-33	-31	-29	-29	-28	-28	-28	-29	0
0	34	-27	-41	-42	-40	-38	-35	-33	-31	-30	-29	-28	-27	-27	-27	0
0	20	-34	-43	-42	-40	-37	-35	-33	-31	-29	-28	-27	-26	-26	-26	0
0	13	-36	-43	-42	-39	-37	-34	-32	-30	-29	-27	-26	-25	-25	-25	0
0	13	-36	-42	-41	-39	-36	-34	-32	-30	-28	-27	-26	-25	-24	-25	0
0	21	-32	-41	-41	-39	-36	-34	-32	-30	-29	-27	-26	-25	-25	-25	0
0	0	0	0	0	0	0	0	0	0	0	0	0	0	0	0	0

B.7 Case 15: 3-D Steady State Solutions of Participating Thermal Cavity, Fluid Ra=1.E4, Mesh=16x16x16

CONVECTION + RADIATION

BC's: No slip; Sides 1 and 6 Non-zero Neumann, Sides 2-5 Adiabatic Walls
Explict Parameters: Ra=1.E4, Pr=0.7, Ar=1.0, Gr=1.43E4, Re=120, Pe=83.6, Bo=40.65
Implict Parameters: Lo=1 m, Nu=15.89E-6 m2/s, To=294.4 K, dTo=3.68E-7, ko=26.3E-6 m2/s
po=2.21E-3 Pa, rho,o=1.16 kg/m3, alpha,o=22.5E-6 m2/s,
Uo=1.9E-3 m/s to=527.4 s, black surfaces, Ka=Kt=1 1/m, Ks=0 1/m

U1 EXP -3 PLANE 9

1:	2:	3:	4:	5:	6:	7:	8:	9:	10:	11:	12:	13:	14:	15:	16:	17:
0	0	0	0	0	0	0	0	0	0	0	0	0	0	0	0	0
0	31	61	87	111	130	144	154	160	163	164	161	156	146	124	76	0
0	46	89	126	157	181	200	214	224	231	234	233	226	208	170	100	0
0	52	98	136	165	186	201	213	223	231	236	237	230	210	167	95	0
0	52	98	133	155	169	177	184	190	197	202	203	196	174	133	71	0
0	50	91	119	134	139	140	142	145	148	151	151	142	120	84	41	0
0	44	77	96	101	99	96	94	94	95	96	92	81	61	35	12	0
0	34	57	64	60	52	45	42	41	40	39	33	21	5	-8	-11	0
0	20	28	23	10	0	-8	-11	-13	-14	-16	-23	-33	-43	-44	-29	0
0	1	-7	-25	-44	-57	-64	-66	-67	-67	-70	-76	-82	-83	-72	-43	0
0	-21	-50	-80	-102	-115	-120	-121	-119	-119	-120	-122	-122	-114	-92	-52	0
0	-48	-95	-134	-158	-170	-174	-172	-169	-166	-163	-160	-153	-136	-105	-58	0
0	-73	-135	-179	-204	-216	-219	-217	-212	-206	-198	-189	-174	-149	-111	-60	0
0	-89	-159	-203	-229	-241	-246	-245	-241	-232	-221	-205	-183	-153	-111	-59	0
0	-88	-153	-193	-215	-228	-235	-237	-235	-229	-217	-200	-175	-143	-102	-53	0
0	-63	-107	-131	-145	-154	-160	-164	-165	-163	-156	-144	-126	-102	-72	-37	0
0	0	0	0	0	0	0	0	0	0	0	0	0	0	0	0	0

U2 EXP -3 PLANE 9

1:	2:	3:	4:	5:	6:	7:	8:	9:	10:	11:	12:	13:	14:	15:	16:	17:
0	0	0	0	0	0	0	0	0	0	0	0	0	0	0	0	0
0	35	55	65	67	62	52	41	30	22	15	11	7	2	-11	-28	0
0	65	103	121	124	114	97	77	57	41	29	20	12	0	-25	-55	0
0	88	139	162	164	149	127	101	76	56	39	25	12	-7	-45	-81	0
0	106	164	187	185	166	139	111	85	62	42	25	6	-22	-69	-104	0
0	120	180	199	190	166	137	108	82	59	38	17	-7	-45	-97	-122	0
0	131	189	199	182	154	124	96	71	48	25	1	-30	-74	-125	-134	0
0	138	190	189	164	133	103	77	54	31	6	-22	-59	-106	-149	-141	0
0	142	183	170	139	108	81	56	33	9	-17	-50	-91	-136	-168	-143	0
0	141	169	145	112	83	58	36	13	-13	-43	-80	-122	-161	-179	-141	0
0	136	149	118	86	61	39	18	-5	-34	-67	-106	-146	-177	-182	-135	0
0	124	124	91	64	44	25	4	-20	-50	-86	-124	-160	-183	-178	-126	0
0	106	98	68	47	31	15	-3	-28	-58	-94	-130	-161	-177	-166	-114	0
0	84	72	48	33	22	10	-6	-28	-56	-88	-120	-146	-157	-144	-96	0
0	58	47	31	21	14	6	-5	-21	-43	-68	-93	-112	-120	-109	-72	0
0	30	23	15	10	6	3	-2	-11	-22	-36	-50	-61	-66	-59	-40	0
0	0	0	0	0	0	0	0	0	0	0	0	0	0	0	0	0

Cont'd:

B.7 Case 15: 3-D Steady State Solutions of Participating Thermal Cavity, Fluid Ra=1.E4

U3 EXP -4 PLANE 8

1:	2:	3:	4:	5:	6:	7:	8:	9:	10:	11:	12:	13:	14:	15:	16:	17:
0	0	0	0	0	0	0	0	0	0	0	0	0	0	0	0	0
0	2	5	7	10	12	12	11	9	6	2	-3	-11	-22	-34	-35	0
0	4	10	17	25	33	38	41	40	36	30	21	9	-8	-29	-37	0
0	5	14	25	39	54	66	74	77	76	69	59	43	20	-9	-25	0
0	5	15	30	50	71	89	103	111	112	106	94	75	47	13	-10	0
0	4	15	33	57	83	107	126	137	139	134	121	99	67	30	3	0
0	2	14	35	63	93	121	142	154	157	151	136	111	77	40	12	0
0	0	13	37	68	101	130	151	164	166	159	141	114	80	45	17	0
0	-2	10	38	72	106	134	154	166	167	158	139	111	77	44	18	0
0	-6	7	37	72	105	132	150	160	160	150	130	102	71	42	18	0
0	-12	1	32	67	97	121	138	146	146	136	117	92	64	37	16	0
0	-21	-8	22	54	81	102	117	125	125	117	101	79	55	32	14	0
0	-31	-21	6	34	56	74	87	96	98	93	81	64	45	27	11	0
0	-40	-35	-12	8	26	40	52	61	65	65	58	47	34	20	8	0
0	-44	-44	-29	-14	-1	9	18	25	31	34	33	28	21	12	5	0
0	-35	-38	-31	-22	-15	-9	-3	0	5	8	10	10	8	5	1	0
0	0	0	0	0	0	0	0	0	0	0	0	0	0	0	0	0

U3 EXP -4 PLANE 9

1:	2:	3:	4:	5:	6:	7:	8:	9:	10:	11:	12:	13:	14:	15:	16:	17:
0	0	0	0	0	0	0	0	0	0	0	0	0	0	0	0	0
0	0	0	0	0	0	0	0	0	0	0	0	0	0	0	0	0
0	0	0	0	0	0	0	0	0	0	0	0	0	0	0	0	0
0	0	0	0	0	0	0	0	0	0	0	0	0	0	0	0	0
0	0	0	0	0	0	0	0	0	0	0	0	0	0	0	0	0
0	0	0	0	0	0	0	0	0	0	0	0	0	0	0	0	0
0	0	0	0	0	0	0	0	0	0	0	0	0	0	0	0	0
0	0	0	0	0	0	0	0	0	0	0	0	0	0	0	0	0
0	0	0	0	0	0	0	0	0	0	0	0	0	0	0	0	0
0	0	0	0	0	0	0	0	0	0	0	0	0	0	0	0	0
0	0	0	0	0	0	0	0	0	0	0	0	0	0	0	0	0
0	0	0	0	0	0	0	0	0	0	0	0	0	0	0	0	0
0	0	0	0	0	0	0	0	0	0	0	0	0	0	0	0	0
0	0	0	0	0	0	0	0	0	0	0	0	0	0	0	0	0
0	0	0	0	0	0	0	0	0	0	0	0	0	0	0	0	0
0	0	0	0	0	0	0	0	0	0	0	0	0	0	0	0	0
0	0	0	0	0	0	0	0	0	0	0	0	0	0	0	0	0
0	0	0	0	0	0	0	0	0	0	0	0	0	0	0	0	0

U3 EXP -4 PLANE 10

1:	2:	3:	4:	5:	6:	7:	8:	9:	10:	11:	12:	13:	14:	15:	16:	17:
0	0	0	0	0	0	0	0	0	0	0	0	0	0	0	0	0
0	-2	-5	-7	-10	-12	-12	-11	-9	-6	-2	3	11	22	34	35	0
0	-4	-10	-17	-25	-33	-38	-41	-40	-36	-30	-21	-9	8	29	37	0
0	-5	-14	-25	-39	-54	-66	-74	-77	-76	-69	-59	-43	-20	9	25	0
0	-5	-15	-30	-50	-71	-89	-103	-111	-112	-106	-94	-75	-47	-13	10	0
0	-4	-15	-33	-57	-83	-107	-126	-137	-139	-134	-121	-99	-67	-30	-3	0
0	-2	-14	-35	-63	-93	-121	-142	-154	-157	-151	-136	-111	-77	-40	-12	0
0	0	-12	-37	-68	-101	-130	-151	-164	-166	-159	-141	-114	-80	-45	-17	0
0	2	-10	-37	-72	-106	-134	-154	-166	-167	-158	-139	-111	-77	-44	-18	0
0	6	-7	-37	-72	-105	-132	-150	-160	-160	-150	-130	-102	-71	-42	-18	0
0	12	-1	-32	-67	-97	-121	-138	-146	-146	-136	-117	-92	-64	-37	-16	0
0	21	8	-22	-54	-81	-102	-117	-125	-125	-117	-101	-79	-55	-32	-14	0
0	31	21	-6	-34	-56	-74	-87	-96	-98	-93	-81	-64	-45	-27	-11	0
0	40	35	12	-8	-26	-40	-52	-61	-65	-65	-58	-47	-34	-20	-8	0
0	44	44	29	14	1	-9	-18	-25	-31	-34	-33	-28	-21	-12	-5	0
0	35	38	31	22	15	9	3	0	-5	-8	-10	-10	-8	-5	-1	0
0	0	0	0	0	0	0	0	0	0	0	0	0	0	0	0	0

(Cont'd)
B.7 Case 15: 3-D Steady State Solutions of Participating Thermal Cavity, Fluid Ra=1.E4

TEMPERATURE EXP -2 PLANE 9

1:	2:	3:	4:	5:	6:	7:	8:	9:	10:	11:	12:	13:	14:	15:	16:	17:
100	97	94	92	89	87	85	83	82	80	77	75	70	63	49	27	0
100	96	94	91	89	87	85	83	81	80	77	75	71	64	52	30	0
100	96	93	91	88	86	84	82	80	79	77	75	72	66	54	32	0
100	96	93	90	87	84	82	80	78	77	75	73	70	65	54	32	0
100	95	91	88	84	81	79	77	75	74	72	70	67	62	51	30	0
100	94	90	85	81	78	75	73	72	70	68	66	63	58	46	26	0
100	93	87	82	78	74	71	69	67	66	64	62	58	52	40	22	0
100	92	85	78	73	70	67	65	63	61	59	57	52	45	34	18	0
100	90	81	74	69	65	62	60	58	57	54	51	46	39	28	15	0
100	88	77	69	64	60	57	55	53	51	49	45	40	33	23	12	0
100	85	73	64	58	55	52	50	48	46	43	39	34	27	19	9	0
100	82	68	59	53	50	47	45	43	40	38	34	29	22	15	7	0
100	80	65	55	49	45	42	40	37	35	32	28	23	18	12	6	0
100	79	63	52	46	41	38	35	33	30	27	23	19	14	9	4	0
100	79	63	52	44	39	36	32	29	26	23	20	16	12	8	4	0
100	80	64	53	45	39	35	31	28	24	21	18	14	11	7	3	0
100	81	66	54	46	40	35	31	27	24	21	17	14	10	7	3	0

RADATIVE FLUX EXP -4 PLANE 9

1:	2:	3:	4:	5:	6:	7:	8:	9:	10:	11:	12:	13:	14:	15:	16:	17:
112	56	44	39	36	34	34	33	33	32	30	26	18	3	-12	-20	-43
111	0	0	0	0	0	0	0	0	0	0	0	0	0	0	0	-53
121	0	0	0	0	0	0	0	0	0	0	0	0	0	0	0	-58
132	0	0	0	0	0	0	0	0	0	0	0	0	0	0	0	-61
141	0	0	0	0	0	0	0	0	0	0	0	0	0	0	0	-61
150	0	0	0	0	0	0	0	0	0	0	0	0	0	0	0	-60
159	0	0	0	0	0	0	0	0	0	0	0	0	0	0	0	-58
168	0	0	0	0	0	0	0	0	0	0	0	0	0	0	0	-55
177	0	0	0	0	0	0	0	0	0	0	0	0	0	0	0	-52
185	0	0	0	0	0	0	0	0	0	0	0	0	0	0	0	-49
192	0	0	0	0	0	0	0	0	0	0	0	0	0	0	0	-46
198	0	0	0	0	0	0	0	0	0	0	0	0	0	0	0	-42
202	0	0	0	0	0	0	0	0	0	0	0	0	0	0	0	-39
204	0	0	0	0	0	0	0	0	0	0	0	0	0	0	0	-36
202	0	0	0	0	0	0	0	0	0	0	0	0	0	0	0	-33
196	0	0	0	0	0	0	0	0	0	0	0	0	0	0	0	-31
141	-30	-76	-84	-81	-74	-66	-59	-52	-46	-40	-35	-31	-27	-23	-21	-35

DIVERGENCE OF RADIATIVE FLUX EXP -4 PLANE 9

1:	2:	3:	4:	5:	6:	7:	8:	9:	10:	11:	12:	13:	14:	15:	16:	17:
0	0	0	0	0	0	0	0	0	0	0	0	0	0	0	0	0
0	310	223	179	155	143	139	141	148	156	162	157	121	22	-134	-220	0
0	350	231	165	126	105	101	108	125	146	166	179	162	76	-107	-244	0
0	368	209	109	46	13	6	19	46	78	111	135	132	60	-114	-257	0
0	363	155	17	-68	-110	-115	-96	-61	-19	20	49	50	-13	-161	-266	0
0	335	71	-102	-202	-243	-241	-212	-169	-122	-79	-49	-50	-107	-215	-269	0
0	282	-44	-244	-345	-374	-357	-316	-265	-214	-171	-144	-147	-191	-254	-265	0
0	201	-188	-400	-485	-491	-456	-402	-344	-290	-247	-222	-223	-248	-271	-254	0
0	90	-353	-556	-611	-589	-534	-469	-405	-349	-306	-280	-272	-276	-270	-241	0
0	-47	-525	-697	-713	-663	-591	-516	-448	-390	-345	-315	-297	-282	-259	-225	0
0	-200	-685	-810	-785	-711	-625	-544	-472	-412	-364	-329	-301	-274	-243	-209	0
0	-347	-812	-885	-825	-732	-637	-552	-478	-417	-367	-326	-291	-258	-225	-193	0
0	-462	-891	-918	-831	-726	-627	-541	-467	-406	-354	-311	-273	-238	-206	-177	0
0	-519	-911	-906	-803	-693	-595	-511	-441	-382	-332	-289	-251	-218	-188	-162	0
0	-502	-860	-841	-739	-634	-543	-466	-402	-348	-302	-262	-228	-197	-170	-147	0
0	-409	-717	-710	-631	-547	-473	-410	-356	-310	-269	-235	-204	-177	-153	-132	0
0	0	0	0	0	0	0	0	0	0	0	0	0	0	0	0	0

Appendix C

2-D Fire Simulation Solutions

C.1 Case 16: 2-D Fire Simulation, Pure Convection, Fluid Ra=1.E4
Implicit Fire Parameters: Ra=3.1E10, Gr=4.43E10, Re=2.1E5, Pe=1.47E5
BC's: No slip; Adiabatic Walls
Explicit Parameters: Ra=1.E4, Pr=0.7, Ar=1.0, Gr=1.43E4, Re=120, Pe=83.6
Implicit Parameters: Lo=3 m, To=830 K, dTo=1072 K, Nu=88.E-6 m2/s, ko=58.E-6 m2/s
rho,o=0.42 kg/m3, alpha,o=125.E-6 m2/s, po=16 Pa, Uo=6.16 m/s
to=0.487 s, q",o=3.05E3 kW/m2

U1 EXP -4 PLANE 1

1:	2:	3:	4:	5:	6:	7:	8:	9:	10:	11:	12:	13:	14:	15:	16:	17:
0	0	0	0	0	0	0	0	0	0	0	0	0	0	0	0	0
0	19	-36	-101	-147	-161	-136	-78	0	78	136	161	147	101	36	-19	0
0	18	-69	-151	-207	-220	-184	-105	0	105	184	220	207	151	69	-18	0
0	17	-81	-168	-228	-241	-201	-115	0	115	201	241	228	168	81	-17	0
0	16	-80	-166	-225	-240	-202	-116	0	116	202	240	225	166	80	-16	0
0	14	-72	-150	-206	-222	-191	-112	0	112	191	222	206	150	72	-14	0
0	10	-59	-123	-171	-187	-164	-99	0	99	164	187	171	123	59	-10	0
0	6	-41	-85	-121	-135	-121	-74	0	74	121	135	121	85	41	-6	0
0	2	-19	-39	-59	-69	-64	-40	0	40	64	69	59	39	19	-2	0
0	-2	5	11	10	6	0	-2	0	2	0	-6	-10	-11	-5	2	0
0	-7	31	65	85	86	68	37	0	-37	-68	-86	-85	-65	-31	7	0
0	-12	58	121	163	171	140	79	0	-79	-140	-171	-163	-121	-58	12	0
0	-16	84	176	240	255	214	122	0	-122	-214	-255	-240	-176	-84	16	0
0	-19	107	222	307	331	282	163	0	-163	-282	-331	-307	-222	-107	19	0
0	-21	112	239	340	377	331	196	0	-196	-331	-377	-340	-239	-112	21	0
0	-23	76	189	284	329	303	191	0	-191	-303	-329	-284	-189	-76	23	0
0	0	0	0	0	0	0	0	0	0	0	0	0	0	0	0	0

U2 EXP -4 PLANE 1

1:	2:	3:	4:	5:	6:	7:	8:	9:	10:	11:	12:	13:	14:	15:	16:	17:
0	0	0	0	0	0	0	0	0	0	0	0	0	0	0	0	0
0	-25	-30	-27	-29	-34	-39	-43	-44	-43	-39	-34	-29	-27	-30	-25	0
0	-81	-106	-92	-56	-10	36	71	84	71	36	-10	-56	-92	-106	-81	0
0	-143	-183	-155	-81	16	115	189	217	189	115	16	-81	-155	-183	-143	0
0	-212	-271	-229	-118	31	183	298	341	298	183	31	-118	-229	-271	-212	0
0	-276	-354	-301	-156	40	245	403	463	403	245	40	-156	-301	-354	-276	0
0	-329	-425	-364	-192	45	297	497	575	497	297	45	-192	-364	-425	-329	0
0	-369	-479	-413	-222	46	336	571	667	571	336	46	-222	-413	-479	-369	0
0	-391	-511	-445	-244	44	359	620	728	620	359	44	-244	-445	-511	-391	0
0	-394	-518	-454	-253	40	365	637	751	637	365	40	-253	-454	-518	-394	0
0	-378	-497	-440	-249	32	349	619	732	619	349	32	-249	-440	-497	-378	0
0	-340	-449	-400	-231	23	313	564	670	564	313	23	-231	-400	-449	-340	0
0	-282	-372	-335	-198	11	255	472	566	472	255	11	-198	-335	-372	-282	0
0	-201	-267	-242	-148	-1	173	334	407	334	173	-1	-148	-242	-267	-201	0
0	-114	-155	-143	-96	-23	66	155	198	155	66	-23	-96	-143	-155	-114	0
0	-18	-20	-17	-21	-34	-52	-69	-74	-69	-52	-34	-21	-17	-20	-18	0
0	0	0	0	0	0	0	0	0	0	0	0	0	0	0	0	0

TEMPERATURE EXP -3 PLANE 1

1:	2:	3:	4:	5:	6:	7:	8:	9:	10:	11:	12:	13:	14:	15:	16:	17:
200	200	202	206	209	213	216	219	219	219	216	213	209	206	202	200	200
200	201	203	207	211	215	218	221	221	221	218	215	211	207	203	201	200
202	203	206	210	215	220	224	227	228	227	224	220	215	210	206	203	202
205	206	209	214	221	227	233	238	239	238	233	227	221	214	209	206	205
209	210	214	220	228	237	246	253	255	253	246	237	228	220	214	210	209
213	215	219	227	237	249	262	272	276	272	262	249	237	227	219	215	213
218	220	225	233	246	261	278	295	303	295	278	261	246	233	225	220	218
223	225	230	240	254	272	293	318	337	318	293	272	254	240	230	225	223
228	230	235	246	261	281	305	334	357	334	305	281	261	246	235	230	228
232	234	240	251	266	287	312	343	366	343	312	287	266	251	240	234	232
236	238	244	254	270	290	316	347	371	347	316	290	270	254	244	238	236
240	241	247	257	272	292	318	349	373	349	318	292	272	257	247	241	240
242	244	249	259	273	293	319	350	374	350	319	293	273	259	249	244	242
244	246	251	261	274	294	319	351	374	351	319	294	274	261	251	246	244
246	248	253	262	276	295	320	351	375	351	320	295	276	262	253	248	246
247	249	254	263	277	296	321	352	376	352	321	296	277	263	254	249	247
247	249	255	264	278	297	322	353	376	353	322	297	278	264	255	249	247

C.2 Case 17: 2-D Fire Simulation, Convection + Radiation, Fluid Ra=1.E4
Implicit Fire Parameters: Ra=3.1E10, Gr=4.43E10, Re=2.1E5, Pe=1.47E5
BC's: No slip; Adiabatic Walls
Explicit Parameters: Ra=1.E4, Pr=0.7, Ar=1.0, Gr=1.43E4, Re=120, Pe=83.6, Bo=40.65
Implicit Parameters: Lo=3 m, To=830 K, dTo=1072 K, Nu=88.E-6 m2/s, ko=58.E-6 m2/s
rho,o=0.42 kg/m3, alpha,o=125.E-6 m2/s, po=16 Pa, Uo=6.16 m/s
to=0.487 s, q",o=3.05E3 kW/m2, Ka=Kt=1 1/m, Ks=0 1/m, black walls

U1 EXP -4 PLANE 1

1:	2:	3:	4:	5:	6:	7:	8:	9:	10:	11:	12:	13:	14:	15:	16:	17:
0	0	0	0	0	0	0	0	0	0	0	0	0	0	0	0	0
0	19	-35	-97	-142	-155	-131	-75	0	75	131	155	142	97	35	-19	0
0	18	-66	-145	-200	-213	-178	-101	0	101	178	213	200	145	66	-18	0
0	18	-78	-163	-220	-233	-195	-111	0	111	195	233	220	163	78	-18	0
0	16	-77	-161	-218	-233	-196	-113	0	113	196	233	218	161	77	-16	0
0	14	-70	-146	-200	-216	-186	-109	0	109	186	216	200	146	70	-14	0
0	10	-58	-120	-167	-183	-161	-97	0	97	161	183	167	120	58	-10	0
0	6	-40	-84	-119	-133	-119	-73	0	73	119	133	119	84	40	-6	0
0	2	-19	-39	-59	-69	-64	-40	0	40	64	69	59	39	19	-2	0
0	-2	4	9	9	4	-1	-2	0	2	1	-4	-9	-9	-4	2	0
0	-7	30	63	82	83	66	36	0	-36	-66	-83	-82	-63	-30	7	0
0	-12	56	117	158	165	136	76	0	-76	-136	-165	-158	-117	-56	12	0
0	-16	82	171	234	249	208	119	0	-119	-208	-249	-234	-171	-82	16	0
0	-20	104	216	299	323	276	159	0	-159	-276	-323	-299	-216	-104	20	0
0	-21	109	233	331	368	323	192	0	-192	-323	-368	-331	-233	-109	21	0
0	-23	74	184	277	321	296	187	0	-187	-296	-321	-277	-184	-74	23	0
0	0	0	0	0	0	0	0	0	0	0	0	0	0	0	0	0

U2 EXP -4 PLANE 1

1:	2:	3:	4:	5:	6:	7:	8:	9:	10:	11:	12:	13:	14:	15:	16:	17:
0	0	0	0	0	0	0	0	0	0	0	0	0	0	0	0	0
0	-24	-29	-27	-29	-34	-39	-43	-44	-43	-39	-34	-29	-27	-29	-24	0
0	-79	-103	-89	-55	-10	34	68	80	68	34	-10	-55	-89	-103	-79	0
0	-139	-177	-150	-79	15	111	183	209	183	111	15	-79	-150	-177	-139	0
0	-206	-262	-222	-114	29	177	289	330	289	177	29	-114	-222	-262	-206	0
0	-267	-343	-292	-152	39	237	390	449	390	237	39	-152	-292	-343	-267	0
0	-319	-412	-353	-187	43	288	482	559	482	288	43	-187	-353	-412	-319	0
0	-358	-465	-402	-217	44	326	555	649	555	326	44	-217	-402	-465	-358	0
0	-380	-496	-433	-237	42	349	603	709	603	349	42	-237	-433	-496	-380	0
0	-383	-503	-442	-247	38	354	621	732	621	354	38	-247	-442	-503	-383	0
0	-368	-484	-429	-243	31	340	603	714	603	340	31	-243	-429	-484	-368	0
0	-332	-437	-390	-225	21	305	550	654	550	305	21	-225	-390	-437	-332	0
0	-275	-363	-326	-193	10	249	461	553	461	249	10	-193	-326	-363	-275	0
0	-197	-260	-236	-144	-1	169	326	397	326	169	-1	-144	-236	-260	-197	0
0	-111	-151	-140	-94	-23	64	151	194	151	64	-23	-94	-140	-151	-111	0
0	-17	-19	-16	-20	-33	-52	-69	-74	-69	-52	-33	-20	-16	-19	-17	0
0	0	0	0	0	0	0	0	0	0	0	0	0	0	0	0	0

TEMPERATURE EXP -3 PLANE 1

1:	2:	3:	4:	5:	6:	7:	8:	9:	10:	11:	12:	13:	14:	15:	16:	17:
199	200	202	205	209	212	215	217	218	217	215	212	209	205	202	200	199
200	201	203	206	210	214	217	219	220	219	217	214	210	206	203	201	200
202	203	205	209	214	219	223	226	227	226	223	219	214	209	205	203	202
205	206	209	213	219	226	232	236	237	236	232	226	219	213	209	206	205
209	210	213	219	227	236	244	250	253	250	244	236	227	219	213	210	209
213	214	218	226	235	247	259	269	272	269	259	247	235	226	218	214	213
218	219	224	232	244	259	275	291	299	291	275	259	244	232	224	219	218
223	224	229	239	252	269	290	314	333	314	290	269	252	239	229	224	223
227	229	235	244	259	278	302	330	352	330	302	278	259	244	235	229	227
232	233	239	249	264	284	309	339	362	339	309	284	264	249	239	233	232
235	237	243	253	268	288	313	343	366	343	313	288	268	253	243	237	235
239	241	246	256	270	290	315	346	369	346	315	290	270	256	246	241	239
242	243	249	258	272	291	316	347	370	347	316	291	272	258	249	243	242
244	245	251	260	273	291	316	347	371	347	316	291	273	260	251	245	244
245	247	252	261	274	293	317	348	372	348	317	293	274	261	252	247	245
246	248	253	262	276	294	318	349	372	349	318	294	276	262	253	248	246
247	248	254	263	276	295	320	350	373	350	320	295	276	263	254	248	247

(Cont'd)
C.2 Case 17: 2-D Fire Simulation, Convection + Radiation, Fluid Ra=1.E4

CONDUCTIVE FLUX EXP -6 PLANE 1

1:	2:	3:	4:	5:	6:	7:	8:	9:	10:	11:	12:	13:	14:	15:	16:	17:
-664	-218	-257	-323	-411	-510	-602	-667	-691	-667	-602	-510	-411	-323	-257	-218	-664
-235	0	0	0	0	0	0	0	0	0	0	0	0	0	0	0	-235
-269	0	0	0	0	0	0	0	0	0	0	0	0	0	0	0	-269
-318	0	0	0	0	0	0	0	0	0	0	0	0	0	0	0	-318
-376	0	0	0	0	0	0	0	0	0	0	0	0	0	0	0	-376
-437	0	0	0	0	0	0	0	0	0	0	0	0	0	0	0	-437
-496	0	0	0	0	0	0	0	0	0	0	0	0	0	0	0	-496
-544	0	0	0	0	0	0	0	0	0	0	0	0	0	0	0	-544
-577	0	0	0	0	0	0	0	0	0	0	0	0	0	0	0	-577
-591	0	0	0	0	0	0	0	0	0	0	0	0	0	0	0	-591
-590	0	0	0	0	0	0	0	0	0	0	0	0	0	0	0	-590
-577	0	0	0	0	0	0	0	0	0	0	0	0	0	0	0	-577
-560	0	0	0	0	0	0	0	0	0	0	0	0	0	0	0	-560
-547	0	0	0	0	0	0	0	0	0	0	0	0	0	0	0	-547
-544	0	0	0	0	0	0	0	0	0	0	0	0	0	0	0	-544
-554	0	0	0	0	0	0	0	0	0	0	0	0	0	0	0	-554
-622	111	128	158	195	226	229	180	134	180	229	226	195	158	128	111	-622

RADIATIVE FLUX EXP -6 PLANE 1

1:	2:	3:	4:	5:	6:	7:	8:	9:	10:	11:	12:	13:	14:	15:	16:	17:
-29	-37	-42	-45	-47	-48	-49	-49	-50	-49	-49	-48	-47	-45	-42	-37	-29
-26	0	0	0	0	0	0	0	0	0	0	0	0	0	0	0	-26
-31	0	0	0	0	0	0	0	0	0	0	0	0	0	0	0	-31
-35	0	0	0	0	0	0	0	0	0	0	0	0	0	0	0	-35
-38	0	0	0	0	0	0	0	0	0	0	0	0	0	0	0	-38
-41	0	0	0	0	0	0	0	0	0	0	0	0	0	0	0	-41
-43	0	0	0	0	0	0	0	0	0	0	0	0	0	0	0	-43
-45	0	0	0	0	0	0	0	0	0	0	0	0	0	0	0	-45
-47	0	0	0	0	0	0	0	0	0	0	0	0	0	0	0	-47
-49	0	0	0	0	0	0	0	0	0	0	0	0	0	0	0	-49
-50	0	0	0	0	0	0	0	0	0	0	0	0	0	0	0	-50
-50	0	0	0	0	0	0	0	0	0	0	0	0	0	0	0	-50
-49	0	0	0	0	0	0	0	0	0	0	0	0	0	0	0	-49
-46	0	0	0	0	0	0	0	0	0	0	0	0	0	0	0	-46
-41	0	0	0	0	0	0	0	0	0	0	0	0	0	0	0	-41
-31	0	0	0	0	0	0	0	0	0	0	0	0	0	0	0	-31
-14	-1	1	9	25	55	109	190	237	190	109	55	25	9	1	-1	-14

DIVERGENCE OF RADIATIVE FLUX EXP -5 PLANE 1

1:	2:	3:	4:	5:	6:	7:	8:	9:	10:	11:	12:	13:	14:	15:	16:	17:
0	0	0	0	0	0	0	0	0	0	0	0	0	0	0	0	0
0	-19	-21	-21	-21	-20	-18	-17	-17	-17	-18	-20	-21	-21	-21	-19	0
0	-22	-24	-24	-22	-20	-18	-16	-15	-16	-18	-20	-22	-24	-24	-22	0
0	-23	-25	-24	-21	-17	-12	-9	-7	-9	-12	-17	-21	-24	-25	-23	0
0	-24	-25	-23	-18	-11	-2	5	8	5	-2	-11	-18	-23	-25	-24	0
0	-24	-25	-22	-14	-1	14	30	37	30	14	-1	-14	-22	-25	-24	0
0	-25	-25	-20	-9	10	38	72	89	72	38	10	-9	-20	-25	-25	0
0	-24	-24	-18	-3	22	66	126	159	126	66	22	-3	-18	-24	-24	0
0	-24	-24	-16	0	33	89	171	218	171	89	33	0	-16	-24	-24	0
0	-24	-23	-15	3	38	102	197	251	197	102	38	3	-15	-23	-24	0
0	-23	-23	-15	3	40	106	206	264	206	106	40	3	-15	-23	-23	0
0	-23	-23	-15	2	37	104	206	265	206	104	37	2	-15	-23	-23	0
0	-22	-22	-16	0	33	98	200	259	200	98	33	0	-16	-22	-22	0
0	-20	-21	-16	-2	28	90	190	248	190	90	28	-2	-16	-21	-20	0
0	-17	-18	-13	-1	25	82	176	232	176	82	25	-1	-13	-18	-17	0
0	-12	-13	-8	1	23	71	150	198	150	71	23	1	-8	-13	-12	0
0	0	0	0	0	0	0	0	0	0	0	0	0	0	0	0	0

C.3 Case 18: 2-D Fire Simulation, Pure Convection, Fluid Ra=1.E5
Implicit Fire Parameters: Ra=3.1E10, Gr=4.43E10, Re=2.1E5, Pe=1.47E5
BC's: No slip; Adiabatic Walls
Explicit Parameters: Ra=1.E5, Pr=0.7, Ar=1.0, Gr=1.43E5, Re=378, Pe=265, Bo=40.65
Implicit Parameters: Lo=3 m, To=830 K, dTo=1072 K, Nu=88.E-6 m2/s, ko=58.E-6 m2/s
rho,o=0.42 kg/m3, alpha,o=125.E-6 m2/s, po=16 Pa, Uo=6.16 m/s
to=0.487 s, q",o=3.05E3 kW/m2, Ka=Kt=1 1/m, Ks=0 1/m, black walls

U1 EXP -3 PLANE 1

1:	2:	3:	4:	5:	6:	7:	8:	9:	10:	11:	12:	13:	14:	15:	16:	17:
0	0	0	0	0	0	0	0	0	0	0	0	0	0	0	0	0
0	-4	-34	-58	-81	-89	-79	-46	0	46	79	89	81	58	34	4	0
0	-7	-51	-82	-109	-112	-94	-53	0	53	94	112	109	82	51	7	0
0	-7	-48	-75	-96	-97	-82	-47	0	47	82	97	96	75	48	7	0
0	-4	-31	-51	-66	-69	-60	-37	0	37	60	69	66	51	31	4	0
0	-1	-10	-21	-30	-34	-33	-23	0	23	33	34	30	21	10	1	0
0	1	8	5	2	-2	-7	-8	0	8	7	2	-2	-5	-8	-1	0
0	3	20	26	27	22	13	3	0	-3	-13	-22	-27	-26	-20	-3	0
0	4	25	37	42	37	26	12	0	-12	-26	-37	-42	-37	-25	-4	0
0	4	25	39	47	43	32	16	0	-16	-32	-43	-47	-39	-25	-4	0
0	3	22	37	47	45	35	18	0	-18	-35	-45	-47	-37	-22	-3	0
0	3	19	33	44	45	37	20	0	-20	-37	-45	-44	-33	-19	-3	0
0	2	16	31	43	48	43	25	0	-25	-43	-48	-43	-31	-16	-2	0
0	2	16	31	45	53	51	32	0	-32	-51	-53	-45	-31	-16	-2	0
0	2	15	31	48	60	62	43	0	-43	-62	-60	-48	-31	-15	-2	0
0	1	11	24	40	53	59	45	0	-45	-59	-53	-40	-24	-11	-1	0
0	0	0	0	0	0	0	0	0	0	0	0	0	0	0	0	0

U2 EXP -3 PLANE 1

1:	2:	3:	4:	5:	6:	7:	8:	9:	10:	11:	12:	13:	14:	15:	16:	17:
0	0	0	0	0	0	0	0	0	0	0	0	0	0	0	0	0
0	-10	-10	-10	-6	-2	4	9	11	9	4	-2	-6	-10	-10	-10	0
0	-41	-48	-41	-24	3	38	68	79	68	38	3	-24	-41	-48	-41	0
0	-72	-82	-67	-35	10	63	108	127	108	63	10	-35	-67	-82	-72	0
0	-99	-114	-90	-46	14	84	148	175	148	84	14	-46	-90	-114	-99	0
0	-111	-132	-105	-54	14	94	170	205	170	94	14	-54	-105	-132	-111	0
0	-111	-138	-112	-60	10	95	182	224	182	95	10	-60	-112	-138	-111	0
0	-100	-131	-111	-63	3	87	180	227	180	87	3	-63	-111	-131	-100	0
0	-85	-117	-105	-64	-3	76	170	220	170	76	-3	-64	-105	-117	-85	0
0	-68	-99	-94	-63	-11	62	155	206	155	62	-11	-63	-94	-99	-68	0
0	-54	-81	-81	-60	-19	48	138	189	138	48	-19	-60	-81	-81	-54	0
0	-42	-64	-68	-54	-23	35	119	168	119	35	-23	-54	-68	-64	-42	0
0	-32	-49	-54	-47	-25	23	99	145	99	23	-25	-47	-54	-49	-32	0
0	-22	-34	-38	-35	-22	12	73	112	73	12	-22	-35	-38	-34	-22	0
0	-14	-21	-24	-24	-17	3	46	74	46	3	-17	-24	-24	-21	-14	0
0	-6	-7	-7	-7	-6	-3	4	11	4	-3	-6	-7	-7	-7	-6	0
0	0	0	0	0	0	0	0	0	0	0	0	0	0	0	0	0

TEMPERATURE EXP -3 PLANE 1

1:	2:	3:	4:	5:	6:	7:	8:	9:	10:	11:	12:	13:	14:	15:	16:	17:
255	259	268	280	290	297	302	305	305	305	302	297	290	280	268	259	255
256	260	271	283	294	301	306	309	310	309	306	301	294	283	271	260	256
257	261	274	288	299	308	315	321	323	321	315	308	299	288	274	261	257
257	262	275	290	301	311	321	330	334	330	321	311	301	290	275	262	257
257	262	274	287	297	307	320	336	344	336	320	307	297	287	274	262	257
256	261	271	282	289	297	313	340	356	340	313	297	289	282	271	261	256
253	258	266	274	279	285	302	342	375	342	302	285	279	274	266	258	253
249	253	260	266	269	273	289	340	397	340	289	273	269	266	260	253	249
242	246	253	257	259	261	277	329	387	329	277	261	259	257	253	246	242
234	238	244	248	249	250	266	319	379	319	266	250	249	248	244	238	234
222	226	232	236	237	239	256	310	370	310	256	239	237	236	232	226	222
208	212	218	223	224	227	245	300	362	300	245	227	224	223	218	212	208
192	196	202	206	209	213	232	291	355	291	232	213	209	206	202	196	192
176	179	184	188	192	199	220	282	351	282	220	199	192	188	184	179	176
162	164	167	172	177	186	210	278	349	278	210	186	177	172	167	164	162
152	153	156	161	167	180	211	281	352	281	211	180	167	161	156	153	152
149	150	153	157	165	182	218	289	356	289	218	182	165	157	153	150	149

C.4 Case 19: 2-D Fire Simulation, Convection + Radiation, Fluid Ra=1.E5
Implicit Fire Parameters: Ra=3.1E10, Gr=4.43E10, Re=2.1E5, Pe=1.47E5
BC's: No slip; Adiabatic Walls
Explicit Parameters: Ra=1.E5, Pr=0.7, Ar=1.0, Gr=1.43E5, Re=378, Pe=265, Bo=40.65
Implicit Parameters: Lo=3 m, To=830 K, dTo=1072 K, Nu=88.E-6 m2/s, ko=58.E-6 m2/s
rho,o=0.42 kg/m3, alpha,o=125.E-6 m2/s, po=16 Pa, Uo=6.16 m/s
to=0.487 s, q",o=3.05E3 kW/m2, Ka=Kt=1 1/m, Ks=0 1/m, black walls

U1 EXP -3 PLANE 1

1:	2:	3:	4:	5:	6:	7:	8:	9:	10:	11:	12:	13:	14:	15:	16:	17:
0	0	0	0	0	0	0	0	0	0	0	0	0	0	0	0	0
0	0	-34	-56	-82	-90	-81	-48	0	48	81	90	82	56	34	0	0
0	0	-52	-79	-109	-113	-97	-55	0	55	97	113	109	79	52	0	0
0	-1	-49	-72	-96	-96	-83	-47	0	47	83	96	96	72	49	1	0
0	-1	-32	-50	-67	-69	-62	-37	0	37	62	69	67	50	32	1	0
0	-2	-11	-22	-31	-34	-34	-23	0	23	34	34	31	22	11	2	0
0	-1	7	4	2	-3	-8	-10	0	10	8	3	-2	-4	-7	1	0
0	0	20	24	27	21	13	3	0	-3	-13	-21	-27	-24	-20	0	0
0	0	26	35	42	36	26	11	0	-11	-26	-36	-42	-35	-26	0	0
0	1	26	38	47	43	32	15	0	-15	-32	-43	-47	-38	-26	-1	0
0	1	23	36	47	45	35	18	0	-18	-35	-45	-47	-36	-23	-1	0
0	1	19	33	44	45	37	20	0	-20	-37	-45	-44	-33	-19	-1	0
0	0	17	30	44	48	44	25	0	-25	-44	-48	-44	-30	-17	0	0
0	1	17	30	46	54	51	31	0	-31	-51	-54	-46	-30	-17	-1	0
0	0	15	30	48	61	64	44	0	-44	-64	-61	-48	-30	-15	0	0
0	0	11	24	40	53	60	48	0	-48	-60	-53	-40	-24	-11	0	0
0	0	0	0	0	0	0	0	0	0	0	0	0	0	0	0	0

U2 EXP -3 PLANE 1

1:	2:	3:	4:	5:	6:	7:	8:	9:	10:	11:	12:	13:	14:	15:	16:	17:
0	0	0	0	0	0	0	0	0	0	0	0	0	0	0	0	0
0	-6	-4	-4	-1	0	0	0	0	0	0	0	-1	-4	-4	-6	0
0	-42	-48	-42	-25	3	39	69	81	69	39	3	-25	-42	-48	-42	0
0	-72	-81	-65	-34	11	62	105	123	105	62	11	-34	-65	-81	-72	0
0	-101	-115	-91	-47	14	85	149	176	149	85	14	-47	-91	-115	-101	0
0	-112	-132	-104	-53	14	94	169	204	169	94	14	-53	-104	-132	-112	0
0	-111	-138	-112	-59	10	95	183	225	183	95	10	-59	-112	-138	-111	0
0	-99	-130	-110	-62	4	88	180	227	180	88	4	-62	-110	-130	-99	0
0	-84	-116	-104	-63	-3	77	171	221	171	77	-3	-63	-104	-116	-84	0
0	-68	-98	-93	-62	-11	63	155	206	155	63	-11	-62	-93	-98	-68	0
0	-54	-80	-81	-59	-18	49	139	189	139	49	-18	-59	-81	-80	-54	0
0	-41	-63	-66	-53	-22	35	119	167	119	35	-22	-53	-66	-63	-41	0
0	-32	-49	-54	-47	-24	23	99	145	99	23	-24	-47	-54	-49	-32	0
0	-22	-32	-36	-33	-20	13	72	109	72	13	-20	-33	-36	-32	-22	0
0	-15	-21	-24	-24	-17	4	48	78	48	4	-17	-24	-24	-21	-15	0
0	-5	-4	-4	-3	-2	-2	-3	-4	-3	-2	-2	-3	-4	-4	-5	0
0	0	0	0	0	0	0	0	0	0	0	0	0	0	0	0	0

TEMPERATURE EXP -3 PLANE 1

1:	2:	3:	4:	5:	6:	7:	8:	9:	10:	11:	12:	13:	14:	15:	16:	17:
252	255	264	275	285	292	297	299	300	299	297	292	285	275	264	255	252
252	256	267	279	289	296	301	304	305	304	301	296	289	279	267	256	252
253	258	270	283	294	303	310	315	317	315	310	303	294	283	270	258	253
254	259	271	285	296	306	316	325	329	325	316	306	296	285	271	259	254
254	259	270	283	293	302	315	331	339	331	315	302	293	283	270	259	254
253	257	267	278	285	293	309	336	351	336	309	293	285	278	267	257	253
250	254	263	271	276	281	299	339	371	339	299	281	276	271	263	254	250
246	250	257	263	266	270	286	337	393	337	286	270	266	263	257	250	246
240	244	250	254	256	259	275	326	384	326	275	259	256	254	250	244	240
231	235	241	245	246	248	264	317	376	317	264	248	246	245	241	235	231
220	224	230	234	236	238	254	308	368	308	254	238	236	234	230	224	220
207	211	217	221	223	226	243	299	361	299	243	226	223	221	217	211	207
192	195	201	205	208	213	232	290	354	290	232	213	208	205	201	195	192
176	179	183	188	192	199	220	282	350	282	220	199	192	188	183	179	176
162	164	168	172	177	186	211	277	348	277	211	186	177	172	168	164	162
153	154	157	161	168	181	211	281	352	281	211	181	168	161	157	154	153
149	150	153	158	166	182	218	289	356	289	218	182	166	158	153	150	149

(Cont'd)
C.4 Case 19: 2-D Fire Simulation, Convection + Radiation, Fluid Ra=1.E5

CONDUCTIVE FLUX EXP -6 PLANE 1

1:	2:	3:	4:	5:	6:	7:	8:	9:	10:	11:	12:	13:	14:	15:	16:	17:
-370	-72	-159	-231	-265	-296	-352	-414	-442	-414	-352	-296	-265	-231	-159	-72	-72
-370	0	0	0	0	0	0	0	0	0	0	0	0	0	0	0	0-370
-426	0	0	0	0	0	0	0	0	0	0	0	0	0	0	0	0-426
-443	0	0	0	0	0	0	0	0	0	0	0	0	0	0	0	0-443
-422	0	0	0	0	0	0	0	0	0	0	0	0	0	0	0	0-422
-379	0	0	0	0	0	0	0	0	0	0	0	0	0	0	0	0-379
-333	0	0	0	0	0	0	0	0	0	0	0	0	0	0	0	0-333
-298	0	0	0	0	0	0	0	0	0	0	0	0	0	0	0	0-298
-280	0	0	0	0	0	0	0	0	0	0	0	0	0	0	0	0-280
-277	0	0	0	0	0	0	0	0	0	0	0	0	0	0	0	0-277
-280	0	0	0	0	0	0	0	0	0	0	0	0	0	0	0	0-280
-275	0	0	0	0	0	0	0	0	0	0	0	0	0	0	0	0-275
-251	0	0	0	0	0	0	0	0	0	0	0	0	0	0	0	0-251
-202	0	0	0	0	0	0	0	0	0	0	0	0	0	0	0	0-202
-143	0	0	0	0	0	0	0	0	0	0	0	0	0	0	0	0-143
-102	0	0	0	0	0	0	0	0	0	0	0	0	0	0	0	0-102
-644	-342	-364	-354	-271	-61	287	392	222	392	287	-61	-271	-354	-364	-342	-342

RADIATIVE FLUX EXP -6 PLANE 1

1:	2:	3:	4:	5:	6:	7:	8:	9:	10:	11:	12:	13:	14:	15:	16:	17:
-14	-1	5	17	29	38	44	47	48	47	44	38	29	17	5	-1	-14
-29	0	0	0	0	0	0	0	0	0	0	0	0	0	0	0	-29
-33	0	0	0	0	0	0	0	0	0	0	0	0	0	0	0	-33
-35	0	0	0	0	0	0	0	0	0	0	0	0	0	0	0	-35
-34	0	0	0	0	0	0	0	0	0	0	0	0	0	0	0	-34
-33	0	0	0	0	0	0	0	0	0	0	0	0	0	0	0	-33
-33	0	0	0	0	0	0	0	0	0	0	0	0	0	0	0	-33
-34	0	0	0	0	0	0	0	0	0	0	0	0	0	0	0	-34
-35	0	0	0	0	0	0	0	0	0	0	0	0	0	0	0	-35
-38	0	0	0	0	0	0	0	0	0	0	0	0	0	0	0	-38
-42	0	0	0	0	0	0	0	0	0	0	0	0	0	0	0	-42
-46	0	0	0	0	0	0	0	0	0	0	0	0	0	0	0	-46
-48	0	0	0	0	0	0	0	0	0	0	0	0	0	0	0	-48
-48	0	0	0	0	0	0	0	0	0	0	0	0	0	0	0	-48
-45	0	0	0	0	0	0	0	0	0	0	0	0	0	0	0	-45
-39	0	0	0	0	0	0	0	0	0	0	0	0	0	0	0	-39
-38	-47	-56	-62	-65	-63	-37	56	127	56	-37	-63	-65	-62	-56	-47	-38

DIVERGENCE OF RADIATIVE FLUX EXP -5 PLANE 1

1:	2:	3:	4:	5:	6:	7:	8:	9:	10:	11:	12:	13:	14:	15:	16:	17:
0	0	0	0	0	0	0	0	0	0	0	0	0	0	0	0	0
0	-4	3	19	33	45	53	59	61	59	53	45	33	19	3	-4	0
0	-4	6	26	45	62	77	90	96	90	77	62	45	26	6	-4	0
0	-3	10	32	53	74	99	126	138	126	99	74	53	32	10	-3	0
0	-2	10	30	48	70	106	153	177	153	106	70	48	30	10	-2	0
0	-3	7	22	35	53	98	176	221	176	98	53	35	22	7	-3	0
0	-4	3	12	19	31	81	198	276	198	81	31	19	12	3	-4	0
0	-6	-1	3	4	11	60	206	310	206	60	11	4	3	-1	-6	0
0	-10	-7	-4	-6	-4	39	185	293	185	39	-4	-6	-4	-7	-10	0
0	-14	-13	-12	-16	-15	21	156	257	156	21	-15	-16	-12	-13	-14	0
0	-19	-19	-20	-24	-25	7	132	227	132	7	-25	-24	-20	-19	-19	0
0	-24	-26	-28	-33	-34	-5	111	199	111	-5	-34	-33	-28	-26	-24	0
0	-29	-32	-36	-41	-43	-17	90	174	90	-17	-43	-41	-36	-32	-29	0
0	-31	-37	-41	-47	-50	-29	73	154	73	-29	-50	-47	-41	-37	-31	0
0	-31	-37	-42	-48	-52	-35	62	141	62	-35	-52	-48	-42	-37	-31	0
0	-28	-33	-37	-42	-46	-32	50	119	50	-32	-46	-42	-37	-33	-28	0
0	0	0	0	0	0	0	0	0	0	0	0	0	0	0	0	0

C.5 Case 20: 2-D Fire Simulation, Pure Convection, Fluid Ra=1.E6
Implicit Fire Parameters: Ra=3.1E10, Gr=4.43E10, Re=2.1E5, Pe=1.47E5
BC's: No slip; Adiabatic Walls
Explicit Parameters: Ra=1.E6, Pr=0.7, Ar=1.0, Gr=1.43E6, Re=1195, Pe=837, Bo=40.65
Implicit Parameters: Lo=3 m, To=830 K, dTo=1072 K, Nu=88.E-6 m2/s, ko=58.E-6 m2/s
rho,o=0.42 kg/m3, alpha,o=125.E-6 m2/s, po=16 Pa, Uo=6.16 m/s
to=0.487 s, q",o=3.05E3 kW/m2, Ka=Kt=1 1/m, Ks=0 1/m, black walls

U1 EXP -3 PLANE 1

1:	2:	3:	4:	5:	6:	7:	8:	9:	10:	11:	12:	13:	14:	15:	16:	17:
0	0	0	0	0	0	0	0	0	0	0	0	0	0	0	0	0
0	14	-62	-141	-206	-259	-279	-193	0	193	279	259	206	141	62	-14	0
0	-3	-79	-160	-218	-183	-150	-92	0	92	150	183	218	160	79	3	0
0	-21	-71	-72	-86	-45	-51	-71	0	71	51	45	86	72	71	21	0
0	-10	-20	-12	-11	0	-16	-17	0	17	16	0	11	12	20	10	0
0	-1	29	21	36	19	40	29	0	-29	-40	-19	-36	-21	-29	1	0
0	5	60	54	61	44	48	1	0	-1	-48	-44	-61	-54	-60	-5	0
0	5	61	69	73	60	61	29	0	-29	-61	-60	-73	-69	-61	-5	0
0	20	51	53	65	73	57	8	0	-8	-57	-73	-65	-53	-51	-20	0
0	0	26	43	67	73	39	24	0	-24	-39	-73	-67	-43	-26	0	0
0	-12	6	38	59	49	28	17	0	-17	-28	-49	-59	-38	-6	12	0
0	6	9	19	26	26	25	19	0	-19	-25	-26	-26	-19	-9	-6	0
0	6	6	9	18	26	33	21	0	-21	-33	-26	-18	-9	-6	-6	0
0	0	9	17	26	31	37	24	0	-24	-37	-31	-26	-17	-9	0	0
0	1	16	24	30	41	53	56	0	-56	-53	-41	-30	-24	-16	-1	0
0	2	16	25	31	44	47	72	0	-72	-47	-44	-31	-25	-16	-2	0
0	0	0	0	0	0	0	0	0	0	0	0	0	0	0	0	0

U2 EXP -3 PLANE 1

1:	2:	3:	4:	5:	6:	7:	8:	9:	10:	11:	12:	13:	14:	15:	16:	17:
0	0	0	0	0	0	0	0	0	0	0	0	0	0	0	0	0
0	0	-11	-22	18	32	26	-12	-13	-12	26	32	18	-22	-11	0	0
0	-67	-93	-136	-101	-10	86	213	293	213	86	-10	-101	-136	-93	-67	0
0	-126	-149	-111	-33	18	71	194	273	194	71	18	-33	-111	-149	-126	0
0	-165	-199	-141	-59	15	109	235	349	235	109	15	-59	-141	-199	-165	0
0	-160	-182	-111	-44	38	63	168	316	168	63	38	-44	-111	-182	-160	0
0	-148	-162	-108	-51	23	58	223	375	223	58	23	-51	-108	-162	-148	0
0	-124	-149	-112	-45	22	41	142	276	142	41	22	-45	-112	-149	-124	0
0	-76	-109	-90	-42	-2	11	156	317	156	11	-2	-42	-90	-109	-76	0
0	-15	-36	-47	-40	-21	0	110	238	110	0	-21	-40	-47	-36	-15	0
0	-29	-56	-72	-62	-32	-17	105	259	105	-17	-32	-62	-72	-56	-29	0
0	-42	-55	-55	-35	-24	-23	80	208	80	-23	-24	-35	-55	-55	-42	0
0	-31	-21	-14	-18	-29	-35	73	212	73	-35	-29	-18	-14	-21	-31	0
0	-24	-22	-18	-20	-20	-28	47	157	47	-28	-20	-20	-18	-22	-24	0
0	-23	-22	-18	-16	-14	-34	37	149	37	-34	-14	-16	-18	-22	-23	0
0	-6	-2	-2	-2	-3	0	0	1	0	0	-3	-2	-2	-2	-6	0
0	0	0	0	0	0	0	0	0	0	0	0	0	0	0	0	0

TEMPERATURE EXP -3 PLANE 1

1:	2:	3:	4:	5:	6:	7:	8:	9:	10:	11:	12:	13:	14:	15:	16:	17:
284	293	314	329	339	345	348	348	348	348	348	345	339	329	314	293	284
286	297	323	335	340	345	352	357	360	357	352	345	340	335	323	297	286
289	303	326	325	314	307	319	351	379	351	319	307	314	325	326	303	289
292	306	319	301	276	265	281	337	386	337	281	265	276	301	319	306	292
293	304	310	289	264	252	260	325	406	325	260	252	264	289	310	304	293
289	299	303	286	268	258	256	323	424	323	256	258	268	286	303	299	289
282	292	297	287	274	266	254	325	455	325	254	266	274	287	297	292	282
274	283	290	286	278	271	251	321	473	321	251	271	278	286	290	283	274
265	274	282	283	278	270	250	318	453	318	250	270	278	283	282	274	265
250	259	270	275	272	263	246	310	445	310	246	263	272	275	270	259	250
230	239	252	258	258	251	241	298	420	298	241	251	258	258	252	239	230
210	220	233	240	240	236	230	281	404	281	230	236	240	240	233	220	210
187	197	208	214	215	215	211	256	379	256	211	215	215	214	208	197	187
157	166	175	178	181	184	181	225	364	225	181	184	181	178	175	166	157
124	131	137	139	141	145	143	187	353	187	143	145	141	139	137	131	124
96	99	102	104	106	109	110	179	367	179	110	109	106	104	102	99	96
86	87	89	91	93	96	112	223	397	223	112	96	93	91	89	87	86

C.6 Case 21: 2-D Fire Simulation, Convection + Radiation, Fluid Ra=1.E6
Implicit Fire Parameters: Ra=3.1E10, Gr=4.43E10, Re=2.1E5, Pe=1.47E5
BC's: No slip; Adiabatic Walls
Explicit Parameters: Ra=1.E6, Pr=0.7, Ar=1.0, Gr=1.43E6, Re=1195, Pe=837, Bo=40.65
Implicit Parameters: Lo=3 m, To=830 K, dTo=1072 K, Nu=88.E-6 m2/s, ko=58.E-6 m2/s
rho,o=0.42 kg/m3, alpha,o=125.E-6 m2/s, po=16 Pa, Uo=6.16 m/s
to=0.487 s, q",o=3.05E3 kW/m2, Ka=Kt=1 1/m, Ks=0 1/m, black walls

U1 EXP -3 PLANE 1

1:	2:	3:	4:	5:	6:	7:	8:	9:	10:	11:	12:	13:	14:	15:	16:	17:
0	0	0	0	0	0	0	0	0	0	0	0	0	0	0	0	0
0	14	-62	-141	-206	-257	-276	-191	0	191	276	257	206	141	62	-14	0
0	-3	-80	-161	-218	-183	-150	-93	0	93	150	183	218	161	80	3	0
0	-22	-72	-73	-88	-47	-53	-72	0	72	53	47	88	73	72	22	0
0	-10	-21	-14	-13	-2	-17	-18	0	18	17	2	13	14	21	10	0
0	-1	29	19	34	17	39	28	0	-28	-39	-17	-34	-19	-29	1	0
0	6	61	53	60	43	47	0	0	0	-47	-43	-60	-53	-61	-6	0
0	5	62	70	73	60	61	28	0	-28	-61	-60	-73	-70	-62	-5	0
0	21	53	55	65	74	58	8	0	-8	-58	-74	-65	-55	-53	-21	0
0	1	28	44	68	75	40	24	0	-24	-40	-75	-68	-44	-28	-1	0
0	-13	6	40	62	52	28	17	0	-17	-28	-52	-62	-40	-6	13	0
0	6	9	20	27	27	25	20	0	-20	-25	-27	-27	-20	-9	-6	0
0	6	6	9	18	27	34	21	0	-21	-34	-27	-18	-9	-6	-6	0
0	0	9	17	26	31	37	24	0	-24	-37	-31	-26	-17	-9	0	0
0	1	16	24	30	41	53	56	0	-56	-53	-41	-30	-24	-16	-1	0
0	2	17	25	31	44	47	72	0	-72	-47	-44	-31	-25	-17	-2	0
0	0	0	0	0	0	0	0	0	0	0	0	0	0	0	0	0

U2 EXP -3 PLANE 1

1:	2:	3:	4:	5:	6:	7:	8:	9:	10:	11:	12:	13:	14:	15:	16:	17:
0	0	0	0	0	0	0	0	0	0	0	0	0	0	0	0	0
0	1	-11	-22	20	33	26	-12	-13	-12	26	33	20	-22	-11	1	0
0	-68	-94	-135	-99	-9	86	214	293	214	86	-9	-99	-135	-94	-68	0
0	-128	-150	-111	-32	19	71	193	270	193	71	19	-32	-111	-150	-128	0
0	-168	-201	-141	-58	17	110	234	348	234	110	17	-58	-141	-201	-168	0
0	-163	-184	-111	-43	40	64	169	316	169	64	40	-43	-111	-184	-163	0
0	-151	-164	-108	-51	24	61	224	375	224	61	24	-51	-108	-164	-151	0
0	-127	-152	-114	-45	25	44	144	277	144	44	25	-45	-114	-152	-127	0
0	-79	-113	-92	-43	0	13	157	318	157	13	0	-43	-92	-113	-79	0
0	-15	-37	-48	-40	-19	2	111	239	111	2	-19	-40	-48	-37	-15	0
0	-28	-55	-72	-63	-31	-15	106	260	106	-15	-31	-63	-72	-55	-28	0
0	-42	-57	-57	-36	-23	-22	80	208	80	-22	-23	-36	-57	-57	-42	0
0	-31	-22	-14	-18	-28	-35	73	212	73	-35	-28	-18	-14	-22	-31	0
0	-25	-22	-18	-20	-20	-28	47	157	47	-28	-20	-20	-18	-22	-25	0
0	-23	-23	-18	-16	-13	-34	37	149	37	-34	-13	-16	-18	-23	-23	0
0	-6	-2	-2	-2	-3	0	0	1	0	0	-3	-2	-2	-2	-6	0
0	0	0	0	0	0	0	0	0	0	0	0	0	0	0	0	0

TEMPERATURE EXP -3 PLANE 1

1:	2:	3:	4:	5:	6:	7:	8:	9:	10:	11:	12:	13:	14:	15:	16:	17:
281	290	310	325	334	340	343	343	343	343	343	340	334	325	310	290	281
283	294	319	330	335	340	347	352	355	352	347	340	335	330	319	294	283
286	300	322	321	311	306	317	348	375	348	317	306	311	321	322	300	286
290	302	315	299	275	265	281	334	382	334	281	265	275	299	315	302	290
290	301	307	287	263	252	260	323	402	323	260	252	263	287	307	301	290
287	297	300	283	266	258	256	320	420	320	256	258	266	283	300	297	287
280	290	295	285	272	265	253	322	451	322	253	265	272	285	295	290	280
272	281	287	284	276	270	250	318	470	318	250	270	276	284	287	281	272
263	272	280	280	276	269	248	315	451	315	248	269	276	280	280	272	263
249	257	268	273	270	262	245	308	443	308	245	262	270	273	268	257	249
229	238	251	257	257	250	240	298	420	298	240	250	257	257	251	238	229
210	220	233	240	240	236	230	281	404	281	230	236	240	240	233	220	210
187	198	209	215	216	216	212	257	381	257	212	216	216	215	209	198	187
158	168	176	180	183	186	183	227	366	227	183	186	183	180	176	168	158
126	133	139	142	144	148	145	189	355	189	145	148	144	142	139	133	126
98	101	104	106	108	112	113	181	370	181	113	112	108	106	104	101	98
87	88	91	93	96	98	114	225	399	225	114	98	96	93	91	88	87

(Cont'd)
C.6 Case 21: 2-D Fire Simulation, Convection + Radiation, Fluid Ra=1.E6

CONDUCTIVE FLUX EXP -6 PLANE 1

1:	2:	3:	4:	5:	6:	7:	8:	9:	10:	11:	12:	13:	14:	15:	16:	17:
-507	-95	-144	-13	122	213	153	-57	-254	-57	153	213	122	-13	-144	-95	-507
-312	0	0	0	0	0	0	0	0	0	0	0	0	0	0	0	-312
-332	0	0	0	0	0	0	0	0	0	0	0	0	0	0	0	-332
-260	0	0	0	0	0	0	0	0	0	0	0	0	0	0	0	-260
-186	0	0	0	0	0	0	0	0	0	0	0	0	0	0	0	-186
-149	0	0	0	0	0	0	0	0	0	0	0	0	0	0	0	-149
-149	0	0	0	0	0	0	0	0	0	0	0	0	0	0	0	-149
-136	0	0	0	0	0	0	0	0	0	0	0	0	0	0	0	-136
-156	0	0	0	0	0	0	0	0	0	0	0	0	0	0	0	-156
-203	0	0	0	0	0	0	0	0	0	0	0	0	0	0	0	-203
-180	0	0	0	0	0	0	0	0	0	0	0	0	0	0	0	-180
-204	0	0	0	0	0	0	0	0	0	0	0	0	0	0	0	-204
-214	0	0	0	0	0	0	0	0	0	0	0	0	0	0	0	-214
-172	0	0	0	0	0	0	0	0	0	0	0	0	0	0	0	-172
-125	0	0	0	0	0	0	0	0	0	0	0	0	0	0	0	-125
-51	0	0	0	0	0	0	0	0	0	0	0	0	0	0	0	-51
-583	-355	-387	-391	-386	-400	-190	496	458	496	-190	-400	-386	-391	-387	-355	-583

RADIATIVE FLUX EXP -6 PLANE 1

1:	2:	3:	4:	5:	6:	7:	8:	9:	10:	11:	12:	13:	14:	15:	16:	17:
-6	31	61	99	128	146	153	153	152	153	153	146	128	99	61	31	-6
-38	0	0	0	0	0	0	0	0	0	0	0	0	0	0	0	-38
-39	0	0	0	0	0	0	0	0	0	0	0	0	0	0	0	-39
-32	0	0	0	0	0	0	0	0	0	0	0	0	0	0	0	-32
-25	0	0	0	0	0	0	0	0	0	0	0	0	0	0	0	-25
-23	0	0	0	0	0	0	0	0	0	0	0	0	0	0	0	-23
-25	0	0	0	0	0	0	0	0	0	0	0	0	0	0	0	-25
-28	0	0	0	0	0	0	0	0	0	0	0	0	0	0	0	-28
-33	0	0	0	0	0	0	0	0	0	0	0	0	0	0	0	-33
-42	0	0	0	0	0	0	0	0	0	0	0	0	0	0	0	-42
-51	0	0	0	0	0	0	0	0	0	0	0	0	0	0	0	-51
-57	0	0	0	0	0	0	0	0	0	0	0	0	0	0	0	-57
-60	0	0	0	0	0	0	0	0	0	0	0	0	0	0	0	-60
-60	0	0	0	0	0	0	0	0	0	0	0	0	0	0	0	-60
-57	0	0	0	0	0	0	0	0	0	0	0	0	0	0	0	-57
-48	0	0	0	0	0	0	0	0	0	0	0	0	0	0	0	-48
-54	-72	-84	-94	-102	-109	-108	-7	88	-7	-108	-109	-102	-94	-84	-72	-54

DIVERGENCE OF RADIATIVE FLUX EXP -5 PLANE 1

1:	2:	3:	4:	5:	6:	7:	8:	9:	10:	11:	12:	13:	14:	15:	16:	17:
0	0	0	0	0	0	0	0	0	0	0	0	0	0	0	0	0
0	28	57	77	76	77	95	134	157	134	95	77	76	77	57	28	0
0	35	56	51	19	1	32	125	188	125	32	1	19	51	56	35	0
0	38	42	8	-44	-71	-37	105	210	105	-37	-71	-44	8	42	38	0
0	33	25	-14	-65	-92	-64	109	248	109	-64	-92	-65	-14	25	33	0
0	25	18	-13	-53	-80	-60	141	313	141	-60	-80	-53	-13	18	25	0
0	17	15	-2	-31	-59	-49	184	393	184	-49	-59	-31	-2	15	17	0
0	10	14	6	-13	-42	-40	209	439	209	-40	-42	-13	6	14	10	0
0	5	12	11	-3	-33	-34	201	419	201	-34	-33	-3	11	12	5	0
0	-4	3	6	-5	-31	-30	178	370	178	-30	-31	-5	6	3	-4	0
0	-17	-12	-8	-16	-35	-31	146	309	146	-31	-35	-16	-8	-12	-17	0
0	-27	-25	-23	-29	-43	-39	104	235	104	-39	-43	-29	-23	-25	-27	0
0	-35	-37	-38	-44	-54	-53	57	160	57	-53	-54	-44	-38	-37	-35	0
0	-41	-47	-51	-57	-66	-70	12	93	12	-70	-66	-57	-51	-47	-41	0
0	-43	-50	-56	-62	-71	-80	-16	49	-16	-80	-71	-62	-56	-50	-43	0
0	-38	-45	-50	-56	-63	-75	-30	20	-30	-75	-63	-56	-50	-45	-38	0
0	0	0	0	0	0	0	0	0	0	0	0	0	0	0	0	0

C.7 Case 22: Accuracy Study of 2-D Fire Simulation, Fluid Ra=1.E6, Mesh=32x32

Implicit Fire Parameters: Ra=3.1E10, Gr=4.43E10, Re=2.1E5, Pe=1.47E5

BC's: No slip; Adiabatic Walls
Explicit Parameters: Ra=1.E6, Pr=0.7, Ar=1.0, Gr=1.43E6, Re=1195, Pe=837, Bo=40.65
Implicit Parameters: Lo=3 m, To=830 K, dTo=1072 K, Nu=88.E-6 m2/s, ko=58.E-6 m2/s
rho,o=0.42 kg/m3, alpha,o=125.E-6 m2/s, po=16 Pa, Uo=6.16 m/s
to=0.487 s

U1 EXP -3 PLANE 1

1:	2:	3:	4:	5:	6:	7:	8:	9:	10:	11:	12:	13:	14:	15:	16:	17:	18:	19:	20:
0	0	0	0	0	0	0	0	0	0	0	0	0	0	0	0	0	0	0	0
0	-4	-5	-13	-46	-42	-5	-113	-210	-169	-178	-221	-234	-202	-146	-72	8	88	156	211
0	-8	-5	-28	-106	-73	-50	-249	-264	-211	-239	-259	-236	-191	-139	-74	5	85	145	192
0	-14	-1	-50	-156	-88	-96	-280	-236	-197	-193	-197	-179	-160	-135	-78	3	83	136	156
0	-20	1	-59	-172	-95	-80	-203	-192	-152	-135	-128	-122	-117	-90	-44	-1	42	88	114
0	-24	-2	-41	-157	-101	-60	-96	-114	-95	-81	-70	-67	-60	-39	-21	-1	16	33	56
0	-24	-12	-10	-110	-99	-60	-51	-50	-44	-37	-31	-29	-25	-30	-29	-2	23	24	21
0	-18	-20	2	-39	-72	-58	-39	-25	-15	-8	-4	-1	-4	-12	-11	-3	5	9	2
0	-8	-19	-3	2	-11	-17	-10	-1	5	10	13	14	10	4	0	-3	-4	-6	-10
0	0	-5	-2	11	22	26	26	25	24	26	27	25	21	12	1	-2	-5	-13	-20
0	4	10	11	21	32	42	44	40	37	39	37	34	28	17	5	-1	-7	-16	-26
0	5	17	24	34	43	52	52	46	48	50	45	39	33	21	9	-1	-10	-20	-31
0	5	20	29	43	55	62	54	51	60	60	49	44	37	23	10	0	-10	-21	-34
0	4	24	38	52	61	58	50	61	74	65	50	48	39	25	13	0	-12	-21	-35
0	3	22	43	59	57	49	57	79	83	60	51	51	39	25	13	0	-11	-21	-35
0	3	14	29	43	47	58	78	92	75	53	55	52	36	24	14	1	-11	-20	-32
0	2	8	15	28	45	68	87	81	55	52	59	50	33	24	13	1	-11	-20	-29
0	1	9	18	31	49	65	66	50	47	58	58	43	30	23	13	1	-10	-20	-26
0	0	7	19	32	41	43	38	42	54	60	50	36	28	21	12	1	-9	-19	-25
0	0	2	9	17	24	29	38	49	56	51	39	31	27	20	11	1	-8	-17	-24
0	0	0	3	8	17	27	38	45	43	37	32	29	25	18	11	1	-7	-16	-23
0	0	1	3	8	15	23	29	31	30	29	29	27	23	17	10	1	-7	-15	-22
0	0	1	4	7	12	16	19	22	25	27	27	25	22	17	10	1	-8	-16	-21
0	0	1	2	5	9	13	16	20	23	24	24	24	22	18	11	1	-8	-17	-22
0	0	1	3	6	9	12	16	19	21	22	23	24	24	20	11	1	-9	-19	-24
0	0	2	4	7	10	13	16	18	20	22	25	26	26	22	12	0	-11	-22	-27
0	0	3	6	9	12	15	18	20	23	25	28	30	30	26	14	0	-14	-26	-31
0	0	4	8	12	15	18	21	24	27	30	33	35	36	30	17	0	-17	-31	-37
0	1	5	9	14	17	21	25	28	31	35	38	41	42	37	22	0	-23	-38	-43
0	1	5	10	15	19	23	27	31	34	38	43	46	48	43	27	0	-28	-45	-50
0	1	5	9	14	18	22	25	29	33	37	42	47	52	53	38	0	-39	-54	-54
0	0	3	7	10	12	15	17	20	23	26	31	36	43	47	37	0	-38	-48	-44
0	0	0	0	0	0	0	0	0	0	0	0	0	0	0	0	0	0	0	0

(Cont'd)
C.7 Case 22: Accuracy Study of 2-D Fire Simulation, Fluid Ra=1.E6, Mesh=32x32

U1 SOLUTION FIELD CONTINUED:

21:	22:	23:	24:	25:	26:	27:	28:	29:	30:	31:	32:	33:
241	236	177	146	192	144	17	26	50	24	18	8	0
234	268	250	202	224	269	84	45	103	50	9	8	0
171	200	199	188	201	284	140	59	142	77	1	10	0
116	126	131	143	170	222	115	68	153	87	-2	13	0
64	68	78	92	114	116	68	77	144	66	-1	17	0
27	30	37	45	52	52	53	81	108	29	4	18	0
1	4	7	13	21	31	46	61	49	6	12	14	0
-14	-13	-10	-5	0	9	16	16	7	3	11	5	0
-24	-25	-24	-22	-21	-18	-15	-12	-7	-1	-1	0	0
-31	-35	-36	-34	-37	-38	-32	-23	-21	-17	-12	0	0
-36	-41	-47	-43	-44	-53	-51	-40	-33	-22	-11	0	0
-40	-44	-56	-54	-44	-56	-68	-57	-38	-17	-10	-3	0
-43	-44	-60	-69	-49	-39	-61	-63	-45	-28	-21	-4	0
-47	-44	-55	-81	-70	-38	-34	-58	-64	-49	-27	-3	0
-49	-48	-44	-76	-92	-68	-44	-42	-51	-38	-18	-3	0
-47	-55	-42	-52	-90	-89	-63	-39	-25	-14	-8	-4	0
-41	-57	-51	-36	-51	-77	-69	-45	-23	-12	-8	-3	0
-33	-51	-58	-46	-32	-37	-48	-45	-33	-20	-8	0	0
-28	-39	-53	-55	-44	-31	-27	-26	-22	-12	-3	1	0
-27	-30	-38	-47	-46	-37	-25	-15	-8	-2	0	0	0
-27	-27	-28	-31	-33	-31	-24	-15	-7	-2	0	0	0
-25	-27	-26	-23	-22	-20	-17	-12	-8	-4	-1	0	0
-24	-25	-25	-22	-19	-15	-12	-9	-6	-3	-1	0	0
-25	-24	-23	-21	-19	-15	-12	-8	-5	-3	-1	0	0
-27	-25	-23	-21	-18	-16	-13	-10	-7	-4	-2	0	0
-31	-29	-26	-23	-20	-17	-15	-12	-9	-6	-3	0	0
-37	-34	-30	-27	-24	-21	-18	-15	-12	-8	-4	0	0
-43	-39	-36	-32	-28	-25	-21	-18	-14	-9	-5	-1	0
-48	-44	-40	-35	-31	-28	-24	-20	-15	-10	-6	-1	0
-49	-43	-38	-34	-30	-26	-23	-19	-15	-10	-5	-1	0
-37	-32	-27	-24	-21	-18	-16	-13	-10	-7	-3	0	0
0	0	0	0	0	0	0	0	0	0	0	0	0

```
  0   0   0   0   0   0   0   0   0   0   0   0   0   0   0   0   0   0   0   0
  0   0  -1 -12  -7  19  -2 -44 -10  -5 -16  -6   9  10   2  -5  -8  -7  -2  10
  0  -8 -13 -32 -22  -5 -57 -84 -56 -67 -38  -2  30  65 114 161 179 159 108  57
  0 -21 -30 -57 -57 -54 -82 -92 -93 -76 -18  19  53 104 158 191 202 191 158  99
  0 -41 -52 -86-111-110 -86 -75 -99 -65 -15  24  67 121 168 208 226 202 163 118
  0 -65 -76-106-158-160-114 -62 -59 -36  -2  32  75 126 196 286 328 280 186 119
  0 -87-103-114-173-195-156 -96 -54 -22   7  39  77 131 219 309 346 309 216 126
  0-100-129-124-140-168-148-100 -55 -16  14  44  77 128 208 292 333 290 205 125
  0-103-147-146-128-115 -98 -71 -41 -10  19  46  77 125 202 302 355 303 202 123
  0 -98-152-165-153-125 -94 -65 -36  -5  22  47  75 117 193 298 353 300 195 116
  0 -90-143-164-164-145-114 -79 -41  -5  22  46  72 109 183 288 346 292 187 109
  0 -77-129-148-147-134-112 -81 -39  -4  20  43  67 100 170 277 339 283 176 101
  0 -63-112-137-138-128-110 -74 -31  -5  14  39  61  90 158 266 331 273 165  92
  0 -55 -97-127-141-137-106 -56 -26 -13   7  34  52  79 145 252 318 261 154  81
  0 -52 -86-105-112 -98 -64 -41 -36 -25   4  29  41  67 134 239 306 249 144  71
  0 -44 -76 -86 -79 -63 -55 -57 -56 -29   5  20  29  57 122 226 292 237 133  61
  0 -32 -63 -83 -89 -90 -92 -88 -62 -18   2   8  18  47 111 214 280 225 122  52
  0 -24 -48 -74 -95-106-102 -74 -31 -10  -8  -3  10  37 100 203 268 214 111  42
  0 -21 -38 -51 -60 -59 -45 -25 -18 -22 -21 -10   2  27  90 193 257 203 101  33
  0 -21 -34 -40 -39 -33 -29 -32 -37 -36 -25 -13  -4  18  82 184 246 193  93  23
  0 -20 -34 -42 -46 -49 -51 -51 -45 -33 -22 -17 -11  11  76 175 236 184  85  16
  0 -19 -31 -38 -44 -47 -47 -41 -31 -24 -21 -22 -17   6  70 167 226 174  78  10
  0 -19 -28 -31 -32 -30 -27 -24 -22 -22 -25 -26 -21   3  64 158 216 165  71   6
  0 -18 -27 -28 -27 -24 -23 -22 -23 -25 -26 -27 -21   0  58 150 206 155  64   3
  0 -18 -26 -27 -26 -25 -24 -23 -23 -24 -25 -25 -21  -1  52 141 196 145  56   0
  0 -17 -24 -25 -24 -22 -21 -20 -20 -20 -22 -23 -20  -3  45 130 184 133  48  -2
  0 -15 -21 -22 -20 -18 -17 -16 -16 -18 -20 -21 -20  -5  38 118 171 120  40  -5
  0 -13 -18 -18 -17 -15 -14 -13 -14 -15 -17 -18 -17  -7  29 103 153 104  30  -6
  0 -10 -14 -14 -13 -12 -11 -11 -11 -13 -14 -16 -16  -9  19  87 134  87  20  -9
  0  -6  -9 -10  -9  -8  -7  -7  -7  -8 -10 -11 -12  -9   9  63 103  63  10  -9
  0  -3  -5  -5  -5  -4  -4  -4  -4  -5  -6  -8  -9  -9   1  41  72  41   1  -9
  0   0  -1  -1   0   0   0   0   0   0  -1  -1  -2  -2   0   9  16   8   0  -2
  0   0   0   0   0   0   0   0   0   0   0   0   0   0   0   0   0   0   0   0
21: 22: 23: 24: 25: 26: 27: 28: 29: 30: 31: 32: 33:  U2 EXP-3 SOLUTION FIELD CONT'D:
  0   0   0   0   0   0   0   0   0   0   0  24   0
 16   2 -18 -12  -2 -39 -18  20   1 -13   4  11   0
 22  -1 -35 -69 -57 -73 -70  -9  -9 -25 -11  -4   0
 43  11 -13 -66 -96 -93 -88 -53 -45 -49 -29 -21   0
 63  20 -11 -59-107 -96 -81 -98 -99 -80 -52 -42   0
 70  28  -4 -39 -71 -68 -92-142-148-105 -74 -64   0   Cont'd  C.7  Case 22
 73  35   4 -23 -51 -82-131-175-167-114-100 -85   0
 73  41  12 -16 -51 -93-137-162-143-121-124 -97   0
 74  43  16 -12 -43 -76-106-124-132-141-141-100   0
 72  44  19  -7 -36 -64 -95-127-151-159-146 -98   0
 70  43  19  -6 -38 -69 -97-128-150-154-140 -96   0
 65  40  17  -5 -39 -74 -95-109-124-135-131 -84   0
 59  36  11  -5 -32 -79-109-118-127-134-116 -60   0
 51  32   5 -13 -22 -61-126-154-154-135 -92 -45   0
 41  28   2 -26 -29 -29 -64-116-126-105 -77 -48   0
 29  20   5 -33 -52 -42 -30 -42 -66 -79 -75 -50   0
 18   7   5 -22 -71 -84 -77 -71 -75 -81 -69 -39   0
  9  -5  -6  -6 -41 -95-116-114-101 -80 -52 -25   0
  3 -13 -21 -16 -11 -30 -63 -78 -71 -54 -37 -19   0
 -3 -15 -29 -35 -29 -18 -16 -25 -34 -37 -33 -20   0
-10 -17 -25 -39 -48 -48 -44 -41 -41 -40 -34 -20   0
-17 -22 -22 -27 -38 -48 -53 -52 -47 -40 -32 -19   0
-21 -27 -25 -22 -22 -26 -31 -34 -34 -32 -28 -19   0
-22 -29 -28 -25 -22 -20 -21 -23 -25 -27 -26 -18   0
-22 -27 -27 -26 -25 -24 -24 -24 -26 -27 -26 -18   0
-20 -24 -23 -22 -21 -22 -22 -23 -25 -26 -24 -17   0
-20 -22 -20 -19 -17 -17 -18 -19 -21 -22 -22 -15   0
-17 -19 -18 -16 -14 -14 -14 -15 -17 -19 -18 -13   0
-16 -16 -15 -13 -12 -11 -12 -12 -14 -15 -14 -10   0
-12 -11 -10  -9  -8  -7  -8  -8  -9 -10 -10  -7   0
 -9  -8  -6  -5  -4  -4  -4  -4  -5  -5  -5  -3   0
 -2  -1  -1   0   0   0   0   0   0  -1  -1   0   0
  0   0   0   0   0   0   0   0   0   0   0   0   0
```

```
288 291 299 310 322 332 340 348 353 356 359 363 365 367 368 368 368 368 367 366
288 291 300 313 326 335 342 351 355 357 360 364 366 369 371 372 372 371 370 367
290 294 304 319 333 339 345 351 352 353 354 356 360 366 372 378 380 377 370 362
292 296 307 324 337 339 342 344 341 338 333 334 340 351 366 379 383 376 361 346
295 299 310 327 336 335 333 327 323 315 307 307 314 331 355 379 389 375 349 325
296 301 312 327 334 330 323 310 301 292 285 284 291 311 343 379 396 375 337 305
298 302 312 324 330 324 315 300 287 277 270 269 276 297 336 382 402 378 331 292
298 302 312 321 324 318 306 292 280 270 264 262 268 288 329 383 410 380 325 284
298 302 310 317 319 312 301 288 277 268 263 261 265 282 324 386 420 385 322 279
296 300 308 314 315 310 300 288 278 270 265 262 264 278 321 391 431 390 320 277
294 298 305 311 312 308 300 290 281 273 268 264 264 276 318 396 445 397 319 275
292 295 302 308 309 307 300 292 284 277 271 267 265 274 315 401 462 403 317 274
288 292 298 304 306 305 300 293 286 280 274 269 266 273 312 406 486 409 315 273
284 287 293 299 302 302 299 293 287 282 276 270 266 272 309 405 509 409 312 272
279 282 288 294 297 298 296 292 288 283 276 270 265 271 306 400 497 404 310 271
273 277 283 288 291 293 292 290 287 282 275 269 264 269 304 395 494 400 308 270
267 270 276 282 286 288 289 288 285 279 273 267 262 267 301 389 486 394 305 268
260 263 269 276 281 284 285 283 279 274 269 264 259 265 297 383 479 388 301 266
252 255 261 267 272 276 277 275 272 269 265 260 256 261 292 376 470 380 296 262
243 246 252 258 263 266 267 267 266 264 259 254 251 257 286 368 460 372 289 257
234 237 243 250 255 258 260 260 259 256 252 248 245 251 279 359 450 362 282 252
224 227 233 240 245 249 251 251 249 247 243 240 239 244 271 348 439 352 273 245
213 216 222 228 233 236 238 238 237 236 234 232 231 236 261 337 427 340 263 236
201 204 210 216 220 223 224 225 225 224 223 221 221 226 249 325 415 327 250 226
188 191 197 202 206 208 210 210 210 210 210 209 209 213 236 312 403 313 237 214
173 176 182 186 190 192 193 194 194 195 195 195 196 200 222 299 391 299 222 200
157 160 165 169 172 174 175 176 176 177 178 179 180 184 206 285 379 285 206 184
141 143 147 151 153 155 155 156 157 158 160 161 163 167 189 271 369 271 189 167
124 126 129 132 134 135 136 137 138 139 140 142 144 149 172 258 361 258 171 149
108 110 112 114 116 117 117 118 119 120 122 124 127 133 157 248 356 248 156 132
 96  97  98 100 101 102 103 103 104 106 107 110 113 121 147 244 358 243 147 121
 88  88  89  90  91  92  93  94  95  96  98 101 106 119 153 254 367 254 153 118
 85  85  86  87  88  89  90  91  92  93  95  98 105 122 168 272 376 272 168 122
21: 22: 23: 24: 25: 26: 27: 28: 29: 30: 31: 32: 33: TEMP EXP-3  FIELD CONTINUED:
364 361 357 353 350 345 338 329 318 299 273 228 171
364 361 358 354 352 348 340 332 323 305 279 244 221
356 353 351 350 348 348 343 335 330 315 288 265 255
335 330 329 333 338 340 340 336 333 322 296 277 271
309 302 303 310 320 325 330 332 333 325 302 285 280  Cont'd C.7  Case 22
287 280 281 289 299 307 318 326 330 324 305 290 285
273 266 267 274 284 296 310 320 326 321 306 293 289
265 259 260 266 276 289 302 313 320 317 306 295 291
262 257 259 264 273 284 297 308 315 313 305 296 292
261 258 260 265 273 283 295 305 311 310 303 295 291
261 260 263 268 275 285 294 303 308 307 300 294 290
262 262 266 271 278 287 295 301 304 303 298 292 288
263 264 269 274 280 288 295 300 301 299 294 288 285
263 265 271 276 281 288 294 298 298 296 290 284 282
262 265 271 277 282 286 291 295 294 290 285 280 277
261 265 271 277 282 285 287 289 288 285 280 275 272
260 263 269 275 281 283 284 284 283 280 275 269 266
258 261 266 271 276 280 281 281 278 274 268 262 259
254 257 262 266 270 273 275 275 271 266 260 254 252
250 253 258 261 264 265 266 265 262 258 252 246 243
245 247 251 255 258 258 258 256 253 249 243 237 234
238 239 243 246 249 250 250 248 245 240 233 227 224
231 231 233 235 237 238 238 236 233 228 222 216 213
221 221 223 224 224 224 224 222 220 215 210 204 201
210 210 210 210 210 210 209 208 205 201 196 190 187
196 196 195 195 194 194 193 191 189 186 181 176 173
180 179 178 177 176 175 175 173 172 169 165 160 157
163 161 160 158 157 156 155 154 153 150 147 142 140
144 142 140 139 137 136 135 134 133 131 128 125 123
127 124 122 120 119 118 117 116 115 113 111 109 107
113 109 107 105 104 103 102 101 100  99  97  96  95
106 100  97  96  94  93  92  91  90  89  88  87  87
105  98  95  92  91  90  89  88  87  86  85  84  84
```

C.8 Case 23: 2-D Fire Simulation, Fluid Ra=1.E6, Small Opening, Mesh=32x16
Implict Fire Parameters: Ra=3.1E10, Gr=4.43E10, Re=2.1E5, Pe=1.47E5)
BC's: No slip; Adiabatic Walls
Explicit Parameters: Ra=1.E6, Pr=0.7, Ar=1.0, Gr=1.43E6, Re=1195, Pe=837, Bo=40.65
Implicit Parameters: Lo=3 m, To=830 K, dTo=1072 K, Nu=88.E-6 m2/s, ko=58.E-6 m2/s
rho,o=0.42 kg/m3, alpha,o=125.E-6 m2/s, po=16 Pa, Uo=6.16 m/s
to=0.487 s, q",o=3.05E3 kW/m2, Ka=Kt=1 1/m, Ks=0 1/m, black walls

U1 EXP -3 PLANE 1

1:	2:	3:	4:	5:	6:	7:	8:	9:	10:	11:	12:	13:	14:	15:	16:	17:	18:	19:	20:
0	0	0	0	0	0	0	0	0	0	0	0	0	0	0	0	0	0	0	0
0	0	-2	2	-4	12	0	12	-38	-20	-85	-8	-100	30	-134	19	0	-67	-146	115
0	4	5	12	-2	-8	-43	-18	-44	28	-38	35	-83	43	-95	-8	0	13	-41	80
0	1	-4	-6	-14	1	-3	15	-14	3	-42	56	-38	99	-45	44	0	23	-50	173
0	-3	-3	-11	-15	-21	-25	-8	-3	63	37	109	61	126	11	123	0	139	-26	198
0	-8	-10	-27	-14	-9	13	51	25	70	70	157	133	185	73	184	0	225	-23	164
0	-5	-12	-23	-6	-6	28	54	63	148	159	229	155	214	89	194	0	247	11	104
0	-4	-15	-18	-3	12	56	69	116	173	153	148	72	132	42	168	0	196	3	43
0	-1	-12	-10	-4	20	42	69	144	122	61	27	10	43	17	113	0	120	-4	-12
0	0	-8	-9	-2	17	43	76	83	22	-9	-34	-13	-15	1	59	0	57	-13	-46
0	0	-3	-5	-4	4	20	27	18	-31	-34	-55	-12	-48	1	2	0	11	-9	-65
0	2	3	0	-7	-11	-5	-9	-30	-59	-42	-67	-13	-66	-3	-34	0	-8	-24	-64
0	3	11	9	-2	-24	-34	-47	-68	-79	-67	-88	-26	-74	-6	6	0	-71	-11	-74
0	4	19	25	13	-22	-53	-73	-91	-99	-107	-112	-81	-97	-94	-59	-157	-100	-54	-49
0	3	23	36	36	4	-43	-83	-106	-120	-128	-129	-122	-137	-134	-152	-122	-71	-58	-37
0	3	24	41	50	34	-19	-76	-107	-89	-83	-92	-94	-107	-105	-103	-93	-72	-45	-26
0	0	0	0	0	0	0	0	0	0	0	0	0	0	0	0	0	0	0	0

U1 SOLUTION FIELD CONTINUED:

21:	22:	23:	24:	25:	26:	27:	28:	29:	30:	31:	32:	33:
0	0	0	0	0	0	0	0	0	0	28	-28	0
-27	139	56	72	14	26	24	37	16	58	35	-9	0
-62	136	117	114	63	53	51	59	38	35	34	-9	0
-19	119	95	103	63	61	62	76	44	37	36	-7	0
42	91	56	70	42	49	56	66	45	35	28	-7	0
51	45	12	26	14	31	34	40	31	26	18	-3	0
21	1	-17	-8	-7	2	5	13	13	14	8	0	0
-12	-29	-31	-29	-26	-22	-14	-6	-1	5	2	2	0
-27	-44	-36	-44	-35	-34	-24	-17	-9	0	-2	4	0
-28	-52	-35	-46	-35	-36	-26	-22	-14	-6	-7	2	0
-19	-52	-26	-41	-28	-32	-24	-23	-17	-11	-9	0	0
-15	-46	-18	-32	-19	-25	-19	-20	-17	-13	-10	0	0
-5	-44	-9	-25	-11	-17	-12	-14	-13	-10	-8	0	0
-22	-27	-8	-13	-3	-6	-4	-6	-7	-6	-5	0	0
-22	-12	-2	1	6	6	5	2	0	-2	-3	1	0
-10	0	7	12	15	16	15	11	7	2	0	0	0
0	0	0	0	0	0	0	0	0	0	0	0	0

U2 EXP -3 PLANE 1

1:	2:	3:	4:	5:	6:	7:	8:	9:	10:	11:	12:	13:	14:	15:	16:	17:	18:	19:	20:
0	0	0	0	0	0	0	0	0	0	0	0	0	0	0	0	0	0	0	0
0	0	0	0	10	5	2	-9	-25	-1	-12	31	-25	57	-67	31	0	-3	-37	-114
0	2	1	-5	-10	-11	-9	-7	-9	-13	0	-22	2	-16	21	0	0	-41	139	99
0	10	-2	4	-3	-1	-11	-18	-15	-32	-1	-19	10	-32	17	-31	0	-60	96	133
0	5	-13	-12	-24	-13	-2	1	10	15	32	22	28	-32	4	-89	0	6	60	181
0	1	-12	-8	-8	6	8	-17	0	-6	59	21	53	-33	-16	-123	0	108	75	122
0	-16	-23	-22	-13	18	31	31	78	73	95	20	23	-67	-34	-153	0	121	73	71
0	-25	-26	-16	15	50	65	59	80	98	76	17	-3	-67	-39	-199	0	111	50	15
0	-39	-35	-19	30	66	103	91	138	122	44	-5	-7	-58	-44	-203	0	80	8	-25
0	-45	-39	-9	50	101	124	110	127	46	-3	-11	-1	-42	-26	-169	0	43	-26	-44
0	-51	-46	-10	54	120	141	135	113	16	-16	-7	-1	-24	-17	-96	0	-17	-48	-56
0	-50	-47	-9	60	132	149	115	60	-16	-10	0	1	-12	-14	-73	0	-48	-67	-49
0	-47	-49	-17	44	121	145	110	53	-9	3	9	-1	4	-26	4	0	-142	-49	-56
0	-34	-39	-18	27	96	123	78	17	-8	10	8	3	22	-8	35	-62	-113	-14	-58
0	-24	-29	-19	5	57	93	79	20	-14	5	1	8	14	-4	-22	-16	-34	-27	-32
0	-6	-6	-5	0	8	12	7	-5	1	5	-4	0	2	0	2	-18	-10	-6	-5
0	0	0	0	0	0	0	0	0	0	0	0	0	0	0	0	0	0	0	0

(Cont'd)
C.8 Case 23: 2-D Fire Simulation, Fluid Ra=1.E6, Small Opening, Mesh=32x1

U2 SOLUTION FIELD CONTINUED:

21:	22:	23:	24:	25:	26:	27:	28:	29:	30:	31:	32:	33:
0	0	0	0	0	0	0	0	0	0	123	45	0
15	31	23	-4	-8	-5	5	-8	-8	28	76	39	0
33	49	11	-11	-29	-32	-7	-4	10	25	41	30	0
66	27	0	-14	-28	-35	-27	-9	0	19	28	18	0
91	29	-14	-17	-26	-27	-37	-17	-6	0	6	2	0
43	9	-19	-12	-23	-27	-35	-21	-15	-6	-4	-8	0
6	-7	-25	-19	-32	-29	-30	-22	-18	-11	-15	-19	0
-27	-22	-30	-22	-25	-18	-17	-13	-10	-10	-21	-24	0
-44	-30	-29	-16	-15	-9	-7	-4	-5	-12	-25	-26	0
-49	-30	-25	-15	-10	-4	-1	0	-1	-10	-22	-23	0
-47	-32	-25	-16	-9	-3	2	5	3	-5	-17	-20	0
-46	-29	-23	-13	-6	0	6	9	7	-1	-10	-15	0
-35	-28	-18	-12	-4	0	7	9	8	1	-7	-12	0
-15	-27	-10	-10	-2	0	6	9	10	5	0	-6	0
-15	-17	-7	-6	-1	0	4	5	6	4	0	-3	0
-3	-3	-2	-2	0	0	0	0	1	1	1	-1	0
0	0	0	0	0	0	0	0	0	0	0	0	0

TEMPERATURE EXP -3 PLANE 1

1:	2:	3:	4:	5:	6:	7:	8:	9:	10:	11:	12:	13:	14:	15:	16:	17:	18:	19:	20:
166	166	165	163	162	160	158	156	154	153	154	155	158	162	166	169	173	180	185	185
165	165	164	162	160	158	156	154	153	152	153	154	158	161	168	168	173	180	184	185
162	161	160	158	156	154	151	150	149	149	149	151	155	158	166	168	173	179	179	181
157	156	154	151	148	145	143	142	143	144	148	150	155	156	162	166	170	174	178	181
151	149	147	143	139	135	133	134	138	142	160	166	178	171	169	165	169	172	179	180
145	143	139	133	129	126	126	129	143	160	199	212	225	211	195	176	174	182	184	171
139	137	132	126	123	123	126	128	182	231	260	262	252	242	223	201	188	195	176	147
133	132	126	121	120	123	133	127	258	301	271	236	219	224	220	215	197	187	149	120
128	127	122	118	120	125	138	142	295	280	195	172	178	193	201	214	189	153	117	100
123	123	119	116	120	129	140	175	303	209	135	136	151	171	185	208	160	114	93	88
118	118	115	113	119	132	145	191	263	132	96	108	123	147	161	173	116	86	78	78
111	113	111	109	116	134	147	180	213	76	66	76	87	105	113	112	76	68	67	68
102	105	105	103	110	135	149	162	161	32	43	45	53	59	63	56	54	60	56	56
90	94	96	93	99	132	157	151	126	9	30	23	31	32	36	40	48	48	43	43
73	77	80	79	84	121	168	163	109	-3	22	12	21	22	28	31	33	31	29	28
59	60	62	65	73	110	173	203	150	2	12	8	12	13	16	16	17	16	15	15
53	54	56	60	75	114	169	227	242	51	3	7	8	9	10	10	10	10	10	10

TEMPERATURE SOLUTION FIELD CONTINUED:

21:	22:	23:	24:	25:	26:	27:	28:	29:	30:	31:	32:	33:
185	184	183	182	181	180	179	178	176	175	171	161	156
184	183	182	181	181	180	179	178	177	175	171	162	157
176	174	174	176	178	179	179	178	177	174	170	162	157
167	159	160	166	172	175	176	176	175	172	168	161	157
158	143	146	155	164	168	171	172	171	169	166	160	156
143	130	136	145	154	159	163	164	165	164	162	158	155
122	119	128	137	144	149	153	156	157	159	159	155	152
108	112	121	128	134	139	143	146	149	153	154	151	148
99	105	112	117	122	126	131	135	141	146	148	146	142
91	96	100	104	108	112	117	124	131	138	141	138	133
81	83	86	89	92	96	102	110	119	126	129	125	120
69	70	71	73	75	79	85	93	101	109	111	107	101
56	56	56	57	58	62	66	73	80	86	88	84	79
41	41	40	40	41	43	47	51	56	60	62	59	55
26	26	25	26	26	28	30	32	35	37	37	35	33
14	14	14	15	16	17	18	20	21	21	20	19	18
10	10	11	11	12	14	15	16	16	16	15	13	13

Appendix D

3-D Fire Simulation Solutions

D.1 Case 24: 3-D Fire Simulation, Fluid Ra=1.E4
Implicit Fire Parameters: Ra=3.1E10, Gr=4.43E10, Re=2.1E5, Pe=1.47E5
BC's: No slip; Adiabatic Walls
Explicit Parameters: Ra=1.E4, Pr=0.7, Ar=1.0, Gr=1.43E4, Re=120, Pe=83.6, Bo=40.65
Implicit Parameters: Lo=3 m, To=830 K, dTo=1072 K, Nu=88.E-6 m2/s, ko=58.E-6 m2/s
rho,o=0.42 kg/m3, alpha,o=125.E-6 m2/s, po=16 Pa, Uo=6.16 m/s
to=0.487 s, q",o=3.05E3 kW/m2, Ka=Kt=1 1/m, Ks=0 1/m, black walls

U1 EXP -4 PLANE 9

1:	2:	3:	4:	5:	6:	7:	8:	9:	10:	11:	12:	13:	14:	15:	16:	17:
0	0	0	0	0	0	0	0	0	0	0	0	0	0	0	0	0
0	-66	-128	-181	-215	-218	-181	-103	0	103	181	218	215	181	128	66	0
0	-69	-131	-177	-198	-190	-150	-83	0	83	150	190	198	177	131	69	0
0	-40	-72	-90	-93	-84	-64	-35	0	35	64	84	93	90	72	40	0
0	-4	-4	0	4	4	0	-3	0	3	0	-4	-4	0	4	4	0
0	23	46	63	70	60	37	13	0	-13	-37	-60	-70	-63	-46	-23	0
0	40	76	101	108	95	63	26	0	-26	-63	-95	-108	-101	-76	-40	0
0	49	92	120	130	117	84	41	0	-41	-84	-117	-130	-120	-92	-49	0
0	53	98	129	140	130	98	52	0	-52	-98	-130	-140	-129	-98	-53	0
0	54	100	132	145	136	106	58	0	-58	-106	-136	-145	-132	-100	-54	0
0	53	99	132	146	139	109	60	0	-60	-109	-139	-146	-132	-99	-53	0
0	52	98	131	146	140	112	62	0	-62	-112	-141	-146	-131	-98	-52	0
0	50	95	128	145	141	114	64	0	-64	-114	-141	-145	-128	-95	-50	0
0	47	90	123	142	141	116	66	0	-66	-116	-141	-142	-123	-90	-47	0
0	42	80	111	131	134	114	67	0	-67	-114	-134	-131	-111	-80	-42	0
0	28	56	80	98	106	98	63	0	-63	-98	-106	-98	-80	-56	-28	0
0	0	0	0	0	0	0	0	0	0	0	0	0	0	0	0	0

U2 EXP -3 PLANE 9

1:	2:	3:	4:	5:	6:	7:	8:	9:	10:	11:	12:	13:	14:	15:	16:	17:
0	0	0	0	0	0	0	0	0	0	0	0	0	0	0	0	0
0	10	20	33	49	68	88	103	109	103	88	68	49	33	20	10	0
0	16	35	58	87	120	154	179	189	179	154	120	87	58	35	16	0
0	21	46	77	114	156	197	229	241	229	197	156	114	77	46	21	0
0	26	55	90	132	178	224	260	274	260	224	178	132	90	55	26	0
0	30	62	100	143	190	238	277	293	277	238	190	143	100	62	30	0
0	32	67	105	147	195	243	284	302	284	243	195	147	105	67	32	0
0	34	69	106	148	193	240	283	303	283	240	193	148	106	69	34	0
0	35	69	105	144	187	233	274	295	274	233	187	144	105	69	35	0
0	35	68	102	138	178	221	261	281	261	221	178	138	102	68	35	0
0	34	65	96	129	166	206	244	262	244	206	166	129	96	65	34	0
0	32	61	89	118	151	187	222	240	222	187	151	118	89	61	32	0
0	29	55	79	104	132	164	196	212	196	164	132	104	79	55	29	0
0	26	47	66	86	109	135	163	178	163	135	109	86	66	47	26	0
0	20	36	50	64	80	100	121	134	121	100	80	64	50	36	20	0
0	12	21	28	35	44	54	67	76	67	54	44	35	28	21	12	0
0	0	0	0	0	0	0	0	0	0	0	0	0	0	0	0	0

U3 EXP -4 PLANE 8 (or "-" Plane 10)

1:	2:	3:	4:	5:	6:	7:	8:	9:	10:	11:	12:	13:	14:	15:	16:	17:
0	0	0	0	0	0	0	0	0	0	0	0	0	0	0	0	0
0	-18	-30	-42	-56	-72	-87	-99	-103	-99	-87	-72	-56	-42	-30	-18	0
0	-20	-32	-43	-54	-64	-74	-80	-83	-80	-74	-64	-54	-43	-32	-20	0
0	-13	-21	-25	-28	-30	-32	-34	-36	-34	-32	-30	-28	-25	-21	-13	0
0	-5	-7	-5	-2	0	0	-2	-3	-2	0	0	-2	-5	-7	-5	0
0	1	4	10	16	20	20	16	13	16	20	20	16	10	4	1	0
0	5	12	20	27	32	33	29	25	29	33	32	27	20	12	5	0
0	8	17	25	33	39	42	42	41	42	42	39	33	25	17	8	0
0	10	20	29	37	44	49	52	52	52	49	44	37	29	20	10	0
0	11	21	30	39	47	53	57	58	57	53	47	39	30	21	11	0
0	12	22	32	40	48	54	59	60	59	54	48	40	32	22	12	0
0	12	23	32	41	49	56	60	62	60	56	49	41	32	23	12	0
0	13	24	33	41	49	56	62	64	62	56	49	41	33	24	13	0
0	14	24	32	41	49	57	63	66	63	57	49	41	32	24	14	0
0	13	22	30	37	46	56	64	67	64	56	46	37	30	22	13	0
0	11	16	21	27	35	46	57	63	57	46	35	27	21	16	11	0
0	0	0	0	0	0	0	0	0	0	0	0	0	0	0	0	0

(Cont'd)
D.1 Case 24: 3-D Fire Simulation, Fluid Ra=1.E4

TEMPERATURE EXP -3 PLANE 9

1:	2:	3:	4:	5:	6:	7:	8:	9:	10:	11:	12:	13:	14:	15:	16:	17:
187	189	193	199	207	215	223	229	231	229	223	215	207	199	193	189	187
188	189	193	200	208	218	227	234	236	234	227	218	208	200	193	189	188
188	190	195	202	212	224	237	246	250	246	237	224	212	202	195	190	188
189	191	196	205	217	232	249	263	268	263	249	232	217	205	196	191	189
190	192	198	207	221	239	261	281	290	281	261	239	221	207	198	192	190
192	193	199	209	224	246	274	305	319	305	274	246	224	209	199	193	192
193	194	200	210	226	250	286	337	375	337	286	250	226	210	200	194	193
193	195	201	212	228	254	293	370	471	370	293	254	228	212	201	195	193
194	196	202	212	229	255	297	380	488	380	297	255	229	212	202	196	194
195	197	203	213	230	256	298	381	488	381	298	256	230	213	203	197	195
195	197	203	214	231	257	299	382	489	382	299	257	231	214	203	197	195
196	198	204	214	231	257	299	382	490	382	299	257	231	214	204	198	196
196	198	204	215	232	258	300	383	490	383	300	258	232	215	204	198	196
197	199	205	215	232	259	301	384	491	384	301	259	232	215	205	199	197
197	199	205	216	233	259	302	385	492	385	302	259	233	216	205	199	197
197	199	205	216	234	260	303	386	494	386	303	260	234	216	205	199	197
197	199	206	217	234	261	304	387	495	387	304	261	234	217	206	199	197

PRESSURE EXP -3 PLANE 9

1:	2:	3:	4:	5:	6:	7:	8:	9:	10:	11:	12:	13:	14:	15:	16:	17:
101	102	103	106	109	113	116	119	120	119	116	113	109	106	103	102	101
89	89	91	93	95	98	101	103	104	103	101	98	95	93	91	89	89
76	77	77	79	80	82	84	85	86	85	84	82	80	79	77	77	76
63	63	64	64	65	66	67	68	68	68	67	66	65	64	64	63	63
50	50	50	50	50	51	51	52	52	52	51	51	50	50	50	50	50
37	37	37	36	36	36	37	37	37	37	37	36	36	36	37	37	37
24	24	24	23	23	23	23	23	23	23	23	23	23	23	24	24	24
11	11	11	10	10	10	10	10	10	10	10	10	10	10	11	11	11
-1	-1	-1	-1	-2	-2	-2	-2	-3	-2	-2	-2	-2	-1	-1	-1	-1
-13	-13	-14	-14	-14	-15	-15	-15	-15	-15	-15	-15	-14	-14	-14	-13	-13
-26	-26	-26	-26	-27	-27	-27	-28	-28	-28	-27	-27	-27	-26	-26	-26	-26
-38	-38	-38	-39	-39	-40	-40	-40	-40	-40	-40	-40	-39	-39	-38	-38	-38
-51	-51	-51	-51	-52	-52	-52	-52	-53	-52	-52	-52	-52	-51	-51	-51	-51
-63	-63	-63	-64	-64	-64	-65	-65	-65	-65	-65	-64	-64	-64	-63	-63	-63
-75	-75	-76	-76	-76	-77	-78	-78	-78	-78	-78	-77	-76	-76	-76	-75	-75
-88	-88	-88	-89	-89	-90	-91	-92	-93	-92	-91	-90	-89	-89	-88	-88	-88
-100	-100	-100	-101	-103	-105	-107	-109	-110	-109	-107	-105	-103	-101	-100	-100	-100

CONDUCTIVE FLUX EXP -5 PLANE 9

1:	2:	3:	4:	5:	6:	7:	8:	9:	10:	11:	12:	13:	14:	15:	16:	17:
-79	-9	-15	-26	-44	-72	-106	-136	-149	-136	-106	-72	-44	-26	-15	-9	-79
-44	0	0	0	0	0	0	0	0	0	0	0	0	0	0	0	-44
-48	0	0	0	0	0	0	0	0	0	0	0	0	0	0	0	-48
-53	0	0	0	0	0	0	0	0	0	0	0	0	0	0	0	-53
-56	0	0	0	0	0	0	0	0	0	0	0	0	0	0	0	-56
-58	0	0	0	0	0	0	0	0	0	0	0	0	0	0	0	-58
-60	0	0	0	0	0	0	0	0	0	0	0	0	0	0	0	-60
-60	0	0	0	0	0	0	0	0	0	0	0	0	0	0	0	-60
-61	0	0	0	0	0	0	0	0	0	0	0	0	0	0	0	-61
-61	0	0	0	0	0	0	0	0	0	0	0	0	0	0	0	-61
-61	0	0	0	0	0	0	0	0	0	0	0	0	0	0	0	-61
-61	0	0	0	0	0	0	0	0	0	0	0	0	0	0	0	-61
-61	0	0	0	0	0	0	0	0	0	0	0	0	0	0	0	-61
-62	0	0	0	0	0	0	0	0	0	0	0	0	0	0	0	-62
-62	0	0	0	0	0	0	0	0	0	0	0	0	0	0	0	-62
-63	0	0	0	0	0	0	0	0	0	0	0	0	0	0	0	-63
-85	2	4	6	9	13	18	21	21	21	18	13	9	6	4	2	-85

(Cont'd)
D.1 Case 24: 3-D Fire Simulation, Fluid Ra=1.E4

RADATIVE FLUX EXP -5 PLANE 9

1:	2:	3:	4:	5:	6:	7:	8:	9:	10:	11:	12:	13:	14:	15:	16:	17:
-1	0	0	0	0	0	0	0	0	0	0	0	0	0	0	0	-1
0	0	0	0	0	0	0	0	0	0	0	0	0	0	0	0	0
-1	0	0	0	0	0	0	0	0	0	0	0	0	0	0	0	-1
-1	0	0	0	0	0	0	0	0	0	0	0	0	0	0	0	-1
-1	0	0	0	0	0	0	0	0	0	0	0	0	0	0	0	-1
-1	0	0	0	0	0	0	0	0	0	0	0	0	0	0	0	-1
-1	0	0	0	0	0	0	0	0	0	0	0	0	0	0	0	-1
-1	0	0	0	0	0	0	0	0	0	0	0	0	0	0	0	-1
-1	0	0	0	0	0	0	0	0	0	0	0	0	0	0	0	-1
-2	0	0	0	0	0	0	0	0	0	0	0	0	0	0	0	-2
-2	0	0	0	0	0	0	0	0	0	0	0	0	0	0	0	-2
-2	0	0	0	0	0	0	0	0	0	0	0	0	0	0	0	-2
-2	0	0	0	0	0	0	0	0	0	0	0	0	0	0	0	-2
-2	0	0	0	0	0	0	0	0	0	0	0	0	0	0	0	-2
-1	0	0	0	0	0	0	0	0	0	0	0	0	0	0	0	-1
-1	0	0	0	0	0	0	0	0	0	0	0	0	0	0	0	-1
0	0	0	0	1	3	10	40	124	40	10	3	1	0	0	0	0

DIVERGENCE OF RADIATIVE FLUX EXP -4 PLANE 9

1:	2:	3:	4:	5:	6:	7:	8:	9:	10:	11:	12:	13:	14:	15:	16:	17:
0	0	0	0	0	0	0	0	0	0	0	0	0	0	0	0	0
0	0	0	0	0	0	1	1	2	1	1	0	0	0	0	0	0
0	0	0	0	0	1	2	3	4	3	2	1	0	0	0	0	0
0	0	0	0	0	2	4	6	7	6	4	2	0	0	0	0	0
0	0	0	0	1	2	5	9	11	9	5	2	1	0	0	0	0
0	0	0	0	1	3	8	15	19	15	8	3	1	0	0	0	0
0	0	0	0	1	3	10	25	43	25	10	3	1	0	0	0	0
0	0	0	0	1	4	11	40	123	40	11	4	1	0	0	0	0
0	0	0	0	1	4	12	45	144	45	12	4	1	0	0	0	0
0	0	0	0	1	3	11	46	144	46	11	3	1	0	0	0	0
0	0	0	0	0	3	11	45	145	45	11	3	0	0	0	0	0
0	0	0	0	0	3	11	45	145	45	11	3	0	0	0	0	0
0	0	0	0	0	3	10	45	145	45	10	3	0	0	0	0	0
0	0	0	0	0	2	9	44	144	44	9	2	0	0	0	0	0
0	0	0	0	0	2	8	41	141	41	8	2	0	0	0	0	0
0	0	0	0	0	1	7	36	131	36	7	1	0	0	0	0	0
0	0	0	0	0	0	0	0	0	0	0	0	0	0	0	0	0

FIRE EXP -2 PLANE 9

1:	2:	3:	4:	5:	6:	7:	8:	9:	10:	11:	12:	13:	14:	15:	16:	17:
0	0	0	0	0	0	0	0	0	0	0	0	0	0	0	0	0
0	0	0	0	0	0	0	0	0	0	0	0	0	0	0	0	0
0	0	0	0	0	0	0	0	0	0	0	0	0	0	0	0	0
0	0	0	0	0	0	0	0	0	0	0	0	0	0	0	0	0
0	0	0	0	0	0	0	0	0	0	0	0	0	0	0	0	0
0	0	0	0	0	0	0	0	0	0	0	0	0	0	0	0	0
0	0	0	0	0	0	0	0	0	0	0	0	0	0	0	0	0
0	0	0	0	0	0	0	0	0	0	0	0	0	0	0	0	0
0	0	0	0	0	0	0	0	237	0	0	0	0	0	0	0	0
0	0	0	0	0	0	0	0	237	0	0	0	0	0	0	0	0
0	0	0	0	0	0	0	0	237	0	0	0	0	0	0	0	0
0	0	0	0	0	0	0	0	237	0	0	0	0	0	0	0	0
0	0	0	0	0	0	0	0	237	0	0	0	0	0	0	0	0
0	0	0	0	0	0	0	0	237	0	0	0	0	0	0	0	0
0	0	0	0	0	0	0	0	237	0	0	0	0	0	0	0	0
0	0	0	0	0	0	0	0	237	0	0	0	0	0	0	0	0
0	0	0	0	0	0	0	0	237	0	0	0	0	0	0	0	0
0	0	0	0	0	0	0	0	237	0	0	0	0	0	0	0	0

D.2 Case 25: 3-D Fire Simulation, Fluid Ra=1.E5
Implicit Fire Parameters: Ra=3.1E10, Gr=4.43E10, Re=2.1E5, Pe=1.47E5
BC's: No slip; Adiabatic Walls
Explicit Parameters: Ra=1.E5, Pr=0.7, Ar=1.0, Gr=1.43E5, Re=378, Pe=265, Bo=40.65
Implicit Parameters: Lo=3 m, To=830 K, dTo=1072 K, Nu=88.E-6 m2/s, ko=58.E-6 m2/s
rho,o=0.42 kg/m3, alpha,o=125.E-6 m2/s, po=16 Pa, Uo=6.16 m/s
to=0.487 s, q",o=3.05E3 kW/m2, Ka=Kt=1 1/m, Ks=0 1/m, black walls

U1 EXP -4 PLANE 9

1:	2:	3:	4:	5:	6:	7:	8:	9:	10:	11:	12:	13:	14:	15:	16:	17:
0	0	0	0	0	0	0	0	0	0	0	0	0	0	0	0	0
0	-80	-160	-221	-195	108	723	744	0	-744	-723	-108	195	221	160	80	0
0	-31	-32	49	264	475	-54	-597	0	597	54	-475	-264	-49	32	31	0
0	41	111	226	323	182	129	342	0	-342	-129	-182	-323	-226	-111	-41	0
0	78	164	247	270	251	135	-141	0	141	-135	-251	-270	-247	-164	-78	0
0	83	163	223	247	224	188	228	0	-228	-188	-224	-247	-223	-163	-83	0
0	77	148	202	233	238	188	19	0	-19	-188	-238	-233	-202	-148	-77	0
0	70	135	189	224	228	201	177	0	-177	-201	-228	-224	-189	-135	-70	0
0	65	127	180	218	230	199	84	0	-84	-199	-230	-218	-180	-127	-65	0
0	63	123	175	215	230	208	152	0	-152	-208	-230	-215	-175	-123	-63	0
0	61	121	174	215	234	212	119	0	-119	-212	-234	-215	-174	-121	-61	0
0	62	122	177	220	241	222	149	0	-149	-222	-241	-220	-177	-122	-62	0
0	65	128	185	229	252	233	145	0	-145	-233	-252	-229	-185	-128	-65	0
0	71	139	199	245	268	251	165	0	-165	-251	-268	-245	-199	-139	-71	0
0	77	150	213	261	287	271	179	0	-179	-272	-287	-261	-213	-150	-77	0
0	67	131	189	238	271	274	196	0	-196	-274	-271	-238	-189	-131	-67	0
0	0	0	0	0	0	0	0	0	0	0	0	0	0	0	0	0

U2 EXP -3 PLANE 9

1:	2:	3:	4:	5:	6:	7:	8:	9:	10:	11:	12:	13:	14:	15:	16:	17:
0	0	0	0	0	0	0	0	0	0	0	0	0	0	0	0	0
0	-6	-4	8	51	164	407	747	919	747	407	164	51	8	-4	-6	0
0	-7	0	28	98	239	452	604	644	603	452	239	98	28	0	-7	0
0	-3	10	51	131	259	410	580	684	580	410	259	131	51	10	-3	0
0	2	22	66	141	249	403	581	666	581	403	249	141	66	22	2	0
0	7	29	73	142	243	385	562	671	562	385	243	142	73	29	7	0
0	10	33	75	139	234	372	548	650	548	372	234	139	75	33	10	0
0	11	35	74	135	224	352	522	633	522	352	224	135	74	35	11	0
0	12	35	72	129	212	334	495	596	495	334	212	129	72	35	12	0
0	11	33	68	121	198	311	463	565	463	311	198	121	68	33	11	0
0	11	30	63	111	181	286	429	523	429	286	181	111	63	30	11	0
0	9	27	55	99	162	257	389	479	389	257	162	99	55	27	9	0
0	7	22	47	84	140	223	343	425	343	223	140	84	47	22	7	0
0	4	16	36	66	112	182	286	360	286	182	112	66	36	16	4	0
0	2	9	23	45	79	132	215	277	215	132	79	45	23	9	2	0
0	0	4	11	23	40	70	120	163	120	70	40	23	11	4	0	0
0	0	0	0	0	0	0	0	0	0	0	0	0	0	0	0	0

U3 EXP -4 PLANE 8 (or "-" Plane 10)

1:	2:	3:	4:	5:	6:	7:	8:	9:	10:	11:	12:	13:	14:	15:	16:	17:
0	0	0	0	0	0	0	0	0	0	0	0	0	0	0	0	0
0	-27	-41	-55	-62	-11	211	569	744	569	211	-11	-62	-55	-41	-27	0
0	-22	-28	-15	33	130	94	-314	-597	-314	94	130	33	-15	-28	-22	0
0	-9	-4	20	61	73	41	183	342	183	41	73	61	20	-4	-9	0
0	0	11	32	58	78	91	-16	-141	-16	91	78	58	32	11	0	0
0	6	17	35	55	73	83	149	228	149	83	73	55	35	17	6	0
0	8	19	35	54	75	97	72	19	72	97	75	54	35	19	8	0
0	8	20	35	53	73	93	133	177	133	93	73	53	35	20	8	0
0	8	20	35	53	74	97	101	84	101	97	74	53	35	20	8	0
0	9	21	35	54	75	98	128	152	128	98	75	54	35	21	9	0
0	10	23	38	56	78	102	119	119	119	102	78	56	38	23	10	0
0	13	27	42	60	82	107	133	149	133	107	82	60	42	27	13	0
0	17	32	48	66	87	112	136	145	136	112	87	66	48	32	17	0
0	22	40	56	73	94	120	150	165	150	120	94	73	56	40	22	0
0	28	46	61	78	99	128	162	179	162	128	99	78	61	46	28	0
0	26	40	53	67	89	123	169	196	169	123	89	67	53	40	26	0
0	0	0	0	0	0	0	0	0	0	0	0	0	0	0	0	0

(cont'd)
D.2 Case 25: 3-D Fire Simulation, Fluid Ra=1.E5

TEMPERATURE EXP -3 PLANE 9

1:	2:	3:	4:	5:	6:	7:	8:	9:	10:	11:	12:	13:	14:	15:	16:	17:
67	69	76	87	105	138	197	287	340	287	197	138	105	87	76	69	67
67	69	75	85	102	134	204	318	381	318	204	134	102	85	75	69	67
65	66	71	79	93	129	219	339	396	339	219	129	93	79	71	66	65
62	63	66	73	89	131	217	351	437	351	217	131	89	73	66	63	62
59	59	63	70	88	130	222	381	482	381	222	130	88	70	63	59	59
56	57	60	69	88	129	221	402	549	402	221	129	88	69	60	57	56
53	55	59	68	88	129	220	435	659	435	220	129	88	68	59	55	53
52	53	57	67	87	130	217	446	785	446	217	130	87	67	57	53	52
50	52	56	67	87	130	218	445	760	445	218	130	87	67	56	52	50
49	51	56	66	87	130	218	447	775	447	218	130	87	66	56	51	49
48	50	55	66	87	130	219	448	770	448	219	130	87	66	55	50	48
48	49	55	66	88	131	220	449	775	449	220	131	88	66	55	49	48
47	49	55	66	88	132	222	452	777	452	222	132	88	66	55	49	47
47	49	55	67	89	134	224	456	783	456	224	134	89	67	55	49	47
47	49	55	68	91	137	229	463	791	463	229	137	91	68	55	49	47
48	50	56	69	95	143	239	475	804	475	239	143	95	69	56	50	48
48	50	57	71	98	149	250	489	819	489	250	149	98	71	57	50	48

PRESSURE EXP -3 PLANE 9

1:	2:	3:	4:	5:	6:	7:	8:	9:	10:	11:	12:	13:	14:	15:	16:	17:
31	32	33	37	44	60	105	208	277	208	105	60	44	37	33	32	31
27	27	28	30	33	38	26	-45	-105	-45	26	38	33	30	28	27	27
22	22	22	23	23	20	13	21	38	21	13	20	23	23	22	22	22
18	18	17	17	16	14	16	24	24	24	16	14	16	17	17	18	18
13	13	13	12	11	11	12	12	14	12	12	11	11	12	13	13	13
9	9	9	8	8	8	8	10	10	10	8	8	8	8	9	9	9
5	5	5	5	4	4	4	4	5	4	4	4	4	5	5	5	5
2	2	1	1	1	1	0	1	1	1	0	1	1	1	1	2	2
-1	-1	-1	-1	-1	-2	-2	-2	-2	-2	-2	-2	-1	-1	-1	-1	-1
-4	-4	-4	-4	-5	-5	-5	-5	-5	-5	-5	-5	-5	-4	-4	-4	-4
-8	-8	-8	-8	-8	-8	-8	-8	-8	-8	-8	-8	-8	-8	-8	-8	-8
-11	-11	-11	-11	-11	-11	-11	-11	-11	-11	-11	-11	-11	-11	-11	-11	-11
-14	-14	-14	-14	-14	-14	-14	-14	-14	-14	-14	-14	-14	-14	-14	-14	-14
-17	-17	-17	-17	-18	-18	-18	-17	-17	-17	-18	-18	-18	-17	-17	-17	-17
-20	-20	-21	-21	-21	-22	-22	-22	-22	-22	-22	-22	-21	-21	-21	-20	-20
-24	-24	-24	-25	-26	-27	-29	-30	-30	-30	-29	-27	-26	-25	-24	-24	-24
-27	-27	-28	-29	-32	-35	-41	-50	-57	-50	-41	-35	-32	-29	-28	-27	-27

CONDUCTIVE FLUX EXP -5 PLANE 9

1:	2:	3:	4:	5:	6:	7:	8:	9:	10:	11:	12:	13:	14:	15:	16:	17:
-13	7	11	20	31	26	-58	-165	-195	-165	-58	26	31	20	11	7	-13
-19	0	0	0	0	0	0	0	0	0	0	0	0	0	0	0	-19
-15	0	0	0	0	0	0	0	0	0	0	0	0	0	0	0	-15
-11	0	0	0	0	0	0	0	0	0	0	0	0	0	0	0	-11
-10	0	0	0	0	0	0	0	0	0	0	0	0	0	0	0	-10
-11	0	0	0	0	0	0	0	0	0	0	0	0	0	0	0	-11
-12	0	0	0	0	0	0	0	0	0	0	0	0	0	0	0	-12
-13	0	0	0	0	0	0	0	0	0	0	0	0	0	0	0	-13
-15	0	0	0	0	0	0	0	0	0	0	0	0	0	0	0	-15
-15	0	0	0	0	0	0	0	0	0	0	0	0	0	0	0	-15
-16	0	0	0	0	0	0	0	0	0	0	0	0	0	0	0	-16
-17	0	0	0	0	0	0	0	0	0	0	0	0	0	0	0	-17
-17	0	0	0	0	0	0	0	0	0	0	0	0	0	0	0	-17
-18	0	0	0	0	0	0	0	0	0	0	0	0	0	0	0	-18
-19	0	0	0	0	0	0	0	0	0	0	0	0	0	0	0	-19
-21	0	0	0	0	0	0	0	0	0	0	0	0	0	0	0	-21
-26	1	4	9	19	36	63	81	89	81	63	36	19	9	4	1	-26

(cont'd)

D.2 Case 26: 3-D Fire Simulation, Fluid Ra=1.E6, t*=5.33 (t=2.6 s)

RADIATIVE FLUX EXP -4 PLANE 9

1:	2:	3:	4:	5:	6:	7:	8:	9:	10:	11:	12:	13:	14:	15:	16:	17:
0	0	0	0	0	0	0	1	2	1	0	0	0	0	0	0	0
0	0	0	0	0	0	0	0	0	0	0	0	0	0	0	0	0
0	0	0	0	0	0	0	0	0	0	0	0	0	0	0	0	0
0	0	0	0	0	0	0	0	0	0	0	0	0	0	0	0	0
0	0	0	0	0	0	0	0	0	0	0	0	0	0	0	0	0
0	0	0	0	0	0	0	0	0	0	0	0	0	0	0	0	0
0	0	0	0	0	0	0	0	0	0	0	0	0	0	0	0	0
0	0	0	0	0	0	0	0	0	0	0	0	0	0	0	0	0
0	0	0	0	0	0	0	0	0	0	0	0	0	0	0	0	0
0	0	0	0	0	0	0	0	0	0	0	0	0	0	0	0	0
0	0	0	0	0	0	0	0	0	0	0	0	0	0	0	0	0
0	0	0	0	0	0	0	0	0	0	0	0	0	0	0	0	0
0	0	0	0	0	0	0	0	0	0	0	0	0	0	0	0	0
0	0	0	0	0	0	0	0	0	0	0	0	0	0	0	0	0
0	0	0	0	0	0	0	0	0	0	0	0	0	0	0	0	0
0	0	0	0	0	0	0	0	0	0	0	0	0	0	0	0	0
0	0	0	0	0	0	0	11	107	11	0	0	0	0	0	0	0

DIVERGENCE OF RADIATIVE FLUX EXP -3 PLANE 9

1:	2:	3:	4:	5:	6:	7:	8:	9:	10:	11:	12:	13:	14:	15:	16:	17:
0	0	0	0	0	0	0	0	0	0	0	0	0	0	0	0	0
0	0	0	0	0	0	0	2	5	2	0	0	0	0	0	0	0
0	0	0	0	0	0	0	3	6	3	0	0	0	0	0	0	0
0	0	0	0	0	0	0	3	9	3	0	0	0	0	0	0	0
0	0	0	0	0	0	0	5	14	5	0	0	0	0	0	0	0
0	0	0	0	0	0	0	6	25	6	0	0	0	0	0	0	0
0	0	0	0	0	0	0	9	54	9	0	0	0	0	0	0	0
0	0	0	0	0	0	0	9	110	9	0	0	0	0	0	0	0
0	0	0	0	0	0	0	9	96	9	0	0	0	0	0	0	0
0	0	0	0	0	0	0	9	104	9	0	0	0	0	0	0	0
0	0	0	0	0	0	0	9	101	9	0	0	0	0	0	0	0
0	0	0	0	0	0	0	9	103	9	0	0	0	0	0	0	0
0	0	0	0	0	0	0	9	104	9	0	0	0	0	0	0	0
0	0	0	0	0	-1	-1	9	107	9	-1	-1	0	0	0	0	0
0	0	0	0	0	-1	-1	8	109	8	-1	-1	0	0	0	0	0
0	0	0	0	0	0	-1	7	108	7	-1	0	0	0	0	0	0
0	0	0	0	0	0	0	0	0	0	0	0	0	0	0	0	0

FIRE EXP -2 PLANE 9

1:	2:	3:	4:	5:	6:	7:	8:	9:	10:	11:	12:	13:	14:	15:	16:	17:
0	0	0	0	0	0	0	0	0	0	0	0	0	0	0	0	0
0	0	0	0	0	0	0	0	0	0	0	0	0	0	0	0	0
0	0	0	0	0	0	0	0	0	0	0	0	0	0	0	0	0
0	0	0	0	0	0	0	0	0	0	0	0	0	0	0	0	0
0	0	0	0	0	0	0	0	0	0	0	0	0	0	0	0	0
0	0	0	0	0	0	0	0	0	0	0	0	0	0	0	0	0
0	0	0	0	0	0	0	0	0	0	0	0	0	0	0	0	0
0	0	0	0	0	0	0	0	0	0	0	0	0	0	0	0	0
0	0	0	0	0	0	0	0	237	0	0	0	0	0	0	0	0
0	0	0	0	0	0	0	0	237	0	0	0	0	0	0	0	0
0	0	0	0	0	0	0	0	237	0	0	0	0	0	0	0	0
0	0	0	0	0	0	0	0	237	0	0	0	0	0	0	0	0
0	0	0	0	0	0	0	0	237	0	0	0	0	0	0	0	0
0	0	0	0	0	0	0	0	237	0	0	0	0	0	0	0	0
0	0	0	0	0	0	0	0	237	0	0	0	0	0	0	0	0
0	0	0	0	0	0	0	0	237	0	0	0	0	0	0	0	0
0	0	0	0	0	0	0	0	237	0	0	0	0	0	0	0	0
0	0	0	0	0	0	0	0	237	0	0	0	0	0	0	0	0

D.3 Case 26: 3-D Fire Simulation, Fluid Ra=1.E6, t*=5.33 (t=2.6 s)
Implicit Fire Parameters: Ra=3.1E10, Gr=4.43E10, Re=2.1E5, Pe=1.47E5
BC's: No slip; Adiabatic Walls
Explicit Parameters: Ra=1.E6, Pr=0.7, Ar=1.0, Gr=1.43E6, Re=1195, Pe=837, Bo=40.65
Implicit Parameters: Lo=3 m, To=830 K, dTo=1072 K, Nu=88.E-6 m2/s, ko=58.E-6 m2/s
rho,o=0.42 kg/m3, alpha,o=125.E-6 m2/s, po=16 Pa, Uo=6.16 m/s
to=0.487 s, q",o=3.05E3 kW/m2, Ka=Kt=1 1/m, Ks=0 1/m, black walls

U1 EXP -2 PLANE 9

1:	2:	3:	4:	5:	6:	7:	8:	9:	10:	11:	12:	13:	14:	15:	16:	17:
0	0	0	0	0	0	0	0	0	0	0	0	0	0	0	0	0
0	-12	-79	-149	-111	-58	2	-52	0	52	-2	58	111	149	79	12	0
0	2	-54	-156	-136	-122	-39	-31	0	31	39	122	136	156	54	-2	0
0	3	16	32	-138	-100	-39	-17	0	17	39	100	138	-32	-16	-3	0
0	4	4	-12	-26	-37	11	15	0	-15	-11	37	26	12	-4	-4	0
0	1	2	2	0	-20	-52	-39	0	39	52	20	0	-2	-2	-1	0
0	0	1	0	3	-14	15	35	0	-35	-15	14	-3	0	-1	0	0
0	0	1	2	1	5	-52	-39	0	39	52	-5	-1	-2	-1	0	0
0	0	1	1	5	0	13	34	0	-34	-13	0	-5	-1	-1	0	0
0	0	1	2	3	1	2	-23	0	23	-2	-1	-3	-2	-1	0	0
0	0	1	1	1	6	-10	12	0	-12	10	-6	-1	-1	-1	0	0
0	0	1	1	2	-1	7	-1	0	1	-7	1	-2	-1	-1	0	0
0	0	1	1	1	3	1	2	0	-2	-1	-3	-1	-1	-1	0	0
0	0	1	1	2	3	0	1	0	-1	0	-3	-2	-1	-1	0	0
0	0	1	2	2	2	4	5	0	-5	-4	-2	-2	-2	-1	0	0
0	0	1	2	3	4	4	1	0	-1	-4	-4	-3	-2	-1	0	0
0	0	0	0	0	0	0	0	0	0	0	0	0	0	0	0	0

U2 EXP -2 PLANE 9

1:	2:	3:	4:	5:	6:	7:	8:	9:	10:	11:	12:	13:	14:	15:	16:	17:
0	0	0	0	0	0	0	0	0	0	0	0	0	0	0	0	0
0	-6	64	172	200	227	290	361	342	361	290	227	200	172	64	-6	0
0	-9	6	-10	13	27	-6	-34	-38	-34	-6	27	13	-10	6	-9	0
0	-8	-5	28	-31	-71	-71	-80	95	-80	-71	-71	-31	28	-5	-8	0
0	-4	0	4	-14	-25	12	130	154	130	12	-25	-14	4	0	-4	0
0	-2	-2	-1	-2	45	49	-5	38	-5	49	45	-2	-1	-2	-2	0
0	-2	-3	-4	-5	-3	16	62	141	62	16	-3	-5	-4	-3	-2	0
0	-2	-3	-3	-7	12	63	76	76	76	63	12	-7	-3	-3	-2	0
0	-1	-3	-3	-4	4	-11	14	86	14	-11	4	-4	-3	-3	-1	0
0	-1	-2	-2	0	1	20	89	96	89	20	1	0	-2	-2	-1	0
0	-1	-2	-2	-1	0	18	15	66	15	18	0	-1	-2	-2	-1	0
0	-1	-1	-1	-1	2	0	53	79	53	0	2	-1	-1	-1	-1	0
0	-1	-1	-1	-1	-1	11	32	62	32	11	-1	-1	-1	-1	-1	0
0	-1	-1	-1	-1	0	4	30	56	30	4	0	-1	-1	-1	-1	0
0	0	-1	-1	-1	-1	0	21	44	21	0	-1	-1	-1	-1	0	0
0	0	0	0	-1	-2	0	15	31	15	0	-2	-1	0	0	0	0
0	0	0	0	0	0	0	0	0	0	0	0	0	0	0	0	0

U3 EXP -2 PLANE 8 (or "-" Plane 10)

1:	2:	3:	4:	5:	6:	7:	8:	9:	10:	11:	12:	13:	14:	15:	16:	17:
0	0	0	0	0	0	0	0	0	0	0	0	0	0	0	0	0
0	0	-13	-28	-24	-21	-25	-16	-52	-16	-25	-21	-24	-28	-13	0	0
0	0	-5	-18	-15	-19	-24	-26	-31	-26	-24	-19	-15	-18	-5	0	0
0	0	2	5	-34	-44	-69	-72	-17	-72	-69	-44	-34	5	2	0	0
0	0	1	0	-5	-13	-3	13	15	13	-3	-13	-5	0	1	0	0
0	0	0	0	0	-6	-16	-33	-39	-33	-16	-6	0	0	0	0	0
0	0	0	0	0	0	-4	24	35	24	-4	0	0	0	0	0	0
0	0	0	0	0	1	-15	-31	-39	-31	-15	1	0	0	0	0	0
0	0	0	0	1	2	4	14	34	14	4	2	1	0	0	0	0
0	0	0	0	0	0	1	-7	-23	-7	1	0	0	0	0	0	0
0	0	0	0	0	1	0	-1	12	-1	0	1	0	0	0	0	0
0	0	0	0	0	0	0	3	-1	3	0	0	0	0	0	0	0
0	0	0	0	0	0	2	0	2	0	2	0	0	0	0	0	0
0	0	0	0	0	1	0	1	1	1	0	1	0	0	0	0	0
0	0	0	0	0	0	1	4	5	4	1	0	0	0	0	0	0
0	0	0	0	0	1	1	1	1	1	1	1	0	0	0	0	0
0	0	0	0	0	0	0	0	0	0	0	0	0	0	0	0	0

(Cont'd)
D.3 Case 26: 3-D Fire Simulation, Fluid Ra=1.E6, t*=5.33 (t=2.6 s)

TEMPERATURE EXP -2 PLANE 9

1:	2:	3:	4:	5:	6:	7:	8:	9:	10:	11:	12:	13:	14:	15:	16:	17:
0	2	14	31	47	47	48	61	63	61	48	47	47	31	14	2	0
0	9	32	53	51	46	48	66	59	66	48	46	51	53	32	9	0
1	6	20	48	44	45	54	65	58	65	54	45	44	48	20	6	1
0	2	5	-2	70	57	26	48	74	48	26	57	70	-2	5	2	0
0	0	2	1	10	35	32	47	94	47	32	35	10	1	2	0	0
0	0	0	0	0	19	44	65	88	65	44	19	0	0	0	0	0
0	0	0	0	0	5	17	37	113	37	17	5	0	0	0	0	0
0	0	0	0	0	8	36	65	123	65	36	8	0	0	0	0	0
0	0	0	0	0	2	-16	16	113	16	-16	2	0	0	0	0	0
0	0	0	0	0	1	14	73	124	73	14	1	0	0	0	0	0
0	0	0	0	0	1	5	12	107	12	5	1	0	0	0	0	0
0	0	0	0	0	2	2	62	129	62	2	2	0	0	0	0	0
0	0	0	0	1	1	7	28	104	28	7	1	1	0	0	0	0
0	0	0	0	0	1	4	47	129	47	4	1	0	0	0	0	0
0	0	0	0	0	1	3	32	113	32	3	1	0	0	0	0	0
0	0	0	0	0	1	2	49	144	50	2	1	0	0	0	0	0
0	0	0	0	0	1	7	58	150	58	7	1	0	0	0	0	0

PRESSURE EXP -2 PLANE 9

1:	2:	3:	4:	5:	6:	7:	8:	9:	10:	11:	12:	13:	14:	15:	16:	17:
32	38	60	57	9	-10	34	83	49	83	34	-10	9	57	60	38	32
28	33	11	-125	-202	-293	-403	-522	-547	-522	-403	-293	-202	-125	11	33	28
20	18	7	-35	-24	-16	39	68	81	68	39	-16	-24	-35	7	18	20
12	11	4	13	-47	-27	0	20	45	20	0	-27	-47	13	4	11	12
8	7	8	6	1	-4	8	-20	-39	-20	8	-4	1	6	8	7	8
6	6	5	4	1	-5	-5	16	31	16	-5	-5	1	4	5	6	6
5	5	4	3	1	1	8	-3	-23	-3	8	1	1	3	4	5	5
4	4	4	3	1	0	-10	-14	-5	-14	-10	0	1	3	4	4	4
4	4	3	3	2	0	3	16	11	16	3	0	2	3	3	4	4
3	3	3	3	2	2	1	-11	-15	-11	1	2	2	3	3	3	3
3	3	3	3	2	2	1	11	16	11	1	2	2	3	3	3	3
3	3	3	3	3	2	3	0	-1	0	3	2	3	3	3	3	3
3	3	3	3	3	3	2	3	4	3	2	3	3	3	3	3	3
3	3	3	3	3	3	3	3	3	3	3	3	3	3	3	3	3
3	3	3	3	3	3	3	3	3	3	3	3	3	3	3	3	3
3	3	3	3	3	3	3	3	2	3	3	3	3	3	3	3	3
3	3	3	3	3	2	2	1	0	1	2	2	3	3	3	3	3

CONDUCTIVE FLUX EXP -5 PLANE 9

1:	2:	3:	4:	5:	6:	7:	8:	9:	10:	11:	12:	13:	14:	15:	16:	17:
-181	-77	-35	-120	-183	-56	97	-8	-18	-8	97	-56	-183	-120	-35	-77	-181
-155	0	0	0	0	0	0	0	0	0	0	0	0	0	0	0	-155
-113	0	0	0	0	0	0	0	0	0	0	0	0	0	0	0	-113
-56	0	0	0	0	0	0	0	0	0	0	0	0	0	0	0	-56
-9	0	0	0	0	0	0	0	0	0	0	0	0	0	0	0	-9
0	0	0	0	0	0	0	0	0	0	0	0	0	0	0	0	0
0	0	0	0	0	0	0	0	0	0	0	0	0	0	0	0	0
-1	0	0	0	0	0	0	0	0	0	0	0	0	0	0	0	-1
-1	0	0	0	0	0	0	0	0	0	0	0	0	0	0	0	-1
-1	0	0	0	0	0	0	0	0	0	0	0	0	0	0	0	-1
-1	0	0	0	0	0	0	0	0	0	0	0	0	0	0	0	-1
-2	0	0	0	0	0	0	0	0	0	0	0	0	0	0	0	-2
-2	0	0	0	0	0	0	0	0	0	0	0	0	0	0	0	-2
-2	0	0	0	0	0	0	0	0	0	0	0	0	0	0	0	-2
-1	0	0	0	0	0	0	0	0	0	0	0	0	0	0	0	-1
-1	0	0	0	0	0	0	0	0	0	0	0	0	0	0	0	-1
-3	-1	-1	-2	-3	-5	54	233	333	233	54	-5	-3	-2	-1	-1	-3

(Cont'd)
D.3 Case 26: 3-D Fire Simulation, Fluid Ra=1.E6, t*5.33 (t=2.6 s)

RADIIATIVE FLUX EXP -3 PLANE 9

1:	2:	3:	4:	5:	6:	7:	8:	9:	10:	11:	12:	13:	14:	15:	16:	17:
0	0	0	0	0	0	1	2	3	2	1	0	0	0	0	0	0
0	0	0	0	0	0	0	0	0	0	0	0	0	0	0	0	0
0	0	0	0	0	0	0	0	0	0	0	0	0	0	0	0	0
0	0	0	0	0	0	0	0	0	0	0	0	0	0	0	0	0
0	0	0	0	0	0	0	0	0	0	0	0	0	0	0	0	0
0	0	0	0	0	0	0	0	0	0	0	0	0	0	0	0	0
0	0	0	0	0	0	0	0	0	0	0	0	0	0	0	0	0
0	0	0	0	0	0	0	0	0	0	0	0	0	0	0	0	0
0	0	0	0	0	0	0	0	0	0	0	0	0	0	0	0	0
0	0	0	0	0	0	0	0	0	0	0	0	0	0	0	0	0
0	0	0	0	0	0	0	0	0	0	0	0	0	0	0	0	0
0	0	0	0	0	0	0	0	0	0	0	0	0	0	0	0	0
0	0	0	0	0	0	0	0	0	0	0	0	0	0	0	0	0
0	0	0	0	0	0	0	0	0	0	0	0	0	0	0	0	0
0	0	0	0	0	0	0	0	0	0	0	0	0	0	0	0	0
0	0	0	0	0	0	0	0	0	0	0	0	0	0	0	0	0
0	0	0	0	0	0	0	1	134	1	0	0	0	0	0	0	0

DIVERGENCE OF RADIATIVE FLUX EXP -2 PLANE 9

1:	2:	3:	4:	5:	6:	7:	8:	9:	10:	11:	12:	13:	14:	15:	16:	17:
0	0	0	0	0	0	0	0	0	0	0	0	0	0	0	0	0
0	0	0	0	1	1	0	1	4	1	0	1	1	0	0	0	0
0	0	0	0	0	0	0	2	4	2	0	0	0	0	0	0	0
0	0	0	0	0	6	0	0	9	0	0	6	0	0	0	0	0
0	0	0	0	0	0	0	0	19	0	0	0	0	0	0	0	0
0	0	0	0	0	0	0	1	21	1	0	0	0	0	0	0	0
0	0	0	0	0	0	0	0	47	0	0	0	0	0	0	0	0
0	0	0	0	0	0	0	2	62	2	0	0	0	0	0	0	0
0	0	0	0	0	0	0	-1	52	-1	0	0	0	0	0	0	0
0	0	0	0	0	0	0	5	67	5	0	0	0	0	0	0	0
0	0	0	0	0	0	0	-1	43	-1	0	0	0	0	0	0	0
0	0	0	0	0	0	0	2	81	2	0	0	0	0	0	0	0
0	0	0	0	0	0	0	-1	38	-1	0	0	0	0	0	0	0
0	0	0	0	0	0	-1	0	76	0	-1	0	0	0	0	0	0
0	0	0	0	0	0	-1	-2	47	-2	-1	0	0	0	0	0	0
0	0	0	0	0	0	-1	-4	100	-4	-1	0	0	0	0	0	0
0	0	0	0	0	0	0	0	0	0	0	0	0	0	0	0	0

FIRE EXP -2 PLANE 9

1:	2:	3:	4:	5:	6:	7:	8:	9:	10:	11:	12:	13:	14:	15:	16:	17:
0	0	0	0	0	0	0	0	0	0	0	0	0	0	0	0	0
0	0	0	0	0	0	0	0	0	0	0	0	0	0	0	0	0
0	0	0	0	0	0	0	0	0	0	0	0	0	0	0	0	0
0	0	0	0	0	0	0	0	0	0	0	0	0	0	0	0	0
0	0	0	0	0	0	0	0	0	0	0	0	0	0	0	0	0
0	0	0	0	0	0	0	0	0	0	0	0	0	0	0	0	0
0	0	0	0	0	0	0	0	0	0	0	0	0	0	0	0	0
0	0	0	0	0	0	0	0	237	0	0	0	0	0	0	0	0
0	0	0	0	0	0	0	0	237	0	0	0	0	0	0	0	0
0	0	0	0	0	0	0	0	237	0	0	0	0	0	0	0	0
0	0	0	0	0	0	0	0	237	0	0	0	0	0	0	0	0
0	0	0	0	0	0	0	0	237	0	0	0	0	0	0	0	0
0	0	0	0	0	0	0	0	237	0	0	0	0	0	0	0	0
0	0	0	0	0	0	0	0	237	0	0	0	0	0	0	0	0
0	0	0	0	0	0	0	0	237	0	0	0	0	0	0	0	0
0	0	0	0	0	0	0	0	237	0	0	0	0	0	0	0	0
0	0	0	0	0	0	0	0	237	0	0	0	0	0	0	0	0

D.4 Case 27: 3-D Fire Simulation, Fluid Ra=1.E5, Non-Uniform Grid
Implicit Fire Parameters: Ra=3.1E10, Gr=4.43E10, Re=2.1E5, Pe=1.47E5
BC's: No slip; Adiabatic Walls
Explicit Parameters: Ra=1.E5, Pr=0.7, Ar=1.0, Gr=1.43E5, Re=378, Pe=265, Bo=40.65
Implicit Parameters: Lo=3 m, To=830 K, dTo=1072 K, Nu=88.E-6 m2/s, ko=58.E-6 m2/s
rho,o=0.42 kg/m3, alpha,o=125.E-6 m2/s, po=16 Pa, Uo=6.16 m/s
to=0.487 s, q",o=3.05E3 kW/m2, Ka=Kt=1 1/m, Ks=0 1/m, black walls

U1 EXP -4 PLANE 9

1:	2:	3:	4:	5:	6:	7:	8:	9:	10:	11:	12:	13:	14:	15:	16:	17:
0	0	0	0	0	0	0	0	0	0	0	0	0	0	0	0	0
0	-98	-182	-224	-184	-86	-6	16	1	-17	8	94	191	221	175	92	0
0	-55	-45	52	168	191	126	52	4	-49	-129	-194	-159	-42	46	51	0
0	27	106	197	221	182	128	68	5	-64	-129	-185	-222	-190	-99	-27	0
0	80	165	220	235	219	168	90	5	-85	-168	-219	-232	-215	-158	-76	0
0	96	171	210	207	159	90	36	4	-30	-90	-162	-206	-205	-165	-91	0
0	95	161	189	178	136	83	35	5	-29	-81	-137	-177	-185	-154	-89	0
0	88	148	172	164	134	94	48	5	-42	-91	-133	-161	-167	-141	-83	0
0	82	137	161	158	132	92	47	5	-40	-89	-130	-154	-156	-131	-77	0
0	78	131	156	154	129	89	46	5	-39	-86	-126	-150	-150	-124	-73	0
0	76	129	155	154	132	94	49	5	-42	-90	-128	-150	-148	-121	-70	0
0	75	129	157	158	137	98	52	5	-45	-95	-134	-153	-150	-121	-70	0
0	77	132	161	164	143	103	54	5	-47	-100	-140	-159	-154	-124	-71	0
0	79	136	167	170	150	109	57	5	-52	-107	-148	-166	-160	-128	-74	0
0	79	136	168	174	157	117	62	5	-58	-116	-155	-170	-161	-129	-74	0
0	64	111	141	153	147	119	68	3	-66	-119	-146	-149	-135	-105	-59	0
0	0	0	0	0	0	0	0	0	0	0	0	0	0	0	0	0

U2 EXP -3 PLANE 9

1:	2:	3:	4:	5:	6:	7:	8:	9:	10:	11:	12:	13:	14:	15:	16:	17:
0	0	0	0	0	0	0	0	0	0	0	0	0	0	0	0	0
0	-3	6	32	85	161	241	296	314	296	237	153	78	29	5	-2	0
0	-2	17	64	136	218	286	326	338	326	283	211	128	58	16	-2	0
0	2	32	88	160	233	294	333	346	334	291	227	152	82	30	2	0
0	9	44	100	168	241	308	354	369	354	305	234	161	94	41	9	0
0	14	51	105	170	242	308	354	369	354	304	235	163	99	48	14	0
0	18	54	105	167	232	294	340	357	340	290	226	160	100	52	17	0
0	20	55	103	159	220	280	327	348	327	276	214	153	98	52	19	0
0	20	53	98	151	209	266	312	331	311	262	203	145	94	51	20	0
0	20	51	92	141	195	248	292	311	292	245	189	135	88	49	19	0
0	18	47	84	129	178	229	270	289	270	225	173	124	81	45	18	0
0	16	42	75	115	160	207	246	264	246	203	156	111	72	40	16	0
0	14	36	65	99	139	181	218	234	217	178	135	95	62	34	13	0
0	10	28	52	80	113	150	183	198	182	147	110	77	49	27	10	0
0	7	19	36	57	82	111	138	152	138	108	79	54	34	18	7	0
0	3	10	19	30	44	61	79	90	79	59	42	28	18	9	3	0
0	0	0	0	0	0	0	0	0	0	0	0	0	0	0	0	0

(Cont'd)
D.4 Case 27: 3-D Fire Simulation, Fluid Ra=1.E5, Non-Uniform Grid

U3 EXP -4 PLANE 8

1:	2:	3:	4:	5:	6:	7:	8:	9:	10:	11:	12:	13:	14:	15:	16:	17:
0	0	0	0	0	0	0	0	0	0	0	0	0	0	0	0	0
0	-16	-27	-38	-43	-31	-9	9	16	9	-11	-34	-44	-38	-26	-16	0
0	-15	-15	-1	27	53	60	55	52	55	60	51	23	-4	-16	-15	0
0	-7	1	21	40	52	59	65	68	66	59	50	38	18	0	-7	0
0	0	11	27	45	63	78	87	90	87	77	61	42	25	9	0	0
0	4	15	29	42	48	46	39	36	39	46	48	40	27	13	3	0
0	6	16	28	37	42	42	38	35	38	42	42	36	26	15	6	0
0	7	17	27	35	41	45	48	48	48	45	41	34	26	16	7	0
0	8	17	27	34	41	45	47	47	47	45	40	34	26	17	8	0
0	9	18	27	34	40	44	46	46	46	44	40	34	26	17	8	0
0	10	19	28	35	41	46	48	49	48	46	41	35	27	19	9	0
0	11	21	29	36	43	48	51	52	51	48	43	36	28	20	11	0
0	13	22	31	38	45	50	53	54	53	50	44	37	30	22	13	0
0	15	24	32	39	46	52	56	58	56	52	46	39	31	24	15	0
0	16	24	31	39	48	55	60	62	60	55	47	38	31	24	16	0
0	13	19	25	33	43	54	64	68	64	54	42	32	25	19	13	0
0	0	0	0	0	0	0	0	0	0	0	0	0	0	0	0	0

U3 EXP -4 PLANE 9

1:	2:	3:	4:	5:	6:	7:	8:	9:	10:	11:	12:	13:	14:	15:	16:	17:
0	0	0	0	0	0	0	0	0	0	0	0	0	0	0	0	0
0	-2	-3	-4	-4	-2	0	0	1	0	0	-2	-4	-4	-3	-2	0
0	-3	-3	-2	0	2	4	4	4	4	3	2	0	-3	-3	-3	0
0	-2	-2	-1	1	3	4	5	5	5	4	2	0	-1	-2	-2	0
0	-2	-1	0	2	4	5	5	5	5	5	3	1	0	-1	-2	0
0	-1	0	1	2	4	4	4	4	4	4	3	2	0	0	-1	0
0	0	0	1	3	4	4	5	5	5	4	4	3	1	0	0	0
0	0	1	2	3	4	5	5	5	5	5	4	3	2	0	0	0
0	0	1	3	4	5	5	5	5	5	5	5	4	3	1	0	0
0	1	2	3	4	5	5	5	5	5	5	5	4	3	2	1	0
0	1	3	4	5	5	5	5	5	5	5	5	5	4	3	1	0
0	2	3	4	5	5	5	5	5	5	5	5	5	4	3	2	0
0	2	4	4	5	5	5	5	5	5	5	5	5	4	3	2	0
0	2	4	4	5	5	5	5	5	5	5	5	5	4	4	2	0
0	2	3	4	4	4	5	5	5	5	5	4	4	4	3	2	0
0	2	2	3	3	3	3	3	3	3	3	3	3	3	2	2	0
0	0	0	0	0	0	0	0	0	0	0	0	0	0	0	0	0

U3 EXP -4 PLANE 10

1:	2:	3:	4:	5:	6:	7:	8:	9:	10:	11:	12:	13:	14:	15:	16:	17:
0	0	0	0	0	0	0	0	0	0	0	0	0	0	0	0	0
0	13	22	33	38	27	7	-10	-17	-10	9	30	38	33	21	13	0
0	10	9	-4	-31	-54	-58	-52	-49	-52	-59	-52	-27	-1	10	10	0
0	1	-7	-26	-42	-51	-56	-62	-64	-62	-56	-50	-40	-23	-6	2	0
0	-4	-15	-30	-44	-60	-74	-83	-85	-83	-73	-58	-42	-28	-14	-4	0
0	-7	-18	-29	-40	-45	-41	-34	-30	-34	-42	-44	-38	-28	-16	-7	0
0	-8	-18	-27	-34	-37	-36	-32	-29	-32	-36	-37	-33	-26	-17	-8	0
0	-8	-16	-24	-30	-35	-39	-41	-42	-41	-39	-35	-30	-23	-16	-8	0
0	-8	-15	-22	-29	-34	-38	-40	-40	-40	-38	-34	-28	-22	-15	-7	0
0	-8	-15	-21	-28	-33	-36	-38	-39	-39	-37	-33	-27	-21	-14	-7	0
0	-8	-15	-21	-28	-34	-38	-41	-42	-41	-38	-33	-27	-21	-14	-7	0
0	-8	-15	-22	-29	-35	-40	-44	-45	-44	-40	-35	-28	-22	-15	-8	0
0	-9	-16	-23	-30	-37	-43	-46	-47	-46	-43	-37	-30	-23	-16	-9	0
0	-11	-18	-25	-32	-40	-46	-50	-52	-51	-46	-39	-32	-24	-18	-10	0
0	-12	-19	-25	-33	-42	-50	-56	-58	-56	-50	-41	-33	-25	-18	-12	0
0	-10	-15	-21	-29	-40	-52	-62	-66	-62	-51	-39	-28	-21	-15	-10	0
0	0	0	0	0	0	0	0	0	0	0	0	0	0	0	0	0

(cont'd)
D.4 Case 27: 3-D Fire Simulation, Fluid Ra=1.E5, Non-Uniform Grid

TEMPERATURE EXP -3 PLANE 9

1:	2:	3:	4:	5:	6:	7:	8:	9:	10:	11:	12:	13:	14:	15:	16:	17:
31	34	41	51	64	78	91	99	102	99	90	77	63	50	41	34	32
31	34	41	51	64	81	98	110	115	110	97	79	62	50	40	34	31
30	33	39	48	62	84	107	123	129	123	105	81	60	47	38	33	31
29	31	36	46	63	88	116	136	143	136	114	85	60	44	36	31	29
28	29	34	45	64	92	126	153	163	153	124	89	61	44	34	30	28
26	28	34	45	65	96	138	175	189	175	134	92	62	44	33	28	27
26	27	33	45	65	98	146	208	244	207	142	93	63	44	33	28	26
25	27	33	45	66	98	148	240	348	237	142	94	63	44	33	27	25
24	26	33	45	66	98	147	236	340	234	142	94	63	44	33	27	25
24	26	33	45	66	99	148	238	343	236	143	94	64	44	33	26	24
24	26	33	46	66	99	148	238	342	235	143	95	64	44	33	26	24
24	26	33	46	67	99	148	239	343	236	143	95	64	45	33	26	24
24	26	33	46	67	100	149	239	344	236	144	95	65	45	33	26	24
24	26	34	47	68	101	150	240	345	237	145	96	65	45	33	27	24
24	27	34	48	70	102	152	242	347	239	146	98	67	46	34	27	24
24	27	35	49	72	105	155	245	349	242	149	100	68	48	34	27	25
24	27	35	50	73	107	158	248	352	245	152	102	70	49	35	27	25

PRESSURE EXP -3 PLANE 9

1:	2:	3:	4:	5:	6:	7:	8:	9:	10:	11:	12:	13:	14:	15:	16:	17:
155	162	183	224	293	393	506	594	626	594	500	382	284	220	182	163	156
134	139	153	178	211	233	231	216	208	216	233	233	208	176	153	140	135
111	113	117	122	125	130	140	153	158	153	140	130	126	122	118	114	112
88	88	86	83	81	83	87	92	94	92	87	83	82	84	87	89	89
66	65	62	57	52	44	32	21	17	21	33	45	53	59	63	66	67
46	45	42	37	30	22	14	10	8	10	15	23	32	38	42	45	47
27	26	23	19	15	12	13	18	21	18	13	12	16	20	24	27	28
10	9	6	3	0	0	-1	-1	-1	-1	-1	0	1	4	7	9	10
-6	-7	-9	-11	-14	-16	-17	-18	-18	-18	-17	-15	-13	-11	-9	-7	-6
-23	-24	-25	-27	-29	-30	-30	-30	-30	-30	-30	-29	-28	-27	-25	-23	-23
-39	-39	-41	-42	-44	-44	-44	-44	-44	-44	-44	-44	-43	-42	-41	-40	-39
-55	-55	-56	-58	-59	-59	-60	-60	-60	-60	-60	-59	-59	-58	-57	-55	-55
-71	-71	-72	-73	-74	-75	-75	-75	-76	-76	-75	-75	-74	-74	-72	-71	-71
-86	-87	-88	-90	-91	-92	-93	-93	-93	-93	-93	-92	-91	-90	-89	-87	-87
-102	-103	-106	-109	-111	-114	-115	-116	-116	-116	-115	-114	-112	-109	-106	-104	-103
-118	-120	-125	-132	-139	-146	-151	-153	-154	-154	-151	-145	-139	-132	-126	-121	-119
-133	-137	-147	-161	-178	-200	-224	-248	-261	-248	-222	-197	-176	-160	-147	-138	-135

CONDUCTIVE FLUX EXP -6 PLANE 9

1:	2:	3:	4:	5:	6:	7:	8:	9:	10:	11:	12:	13:	14:	15:	16:	17:
-222	37	65	90	45	-147	-447	-694	-783	-695	-427	-121	56	88	62	37	-202
-157	0	0	0	0	0	0	0	0	0	0	0	0	0	0	0	-151
-136	0	0	0	0	0	0	0	0	0	0	0	0	0	0	0	-130
-114	0	0	0	0	0	0	0	0	0	0	0	0	0	0	0	-109
-107	0	0	0	0	0	0	0	0	0	0	0	0	0	0	0	-102
-112	0	0	0	0	0	0	0	0	0	0	0	0	0	0	0	-107
-121	0	0	0	0	0	0	0	0	0	0	0	0	0	0	0	-116
-130	0	0	0	0	0	0	0	0	0	0	0	0	0	0	0	-125
-137	0	0	0	0	0	0	0	0	0	0	0	0	0	0	0	-132
-142	0	0	0	0	0	0	0	0	0	0	0	0	0	0	0	-137
-147	0	0	0	0	0	0	0	0	0	0	0	0	0	0	0	-141
-150	0	0	0	0	0	0	0	0	0	0	0	0	0	0	0	-144
-154	0	0	0	0	0	0	0	0	0	0	0	0	0	0	0	-148
-159	0	0	0	0	0	0	0	0	0	0	0	0	0	0	0	-152
-166	0	0	0	0	0	0	0	0	0	0	0	0	0	0	0	-159
-176	0	0	0	0	0	0	0	0	0	0	0	0	0	0	0	-168
-299	13	35	68	108	149	184	183	162	174	175	140	100	62	31	12	-276

D.5 Case 28: 3-D Fire Simulation, Fluid Ra=1.E6, Non-Uniform Grid, t*=16.4
Implicit Fire Parameters: Ra=3.1E10, Gr=4.43E10, Re=2.1E5, Pe=1.47E5
BC's: No slip; Adiabatic Walls
Explicit Parameters: Ra=1.E6, Pr=0.7, Ar=1.0, Gr=1.43E6, Re=1195, Pe=837, Bo=40.65
Implicit Parameters: Lo=3 m, To=830 K, dTo=1072 K, Nu=88.E-6 m2/s, ko=58.E-6 m2/s
rho,o=0.42 kg/m3, alpha,o=125.E-6 m2/s, po=16 Pa, Uo=6.16 m/s
to=0.487 s, q",o=3.05E3 kW/m2, Ka=Kt=1 1/m, Ks=0 1/m, black walls

U1 EXP -2 PLANE 9

1:	2:	3:	4:	5:	6:	7:	8:	9:	10:	11:	12:	13:	14:	15:	16:	17:
0	0	0	0	0	0	0	0	0	0	0	0	0	0	0	0	0
0	121	22	-66	21	-24	14	-8	0	10	-17	26	-12	43	-49	-172	0
0	-70	-12	11	-6	20	0	-10	1	11	-1	-27	26	-36	51	112	0
0	-170	-37	-117	93	-43	-4	6	2	-9	8	44	-110	119	8	163	0
0	-133	-47	-104	-89	-43	13	6	2	0	-3	34	86	93	50	138	0
0	-90	-120	-73	-113	-20	-3	19	0	-14	11	46	99	102	89	118	0
0	-1	54	37	38	14	-23	-18	4	25	21	-29	-23	-52	-43	0	0
0	-12	-127	-75	-59	-37	-24	0	-7	0	43	34	66	74	133	29	0
0	12	16	23	22	32	43	-16	6	10	-64	-19	-28	-17	-16	-13	0
0	6	12	-20	-38	-65	-74	-33	-1	35	79	61	37	12	-11	-6	0
0	5	4	19	18	41	60	45	0	-50	-60	-36	-18	-16	-3	-5	0
0	3	6	-8	-30	-14	6	20	-2	-24	-1	15	30	6	-6	-3	0
0	2	4	2	1	-6	55	-1	1	-2	-50	9	5	-4	-4	-2	0
0	2	5	4	6	-63	-68	-42	3	42	70	53	-16	-3	-5	-2	0
0	2	2	13	-5	29	-10	-14	0	17	-12	-25	0	-11	-3	-2	0
0	1	4	2	-4	-20	0	5	0	-6	6	20	3	-3	-4	-1	0
0	0	0	0	0	0	0	0	0	0	0	0	0	0	0	0	0

U2 EXP -2 PLANE 9

1:	2:	3:	4:	5:	6:	7:	8:	9:	10:	11:	12:	13:	14:	15:	16:	17:
0	0	0	0	0	0	0	0	0	0	0	0	0	0	0	0	0
0	-26	337	363	361	339	304	293	294	295	307	364	357	358	315	-101	0
0	103	6	-9	18	37	6	41	44	42	4	47	14	-15	45	129	0
0	-33	-57	-6	-106	-219	-61	117	84	119	-58	-285	-69	-26	-63	-47	0
0	28	-34	57	-2	139	64	59	54	55	69	100	-14	71	-32	32	0
0	-10	-65	-96	-139	-121	-92	-10	-25	2	-117	-122	-146	-120	-71	-15	0
0	-14	9	138	154	110	126	193	195	188	113	120	160	130	19	-13	0
0	-1	24	-22	14	44	22	3	10	1	25	40	10	-22	21	3	0
0	-13	-12	3	19	27	22	38	63	28	25	26	15	0	-9	-15	0
0	-6	-6	18	41	54	56	53	50	54	52	51	37	17	-6	-6	0
0	-4	-3	0	5	8	8	9	11	9	11	9	6	0	-3	-4	0
0	-2	-3	3	13	15	24	15	6	16	25	15	12	2	-4	-2	0
0	-2	-3	-2	-4	24	31	10	7	12	45	12	-5	-3	-3	-2	0
0	-1	-2	-3	-8	62	30	45	36	38	40	53	-14	-1	-3	-1	0
0	-1	-1	-3	9	8	27	12	19	18	23	11	5	-2	-1	-1	0
0	0	0	1	8	15	2	2	-1	1	4	15	7	0	0	0	0
0	0	0	0	0	0	0	0	0	0	0	0	0	0	0	0	0

(Cont'd)

D.5 Case 28: 3-D Fire Simulation, Fluid Ra=1.E6, Non-Uniform Grid, t*=16.4, (t=8 s)

U3 EXP -2 PLANE 8

1:	2:	3:	4:	5:	6:	7:	8:	9:	10:	11:	12:	13:	14:	15:	16:	17:
0	0	0	0	0	0	0	0	0	0	0	0	0	0	0	0	0
0	8	-19	1	0	11	11	-10	-8	-9	17	11	2	4	-21	11	0
0	0	-32	-2	-1	30	3	-12	-10	-11	9	28	-3	-3	-28	3	0
0	-8	-13	-2	28	17	1	7	6	7	4	38	11	-2	-17	-3	0
0	-10	-14	-17	-41	-48	-23	0	6	2	-19	-61	-24	-7	-15	-10	0
0	-2	-7	-19	-53	-27	9	14	19	10	8	-27	-54	-18	-11	0	0
0	0	4	17	40	41	-16	-21	-18	-20	-9	43	43	20	4	0	0
0	-1	-15	-26	-31	-23	-16	-8	0	-15	-22	-20	-34	-27	-16	-3	0
0	0	0	6	20	17	31	2	-16	16	28	9	22	4	0	0	0
0	0	1	-3	-16	-20	-36	-39	-33	-45	-34	-17	-14	-1	0	0	0
0	0	0	1	9	9	21	37	45	35	12	7	8	0	0	0	0
0	0	1	-1	-5	-4	-1	13	20	15	0	-4	-4	0	0	0	0
0	0	0	0	0	-1	26	18	0	21	12	-2	0	0	0	0	0
0	0	1	0	4	-12	-23	-48	-42	-45	-20	-9	6	0	1	0	0
0	0	0	2	3	2	-9	-16	-14	-17	-4	2	3	2	0	0	0
0	0	0	1	-2	-2	0	1	5	1	-1	-1	-1	1	0	0	0
0	0	0	0	0	0	0	0	0	0	0	0	0	0	0	0	0

U3 EXP -2 PLANE 9

1:	2:	3:	4:	5:	6:	7:	8:	9:	10:	11:	12:	13:	14:	15:	16:	17:
0	0	0	0	0	0	0	0	0	0	0	0	0	0	0	0	0
0	0	-2	1	0	0	0	0	0	0	0	1	-1	-1	0	0	0
0	-1	-1	0	1	0	0	1	1	1	0	2	1	0	0	0	0
0	0	2	0	1	-3	0	1	2	1	0	-3	4	0	1	0	0
0	0	-1	0	-2	0	-1	1	2	2	-1	1	-3	0	0	0	0
0	0	0	0	-1	0	1	0	0	0	1	0	-2	0	0	1	0
0	-1	1	2	5	4	4	5	4	5	4	5	6	2	1	0	0
0	0	0	-2	-1	0	1	-4	-7	-3	1	-1	-2	-2	0	0	0
0	0	0	0	1	1	-4	3	6	2	-2	2	1	0	0	0	0
0	0	0	0	0	0	1	0	-1	0	0	-1	0	0	0	0	0
0	0	0	0	0	0	-2	-2	0	-1	0	0	0	0	0	0	0
0	0	0	0	0	0	0	0	-2	0	0	0	0	0	0	0	0
0	0	0	0	0	0	-1	-1	1	0	0	0	0	0	0	0	0
0	0	0	0	0	0	0	2	3	1	0	0	0	0	0	0	0
0	0	0	0	0	0	-1	0	0	0	0	0	0	0	0	0	0
0	0	0	0	0	0	0	0	0	0	0	0	0	0	0	0	0
0	0	0	0	0	0	0	0	0	0	0	0	0	0	0	0	0

U3 EXP -2 PLANE 10

1:	2:	3:	4:	5:	6:	7:	8:	9:	10:	11:	12:	13:	14:	15:	16:	17:
0	0	0	0	0	0	0	0	0	0	0	0	0	0	0	0	0
0	-10	18	1	0	-9	-11	9	10	7	-13	-12	0	-1	23	-12	0
0	0	27	5	0	-24	-4	12	11	9	-4	-25	4	3	26	-2	0
0	5	15	1	-30	-3	1	-9	-9	-10	-2	-9	-22	2	21	2	0
0	10	12	11	37	38	24	6	0	2	24	39	22	1	15	10	0
0	5	7	11	49	30	-1	-7	-14	-3	1	30	46	10	9	3	0
0	-1	-2	-11	-38	-42	16	28	25	27	9	-43	-39	-15	-2	-2	0
0	0	14	21	30	21	15	7	0	12	21	18	31	22	15	2	0
0	-1	0	-6	-19	-16	-33	-12	10	-22	-28	-7	-21	-4	-1	-1	0
0	0	-1	2	16	18	33	41	35	45	30	15	14	0	-1	-1	0
0	0	-1	-1	-11	-10	-24	-43	-50	-39	-14	-8	-9	0	-1	0	0
0	0	-1	0	5	4	1	-15	-24	-15	-1	3	3	0	-1	0	0
0	0	-1	0	0	1	-24	-20	-2	-22	-12	2	0	0	-1	0	0
0	0	-1	0	-4	13	22	50	42	45	18	9	-6	0	-1	0	0
0	0	0	-2	-3	-4	7	20	17	19	2	-2	-3	-2	0	0	0
0	0	-1	-1	1	2	0	-3	-6	-3	1	1	0	-1	0	0	0
0	0	0	0	0	0	0	0	0	0	0	0	0	0	0	0	0

(cont'd)

D.5 Case 28: 3-D Fire Simulation, Fluid Ra=1.E6, Non-Uniform Grid, t*=16.4, (t=8 s)

TEMPERATURE EXP -2 PLANE 9

1:	2:	3:	4:	5:	6:	7:	8:	9:	10:	11:	12:	13:	14:	15:	16:	17:
21	36	43	49	44	45	50	50	50	49	50	43	45	51	38	38	21
23	25	43	50	43	44	49	49	50	48	48	43	43	52	40	18	26
22	41	44	49	43	44	49	49	50	48	48	43	43	51	43	44	23
35	55	49	46	38	45	46	47	48	46	46	45	38	46	47	52	37
30	47	31	49	38	48	45	47	52	48	43	49	38	40	33	45	33
4	55	41	42	57	38	44	54	69	57	39	49	47	49	29	57	22
2	6	20	21	12	21	43	69	85	67	40	9	18	17	22	13	2
-3	15	46	24	45	28	32	61	85	52	32	23	42	29	47	22	-4
0	1	2	3	-1	3	31	85	97	76	10	6	-3	4	2	2	0
0	1	0	14	24	35	46	50	77	42	46	28	21	13	0	1	0
0	0	2	-1	2	-5	-8	24	72	17	-10	0	1	0	2	0	0
0	0	0	7	27	38	44	55	87	50	43	31	24	6	0	0	0
0	0	0	2	6	47	26	66	100	62	32	45	8	2	0	0	0
0	0	1	-1	15	80	75	75	96	74	82	69	2	1	0	0	0
0	0	0	0	12	9	100	112	133	121	68	-4	10	0	1	0	0
0	0	0	1	17	36	27	58	87	53	29	37	14	0	0	0	0
0	0	0	2	11	24	42	65	102	66	41	20	9	1	0	0	0

PRESSURE EXP -2 PLANE 9

1:	2:	3:	4:	5:	6:	7:	8:	9:	10:	11:	12:	13:	14:	15:	16:	17:
7	50	19	14	41	25	39	54	58	54	40	22	43	14	33	51	-10
20	-54	-265	-286	-282	-270	-236	-230	-236	-230	-237	-272	-283	-275	-269	-57	3
11	-25	6	59	49	55	38	26	28	27	41	57	48	56	12	-25	0
23	-24	12	36	47	34	-2	-13	-15	-13	0	39	48	28	20	-29	21
15	0	5	16	9	25	37	41	43	42	38	26	11	15	6	-5	16
11	12	-8	9	-4	12	28	37	36	37	20	4	-17	5	-7	8	13
10	8	2	-39	-41	-50	-68	-89	-94	-91	-66	-49	-38	-34	2	8	11
7	8	0	7	11	0	0	10	16	8	-2	1	9	10	-2	10	8
6	4	1	2	2	5	1	-9	-15	-8	2	5	3	3	1	5	6
5	4	3	3	0	-3	-6	-5	-3	-5	-5	-2	0	4	4	4	5
4	4	4	3	3	5	8	9	9	9	8	5	4	4	4	4	5
4	4	4	4	5	5	6	5	6	5	6	5	5	4	4	4	4
4	4	4	4	5	7	3	0	-1	0	4	8	5	4	4	4	4
4	4	4	4	4	3	-4	-9	-14	-7	-3	3	4	4	4	4	4
4	4	4	4	3	3	6	8	9	8	5	2	3	4	4	4	4
4	4	4	4	4	4	3	3	3	3	3	4	4	4	4	4	4
4	4	4	4	3	3	3	2	2	2	3	3	3	4	4	4	4

CONDUCTIVE FLUX EXP -5 PLANE 9

1:	2:	3:	4:	5:	6:	7:	8:	9:	10:	11:	12:	13:	14:	15:	16:	17:
-370	125	93	-43	26	14	6	32	26	36	6	19	21	-26	127	114	-210
-127	0	0	0	0	0	0	0	0	0	0	0	0	0	0	0	-68
-109	0	0	0	0	0	0	0	0	0	0	0	0	0	0	0	-82
-162	0	0	0	0	0	0	0	0	0	0	0	0	0	0	0	-142
-144	0	0	0	0	0	0	0	0	0	0	0	0	0	0	0	-122
-398	0	0	0	0	0	0	0	0	0	0	0	0	0	0	0	-281
-51	0	0	0	0	0	0	0	0	0	0	0	0	0	0	0	-100
-249	0	0	0	0	0	0	0	0	0	0	0	0	0	0	0	-305
-6	0	0	0	0	0	0	0	0	0	0	0	0	0	0	0	-9
-6	0	0	0	0	0	0	0	0	0	0	0	0	0	0	0	-5
-9	0	0	0	0	0	0	0	0	0	0	0	0	0	0	0	-8
-2	0	0	0	0	0	0	0	0	0	0	0	0	0	0	0	-3
-2	0	0	0	0	0	0	0	0	0	0	0	0	0	0	0	-2
-3	0	0	0	0	0	0	0	0	0	0	0	0	0	0	0	-2
-3	0	0	0	0	0	0	0	0	0	0	0	0	0	0	0	-3
-2	0	0	0	0	0	0	0	0	0	0	0	0	0	0	0	-2
-8	-1	-6	20	-46	8	-276	-229	-55	-247	-117	35	-35	20	-7	0	-8

(cont'd)

D.5 Case 28: 3-D Fire Simulation, Fluid Ra=1.E6, Non-Uniform Grid,

RADIATIVE FLUX EXP -4 PLANE 9

1:	2:	3:	4:	5:	6:	7:	8:	9:	10:	11:	12:	13:	14:	15:	16:	17:
-3	0	10	7	6	5	12	12	13	11	11	4	7	11	7	0	-2
-5	0	0	0	0	0	0	0	0	0	0	0	0	0	0	0	-4
-5	0	0	0	0	0	0	0	0	0	0	0	0	0	0	0	-5
-4	0	0	0	0	0	0	0	0	0	0	0	0	0	0	0	-4
-5	0	0	0	0	0	0	0	0	0	0	0	0	0	0	0	-5
-5	0	0	0	0	0	0	0	0	0	0	0	0	0	0	0	-5
-5	0	0	0	0	0	0	0	0	0	0	0	0	0	0	0	-5
-4	0	0	0	0	0	0	0	0	0	0	0	0	0	0	0	-4
-4	0	0	0	0	0	0	0	0	0	0	0	0	0	0	0	-4
-4	0	0	0	0	0	0	0	0	0	0	0	0	0	0	0	-3
-3	0	0	0	0	0	0	0	0	0	0	0	0	0	0	0	-3
-4	0	0	0	0	0	0	0	0	0	0	0	0	0	0	0	-3
-4	0	0	0	0	0	0	0	0	0	0	0	0	0	0	0	-3
-3	0	0	0	0	0	0	0	0	0	0	0	0	0	0	0	-3
-3	0	0	0	0	0	0	0	0	0	0	0	0	0	0	0	-3
-3	0	0	0	0	0	0	0	0	0	0	0	0	0	0	0	-3
-3	-2	-2	-4	-6	-9	-7	26	274	29	-6	-8	-5	-3	-2	-2	-3

DIVERGENCE OF RADIATIVE FLUX EXP -3 PLANE 9

1:	2:	3:	4:	5:	6:	7:	8:	9:	10:	11:	12:	13:	14:	15:	16:	17:
0	0	0	0	0	0	0	0	0	0	0	0	0	0	0	0	0
0	-1	5	7	4	3	10	8	9	7	9	2	4	11	1	-3	0
0	-3	5	10	4	3	11	9	11	8	10	2	4	14	1	-2	0
0	16	9	12	0	4	10	7	8	5	8	3	-1	10	7	15	0
0	11	-1	9	4	6	9	7	11	6	7	8	1	3	0	9	0
0	9	12	-1	22	-1	1	12	47	15	0	1	9	2	0	24	0
0	-3	-3	-2	-4	-4	3	48	136	50	0	-5	-4	-3	-3	-3	0
0	-2	12	-2	2	-1	-4	21	130	8	-4	-4	3	-1	13	-2	0
0	-2	-2	-3	-4	-5	-1	138	186	103	-6	-4	-4	-3	-2	-2	0
0	-2	-2	-3	-3	-1	5	20	136	2	4	-3	-3	-3	-2	-2	0
0	-2	-2	-3	-4	-5	-7	0	142	-4	-6	-5	-4	-3	-2	-2	0
0	-2	-2	-3	-3	-2	5	12	112	8	2	-4	-3	-3	-2	-2	0
0	-2	-2	-3	-5	-2	-9	43	265	23	-8	-2	-5	-3	-2	-1	0
0	-1	-2	-4	-6	94	26	7	122	6	64	55	-5	-3	-2	-1	0
0	-1	-2	-3	-6	-13	344	441	891	621	81	-10	-5	-3	-2	-1	0
0	-1	-2	-3	-5	-5	-18	-6	102	-16	-16	-3	-4	-2	-1	-1	0
0	0	0	0	0	0	0	0	0	0	0	0	0	0	0	0	0

FIRE EXP -2 PLANE 9

1:	2:	3:	4:	5:	6:	7:	8:	9:	10:	11:	12:	13:	14:	15:	16:	17:
0	0	0	0	0	0	0	0	0	0	0	0	0	0	0	0	0
0	0	0	0	0	0	0	0	0	0	0	0	0	0	0	0	0
0	0	0	0	0	0	0	0	0	0	0	0	0	0	0	0	0
0	0	0	0	0	0	0	0	0	0	0	0	0	0	0	0	0
0	0	0	0	0	0	0	0	0	0	0	0	0	0	0	0	0
0	0	0	0	0	0	0	0	0	0	0	0	0	0	0	0	0
0	0	0	0	0	0	0	0	0	0	0	0	0	0	0	0	0
0	0	0	0	0	0	0	0	237	0	0	0	0	0	0	0	0
0	0	0	0	0	0	0	0	237	0	0	0	0	0	0	0	0
0	0	0	0	0	0	0	0	237	0	0	0	0	0	0	0	0
0	0	0	0	0	0	0	0	237	0	0	0	0	0	0	0	0
0	0	0	0	0	0	0	0	237	0	0	0	0	0	0	0	0
0	0	0	0	0	0	0	0	237	0	0	0	0	0	0	0	0
0	0	0	0	0	0	0	0	237	0	0	0	0	0	0	0	0
0	0	0	0	0	0	0	0	237	0	0	0	0	0	0	0	0
0	0	0	0	0	0	0	0	237	0	0	0	0	0	0	0	0
0	0	0	0	0	0	0	0	237	0	0	0	0	0	0	0	0

Appendix E

A Sample of Discrete Exchange Factor Subroutine

```
cxxxxxxxxxx          view_factors                    xxxxxxxxxxxxxxxxxxxx

          subroutine view_factors

      implicit double precision (a-h,o-z)
      double precision Ka,Ks,Kt,VF_sum(5000)
      real*4 VF(5000)

      common /global_areas/ d_Area(5000)
      common /global_volumes/ d_Vol(5000)
      common /rad_properties/ emissivity(5000),Ka,Ks,Kt,omega,SBC,pi
c     common /VF_out/VF(5000,5000)
      common /VF_adjusting/ VF_coeff
      common /mesh/ m_rows_x1,m_rows_x2,m_rows_x3
      common /nodes/ number_tot_nodes,number_x1_x2_plane_nodes,
     $               number_tot_B_nodes,Node_BD(400),Node_B(2000)
      common /domain_corners/  Node_domain_corners(8)


c     The most complicated and challenging portion of the code is
c     to identify and calculate the four major different types of
c     view factors:

c     (1) dsi_dsj (dss) = both from i-th and to j-th nodes are on the
c                 boundary surfaces of the domain;
c     (2) dsi_dgj (dsg) = from i-th boundary node to j-th gas (interior)
c                 node of the domain;
c     (3) dgi_dsj (dgs) = from i-th gas node to j-th boundary node; and
c     (4) dgi_dgj (dgg) = from i-th gas node to j-th gas node

c     For non-participating media, the only set of view factors that
c     is required is dss.  And, in essence, tau=transmittance=1.0
c     because the media (gas) is "transparent".  So, when executing
c     Subroutine Gauss_Seidel, which assembles the "invisible"
c     augmented matrix for solving all the nodal radiosities
c     simultaneously and globally including both boundary and gas
c     (interior) nodes, we need to identify both i-th and j-th nodes
c     in terms of boundary or gas node and then evaluate one of the
c     above appropriate view factors.

c          Kt=extinction coefficient, 1/m
c     tau=transmittance=exp(-Kt*|distance_vector|)

      write(2,'(/" Nodal View Factor Summations:")')

      open(50,file='/usr/tmp/dhwong',form='unformatted')

      do 5500 i=1,number_tot_nodes
        VF_sum(i)=0.d0
        do 6000 j=1,number_tot_nodes

c     Assume both i-th and j-th nodes are gas nodes to begin with:
      i_type=0
      j_type=0

      do 100 n1=1,number_tot_B_Nodes
        if(i.eq.Node_B(n1))then
          i_type=1
          goto 99
        end if
100     continue
99      do 200 n1=1,number_tot_B_Nodes
```

```
          if(j.eq.Node_B(n1))then
            j_type=1
            goto 9999
          end if
200      continue

c        Look for identical i-th and j-th nodes:

9999     if(i.eq.j.and.i_type.eq.1)then   ! i-th node is a boundary node
          call self_VF(i,Fdi_dj)
          VF(j)=VF_coeff*Fdi_dj
          goto 888
         end if
         if(i.eq.j)then  ! i-th node is a gas node
          VF(j)=0.d0
          goto 888
         end if

c        Despite whether i-th and j-th nodes are boundary or gas nodes,
c        we must compute the distance vector components and
c        transmittance first:
999      call distance_vector(i,j,x1_distance_vector,
     S                    x2_distance_vector,x3_distance_vector,R,
     S                    R_square)
c        write(8,3020)x1_distance_vector,x2_distance_vector,
c     S             x3_distance_vector,R,R_square,r_length_j

         a1=-Kt*R
         tau=dexp(a1)
c         tau=1.d0

c        if the i-th node is a boundary node:
         if(i_type.eq.1) then
          call unit_normal_vector(i,x1_norm_vector_i,
     S                        x2_norm_vector_i,x3_norm_vector_i)
c         write(8,3010)i,x1_norm_vector_i,x2_norm_vector_i,
c     S              x3_norm_vector_i
          cos_theta_i=cosine_angle(x1_norm_vector_i,
     S              x2_norm_vector_i,x3_norm_vector_i,
     S              x1_distance_vector,x2_distance_vector,
     S              x3_distance_vector,R)
         end if

c        if the j-th node is a boundary node:
         if(j_type.eq.1)then
          call unit_normal_vector(j,x1_norm_vector_j,
     S                         x2_norm_vector_j,x3_norm_vector_j)
c         write(8,3010)j,x1_norm_vector_j,x2_norm_vector_j,
c     S             x2_norm_vector_j
          cos_theta_j=cosine_angle(x1_norm_vector_j,
     S              x2_norm_vector_j,x3_norm_vector_j,
     S              -x1_distance_vector,-x2_distance_vector,
     S              -x3_distance_vector,R)
         end if

c        write(8,3030)cos_theta_i,cos_theta_j,tau,dA_j

         if(i_type.eq.1.and.j_type.eq.1)   ! dss
     S    VF(j)=VF_coeff*cos_theta_i*cos_theta_j*tau*d_Area(j)
     S          /(pi*R_square)
         if(i_type.eq.1.and.j_type.eq.0)   ! dsg
     S    VF(j)=VF_coeff*cos_theta_i*Kt*tau*d_Vol(j)/(pi*R_square)
```

```
      if(i_type.eq.0.and.j_type.eq.1)   ! dgs
     $   VF(j)=VF_coeff*cos_theta_j*tau*d_Area(j)/(4.d0*pi*R_square)
      if(i_type.eq.0.and.j_type.eq.0)   ! dgg
     $   VF(j)=VF_coeff*Kt*tau*d_Vol(j)/(4.d0*pi*R_square)
888    VF_sum(i)=VF_sum(i)+VF(j)
c      write(3,'(1x,12hfrom Node_B(,i5,2h)=,i5,11h to Node_B(,
c     $          i5,2h)=,i5,6h;  VF=,d20.10)')i,Node_B(i),j,
c     $          Node_B(j),VF(j)
c      write(2,'(1x,7hNode_B(,i5,2h)=,i5,7h ; sum=,d20.10)')
c     $           i,Node_B(i),sum
c      write(3,'(1x,7hNode_B(,i5,2h)=,i5,7h ; sum=,d20.10)')
c     $           i,Node_B(i),sum
6000    continue
        sum=0.d0
        do 6500 j=1,number_tot_nodes
          VF(j)=VF(j)/VF_sum(i)
6500        sum=sum+VF(j)
        write(50) VF
c       write(50,9001) VF
9001      format(15f7.4)
        write(2,'(1x,5hNode(,i5,2h)=,5x,7h ; sum=,d20.10)')i,sum
        write(3,'(1x,5hNode(,i5,2h)=,5x,7h ; sum=,d20.10)')i,sum
5500    continue

      return
      end
```

Appendix F

AKCESS*. Model File for Ra=1.E5, 3-D Fire Simulation

```
TITLE      **** MODEL FILE ****
   3D FIRE AT RA=1.E5   NON-UNIFORM GRID
INTEGRATION FACTORS
  0.      $ INITIAL_TIME
  30.   $ FINAL_TIME
  1.E-4   $ PROBLEM_CONVERGENCE_CRITERIA
  1.0    $ MAXIMUM_CHANGE_IN_Q__(DQ)
  -0.01    $ INITIAL_TIME_STEP
  1.25       $ TIME_STEP_MULTIPLIER
  0.25    $ MAXIMUM_TIME_STEP
  1.0    $ CRITERIA_TO_RAISE_MAX_TIME_STEP
  10000       $ MAXIMUM_NUMBER_OF_STEPS
  11      $ MAXIMUM_NUMBER_OF_ITERATIONS_PER_STEP
  0.001   $ ITERATION_CONVERGENCE_CRITERIA
#  0.5      $ THETA__IMPLICITNESS_FACTOR
  0.5      $ THETA__IMPLICITNESS_FACTOR
  0.5      $ MAXIMUM_VALUE_OF_ANY_DELTA_Q
GLOBAL SCALARS
  [ 0. ]      $ HT
MATERIALS
  2  1  #  ALLOW FOR 2 MATERIALS, NO INTERPOLATION
  [   1., -1.,  0.,  0.          $ ONE,-ONE,DUM1,DUM2
#      .0011832,  0.,  0.,  0.,  0.       $ REI,RE2I,-GR,PEI,BOLTZ
#      .000836666,  0.,  0.,  0.,  0.       $ REI,RE2I,-GR,PEI,BOLTZ
#      .00836666,  0.,  0.,  0.,  0.       $ REI,RE2I,-GR,PEI,BOLTZ
      .002645,  0.,  0.,  0.,  0.       $ REI,RE2I,-GR,PEI,BOLTZ
     1.,  0.,  1.,  0.,  0.          $ CNDI,RAYLE,ARCHI,PECLET,REYTRB
     0.,  0.,  0.,  0.,  0.       $ PHIHT,PHIMM,DUM3,PBC4,PBC5
     1.,  0.,  0.,  0.,  0. ]     $ JOBC1,JOBC2,JOBC3,SGR,SQHT
   [ 0.,  0.,  0.,  0.,           $ ONE,-ONE,DUM1,DUM2
     0.,  0.,  0.,  0.,  0.       $ REI,RE2I,-GR,PEI,BOLTZ
     0.,  0.,  0.,  0.,  0.       $ CNDI,RAYLE,ARCHI,PECLET,REYTRB
     0.,  0.,  0.,  0.,  0.       $ PHIHT,PHIMM,DUM3,PBC4,PBC5
     0.,  0.,  0.,  0.,  0. ]     $ JOBC1,JOBC2,JOBC3,SGR,SQHT
PRINT
    17    17    17   # GRID SIZE    TOTAL OF    441 NODES
             1    # PRINT INTERVAL (STEPS)
         -1    17   # I WINDOW
          1    17   # J WINDOW
          1    17   # K WINDOW
#  NONE      #  VARIABLES
   U1 U2 U3 TEMP OFWL QFLX # VARIABLES
   NONE     #  VARIABLES FIRST STEP ONLY
#  X1 X2 X3  # VARIABLES FIRST STEP ONLY
(1P,3(1X,5E13.6/),1X,2E13.6)   # FORMAT
DEBUG
     NONE         # STEP NUMBER TO PRINT ALL ITERATIONS
#     1         # STEP NUMBER TO PRINT ALL ITERATIONS
     NONE          # TYPE OF DEBUG PRINT
     1           # ITERATION NUMBER
     142,1,1        # I,J,K  LOCATION, (K=0, ALL PLANES)
     ALL           # VARIABLE OR ALL
     ALL          # TERM NUMBER OR (- FOR SET NO.), OR ALL
OTHERS
  7.         T  FTHERM
  1. 1. 10. 70.0 730.0 4*0.0  T  ALC, REFLEN UREF TREF DELTEM
  0  10      T   ISCALAR(9)
     1       T   IETKJ
  8.         T   VECTOR(8)
  7*0.0      T   MULTIPLIERS - NO. OF VARIABLES
  9.         T   VECTOR(9)
  7*1.0      T   MULTIPLIERS FOR OUTPUT VARIABLES
```

```
#  0      36 T
#  1        T IPRSGD  APPLY PHI B.C.
  0      32 T ISMPHI
#1        1  T MAX NO. OF TIMES TO UPDATE SUMPHI AT EACH STEP
  5       1  T MAX NO. OF TIMES TO UPDATE SUMPHI AT EACH STEP
  0      71 T # RESET THETA AFTER FIRST TIME STEP
# 0   0   0  T ISCALR (71-80) # 1-RESET THETA
  1   1   0  T ISCALR (71-80) # 1-RESET THETA
  0  72 T $ NON-DIMENSIONALIZE INPUT, UNITS
  0  1  T ISCALR (72-73) $ 0-NO,1-YES; 0-BGU,1-SI
# 1 0  T ISCALR (72-73) $ 0-NO,1-YES; 0-BGU,1-SI
  0  74 T $ HEAT FLUX CALCULATIONS
  1    T
  0  75 T $ RADIATION CALCULATIONS
  3  T ISCALR (75) $ 0-NO; 1-YES
  0. 71 T RSCALR (71-80)
  1.25 0.8 1.0 T HRAT(MAX) HRAT(MIN) HRAT(PRS) EPS(SUMP UPDATE)
GRAPHICS  T  PLOT VARIABLE LIST
  X1 X2 X3 U1 U2 U3 TEMP PRES
THREE INTEGER  T  INTEGER PRINT FIELD
X1 X2 X3 U1 U2 U3 TEMP SPHI PRES OFWL QFLX SRAD SRCT FIRE T
#  54 55 56 1 2 3 4 7 T
BOUNDARY CONDITIONS
 WALL_NS 1 [ 289I1 1
          1711 290 15I17 307 15I17 323 1711 562
          1711 579 15I17 596 15I17 612 1711 851
          1711 868 15I17 885 15I17 901 1711 1140
          1711 1157 15I17 1174 15I17 1190 1711 1429
          1711 1446 15I17 1463 15I17 1479 1711 1718
          1711 1735 15I17 1752 15I17 1768 1711 2007
          1711 2024 15I17 2041 15I17 2057 1711 2296
          1711 2313 15I17 2330 15I17 2346 1711 2585
          1711 2602 15I17 2619 15I17 2635 1711 2874
          1711 2891 15I17 2908 15I17 2924 1711 3163
          1711 3180 15I17 3197 15I17 3213 1711 3452
          1711 3469 15I17 3486 15I17 3502 1711 3741
          1711 3758 15I17 3775 15I17 3791 1711 4030
          1711 4047 15I17 4064 15I17 4080 1711 4319
          1711 4336 15I17 4353 15I17 4369 1711 4608
          28911 4625 |
# RHFLUX  1  | 289I17  1 |
# RHFLUX  2  | 289I17  17 |
INITIAL CONDITIONS
  | 17(289*0. ) |    $ U1  1
  | 17(289*0. ) |    $ U2  2
  | 17(289*0. ) |    $ U3  3
  | 17(289*0. ) |    $ TEMP 4
  | 17(289*0.) |  $ PHI  5
  | 17(289*0.) |  $ PRES  6
  | 17(289*0.) |  $ SPHI  7
  | 17(289*0.) |  $ TAU1  8
  | 17(289*0.) |  $ TAU2  9
  | 17(289*0.) |  $ TAU3  10
  | 17(289*0.) |  $ QFLX  11
  | 17(289*0.) |  $ SRAD  12
  | 17(289*0.) |  $ SRCT  13
  | 17(289*0.) |  $ FIRE  14
  | 17(289*0.) |  $ TREF  15
  | 17(289*0.) |  $ USJN  16
  | 17(289*0.) |  $ SORC  17
# |17(1. 15*0. -1.) 17(1. 15*0. -1.) 17(1. 15*0. -1.) 17(1. 15*0. -1.)
#  17(1. 15*0. -1.) 17(1. 15*0. -1.) 17(1. 15*0. -1.) 17(1. 15*0. -1.)
```

```
#  17(1. 15*0. -1.) 17(1. 15*0. -1.) 17(1. 15*0. -1.) 17(1. 15*0. -1.)
#  17(1. 15*0. -1.) 17(1. 15*0. -1.) 17(1. 15*0. -1.) 17(1. 15*0. -1.)
#  17(1. 15*0. -1.) ]     $ OFWL   60
 [17(1. 15*2. 17. 5. 15*0. 3. 5. 15*0. 3. 5. 15*0. 3. 5. 15*0. 3.
    5. 15*0. 3.  5. 15*0. 3. 5. 15*0. 3. 5. 15*0. 3. 5. 15*0. 3.
    5. 15*0. 3.  5. 15*0. 3. 5. 15*0. 3. 5. 15*0. 3. 5. 15*0. 3.
    5. 15*0. 3.  273. 15*4.0  289.) ]   $  OFWL 60
# [ 17(1. 15*2. 17. 15(5. 15*0. 3.) 273. 15*4. 289.) ] $ OFWL 60
 [289*1. 255(2. 15*0. -2.) 289*-1.)]  $  SURF 61
 [17(289*0.0)]     $  SRFN 62
  [  17(289*0.)  ]   $  BC1   18
  [  17(289*0.)  ]   $  BC2   19
  [  17(289*0.)  ]   $  COSX  20
  [  17(289*0.)  ]   $  COSY  21
  [  17(289*0.)  ]   $  COSZ  22
  [  17(289*0.)  ]   $  TDT4  23
  [  17(289*0.)  ]   $  TDT5  24
  [  17(289*0.)  ]   $  TDT6  25
  [  17(289*1.)  ]   $  MTRL  26
  [  17(289*0.)  ]   $  DETJ  27
  [  17(289*0.)  ]   $  DETC  28
  [  17(289*0.)  ]   $  ETKJ  29
  [  17(289*0.)  ]   $  EJK2  30
  [  17(289*0.)  ]   $  EJK3  31
  [  17(289*0.)  ]   $  EJK4  32
  [  17(289*0.)  ]   $  EJK5  33
  [  17(289*0.)  ]   $  EJK6  34
  [  17(289*0.)  ]   $  EJK7  35
  [  17(289*0.)  ]   $  EJK8  36
  [  17(289*0.)  ]   $  EJK9  37
  [  17(289*0.)  ]   $  U1L   38
  [  17(289*0.)  ]   $  U2L   39
  [  17(289*0.)  ]   $  U3L   40
  [  17(289*0.)  ]   $  TEML  41
  [  17(289*0.)  ]   $  PHIL  42
  [  17(289*0.)  ]   $  PREL  43
  [  17(289*0.)  ]   $  F1    44
  [  17(289*0.)  ]   $  F2    45
  [  17(289*0.)  ]   $  F3    46
  [  17(289*0.)  ]   $  F4    47
  [  17(289*0.)  ]   $  F5    48
  [  17(289*0.)  ]   $  F6    49
  [  17(289*0.)  ]   $  G1    50
  [  17(289*0.)  ]   $  G2    51
  [  17(289*0.)  ]   $  G3    52
  [  17(289*0.)  ]   $  G4    53
  [  17(289*0.)  ]   $  G5    54
  [  17(289*0.)  ]   $  G6    55
  [289(0. 8R.85   .5  8R1.15  1. ) ]  $  X1  56
#  [289(0. 8R1.   .5  8R1.  1. ) ]  $  X1  56
  [ -17(0. 8R1. 0.5 8R1. 1.)
    -17(0. 8R1. 0.5 8R1. 1.)
    -17(0. 8R1. 0.5 8R1. 1.)
    -17(0. 8R1. 0.5 8R1. 1.)
    -17(0. 8R1. 0.5 8R1. 1.)
    -17(0. 8R1. 0.5 8R1. 1.)
    -17(0. 8R1. 0.5 8R1. 1.)
    -17(0. 8R1. 0.5 8R1. 1.)
    -17(0. 8R1. 0.5 8R1. 1.)
    -17(0. 8R1. 0.5 8R1. 1.)
    -17(0. 8R1. 0.5 8R1. 1.)
    -17(0. 8R1. 0.5 8R1. 1.)
```

```
   -17(0. 8R1. 0.5 8R1. 1.)
   -17(0. 8R1. 0.5 8R1. 1.)
   -17(0. 8R1. 0.5 8R1. 1.)
   -17(0. 8R1. 0.5 8R1. 1.)
   -17(0. 8R1. 0.5 8R1. 1.) ]  $ X2   57
  [ -289(0. 8R.85 .5  8R1.15  1.) ] $ X3   58
#  [ -289(0. 8R1. .5  8R1.  1.) ] $ X3   58
  [  17(289*1.) ]    T ONES    59
END
```

Appendix G

AKCESS*. Template File for Ra=1.E5, 3-D Fire Simulation

```
INTEGRATION FACTORS
  INITIAL_TIME
  FINAL_TIME
  PROBLEM_CONVERGENCE_CRITERIA
  MAXIMUM_CHANGE_IN_Q__(DQ)
  INITIAL_TIME_STEP
  TIME_STEP_MULTIPLIER
  MAXIMUM_TIME_STEP
  CRITERIA_TO_RAISE_MAX_TIME_STEP
  MAXIMUM_NUMBER_OF_STEPS
  MAXIMUM_NUMBER_OF_ITERATIONS_PER_STEP
  ITERATION_CONVERGENCE_CRITERIA
  THETA__IMPLICITNESS_FACTOR
  MAXIMUM_VALUE_OF_ANY_DELTA_Q

TRANSFORMATION ARRAYS
    ETKJ    1.
    DETJ    1.

BOUNDARY CONDITIONS
        U1 U2 U3 TEMP PHI PRES    # ORDER
#  FLUX    0 0 0 4 0 0     # HEAT FLUX
#  CONV    0 0 0 |-3 3| 0 0 # HEAT FLUX
  HFLUX   0 0 0 5 0 0    # FD CONVECTIVE FLUX
  RFLUX   0 0 0 6 0 0    # RADIATIVE FLUX
  RHFLUX  0 0 0 7 0 0    # CONVECTIVE+RADIATIVE FLUX
 INLT_P   0 0 0 0 0 3 # INLET
 DIRI_U   D 0 0 0 0 0 # DIRICHLET U
 DIRI_V   0 D 0 0 0 0 # DIRICHLET V
 DIRI_W   0 0 D 0 0 0 # DIRICHLET W
 WALL_NS  D D D 0 0 0 # NO SLIP WALL
 WALL_SL  [-4 4][-4 4][-4 4] 0 4 0 # SLIP WALL
 DIRI_T   0 0 0 D 0 0 # WALL TEMPERATURE
 BLANK    D D D D D D # BLANK REGION
 DIRI_P   0 0 0 0 0 D # THROUGHFLOW PRESSURE
 DIRI_PH| 0 0 0 0 D 0 # THROUGHFLOW PRESSURE

TITLE           **** TEMPLATE FILE TEMP.UVWT ****
 CONTINUITY CONSTRAINT TENSOR MATRIX A JACOBIANS (2/10/94)

RESIDUALS

 U1   1   T  EQN#, SET#, # OF TERMS --- TEMPORAL DERIV. SET (U1)
 ()()()(0;1)(C200)(-U1)
+(PHIMM)()()(1;0)(C201)(SPHI)
+(PHIMM)()()(4;0)(C202)(SPHI)
+(PHIMM)()()(7;0)(C203)(SPHI)
 U1   2   T  EQN#, SET#, # OF TERMS --- SPATIAL FIELD SET (U1)
 ()()(U1+U2+U3)(102030;0)(C3001)(U1)
+()()(U1+U2+U3)(405060;0)(C3002)(U1)
+()()(U1+U2+U3)(708090;0)(C3003)(U1)
+(PHIHT)()()(1;0)(C201)(SPHI)
+(PHIHT)()()(4;0)(C202)(SPHI)
+(PHIHT)()()(7;0)(C203)(SPHI)
+()()()(1;0)(C201)(PRES)
+()()()(4;0)(C202)(PRES)
+()()()(7;0)(C203)(PRES)
+(REI)()()(112233;-1)(C211)(U1)
+(REI)()()(445566;-1)(C222)(U1)
+(REI)()()(778899;-1)(C233)(U1)
+(REI)()()(142536;-1)(C221)(U1)
+(REI)()()(142536;-1)(C212)(U1)
```

```
+(REI)()()(172839;-1)(C231)(U1)
+(REI)()()(172839;-1)(C213)(U1)
+(REI)()()(475869;-1)(C223)(U1)
+(REI)()()(475869;-1)(C232)(U1)
 U1   4   T  EQN#, SET#,  # OF TERMS --- BOUNDARY SET (U1)
 (REI)()()(;1)(B200)(TAU1)

 U2   1   T  EQN#, SET#, # OF TERMS --- TEMPORAL DERIV. SET (U2)
 ()()()(0;1)(C200)(-U2)
+(PHIMM)()()(2;0)(C201)(SPHI)
+(PHIMM)()()(5;0)(C202)(SPHI)
+(PHIMM)()()(8;0)(C203)(SPHI)
 U2   2   T  EQN#, SET#, # OF TERMS --- SPATIAL FIELD SET (U2)
 ()()(U1+U2+U3)(102030;0)(C3001)(U2)
+()()(U1+U2+U3)(405060;0)(C3002)(U2)
+()()(U1+U2+U3)(708090;0)(C3003)(U2)
+(PHIHT)()()(2;0)(C201)(SPHI)
+(PHIHT)()()(5;0)(C202)(SPHI)
+(PHIHT)()()(8;0)(C203)(SPHI)
+()()()(2;0)(C201)(PRES)
+()()()(5;0)(C202)(PRES)
+()()()(8;0)(C203)(PRES)
+(REI)()()(112233;-1)(C211)(U2)
+(REI)()()(445566;-1)(C222)(U2)
+(REI)()()(778899;-1)(C233)(U2)
+(REI)()()(142536;-1)(C221)(U2)
+(REI)()()(142536;-1)(C212)(U2)
+(REI)()()(172839;-1)(C231)(U2)
+(REI)()()(172839;-1)(C213)(U2)
+(REI)()()(475869;-1)(C223)(U2)
+(REI)()()(475869;-1)(C232)(U2)
+(-GR,RE21)()()(;1)(C200)(TEMP)
 U2   4   T  EQN#, SET#,  # OF TERMS --- BOUNDARY SET (U2)
 (-,REI)()()(;1)(B200)(TAU2)

 U3   1   T  EQN#, SET#, # OF TERMS --- TEMPORAL DERIV. SET (U3)
 ()()()(0;1)(C200)(-U3)
+(PHIMM)()()(3;0)(C201)(SPHI)
+(PHIMM)()()(6;0)(C202)(SPHI)
+(PHIMM)()()(9;0)(C203)(SPHI)
 U3   2   T  EQN#, SET#, # OF TERMS --- SPATIAL FIELD SET (U3)
 ()()(U1+U2+U3)(102030;0)(C3001)(U3)
+()()(U1+U2+U3)(405060;0)(C3002)(U3)
+()()(U1+U2+U3)(708090;0)(C3003)(U3)
+(PHIHT)()()(3;0)(C201)(SPHI)
+(PHIHT)()()(6;0)(C202)(SPHI)
+(PHIHT)()()(9;0)(C203)(SPHI)
+()()()(3;0)(C201)(PRES)
+()()()(6;0)(C202)(PRES)
+()()()(9;0)(C203)(PRES)
+(REI)()()(112233;-1)(C211)(U3)
+(REI)()()(445566;-1)(C222)(U3)
+(REI)()()(778899;-1)(C233)(U3)
+(REI)()()(142536;-1)(C221)(U3)
+(REI)()()(142536;-1)(C212)(U3)
+(REI)()()(172839;-1)(C231)(U3)
+(REI)()()(172839;-1)(C213)(U3)
+(REI)()()(475869;-1)(C223)(U3)
+(REI)()()(475869;-1)(C232)(U3)
 U3   4   T  EQN#, SET#,  # OF TERMS --- BOUNDARY SET (U3)
 (-,REI)()()(;1)(B200)(TAU3)
```

```
 TEMP   1   T  EQN#, SET#, # OF TERMS --- TEMPORAL DERIV. SET (TEMP)
()()()(0;1)(C200)(-TEMP)
 TEMP   2   T  EQN#, SET#, # OF TERMS --- SPATIAL FIELD SET (TEMP)
()()(U1+U2+U3)(102030;0)(C3001)(TEMP)
+()()(U1+U2+U3)(405060;0)(C3002)(TEMP)
+()()(U1+U2+U3)(708090;0)(C3003)(TEMP)
+(PEI)()()(112233;-1)(C211)(TEMP)
+(PEI)()()(445566;-1)(C222)(TEMP)
+(PEI)()()(778899;-1)(C233)(TEMP)
+(PEI)()()(142536;-1)(C221)(TEMP)
+(PEI)()()(142536;-1)(C212)(TEMP)
+(PEI)()()(172839;-1)(C231)(TEMP)
+(PEI)()()(172839;-1)(C213)(TEMP)
+(PEI)()()(475869;-1)(C223)(TEMP)
+(PEI)()()(475869;-1)(C232)(TEMP)
+(-)()()(;1)(C200)(SRCT)
+(-)()()(;1)(C200)(FIRE)
# TEMP   3   T  EQN#, SET#,  # OF TERMS --- BOUNDARY SET (TEMP)
#  ()(NUSL)()(;1)(B200)(TEMP)
# +(-)(NUSL)()(;1)(B200)(TREF)
 TEMP   5   #  VARBL, SET NO.,  --- BOUNDARY SET (TEMP)
(-)()()(0;1)(B200)(QFLX)
 TEMP   6   #  VARBL, SET NO.,  --- BOUNDARY SET (TEMP)
(WONG)()()(0;1)(B200)(SRAD)
 TEMP   7   #  VARBL, SET NO.,  --- BOUNDARY SET (TEMP)
(WONG)()()(0;1)(B200)(SRAD)
+(-)()()(0;1)(B200)(QFLX)

JACOBIANS

 U1 U1   1   1   T
 ()()()(;0)(A200)(DETJ)
 U1 U1   2   1   T
+()()(U1+U2+U3)(102030;0)(A3001)()
+()()(U1)(1;0)(A3100)()
+(REI)()()(112233;-1)(A211)()
 U1 U2   2   1   T
 ()()(U1)(2;0)(A3100)()
 U1 U3   2   1   T
 ()()(U1)(3;0)(A3100)()

 U2 U1   2   1   T
 ()()(U2)(1;0)(A3100)()
 U2 U2   1   1   T
 ()()()(;0)(A200)(DETJ)
 U2 U2   2   1   T
+()()(U1+U2+U3)(102030;0)(A3001)()
+()()(U2)(2;0)(A3100)()
+(REI)()()(112233;-1)(A211)()
 U2 U3   2   1   T
 ()()(U2)(3;0)(A3100)()
 U2 TEMP   2   1   T
 (-,SGR,REI,SQHT)()()(;0)(A200)(DETJ)

 U3 U1   2   1   T
 ()()(U3)(1;0)(A3100)()
 U3 U2   2   1   T
 ()()(U3)(2;0)(A3100)()
 U3 U3   1   1   T
 ()()()(;0)(A200)(DETJ)
 U3 U3   2   1   T
 ()()(U1+U2+U3)(102030;0)(A3001)()
```

```
+()()(U3)(3;0)(A3100)()
+(REI)()()(112233;-1)(A211)()

 TEMP U1  2  1  T
 ()()(TEMP)(1;0)(A3100)()
 TEMP  U2  2  1  T
 ()()(TEMP)(2;0)(A3100)()
 TEMP  U3  2  1  T
 ()()(TEMP)(3;0)(A3100)()
 TEMP TEMP  1  1  T
 ()()()(;0)(A200)(DETJ)
 TEMP TEMP  2  1  T
+()()(U1+U2+U3)(102030;0)(A3001)()
+(PEI)()()(112233;-1)(A211)()
#TEMP TEMP  3  1  T
# ()(NUSL)()(;0)(A200)(DETJ)

 U1 U1  1   2  T
 ()()()(;0)(A200)(DETJ)
 U1 U1  2   2  T
+()()(U1+U2+U3)(405060;0)(A3001)()
+()()(U1)(4;0)(A3100)()
+(REI)()()(445566;-1)(A211)()
 U1 U2  2   2  T
 ()()(U1)(5;0)(A3100)()
 U1 U3  2   2  T
 ()()(U1)(6;0)(A3100)()

 U2 U1  2  2  T
 ()()(U2)(4;0)(A3100)()
 U2 U2  1  2  T
 ()()()(;0)(A200)(DETJ)
 U2 U2  2  2  T
+()()(U1+U2+U3)(405060;0)(A3001)()
+()()(U2)(5;0)(A3100)()
+(REI)()()(445566;-1)(A211)()
 U2 U3  2  2  T
 ()()(U3)(6;0)(A3100)()
 U2 TEMP  2  2  T
 (SGR,REI,SQHT)()()(;0)(A200)(DETJ)

 U3 U1  2  2  T
 ()()(U3)(4;0)(A3100)()
 U3 U2  2  2  T
 ()()(U3)(5;0)(A3100)()
 U3 U3  1  2  T
 ()()()(;0)(A200)(DETJ)
 U3 U3  2  2  T
 ()()(U1+U2+U3)(405060;0)(A3001)()
+()()(U3)(6;0)(A3100)()
+(REI)()()(445566;-1)(A211)()

 TEMP  U1  2  2  T
 ()()(TEMP)(4;0)(A3100)()
 TEMP  U2  2  2  T
 ()()(TEMP)(5;0)(A3100)()
 TEMP  U3  2  2  T
 ()()(TEMP)(6;0)(A3100)()
 TEMP TEMP  1  2  T
 ()()()(;0)(A200)(DETJ)
 TEMP TEMP  2  2  T
 ()()(U1+U2+U3)(405060;0)(A3001)()
```

```
+(PEI)()()(445566;-1)(A211)()
# TEMP TEMP  3  2  T
# ()(NUSL)()(;0)(A200)(DETJ)

 U1 U1  1  3  T
 ()()()(;0)(A200)(DETJ)
 U1 U1  2  3  T
 ()()(U1+U2+U3)(708090;0)(A3001)()
+()()(U1)(7;0)(A3100)()
+(REI)()()(778899;-1)(A211)()
 U1 U2  2  3  T
 ()()(U1)(8;0)(A3100)()
 U1 U3  2  3  T
 ()()(U1)(9;0)(A3100)()

 U2 U1  2  3  T
 ()()(U2)(7;0)(A3100)()
 U2 U2  1  3  T
 ()()()(;0)(A200)(DETJ)
 U2 U2  2  3  T
 ()()(U1+U2+U3)(708090;0)(A3001)()
+()()(U2)(8;0)(A3100)()
+(REI)()()(778899;-1)(A211)()
 U2 U3  2  3  T
 ()()(U2)(9;0)(A3100)()
 U2 TEMP  2  3  T
 (-,SGR,REI,SQHT)()()(;0)(A200)(DETJ)

 U3 U1  2  3  T
 ()()(U3)(7;0)(A3100)()
 U3 U2  2  3  T
 ()()(U3)(8;0)(A3100)()
 U3 U3  1  3  T
 ()()()(;0)(A200)(DETJ)
 U3 U3  2  3  T
 ()()(U1+U2+U3)(708090;0)(A3001)()
+()()(U3)(9;0)(A3100)()
+(REI)()()(778899;-1)(A211)()

 TEMP U1  2  3  T
 ()()(TEMP)(7;0)(A3100)()
 TEMP U2  2  3  T
 ()()(TEMP)(8;0)(A3100)()
 TEMP U3  2  3  T
 ()()(TEMP)(9;0)(A3100)()
 TEMP TEMP  1  3  T
 ()()()(;0)(A200)(DETJ)
 TEMP TEMP  2  3  T
 ()()(U1+U2+U3)(708090;0)(A3001)()
+(PEI)()()(778899;-1)(A211)()
# TEMP TEMP  3  3  T
# ()(NUSL)()(;0)(A200)(DETJ)

GROUP FREQUENCY
   1
SOLUTION TYPE
 DELTA_Q
 FACTORED_GAUSS_ELIMINATION
 IMPLICIT_EULER

END
```

```
TITLE          **** TEMPLATE FILE  TEMP.PH.UVWT ****
 INS3D  PHI ALGORITHM,  DELSQ PHI SOLVE  03/20/92

RESIDUALS
 PHI   2   T  EQN#, SET#, # OF TERMS --- SPATIAL FIELD SET (PHI)
 ()()()(1;0)(C201)(U1)
+()()()(4;0)(C202)(U1)
+()()()(7;0)(C203)(U1)
+()()()(2;0)(C201)(U2)
+()()()(5;0)(C202)(U2)
+()()()(8;0)(C203)(U2)
+()()()(3;0)(C201)(U3)
+()()()(6;0)(C202)(U3)
+()()()(9;0)(C203)(U3)
 PHI   4     #  VARBL, SET NO.,  --- BOUNDARY SET (PHI)
 (DUM1)()(COSY)(;1)(A200)(U1)
+(DUM2)()(COSX)(;1)(A200)(U2)
+(DUM3)()(COSZ)(;1)(A200)(U3)

JACOBIANS
 PHI PHI   2  1  T EQN, VARDIF, SET, TERMS, DIRECTION
 ()()()(112233;-1)(C211)()
+()()()(445566;-1)(C222)()
+()()()(778899;-1)(C233)()
+()()()(142536;-1)(C221)()
+()()()(142536;-1)(C212)()
+()()()(172839;-1)(C231)()
+()()()(172839;-1)(C213)()
+()()()(475869;-1)(C223)()
+()()()(475869;-1)(C232)()

GROUP FREQUENCY
      1
SOLUTION TYPE
 Q
 LU_FACTORIZATION_INCOMPLETE
#  CONJ_GRAD_INCOMPLETE_CHOLESKY
#  GAUSS_ELIMINATION
 IMPLICIT_EULER

END

TITLE          **** TEMPLATE FILE  TEMP.PH.UVWT ****
 INS3D  PHI ALGORITHM,  DELSQ PRESSURE SOLVE  03/20/92

RESIDUALS
 PRES   2  T  EQN#, SET#, # OF TERMS --- SPATIAL FIELD SET (PRES)
 ()(U1)()(11;-1)(C211)(U1)
+()(U2)()(12;-1)(C211)(U1)
+()(U3)()(13;-1)(C211)(U1)
+()(U1)()(21;-1)(C211)(U2)
+()(U2)()(22;-1)(C211)(U2)
+()(U3)()(23;-1)(C211)(U2)
+()(U1)()(31;-1)(C211)(U3)
+()(U2)()(32;-1)(C211)(U3)
+()(U3)()(33;-1)(C211)(U3)
+()(U1)()(14;-1)(C212)(U1)
+()(U2)()(15;-1)(C212)(U1)
+()(U3)()(16;-1)(C212)(U1)
+()(U1)()(24;-1)(C212)(U2)
+()(U2)()(25;-1)(C212)(U2)
+()(U3)()(26;-1)(C212)(U2)
```

+()(U1)()(34;-1)(C212)(U3)
+()(U2)()(35;-1)(C212)(U3)
+()(U3)()(36;-1)(C212)(U3)
+()(U1)()(17;-1)(C213)(U1)
+()(U2)()(18;-1)(C213)(U1)
+()(U3)()(19;-1)(C213)(U1)
+()(U1)()(27;-1)(C213)(U2)
+()(U2)()(28;-1)(C213)(U2)
+()(U3)()(29;-1)(C213)(U2)
+()(U1)()(37;-1)(C213)(U3)
+()(U2)()(38;-1)(C213)(U3)
+()(U3)()(39;-1)(C213)(U3)
+()(U1)()(41;-1)(C221)(U1)
+()(U2)()(42;-1)(C221)(U1)
+()(U3)()(43;-1)(C221)(U1)
+()(U1)()(51;-1)(C221)(U2)
+()(U2)()(52;-1)(C221)(U2)
+()(U3)()(53;-1)(C221)(U2)
+()(U1)()(61;-1)(C221)(U3)
+()(U2)()(62;-1)(C221)(U3)
+()(U3)()(63;-1)(C221)(U3)
+()(U1)()(44;-1)(C222)(U1)
+()(U2)()(45;-1)(C222)(U1)
+()(U3)()(46;-1)(C222)(U1)
+()(U1)()(54;-1)(C222)(U2)
+()(U2)()(55;-1)(C222)(U2)
+()(U3)()(56;-1)(C222)(U2)
+()(U1)()(64;-1)(C222)(U3)
+()(U2)()(65;-1)(C222)(U3)
+()(U3)()(66;-1)(C222)(U3)
+()(U1)()(47;-1)(C223)(U1)
+()(U2)()(48;-1)(C223)(U1)
+()(U3)()(49;-1)(C223)(U1)
+()(U1)()(57;-1)(C223)(U2)
+()(U2)()(58;-1)(C223)(U2)
+()(U3)()(59;-1)(C223)(U2)
+()(U1)()(67;-1)(C223)(U3)
+()(U2)()(68;-1)(C223)(U3)
+()(U3)()(69;-1)(C223)(U3)
+()(U1)()(71;-1)(C231)(U1)
+()(U2)()(72;-1)(C231)(U1)
+()(U3)()(73;-1)(C231)(U1)
+()(U1)()(81;-1)(C231)(U2)
+()(U2)()(82;-1)(C231)(U2)
+()(U3)()(83;-1)(C231)(U2)
+()(U1)()(91;-1)(C231)(U3)
+()(U2)()(92;-1)(C231)(U3)
+()(U3)()(93;-1)(C231)(U3)
+()(U1)()(74;-1)(C232)(U1)
+()(U2)()(75;-1)(C232)(U1)
+()(U3)()(76;-1)(C232)(U1)
+()(U1)()(84;-1)(C232)(U2)
+()(U2)()(85;-1)(C232)(U2)
+()(U3)()(86;-1)(C232)(U2)
+()(U1)()(94;-1)(C232)(U3)
+()(U2)()(95;-1)(C232)(U3)
+()(U3)()(96;-1)(C232)(U3)
+()(U1)()(77;-1)(C233)(U1)
+()(U2)()(78;-1)(C233)(U1)
+()(U3)()(79;-1)(C233)(U1)
+()(U1)()(87;-1)(C233)(U2)
+()(U2)()(88;-1)(C233)(U2)

```
+()(U3)()(89;-1)(C233)(U2)
+()(U1)()(97;-1)(C233)(U3)
+()(U2)()(98;-1)(C233)(U3)
+()(U3)()(99;-1)(C233)(U3)
+(-GR,RE2I)()()(2;0)(C210)(TEMP)
+(-GR,RE2I)()()(5;0)(C220)(TEMP)
+(-GR,RE2I)()()(8;0)(C230)(TEMP)
 PRES  3   T
(REI)()()(1;-1)(A201)(TAU1)
+(-,JOBC1,REI)()()(55;-1)(B222)(U1)
+(-,JOBC1,REI)()()(11;-1)(B211)(U1)
 PRES  4  T
(REI)()()(1;-1)(A201)(TAU1)
 PRES  5     T
(REI)()()(5;-1)(A201)(TAU1)
 PRES  6     T
(REI)()()(5;-1)(A201)(TAU1)
 PRES  7     T
(REI)()()(9;-1)(A201)(TAU1)
  PRES  8     T
(REI)()()(9;-1)(A201)(TAU1)
  PRES  10    T
(JOBC2,REI)()()(55;-1)(B222)(U1)
+(JOBC2,REI)()()(11;-1)(B211)(U1)
  PRES  11    T
(JOBC3,REI)()()(55;-1)(B222)(U1)
+(JOBC3,REI)()()(11;-1)(B211)(U1)

JACOBIANS

 PRES PRES  1  1  T EQN, VARDIF, SET, TERMS, DIRECTION
 ()()()(112233;-1)(C211)()
+()()()(445566;-1)(C222)()
+()()()(778899;-1)(C233)()
+()()()(142536;-1)(C221)()
+()()()(142536;-1)(C212)()
+()()()(172839;-1)(C231)()
+()()()(172839;-1)(C213)()
+()()()(475869;-1)(C223)()
+()()()(475869;-1)(C232)()

GROUP FREQUENCY
      -3
SOLUTION TYPE
 Q
 LU_FACTORIZATION_INCOMPLETE
#  CONJ_GRAD_INCOMPLETE_CHOLESKY
 IMPLICIT_EULER

END
```

Appendix H

AKCESS*. Cdata File for Ra=1.E4, 2-D CFD-Radiation and Fire Simulation

4. T IQNOW
0.000000E+00 0.000000E+00 0.000000E+00 0.000000E+00 0.000000E+00
0.000000E+00 0.000000E+00 0.000000E+00 0.000000E+00 0.000000E+00
0.000000E+00 0.000000E+00 0.000000E+00 0.000000E+00 0.000000E+00
0.000000E+00 0.000000E+00 0.000000E+00-2.572526E-02-6.332994E-02
-9.002969E-02-1.023930E-01-1.079351E-01-1.128174E-01-1.184001E-01
-1.239839E-01-1.271089E-01-1.247274E-01-1.146206E-01-9.542859E-02
-6.778258E-02-3.613317E-02-1.041382E-02 0.000000E+00 0.000000E+00
-2.729276E-02-7.571801E-02-1.172910E-01-1.418686E-01-1.573024E-01
-1.691930E-01-1.779208E-01-1.840831E-01-1.849012E-01-1.778357E-01
-1.601344E-01-1.310608E-01-9.277941E-02-4.993929E-02-1.473063E-02
0.000000E+00 0.000000E+00-2.208899E-02-6.948953E-02-1.153946E-01
-1.460907E-01-1.680738E-01-1.831069E-01-1.919652E-01-1.968573E-01
-1.943485E-01-1.853622E-01-1.665939E-01-1.361438E-01-9.729712E-02
-5.270943E-02-1.511536E-02 0.000000E+00 0.000000E+00-1.559009E-02
-5.574616E-02-9.882924E-02-1.304703E-01-1.541493E-01-1.683495E-01
-1.751861E-01-1.786355E-01-1.746170E-01-1.662064E-01-1.512287E-01
-1.260758E-01-9.235964E-02-5.119359E-02-1.487798E-02 0.000000E+00
0.000000E+00-9.224827E-03-3.880915E-02-7.451677E-02-1.031573E-01
-1.247637E-01-1.368284E-01-1.408738E-01-1.421313E-01-1.386335E-01
-1.322453E-01-1.226381E-01-1.060452E-01-8.086515E-02-4.692236E-02
-1.441580E-02 0.000000E+00 0.000000E+00-3.068982E-03-2.058712E-02
-4.630660E-02-6.930483E-02-8.666169E-02-9.632631E-02-9.828032E-02
-9.700457E-02-9.399849E-02-9.002247E-02-8.545305E-02-7.781589E-02
-6.332788E-02-3.946414E-02-1.310925E-02 0.000000E+00 0.000000E+00
2.380217E-03-2.608041E-03-1.646468E-02-3.204947E-02-4.435526E-02
-5.114155E-02-5.180695E-02-4.897939E-02-4.567422E-02-4.360421E-02
-4.345033E-02-4.370791E-02-4.024548E-02-2.839911E-02-1.063652E-02
0.000000E+00 0.000000E+00 7.045628E-03 1.403748E-02 1.300725E-02
6.320572E-03-4.818712E-04-4.048979E-03-3.398098E-03-4.584952E-09
3.398091E-03 4.048973E-03 4.818632E-04-6.320576E-03-1.300725E-02
-1.403748E-02-7.045624E-03 0.000000E+00 0.000000E+00 1.063652E-02
2.839911E-02 4.024549E-02 4.370792E-02 4.345034E-02 4.360422E-02
4.567423E-02 4.897940E-02 5.180697E-02 5.114156E-02 4.435527E-02
3.204948E-02 1.646467E-02 2.608055E-03-2.380226E-03 0.000000E+00
0.000000E+00 1.310925E-02 3.946415E-02 6.332787E-02 7.781589E-02
8.545304E-02 9.002246E-02 9.399848E-02 9.700456E-02 9.828031E-02
9.632630E-02 8.666169E-02 6.930482E-02 4.630661E-02 2.058711E-02
3.068993E-03 0.000000E+00 0.000000E+00 1.441580E-02 4.692235E-02
8.086517E-02 1.060452E-01 1.226381E-01 1.322453E-01 1.386335E-01
1.421313E-01 1.408738E-01 1.368284E-01 1.247637E-01 1.031573E-01
7.451675E-02 3.880917E-02 9.224815E-03 0.000000E+00 0.000000E+00
1.487797E-02 5.119360E-02 9.235962E-02 1.260758E-01 1.512286E-01
1.662064E-01 1.746170E-01 1.786355E-01 1.751861E-01 1.683495E-01
1.541493E-01 1.304703E-01 9.882928E-02 5.574614E-02 1.559010E-02
0.000000E+00 0.000000E+00 1.511537E-02 5.270941E-02 9.729715E-02
1.361438E-01 1.665940E-01 1.853622E-01 1.943485E-01 1.968573E-01
1.919652E-01 1.831069E-01 1.680738E-01 1.460907E-01 1.153946E-01
6.948955E-02 2.208899E-02 0.000000E+00 0.000000E+00 1.473063E-02
4.993930E-02 9.277937E-02 1.310608E-01 1.601344E-01 1.778357E-01
1.849012E-01 1.840831E-01 1.779208E-01 1.691930E-01 1.573024E-01
1.418686E-01 1.172910E-01 7.571799E-02 2.729277E-02 0.000000E+00
0.000000E+00 1.041383E-02 3.613316E-02 6.778261E-02 9.542858E-02
1.146206E-01 1.247274E-01 1.271089E-01 1.239839E-01 1.184001E-01
1.128174E-01 1.079351E-01 1.023930E-01 9.002966E-02 6.332995E-02
2.572526E-02 0.000000E+00 0.000000E+00 0.000000E+00 0.000000E+00
0.000000E+00 0.000000E+00 0.000000E+00 0.000000E+00 0.000000E+00
0.000000E+00 0.000000E+00 0.000000E+00 0.000000E+00 0.000000E+00
0.000000E+00 0.000000E+00 0.000000E+00 0.000000E+00 $ U1
0.000000E+00 0.000000E+00 0.000000E+00 0.000000E+00 0.000000E+00
0.000000E+00 0.000000E+00 0.000000E+00 0.000000E+00 0.000000E+00
0.000000E+00 0.000000E+00 0.000000E+00 0.000000E+00 0.000000E+00

0.000000E+00 0.000000E+00 0.000000E+00 2.444424E-02 1.673957E-02
5.830826E-03 7.652210E-04 5.845587E-04 1.635893E-03 2.347153E-03
2.446694E-03 9.755201E-04-2.047730E-03-6.530681E-03-1.120792E-02
-1.516809E-02-1.579066E-02-1.059407E-02 0.000000E+00 0.000000E+00
6.913190E-02 5.588365E-02 2.924994E-02 1.423886E-02 1.016387E-02
9.563803E-03 9.163128E-03 6.172861E-03-3.872392E-04-1.087307E-02
-2.546809E-02-4.008433E-02-5.059366E-02-5.118296E-02-3.542395E-02
0.000000E+00 0.000000E+00 1.163440E-01 1.049561E-01 6.534122E-02
3.844176E-02 2.635619E-02 2.107501E-02 1.715275E-02 9.021798E-03
-4.750306E-03-2.420632E-02-4.939458E-02-7.514493E-02-9.363819E-02
-9.451511E-02-6.636901E-02 0.000000E+00 0.000000E+00 1.554229E-01
1.522072E-01 1.048312E-01 6.633089E-02 4.462166E-02 3.279929E-02
2.319980E-02 1.008338E-02-9.940983E-03-3.761909E-02-7.139238E-02
-1.072288E-01-1.343581E-01-1.371212E-01-9.793970E-02 0.000000E+00
0.000000E+00 1.831253E-01 1.919191E-01 1.417143E-01 9.341326E-02
6.202686E-02 4.283772E-02 2.673314E-02 8.985489E-03-1.492426E-02
-4.789138E-02-8.804458E-02-1.321199E-01-1.681698E-01-1.757275E-01
-1.284031E-01 0.000000E+00 0.000000E+00 1.986582E-01 2.206582E-01
1.722101E-01 1.171401E-01 7.664632E-02 4.982959E-02 2.827186E-02
6.589952E-03-1.935745E-02-5.378306E-02-9.724224E-02-1.472194E-01
-1.921561E-01-2.073716E-01-1.562276E-01 0.000000E+00 0.000000E+00
2.024409E-01 2.366884E-01 1.938688E-01 1.358666E-01 8.801559E-02
5.376384E-02 2.762937E-02 3.597667E-03-2.272616E-02-5.590337E-02
-9.929306E-02-1.523164E-01-2.047267E-01-2.292635E-01-1.792131E-01
0.000000E+00 0.000000E+00 1.953712E-01 2.395204E-01 2.051999E-01
1.481503E-01 9.584093E-02 5.565448E-02 2.541012E-02 6.109068E-08
-2.541001E-02-5.565435E-02-9.584082E-02-1.481502E-01-2.051998E-01
-2.395203E-01-1.953711E-01 0.000000E+00 0.000000E+00 1.792130E-01
2.292634E-01 2.047266E-01 1.523162E-01 9.929295E-02 5.590325E-02
2.272605E-02-3.597788E-03-2.762948E-02-5.376397E-02-8.801570E-02
-1.358667E-01-1.938689E-01-2.366885E-01-2.024410E-01 0.000000E+00
0.000000E+00 1.562278E-01 2.073716E-01 1.921562E-01 1.472195E-01
9.724234E-02 5.378318E-02 1.935755E-02-6.589840E-03-2.827176E-02
-4.982948E-02-7.664622E-02-1.171400E-01-1.722099E-01-2.206582E-01
-1.986581E-01 0.000000E+00 0.000000E+00 1.284030E-01 1.757274E-01
1.681697E-01 1.321198E-01 8.804449E-02 4.789128E-02 1.492416E-02
-8.985586E-03-2.673324E-02-4.283781E-02-6.202696E-02-9.341335E-02
-1.417144E-01-1.919191E-01-1.831254E-01 0.000000E+00 0.000000E+00
9.793979E-02 1.371212E-01 1.343582E-01 1.072288E-01 7.139246E-02
3.761917E-02 9.941061E-03-1.008330E-02-2.319972E-02-3.279922E-02
-4.462158E-02-6.633082E-02-1.048311E-01-1.522072E-01-1.554228E-01
0.000000E+00 0.000000E+00 6.636894E-02 9.451507E-02 9.363813E-02
7.514487E-02 4.939452E-02 2.420626E-02 4.750240E-03-9.021852E-03
-1.715282E-02-2.107506E-02-2.635625E-02-3.844181E-02-6.534129E-02
-1.049561E-01-1.163441E-01 0.000000E+00 0.000000E+00 3.542400E-02
5.118299E-02 5.059371E-02 4.008437E-02 2.546813E-02 1.087310E-02
3.872841E-04-6.172826E-03-9.163083E-03-9.563772E-03-1.016383E-02
-1.423884E-02-2.924989E-02-5.588361E-02-6.913185E-02 0.000000E+00
0.000000E+00 1.059404E-02 1.579065E-02 1.516808E-02 1.120788E-02
6.530674E-03 2.047698E-03-9.755375E-04-2.446721E-03-2.347165E-03
-1.635926E-03-5.845578E-04-7.652621E-04-5.830834E-03-1.673958E-02
-2.444426E-02 0.000000E+00 0.000000E+00 0.000000E+00 0.000000E+00
0.000000E+00 0.000000E+00 0.000000E+00 0.000000E+00 0.000000E+00
0.000000E+00 0.000000E+00 0.000000E+00 0.000000E+00 0.000000E+00
0.000000E+00 0.000000E+00 0.000000E+00 0.000000E+00 $ U2
1.000000E+00 7.980487E-01 6.181677E-01 4.771338E-01 3.782750E-01
3.133214E-01 2.707267E-01 2.409647E-01 2.175876E-01 1.966046E-01
1.756365E-01 1.532585E-01 1.285852E-01 1.010282E-01 7.021504E-02
3.619750E-02 0.000000E+00 1.000000E+00 7.911643E-01 6.054865E-01
4.635313E-01 3.679167E-01 3.071695E-01 2.680139E-01 2.406629E-01
2.188916E-01 1.989861E-01 1.787471E-01 1.568098E-01 1.322610E-01
1.044662E-01 7.300044E-02 3.782696E-02 0.000000E+00 1.000000E+00

7.845471E-01 5.928802E-01 4.498101E-01 3.584982E-01 3.041083E-01
2.709170E-01 2.484032E-01 2.304566E-01 2.136104E-01 1.956831E-01
1.750521E-01 1.503055E-01 1.203855E-01 8.484270E-02 4.408498E-02
0.000000E+00 1.000000E+00 7.846222E-01 5.923752E-01 4.503097E-01
3.627733E-01 3.139229E-01 2.866909E-01 2.698076E-01 2.570468E-01
2.448429E-01 2.305523E-01 2.117443E-01 1.859656E-01 1.513045E-01
1.073505E-01 5.568164E-02 0.000000E+00 1.000000E+00 7.907682E-01
6.032084E-01 4.647218E-01 3.808574E-01 3.366384E-01 3.148365E-01
3.037152E-01 2.967206E-01 2.899041E-01 2.798563E-01 2.629140E-01
2.352636E-01 1.938706E-01 1.382696E-01 7.157686E-02 0.000000E+00
1.000000E+00 8.015423E-01 6.227932E-01 4.900738E-01 4.099596E-01
3.694528E-01 3.521282E-01 3.461714E-01 3.445828E-01 3.428688E-01
3.368477E-01 3.215794E-01 2.916906E-01 2.427746E-01 1.740193E-01
9.006748E-02 0.000000E+00 1.000000E+00 8.157673E-01 6.488919E-01
5.236631E-01 4.474000E-01 4.096332E-01 3.954466E-01 3.933331E-01
3.959650E-01 3.983142E-01 3.955581E-01 3.817310E-01 3.498342E-01
2.937020E-01 2.116826E-01 1.097374E-01 0.000000E+00 1.000000E+00
8.324754E-01 6.797633E-01 5.634694E-01 4.912528E-01 4.553523E-01
4.428477E-01 4.428866E-01 4.480653E-01 4.530251E-01 4.525172E-01
4.398279E-01 4.064225E-01 3.439917E-01 2.494095E-01 1.296405E-01
0.000000E+00 1.000000E+00 8.508925E-01 7.140404E-01 6.079876E-01
5.402729E-01 5.056758E-01 4.935579E-01 4.940663E-01 5.000000E-01
5.059337E-01 5.064421E-01 4.943242E-01 4.597271E-01 3.920124E-01
2.859596E-01 1.491075E-01 0.000000E+00 1.000000E+00 8.703595E-01
7.505905E-01 6.560083E-01 5.935775E-01 5.601721E-01 5.474828E-01
5.469749E-01 5.519347E-01 5.571134E-01 5.571523E-01 5.446477E-01
5.087472E-01 4.365306E-01 3.202367E-01 1.675246E-01 0.000000E+00
1.000000E+00 8.902626E-01 7.883174E-01 7.062980E-01 6.501658E-01
6.182690E-01 6.044419E-01 6.016858E-01 6.040350E-01 6.066669E-01
6.045534E-01 5.903668E-01 5.526000E-01 4.763369E-01 3.511081E-01
1.842327E-01 0.000000E+00 1.000000E+00 9.099325E-01 8.259807E-01
7.572254E-01 7.083094E-01 6.784206E-01 6.631523E-01 6.571312E-01
6.554172E-01 6.538286E-01 6.478718E-01 6.305472E-01 5.900404E-01
5.099262E-01 3.772068E-01 1.984577E-01 0.000000E+00 1.000000E+00
9.284231E-01 8.617304E-01 8.061293E-01 7.647364E-01 7.370860E-01
7.201437E-01 7.100959E-01 7.032794E-01 6.962848E-01 6.851635E-01
6.633616E-01 6.191426E-01 5.352782E-01 3.967916E-01 2.092318E-01
0.000000E+00 1.000000E+00 9.443184E-01 8.926495E-01 8.486955E-01
8.140344E-01 7.882557E-01 7.694477E-01 7.551571E-01 7.429532E-01
7.301924E-01 7.133091E-01 6.860771E-01 6.372267E-01 5.496903E-01
4.076248E-01 2.153778E-01 0.000000E+00 1.000000E+00 9.559150E-01
9.151573E-01 8.796145E-01 8.496945E-01 8.249479E-01 8.043169E-01
7.863896E-01 7.695434E-01 7.515968E-01 7.290830E-01 6.958917E-01
6.415018E-01 5.501899E-01 4.071198E-01 2.154529E-01 0.000000E+00
1.000000E+00 9.621730E-01 9.269996E-01 8.955338E-01 8.677390E-01
8.431902E-01 8.212529E-01 8.010139E-01 7.811084E-01 7.593371E-01
7.319861E-01 6.928305E-01 6.320833E-01 5.364687E-01 3.945135E-01
2.088357E-01 0.000000E+00 1.000000E+00 9.638025E-01 9.297850E-01
8.989718E-01 8.714148E-01 8.467415E-01 8.243635E-01 8.033954E-01
7.824124E-01 7.590353E-01 7.292733E-01 6.866786E-01 6.217250E-01
5.228662E-01 3.818323E-01 2.019513E-01 0.000000E+00 $ TEMP 3
289*0. $ PHI 4
289*0. $ PRES 5
289*0. $ OMGA 6
289*0. $ PSI 7
289*0. $ SPHI 8
289*0. $ AVEL 9
289*0. $ TAU2W 10
289*0. $ UMAG 11
289*0. $ YPLS 12
289*0. $ PHIW 13
289*0. $ PARU 14

```
   289*0.     $ PARV    15
   289*0.     $ COSX    16
   289*0.     $ COSY    17
   289*0.     $ PTBL    18
   289*0.     $ SRCT    19
   289*0.     $ FIRE    19
   289*0.     $ TREF    20
   289*0.     $ NUSL    21
 5.568302E-02 1.303151E-03 2.427104E-03 2.616159E-03 1.926350E-03
 9.821893E-04 1.612478E-04-4.562051E-04-9.059922E-04-1.239310E-03
-1.480296E-03-1.620143E-03-1.623415E-03-1.457162E-03-1.113109E-03
-6.083591E-04-1.108947E-02 3.856838E-02 0.000000E+00 0.000000E+00
 0.000000E+00 0.000000E+00 0.000000E+00 0.000000E+00 0.000000E+00
 0.000000E+00 0.000000E+00 0.000000E+00 0.000000E+00 0.000000E+00
 0.000000E+00 0.000000E+00 0.000000E+00-7.084510E-03 3.979722E-02
 0.000000E+00 0.000000E+00 0.000000E+00 0.000000E+00 0.000000E+00
 0.000000E+00 0.000000E+00 0.000000E+00 0.000000E+00 0.000000E+00
 0.000000E+00 0.000000E+00 0.000000E+00 0.000000E+00 0.000000E+00
-8.241548E-03 3.982470E-02 0.000000E+00 0.000000E+00 0.000000E+00
 0.000000E+00 0.000000E+00 0.000000E+00 0.000000E+00 0.000000E+00
 0.000000E+00 0.000000E+00 0.000000E+00 0.000000E+00 0.000000E+00
 0.000000E+00 0.000000E+00-1.042164E-02 3.873932E-02 0.000000E+00
 0.000000E+00 0.000000E+00 0.000000E+00 0.000000E+00 0.000000E+00
 0.000000E+00 0.000000E+00 0.000000E+00 0.000000E+00 0.000000E+00
 0.000000E+00 0.000000E+00 0.000000E+00 0.000000E+00-1.341419E-02
 3.679867E-02 0.000000E+00 0.000000E+00 0.000000E+00 0.000000E+00
 0.000000E+00 0.000000E+00 0.000000E+00 0.000000E+00 0.000000E+00
 0.000000E+00 0.000000E+00 0.000000E+00 0.000000E+00 0.000000E+00
 0.000000E+00-1.688143E-02 3.422102E-02 0.000000E+00 0.000000E+00
 0.000000E+00 0.000000E+00 0.000000E+00 0.000000E+00 0.000000E+00
 0.000000E+00 0.000000E+00 0.000000E+00 0.000000E+00 0.000000E+00
 0.000000E+00 0.000000E+00 0.000000E+00-2.054639E-02 3.117956E-02
 0.000000E+00 0.000000E+00 0.000000E+00 0.000000E+00 0.000000E+00
 0.000000E+00 0.000000E+00 0.000000E+00 0.000000E+00 0.000000E+00
 0.000000E+00 0.000000E+00 0.000000E+00 0.000000E+00 0.000000E+00
-2.423032E-02 2.781115E-02 0.000000E+00 0.000000E+00 0.000000E+00
 0.000000E+00 0.000000E+00 0.000000E+00 0.000000E+00 0.000000E+00
 0.000000E+00 0.000000E+00 0.000000E+00 0.000000E+00 0.000000E+00
 0.000000E+00 0.000000E+00-2.781115E-02 2.423032E-02 0.000000E+00
 0.000000E+00 0.000000E+00 0.000000E+00 0.000000E+00 0.000000E+00
 0.000000E+00 0.000000E+00 0.000000E+00 0.000000E+00 0.000000E+00
 0.000000E+00 0.000000E+00 0.000000E+00 0.000000E+00-3.117956E-02
 2.054639E-02 0.000000E+00 0.000000E+00 0.000000E+00 0.000000E+00
 0.000000E+00 0.000000E+00 0.000000E+00 0.000000E+00 0.000000E+00
 0.000000E+00 0.000000E+00 0.000000E+00 0.000000E+00 0.000000E+00
 0.000000E+00-3.422102E-02 1.688143E-02 0.000000E+00 0.000000E+00
 0.000000E+00 0.000000E+00 0.000000E+00 0.000000E+00 0.000000E+00
 0.000000E+00 0.000000E+00 0.000000E+00 0.000000E+00 0.000000E+00
 0.000000E+00 0.000000E+00 0.000000E+00-3.679867E-02 1.341419E-02
 0.000000E+00 0.000000E+00 0.000000E+00 0.000000E+00 0.000000E+00
 0.000000E+00 0.000000E+00 0.000000E+00 0.000000E+00 0.000000E+00
 0.000000E+00 0.000000E+00 0.000000E+00 0.000000E+00 0.000000E+00
-3.873932E-02 1.042163E-02 0.000000E+00 0.000000E+00 0.000000E+00
 0.000000E+00 0.000000E+00 0.000000E+00 0.000000E+00 0.000000E+00
 0.000000E+00 0.000000E+00 0.000000E+00 0.000000E+00 0.000000E+00
 0.000000E+00 0.000000E+00-3.982470E-02 8.241550E-03 0.000000E+00
 0.000000E+00 0.000000E+00 0.000000E+00 0.000000E+00 0.000000E+00
 0.000000E+00 0.000000E+00 0.000000E+00 0.000000E+00 0.000000E+00
 0.000000E+00 0.000000E+00 0.000000E+00 0.000000E+00-3.979722E-02
 7.084510E-03 0.000000E+00 0.000000E+00 0.000000E+00 0.000000E+00
 0.000000E+00 0.000000E+00 0.000000E+00 0.000000E+00 0.000000E+00
 0.000000E+00 0.000000E+00 0.000000E+00 0.000000E+00 0.000000E+00
```

```
0.000000E+00-3.856838E-02 1.108947E-02 6.083629E-04 1.113112E-03
1.457162E-03 1.623415E-03 1.620143E-03 1.480296E-03 1.239310E-03
9.059922E-04 4.562051E-04-1.612478E-04-9.821893E-04-1.926350E-03
-2.616159E-03-2.427104E-03-1.303151E-03-5.568302E-02  $  QFLX 22
1. 15*2. 17. 15(5. 15*0. 3.) 273. 15*4. 289.  $ OFWL 23
  289*0.      $ BC1    24
  289*0.      $ BC2    25
  16*1.0 17 15( -17 15*0 17) -17 16*-1      $ SURF    26
  289*0.      $ SRFN    27
  289*0.      $ SRAD    28
  289*0.      $ PBIN    29
 289*001.
  $  MTRL      30
  289*0.      $ DETJ    31
  289*0.      $ DETC    32
  289*0.      $ ETKJ    33
  289*0.      $ EJK2    34
  289*0.      $ EJK3    35
  289*0.      $ EJK4    36
  289*0.      $ EJK5    37
  289*0.      $ EJK6    38
  289*0.      $ EJK7    39
  289*0.      $ EJK8    40
  289*0.      $ EJK9    41
  289*0.      $ U1L    42
  289*0.      $ U2L    43
  289*0.      $ TEML    44
  289*0.      $ PHIL    45
  289*0.      $ PREL    46
  289*0.      $ OMGL    47
  289*0.      $ PSIL    48
  289*0.      $ F1    49
  289*0.      $ F2    50
  289*0.      $ F3    51
  289*0.      $ F4    52
  289*0.      $ F5    53
  289*0.      $ F6    54
  289*0.      $ F7    55
  289*0.      $ G1    56
  289*0.      $ G2    57
  289*0.      $ G3    58
  289*0.      $ G4    59
  289*0.      $ G5    60
  289*0.      $ G6    61
  289*0.      $ G7    62
0.00000D+00  6.25000D-02  1.25000D-01  1.87500D-01  2.50000D-01
3.12500D-01  3.75000D-01  4.37500D-01  5.00000D-01  5.62500D-01
6.25000D-01  6.87500D-01  7.50000D-01  8.12500D-01  8.75000D-01
9.37500D-01  1.00000D+00
0.00000D+00  6.25000D-02  1.25000D-01  1.87500D-01  2.50000D-01
3.12500D-01  3.75000D-01  4.37500D-01  5.00000D-01  5.62500D-01
6.25000D-01  6.87500D-01  7.50000D-01  8.12500D-01  8.75000D-01
9.37500D-01  1.00000D+00
0.00000D+00  6.25000D-02  1.25000D-01  1.87500D-01  2.50000D-01
3.12500D-01  3.75000D-01  4.37500D-01  5.00000D-01  5.62500D-01
6.25000D-01  6.87500D-01  7.50000D-01  8.12500D-01  8.75000D-01
9.37500D-01  1.00000D+00
0.00000D+00  6.25000D-02  1.25000D-01  1.87500D-01  2.50000D-01
3.12500D-01  3.75000D-01  4.37500D-01  5.00000D-01  5.62500D-01
6.25000D-01  6.87500D-01  7.50000D-01  8.12500D-01  8.75000D-01
9.37500D-01  1.00000D+00
0.00000D+00  6.25000D-02  1.25000D-01  1.87500D-01  2.50000D-01
```

3.12500D-01 3.75000D-01 4.37500D-01 5.00000D-01 5.62500D-01
6.25000D-01 6.87500D-01 7.50000D-01 8.12500D-01 8.75000D-01
9.37500D-01 1.00000D+00
0.00000D+00 6.25000D-02 1.25000D-01 1.87500D-01 2.50000D-01
3.12500D-01 3.75000D-01 4.37500D-01 5.00000D-01 5.62500D-01
6.25000D-01 6.87500D-01 7.50000D-01 8.12500D-01 8.75000D-01
9.37500D-01 1.00000D+00
0.00000D+00 6.25000D-02 1.25000D-01 1.87500D-01 2.50000D-01
3.12500D-01 3.75000D-01 4.37500D-01 5.00000D-01 5.62500D-01
6.25000D-01 6.87500D-01 7.50000D-01 8.12500D-01 8.75000D-01
9.37500D-01 1.00000D+00
0.00000D+00 6.25000D-02 1.25000D-01 1.87500D-01 2.50000D-01
3.12500D-01 3.75000D-01 4.37500D-01 5.00000D-01 5.62500D-01
6.25000D-01 6.87500D-01 7.50000D-01 8.12500D-01 8.75000D-01
9.37500D-01 1.00000D+00
0.00000D+00 6.25000D-02 1.25000D-01 1.87500D-01 2.50000D-01
3.12500D-01 3.75000D-01 4.37500D-01 5.00000D-01 5.62500D-01
6.25000D-01 6.87500D-01 7.50000D-01 8.12500D-01 8.75000D-01
9.37500D-01 1.00000D+00
0.00000D+00 6.25000D-02 1.25000D-01 1.87500D-01 2.50000D-01
3.12500D-01 3.75000D-01 4.37500D-01 5.00000D-01 5.62500D-01
6.25000D-01 6.87500D-01 7.50000D-01 8.12500D-01 8.75000D-01
9.37500D-01 1.00000D+00
0.00000D+00 6.25000D-02 1.25000D-01 1.87500D-01 2.50000D-01
3.12500D-01 3.75000D-01 4.37500D-01 5.00000D-01 5.62500D-01
6.25000D-01 6.87500D-01 7.50000D-01 8.12500D-01 8.75000D-01
9.37500D-01 1.00000D+00
0.00000D+00 6.25000D-02 1.25000D-01 1.87500D-01 2.50000D-01
3.12500D-01 3.75000D-01 4.37500D-01 5.00000D-01 5.62500D-01
6.25000D-01 6.87500D-01 7.50000D-01 8.12500D-01 8.75000D-01
9.37500D-01 1.00000D+00
0.00000D+00 6.25000D-02 1.25000D-01 1.87500D-01 2.50000D-01
3.12500D-01 3.75000D-01 4.37500D-01 5.00000D-01 5.62500D-01
6.25000D-01 6.87500D-01 7.50000D-01 8.12500D-01 8.75000D-01
9.37500D-01 1.00000D+00
0.00000D+00 6.25000D-02 1.25000D-01 1.87500D-01 2.50000D-01
3.12500D-01 3.75000D-01 4.37500D-01 5.00000D-01 5.62500D-01
6.25000D-01 6.87500D-01 7.50000D-01 8.12500D-01 8.75000D-01
9.37500D-01 1.00000D+00
0.00000D+00 6.25000D-02 1.25000D-01 1.87500D-01 2.50000D-01
3.12500D-01 3.75000D-01 4.37500D-01 5.00000D-01 5.62500D-01
6.25000D-01 6.87500D-01 7.50000D-01 8.12500D-01 8.75000D-01
9.37500D-01 1.00000D+00
$ X1 63
0.00000D+00 0.00000D+00 0.00000D+00 0.00000D+00 0.00000D+00
0.00000D+00 0.00000D+00 0.00000D+00 0.00000D+00 0.00000D+00
0.00000D+00 0.00000D+00 0.00000D+00 0.00000D+00 0.00000D+00
0.00000D+00 0.00000D+00
6.25000D-02 6.25000D-02 6.25000D-02 6.25000D-02 6.25000D-02
6.25000D-02 6.25000D-02 6.25000D-02 6.25000D-02 6.25000D-02
6.25000D-02 6.25000D-02 6.25000D-02 6.25000D-02 6.25000D-02
6.25000D-02 6.25000D-02
1.25000D-01 1.25000D-01 1.25000D-01 1.25000D-01 1.25000D-01
1.25000D-01 1.25000D-01 1.25000D-01 1.25000D-01 1.25000D-01

```
1.25000D-01  1.25000D-01  1.25000D-01  1.25000D-01  1.25000D-01
1.25000D-01  1.25000D-01
1.87500D-01  1.87500D-01  1.87500D-01  1.87500D-01  1.87500D-01
1.87500D-01  1.87500D-01  1.87500D-01  1.87500D-01  1.87500D-01
1.87500D-01  1.87500D-01  1.87500D-01  1.87500D-01  1.87500D-01
1.87500D-01  1.87500D-01
2.50000D-01  2.50000D-01  2.50000D-01  2.50000D-01  2.50000D-01
2.50000D-01  2.50000D-01  2.50000D-01  2.50000D-01  2.50000D-01
2.50000D-01  2.50000D-01  2.50000D-01  2.50000D-01  2.50000D-01
2.50000D-01  2.50000D-01
3.12500D-01  3.12500D-01  3.12500D-01  3.12500D-01  3.12500D-01
3.12500D-01  3.12500D-01  3.12500D-01  3.12500D-01  3.12500D-01
3.12500D-01  3.12500D-01  3.12500D-01  3.12500D-01  3.12500D-01
3.12500D-01  3.12500D-01
3.75000D-01  3.75000D-01  3.75000D-01  3.75000D-01  3.75000D-01
3.75000D-01  3.75000D-01  3.75000D-01  3.75000D-01  3.75000D-01
3.75000D-01  3.75000D-01  3.75000D-01  3.75000D-01  3.75000D-01
3.75000D-01  3.75000D-01
4.37500D-01  4.37500D-01  4.37500D-01  4.37500D-01  4.37500D-01
4.37500D-01  4.37500D-01  4.37500D-01  4.37500D-01  4.37500D-01
4.37500D-01  4.37500D-01  4.37500D-01  4.37500D-01  4.37500D-01
4.37500D-01  4.37500D-01
5.00000D-01  5.00000D-01  5.00000D-01  5.00000D-01  5.00000D-01
5.00000D-01  5.00000D-01  5.00000D-01  5.00000D-01  5.00000D-01
5.00000D-01  5.00000D-01  5.00000D-01  5.00000D-01  5.00000D-01
5.00000D-01  5.00000D-01
5.62500D-01  5.62500D-01  5.62500D-01  5.62500D-01  5.62500D-01
5.62500D-01  5.62500D-01  5.62500D-01  5.62500D-01  5.62500D-01
5.62500D-01  5.62500D-01  5.62500D-01  5.62500D-01  5.62500D-01
5.62500D-01  5.62500D-01
6.25000D-01  6.25000D-01  6.25000D-01  6.25000D-01  6.25000D-01
6.25000D-01  6.25000D-01  6.25000D-01  6.25000D-01  6.25000D-01
6.25000D-01  6.25000D-01  6.25000D-01  6.25000D-01  6.25000D-01
6.25000D-01  6.25000D-01
6.87500D-01  6.87500D-01  6.87500D-01  6.87500D-01  6.87500D-01
6.87500D-01  6.87500D-01  6.87500D-01  6.87500D-01  6.87500D-01
6.87500D-01  6.87500D-01  6.87500D-01  6.87500D-01  6.87500D-01
6.87500D-01  6.87500D-01
7.50000D-01  7.50000D-01  7.50000D-01  7.50000D-01  7.50000D-01
7.50000D-01  7.50000D-01  7.50000D-01  7.50000D-01  7.50000D-01
7.50000D-01  7.50000D-01  7.50000D-01  7.50000D-01  7.50000D-01
7.50000D-01  7.50000D-01
8.12500D-01  8.12500D-01  8.12500D-01  8.12500D-01  8.12500D-01
8.12500D-01  8.12500D-01  8.12500D-01  8.12500D-01  8.12500D-01
8.12500D-01  8.12500D-01  8.12500D-01  8.12500D-01  8.12500D-01
8.12500D-01  8.12500D-01
8.75000D-01  8.75000D-01  8.75000D-01  8.75000D-01  8.75000D-01
8.75000D-01  8.75000D-01  8.75000D-01  8.75000D-01  8.75000D-01
8.75000D-01  8.75000D-01  8.75000D-01  8.75000D-01  8.75000D-01
8.75000D-01  8.75000D-01
9.37500D-01  9.37500D-01  9.37500D-01  9.37500D-01  9.37500D-01
9.37500D-01  9.37500D-01  9.37500D-01  9.37500D-01  9.37500D-01
9.37500D-01  9.37500D-01  9.37500D-01  9.37500D-01  9.37500D-01
9.37500D-01  9.37500D-01
1.00000D+00  1.00000D+00  1.00000D+00  1.00000D+00  1.00000D+00
1.00000D+00  1.00000D+00  1.00000D+00  1.00000D+00  1.00000D+00
1.00000D+00  1.00000D+00  1.00000D+00  1.00000D+00  1.00000D+00
1.00000D+00  1.00000D+00
 $  X2       64
 289*0.     $ ONES   65
18*1.  15*0.  2*1.  15*0.  2*1.  15*0.
2*1.  15*0.  2*1.  15*0.  2*1.  15*0.
```

```
 2*1.  15*0.  2*1.  15*0.  2*1.  15*0.
 2*1.  15*0.  2*1.  15*0.  2*1.  15*0.
 2*1.  15*0.  2*1.  15*0.  2*1.  15*0.
 18*1.    $ FIXEDSET 1
 18*1.  15*0.  2*1.  15*0.  2*1.  15*0.
 2*1.  15*0.  2*1.  15*0.  2*1.  15*0.
 2*1.  15*0.  2*1.  15*0.  2*1.  15*0.
 2*1.  15*0.  2*1.  15*0.  2*1.  15*0.
 2*1.  15*0.  2*1.  15*0.  2*1.  15*0.
 18*1.    $ FIXEDSET 2
 289*0.   $ FIXEDSET 3
 289*0.   $ FIXEDSET 4
 289*0.   $ FIXEDSET 5
 289*0.   $ FIXEDSET 6
 18*1.  15*0.  2*1.  15*0.  2*1.  15*0.
 2*1.  15*0.  2*1.  15*0.  2*1.  15*0.
 2*1.  15*0.  2*1.  15*0.  2*1.  15*0.
 2*1.  15*0.  2*1.  15*0.  2*1.  15*0.
 2*1.  15*0.  2*1.  15*0.  2*1.  15*0.
 18*1.    $ FIXEDSET 7
T END OF INITIAL CONDITIONS
```

Vita

Born and raised in the British Colony of Hong Kong, Dee graduated from Hoh Fuk Tong College (a local high school) in 1970. After one year of post-secondary education, he was appointed by the Director of Hong Kong Fire Services Department as an Assistant Station Fire Officer (Fire Officer III) in 1971. In 1974, he was promoted to Station Officer (Fire Officer II), who was in charge small and medium fire stations and commanded all first-attendance fire and emergency incidents. Towards the end of his career with the Department, he functioned as a Fire Prevention Officer performing multifarious fire prevention tasks.

Inspired by the engineering and scientific applications in forensic science and fire investigations, he resigned from the Department and pursued higher education in California, USA. He received his first Bachelor degree in Mechanical Engineering from The University of California, Berkeley in 1982 and his second Bachelor degree in Fire Protection Engineering from The University of Maryland, College Park in 1984. Since 1982, Dee has been fully engaged in the profession of fire protection consulting engineering in addition to fire research and testing. Currently, Dee is a registered professional engineer in both disciplines of mechanical and fire protection engineering with States of California and Washington. As a part-time student, he had completed his master degree program in Mechanical Engineering at San Jose State University.

In 1991, he launched a part-time doctoral engineering program at The University of Tennessee, Knoxville. Since January 1994, he has become a full-time student to conduct his doctoral research program.